The Use of Solubility Parameters to Select Membrane Materials for Pervaporation of Organic Mixtures

THE UNIVERSITY OF
WAIKATO
Te Whare Wānanga o Waikato

A thesis submitted in partial fulfilment of the
requirements for the degree of
Doctor of Philosophy
at the University of Waikato by

Marion K. Buckley-Smith

The University of Waikato,
Hamilton, New Zealand
January 2006.

Abstract

Pevaporation is a method for separating volatile components from liquid mixtures at ambient temperatures. The paint processing industry uses Hansen solubility parameters (HSP) to indicate polymer solubility. The potential of this method to predict solvent-polymer affinity was investigated for screening potential membrane materials for the pervaporation of a model solution containing linalool and linalyl acetate (major components of lavender essential oil), in ethanol.

Published HSP values were collated for various polymers, and statistically analysed to determine variations in HSP values for polymer species. An investigation of published research into pervaporation of organic/organic binary solutions separated by homogeneous membranes indicated that the solvent whose HSP value was closest to that of the polymer would preferentially permeate. This relationship did not always hold for halogenated solvents or aqueous/organic solutions. Conflicting literature regarding the relationship between solvent uptake by polymers and HSP relative energy differences was resolved using a logarithmic relationship between these two parameters.

The following membranes were selected, using their HSP to indicate their potential to interact with lavender oil components: Polyamide (PA: 26.9 μm), Polycarbonate (PC: 20.5 μm), Poly(ether imide) (PEI: 29.2 μm), Poly(ether sulphone) (PES: 27.6 μm), Polyethylene (HDPE: 10 μm, LDPE: 13-30 μm), Polyimide (PI: 30.0 μm), Poly(methyl methacrylate) (PMMA: 50 μm), Polypropylene (PP: 15.9 μm), and Poly(tetrafluoro ethylene) (PTFE: 26.7 μm). The HSP (dispersive, polar & hydrogen bonding components) for each membrane were calculated using the mean value obtained from swelling experiments, group contribution (calculated using Hoftyzer-Van Krevelen, Hoy and Beerbower methods), refractive indices (dispersive component), dielectric constants (polar component), and published HSP values.

Pervaporation experiments investigated the effect of membrane thickness, process temperature, permeate pressure, impinging jet heights, feed flow rates and concentrations, and pre-soaking the membrane; on flow rate and selectivity in a polyethylene membrane. Membrane thickness was the dominant factor in membrane selectivity; the thinnest membranes (11.3-14.8 μm) had much poorer selectivity than membranes >24.7 μm. Temperatures between 22-34°C, permeate pressure <10 kPa, impinging jet heights between 0.36-3.36 mm, feed flow rates between 541-1328 mL/min and

concentrations between 1.78-6.01 % v/v of linalool and linalyl acetate in ethanol did not significantly affect selectivity. Flow rates increased with operating temperature, permeate pressure, and impinging jet heights. However, feed flow rate and concentration had no effect on membrane flux rate. Pre-soaking the membrane reduced the time to reach steady-state.

Selected membranes were further investigated under standard operating conditions (permeate temperature 30°C, permeate pressure <10 kPa, impinging jet height 1.36 mm, feed flow rate 804 mL/min and feed concentration of 5% v/v of linalool and linalyl acetate in ethanol). PMMA completely disintegrated in feed solution, and PC was too brittle to make an effective homogeneous membrane. PA, PC, PEI and PTFE had the highest efficiency (selectivity x flow rate) in their homogeneous form. However, PEI, PI and PTFE had the greatest selectivity, thus further trials should be done to improve stability and flow rates through these membranes.

Pervaporation selectivity did not always follow trends predicted by HSP. Although polymers such as PA, PEI, PES, and PI preferentially permeated linalool as predicted, PC, PP and PTFE did not preferentially permeate linalyl acetate. This may have been due to the difference in size and diffusivity of these molecules (linalyl acetate, the larger molecule, did not follow the sorption selectivity predictions), or reliability of literature HSP values and those calculated by group contribution.

This research shows that HSP is a good screening method for pervaporation membranes, especially where the molecules being separated are of comparable size. Polymers that have HSP close to the desired component and not to other components tend to have the best selectivity and flux characteristics. However, diffusion is an important factor, and is not completely accounted for by HSP.

Recommendations for further research include: carrying out pervaporation analyses of selected polymers using pure lavender essential oil; modifying polymers to form asymmetric or composite membranes with improved permeation characteristics; and potential use of thin channel inverse gas chromatography to determine a more accurate HSP which includes diffusivity.

Acknowledgements

I would like to take this opportunity to thank all those who have contributed to my life in the past few years and helped make this work possible.

Moral support

To my friends and family, thank you for the time, care and support you have offered as I have strived to complete this mammoth task.

Academic support

To my chief supervisor Conan Fee, thank you for walking with me on this road of learning. Thanks also to Janis Swan for her assistance in honing my writing technique, and to the technical staff; Brett Nichol, Paul Ewart, Lisa Li, Peter Jarman, Steve Hardy and Steve Newcombe who helped make my experimental work possible. Thanks also to the other staff members of the Department of Materials & Process Engineering who were there at morning and afternoon tea times to bounce ideas off, and help make the research process that much more enjoyable.

Financial support

Thanks to Dr Max Kennedy and other members of Industrial Research Ltd for obtaining FoRST funding for my project.

Thanks to Waikato Raupatu Lands Trust (Tainui Maori Trust Board) and Ngati Mahanga hapuu for the author's scholarship.

Table of Contents

List of Figures

List of Tables

Glossary

Alphabetical abbreviations

a	activity gradient
i	preferential component
j	secondary component
k	Boltzman constant
lool	Linalool
lyl	Linalyl acetate
M_r	molecular weight
n	refractive index
N	Avogadro's number
p	pressure
$^{P}\delta$	Hansen parameter for polymer.
P_p	permeate pressure
$\widetilde{P}_p$	steady-state permeate pressure
$\overline{P}_p$	average permeate pressure
P^o	vapour pressure of liquid
P_o	electric polarizability
R	gas constant
R_o	radius of interaction for the polymer
R^2	coefficient of determination
RED	relative energy difference
$^{S}\delta$	Hansen parameter for solvent.
T	absolute temperature (K)
$\widetilde{T}_f$	steady state feed temperature
$\widetilde{T}_p$	steady state permeate temperature
$\widetilde{T}_r$	steady state retentate temperature
V	molar volume (cm^3/mol)
x_p	permeate
x_f	feed

Greek abbreviations

α	selectivity or separation factor
α_S	sorption selectivity
α_D	diffusion selectivity
δ	solubility parameter
δ_a	polar interactions of the molecule ($\delta_h + \delta_p$)
δ_d	dispersion component of solubility parameter
δ_h	hydrogen bonding component of solubility parameter
δ_p	polar component of solubility parameter
δ_t	total solubility parameter ($\delta_t^2 = \delta_d^2 + \delta_p^2 + \delta_h^2$)
δ_H	Hildebrand and Scott (1950) solubility parameter
δ_v	combined the dispersion and polar components ($\delta_v = (\delta_d^2 + \delta_p^2)^{½}$)
$\Delta\delta_{(S-P)}$	distance between solute and centre of polymers solubility sphere.
ΔE_{coh}	cohesive energy of a material
ΔH	enthalpy of mixing
ΔH_{vap}	heat of vaporisation
ΔG	free energy of mixing
ΔS	entropy
ε	dielectric constant
φ_x	volume fraction
μ	chemical potential
μ	dipole moment
ρ	density

The Use of Solubility Parameters to Select Membrane Materials for Pervaporation of Organic Mixtures

THE UNIVERSITY OF
WAIKATO
Te Whare Wānanga o Waikato

A thesis submitted in partial fulfilment of the
requirements for the degree of
Doctor of Philosophy
at the University of Waikato by

Marion K. Buckley-Smith

The University of Waikato,
Hamilton, New Zealand
January 2006.

Abstract

Pevaporation is a method for separating volatile components from liquid mixtures at ambient temperatures. The paint processing industry uses Hansen solubility parameters (HSP) to indicate polymer solubility. The potential of this method to predict solvent-polymer affinity was investigated for screening potential membrane materials for the pervaporation of a model solution containing linalool and linalyl acetate (major components of lavender essential oil), in ethanol.

Published HSP values were collated for various polymers, and statistically analysed to determine variations in HSP values for polymer species. An investigation of published research into pervaporation of organic/organic binary solutions separated by homogeneous membranes indicated that the solvent whose HSP value was closest to that of the polymer would preferentially permeate. This relationship did not always hold for halogenated solvents or aqueous/organic solutions. Conflicting literature regarding the relationship between solvent uptake by polymers and HSP relative energy differences was resolved using a logarithmic relationship between these two parameters.

The following membranes were selected, using their HSP to indicate their potential to interact with lavender oil components: Polyamide (PA: 26.9 μm), Polycarbonate (PC: 20.5 μm), Poly(ether imide) (PEI: 29.2 μm), Poly(ether sulphone) (PES: 27.6 μm), Polyethylene (HDPE: 10 μm, LDPE: 13-30 μm), Polyimide (PI: 30.0 μm), Poly(methyl methacrylate) (PMMA: 50 μm), Polypropylene (PP: 15.9 μm), and Poly(tetrafluoro ethylene) (PTFE: 26.7 μm). The HSP (dispersive, polar & hydrogen bonding components) for each membrane were calculated using the mean value obtained from swelling experiments, group contribution (calculated using Hoftyzer-Van Krevelen, Hoy and Beerbower methods), refractive indices (dispersive component), dielectric constants (polar component), and published HSP values.

Pervaporation experiments investigated the effect of membrane thickness, process temperature, permeate pressure, impinging jet heights, feed flow rates and concentrations, and pre-soaking the membrane; on flow rate and selectivity in a polyethylene membrane. Membrane thickness was the dominant factor in membrane selectivity; the thinnest membranes (11.3-14.8 μm) had much poorer selectivity than membranes >24.7 μm. Temperatures between 22-34°C, permeate pressure <10 kPa, impinging jet heights between 0.36-3.36 mm, feed flow rates between 541-1328 mL/min and

concentrations between 1.78-6.01 % v/v of linalool and linalyl acetate in ethanol did not significantly affect selectivity. Flow rates increased with operating temperature, permeate pressure, and impinging jet heights. However, feed flow rate and concentration had no effect on membrane flux rate. Pre-soaking the membrane reduced the time to reach steady-state.

Selected membranes were further investigated under standard operating conditions (permeate temperature 30°C, permeate pressure <10 kPa, impinging jet height 1.36 mm, feed flow rate 804 mL/min and feed concentration of 5% v/v of linalool and linalyl acetate in ethanol). PMMA completely disintegrated in feed solution, and PC was too brittle to make an effective homogeneous membrane. PA, PC, PEI and PTFE had the highest efficiency (selectivity x flow rate) in their homogeneous form. However, PEI, PI and PTFE had the greatest selectivity, thus further trials should be done to improve stability and flow rates through these membranes.

Pervaporation selectivity did not always follow trends predicted by HSP. Although polymers such as PA, PEI, PES, and PI preferentially permeated linalool as predicted, PC, PP and PTFE did not preferentially permeate linalyl acetate. This may have been due to the difference in size and diffusivity of these molecules (linalyl acetate, the larger molecule, did not follow the sorption selectivity predictions), or reliability of literature HSP values and those calculated by group contribution.

This research shows that HSP is a good screening method for pervaporation membranes, especially where the molecules being separated are of comparable size. Polymers that have HSP close to the desired component and not to other components tend to have the best selectivity and flux characteristics. However, diffusion is an important factor, and is not completely accounted for by HSP.

Recommendations for further research include: carrying out pervaporation analyses of selected polymers using pure lavender essential oil; modifying polymers to form asymmetric or composite membranes with improved permeation characteristics; and potential use of thin channel inverse gas chromatography to determine a more accurate HSP which includes diffusivity.

Acknowledgements

I would like to take this opportunity to thank all those who have contributed to my life in the past few years and helped make this work possible.

Moral support

To my friends and family, thank you for the time, care and support you have offered as I have strived to complete this mammoth task.

Academic support

To my chief supervisor Conan Fee, thank you for walking with me on this road of learning. Thanks also to Janis Swan for her assistance in honing my writing technique, and to the technical staff; Brett Nichol, Paul Ewart, Lisa Li, Peter Jarman, Steve Hardy and Steve Newcombe who helped make my experimental work possible. Thanks also to the other staff members of the Department of Materials & Process Engineering who were there at morning and afternoon tea times to bounce ideas off, and help make the research process that much more enjoyable.

Financial support

Thanks to Dr Max Kennedy and other members of Industrial Research Ltd for obtaining FoRST funding for my project.

Thanks to Waikato Raupatu Lands Trust (Tainui Maori Trust Board) and Ngati Mahanga hapuu for the author's scholarship.

Table of Contents

List of Figures

List of Tables

Glossary

Alphabetical abbreviations

a	activity gradient
i	preferential component
j	secondary component
k	Boltzman constant
lool	Linalool
lyl	Linalyl acetate
M_r	molecular weight
n	refractive index
N	Avogadro's number
p	pressure
$^{P}\delta$	Hansen parameter for polymer.
P_p	permeate pressure
$\widetilde{P}_p$	steady-state permeate pressure
$\overline{P}_p$	average permeate pressure
P^o	vapour pressure of liquid
P_o	electric polarizability
R	gas constant
R_o	radius of interaction for the polymer
R^2	coefficient of determination
RED	relative energy difference
$^{S}\delta$	Hansen parameter for solvent.
T	absolute temperature (K)
$\widetilde{T}_f$	steady state feed temperature
$\widetilde{T}_p$	steady state permeate temperature
$\widetilde{T}_r$	steady state retentate temperature
V	molar volume (cm^3/mol)
x_p	permeate
x_f	feed

Greek abbreviations

α	selectivity or separation factor
α_S	sorption selectivity
α_D	diffusion selectivity
δ	solubility parameter
δ_a	polar interactions of the molecule ($\delta_h + \delta_p$)
δ_d	dispersion component of solubility parameter
δ_h	hydrogen bonding component of solubility parameter
δ_p	polar component of solubility parameter
δ_t	total solubility parameter ($\delta_t^2 = \delta_d^2 + \delta_p^2 + \delta_h^2$)
δ_H	Hildebrand and Scott (1950) solubility parameter
δ_v	combined the dispersion and polar components ($\delta_v = (\delta_d^2 + \delta_p^2)^{½}$)
$\Delta\delta_{(S-P)}$	distance between solute and centre of polymers solubility sphere.
ΔE_{coh}	cohesive energy of a material
ΔH	enthalpy of mixing
ΔH_{vap}	heat of vaporisation
ΔG	free energy of mixing
ΔS	entropy
ε	dielectric constant
φ_x	volume fraction
μ	chemical potential
μ	dipole moment
ρ	density

Polymer abbreviations

ABS	Acrylonitrile - butadiene - styrene copolymer
CA	Cellulose acetate
CAB	Cellulose acetobutyrate
CBR	Chloro-butadiene rubber
CN	Cellulose nitrate
CPN	Cellophane
CTFE	Poly(chloro-trifluoro ethylene)
CTP	Cellulose tripropionate
E-CTFE	Ethylene-Chloro-trifluoro ethylene copolymer
FEP	Fluorinated Ethylene Propylene Copolymer
HDPE	High density polyethylene
HSP	Hansen solubility parameter
LDPE	Low density polyethylene
NBR	Acrylonitrile - butadiene rubber
NR	Natural rubber
PA	Nylon (polyamide)
PA 6,6	Polyamide 6,6
PA 11	Polyamide 11
PA 12	Polyamide 12
PBT	Poly(butylene terephthalate)
PC	Polycarbonate
PE	Polyethylene
PEI	Poly(ether imide)
PES	Poly(ether sulphone)
PET(P)	Poly(ethylene terephthalate) (polyester)
PF(A)	Phenol formaldehyde resin
PI	Polyimide
PMMA	Poly(methyl methacrylate)
POM	Polyoxymethylene – Homopolymer (Acetal – Homopolymer)
PP	Polypropylene
PPO	Polyphenyleneoxide
PPS	Poly(phenylene sulphide)
PS	Polystyrene (also STY)
PSU	Polysulphone
PTFE	Teflon (polytetrafluoro ethylene)
PUR	Polyurethane
PVA	Poly(vinyl alcohol)
PVAC	Poly(vinyl acetate)
PVC	Poly(vinyl chloride)
PVDC	Poly(vinylidene chloride)
PVDF	Poly(vinylidene fluoride)
STY	Polystyrene
Sty-AA	Poly(styrene acrylic acid)
TPX	Poly(methyl pentene)

Chapter

1

Introduction

1.1 Membrane separations

A membrane is a physical barrier separating two phases that selectively restricts transport of chemical species (Srikanth, 2000). Membranes used in separation processes divide an influent stream into two streams called the permeate (fluid that passes through the semi-permeable membrane) and retentate, which contains constituents rejected by the membrane (Srikanth, 2000). Membrane selectivity can be based on characteristics such as differences in size, shape, electrical charge, concentration, partial pressure, or solubility in the membrane (Peng, 2004).

Common membrane processes include micro-filtration (MF), ultra-filtration (UF), reverse osmosis (RO), electro-dialysis (ED), gas separation (GS), nano-filtration (NF), and pervaporation (PV). Pervaporation separates non-particulate liquids, and differs from other membrane separation techniques, due to a phase change occurring (Hickey *et al.*, 1992).

1.1.1 Pervaporation

The term pervaporation is derived from the words permeation and evaporation (Bowen, 2003), which are the primary mechanisms in this process. The basic PV system has a membrane module, a feed delivery system, and a permeate condensation/recovery system (Peng, 2004). A PV membrane is usually a synthetic polymer film, and components of a liquid feed first dissolve in the membrane and then diffuse across a concentration gradient. A vacuum is usually maintained on the downstream side, removing all molecules migrating to this stream (Shao, 2003).

The main advantage of PV is that it uses much less energy than other phase-change separations such as distillation, due to the highly selective permeation mechanism (solution diffusion) (Shao, 2003). PV systems do not have emission problems or require expensive regeneration steps. They can operate continuously without consuming sorbents, can be used to recycle/re-use solvents, and cost less to operate than many other applications (Bowen, 2003; Peng, 2004). PV has the additional advantages of flexible, compact modular design, ideal for variable feed and product compositions. This is advantageous when producing fine chemicals and pharmaceuticals, where several solvents are used in processing, and when waste streams vary significantly from batch to batch (Drioli and Romano, 2001).

The most attractive features of PV include its capability for separating azeotropic, close-boiling, and heat-sensitive mixtures. Unlike distillation, where separation is based on the boiling point differences of the components, PV does not require such high temperatures and can be run at room temperature. PV is based on the sorption and diffusion properties of the feed components and membrane permselectivity (Villaluenga and Tabe-Mohammadi, 2000).

1.1.2 Pervaporation applications

There are three common applications of pervaporation (Koops and Smolders, 1991; Feng and Huang, 1997):

- Dehydrating organic solvents using hydrophilic membranes (i.e., water-alcohol, -ethers, -ketones, -carboxylic acids),
- Removing organic compounds from aqueous solutions using hydrophobic membranes (i.e., water-chlorinated hydrocarbons, -phenol), and
- Separating anhydrous organic mixtures using organo-selective membranes (i.e., MTBE/methanol).

These categories are detailed in Figure 1:01. The dehydration of organic solvents such as ethanol is the best developed pervaporation process, followed closely by waste-water treatment; organic-organic separations are a distant third.

Components in organic-organic liquid mixtures have very similar physicochemical properties, and are considered more difficult to separate than aqueous-organic mixtures. Consequently, it can be difficult to find a membrane that demonstrates adequate preferential affinity for one component in an organic-organic mixture.

As well as common PV applications (Figure 1:01), PV of organic liquid mixtures has significant potential value in the natural extracts and synthetic chemicals industries. Recently there has been increased use of natural flavour and fragrance compounds in many household products (Runham, 1996), mainly because animal and synthetic extracts have such a poor image. This is due partly to reports about bovine spongiform encephalitis (BSE) (Aburjai and Natsheh, 2003) and a widespread mistrust of synthetic chemicals as food additives, because they may contain impurities from the reaction process (Clark, 1988).

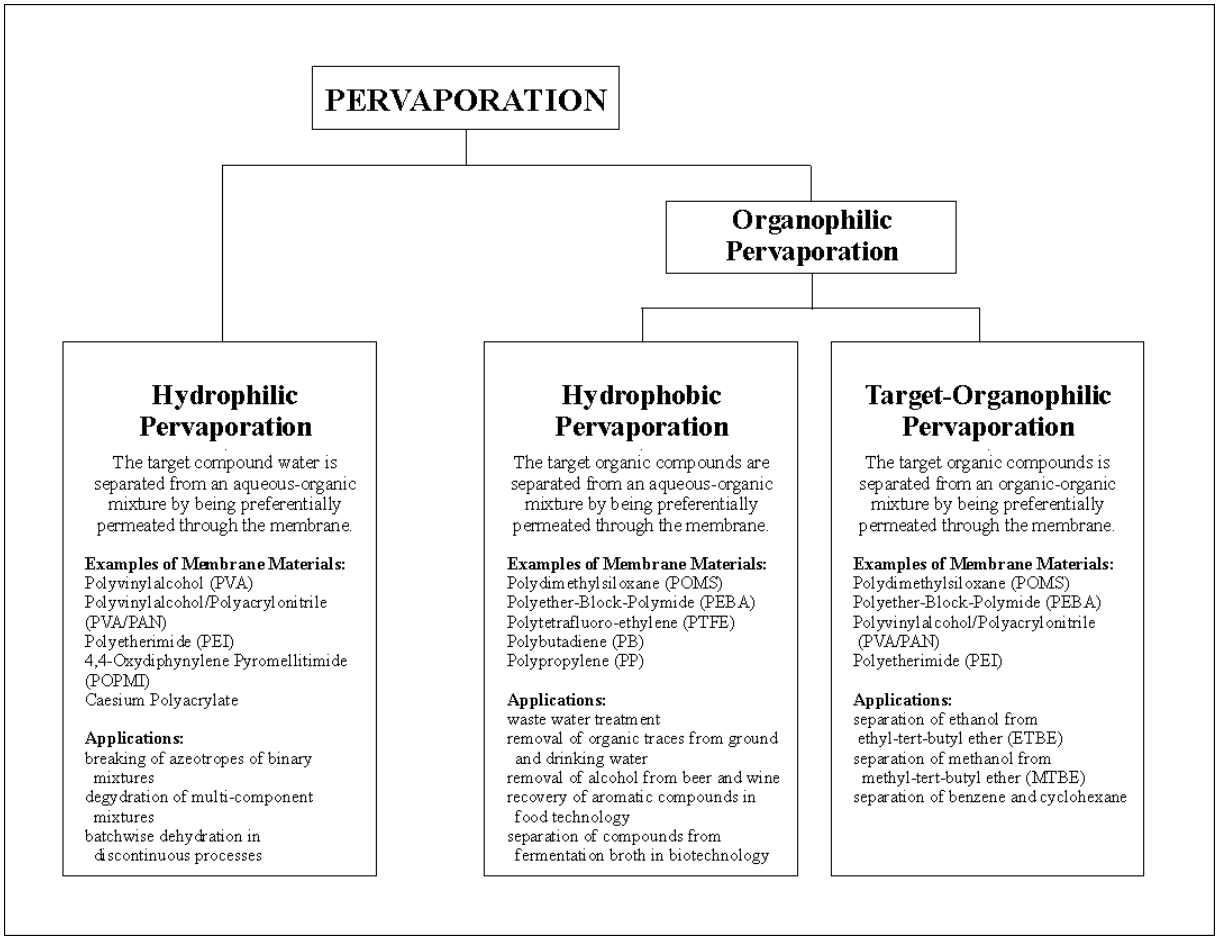

Figure 1:01 Pervaporation research: membranes and applications (Lipnizki et al., 1999).

The potential uses for PV in the natural products industries could include post-extraction processing or "folding" of essential oils to reach industry standards for desirable chemotypes (Bienvenu, 1995), and enrichment or extraction of valuable pharmaceutical products from essential oils (Akgün *et al.*, 2000). As with many natural extracts, essential oils contain thermo-labile components that can degrade under high temperature processing conditions, making PV an ideal alternative to conventional separation techniques such as distillation.

Essential oils and plant extracts are being used in an ever-increasing array of products including: food flavourings in alcoholic and non-alcoholic beverages, frozen desserts, baked goods, meat and meat products (Mastelic *et al.*, 2000); fragrance, perfumery and cosmetics products such as toiletries (including personal care products, fine fragrances, skincare, bath products, deodorants, hair products, etc.), and household products (including air fresheners, laundry products, liquid detergents, surface cleaners and disinfectants) (Clark, 1988; Aburjai and Natsheh, 2003). Other uses include pharmaceuticals (Akgün *et al.*, 2000), herbal

products, antioxidants, aromatherapy, natural insecticides, pesticides, and sprout suppressants (Bienvenu, 1995; Runham, 1996; Al-Amier *et al.*, 1999).

1.2 Aims of the thesis

Materials used for pervaporation membranes are typically found by trial and error because there are no well-established predictive criteria for their selection (Feng and Huang, 1997). A membrane selection method needs to be quick, easy, reproducible and valid for separating a variety of organic liquid mixtures. This thesis uses Hansen solubility parameters (HSP) to select membrane materials. As well as satisfying the above criteria, HSP quantifies the physicochemical properties of polymer and solution components, which can then be linked to sorption and diffusion occurring during membrane permeation. For components of comparable size and mass, selective permeation is governed mainly by differences in components sorption onto the membrane, which depends on the degree of solute-polymer interaction (Ray *et al.*, 1997). Polymers with high selectivity should be chosen because it is easier to increase flux than to increase selectivity (Koops and Smolders, 1991).

The primary objective of this thesis was to find a suitable method to select membrane materials for pervaporation of organic liquid mixtures, and to validate this method by investigating membrane performance when fractionating a model organic liquid mixture.

1.3 Scope

Common methods used in selecting pervaporation membranes include, Hansen solubility parameters, surface thermodynamics, gas-liquid chromatography, contact angle, polarity parameter (Feng and Huang, 1997), sorption equilibrium methods (Ferreira *et al.*, 2001), and gas chromatography retention data (Roberts *et al.*, 2000). Three methods which consider membrane selection from different angles were chosen for preliminary study: Hansen solubility parameters, inverse gas chromatography (I-GC), and solvatochromic polarity parameters. The HSP method uses a theoretical and predictive view, whilst the I-GC and solvatochromic methods determine polymer-solvent interaction in the vapour and liquid phases respectively. Surface thermodynamics and polarity parameters can be predicted by HSP, but there is limited retention data (I-GC) for the polymers typically used in membranes, plus I-GC and solvatochromic methods require potential polymers to be individually

evaluated and have limited scope for predicting the pervaporative selectivity of novel membrane materials.

This study was limited to commercially available homogeneous polymer films approximately 25 μm thick (range: 10-30 μm). The model organic liquid mixture was based on the major components of lavender essential oil *Lavandula angustifolia* (Bienvenu, 1995) primarily because of its low toxicity, is readily available, and contains a range of molecules (alcohol, acetate, ketone, alkene, etc.) with differing physicochemical properties. The PV process variables studied included feed composition and concentration, feed and permeate temperatures, turbulence over membrane surfaces, downstream pressures, membrane type, thickness and swelling, and membrane concentration polarization or fouling.

The cost of high purity organic solution components such as linalool and linalyl acetate limited feed composition and concentrations that could be used. Thus, these organics were diluted in ethanol and concentration trials were restricted to the range 2-10% solutions under normal PV conditions.

1.4 Development of hypotheses

Initial hypotheses on PV membrane selection procedures were formed primarily from preliminary readings, especially the review article published by Feng and Huang (1997). Preliminary investigations into HSP, I-GC, and solvatochromic polarity parameters identified that the latter two methods lacked predictive ability, which limited their usefulness in selecting innovative membranes for separating novel organic liquid mixtures.

The primary hypothesis of this thesis was to determine whether HSP was a suitable method for selecting membrane materials for pervaporative fractionation of a model organic liquid mixture made from essential oil components. The secondary hypothesis was to determine whether feed concentration, temperature, turbulence over membrane surfaces, downstream pressure, membrane thickness and swelling, and membrane material composition significantly affected PV of the model organic liquid mixture.

1.5 Overview of thesis

Chapter 2 begins with a brief historical review of PV and then describes current theory and practice. Later sections discuss membrane selection procedures, including a detailed summary of literature on Hansen solubility parameters.

Chapter 3 investigates the ability of Hansen solubility parameters to predict preferential permeation of PV mixtures found in the literature, and the capability of selecting appropriate membranes for organic/organic PV by relating HSP values to PV performance. This chapter also shows methods for calculating HSP and selection of membrane materials.

Experimental method for organic/organic PV separations are given in Chapter 4. Chapter 5 discusses the data obtained, and the conclusions and recommendations are given in Chapter 6.

Chapter 2

Literature Review

2.1 Pervaporation

In Pervaporation (PV), components of a volatile liquid feed will permeate through a non-porous permselective membrane and evaporate into the permeate space (Figure 2:01). The feed components undergo a phase change, making PV a unique membrane processes (Néel, 1991; Villaluenga and Tabe-Mohammadi, 2000).

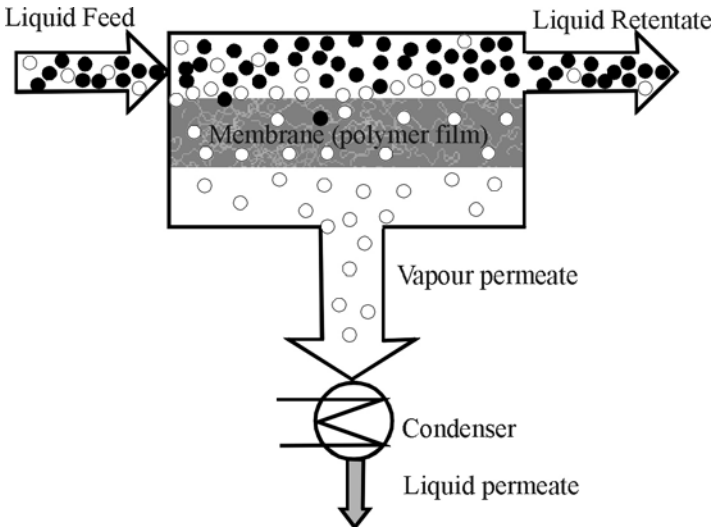

Figure 2:01 The pervaporation process (Schleiffelder and Claudia, 2001).

Liquid feed flows along one side of the membrane and various feed components selectively permeate into and through the membrane. In laboratory-scale batch-PV, liquid retentate is returned to the feed tank, depleted in preferentially permeating components. The enriched permeate vapour is swept from the membranes downstream surface under vacuum conditions or by an inert sweep gas, and is collected in a condenser (Feng and Huang, 1997; Schleiffelder and Claudia, 2001).

2.1.1 Origins of pervaporation

The PV technique was first described in 1917 when Kober was dialysing and noticed liquid evaporated through a tightly closed collodion bag suspended in air (Kober, 1917; Karlsson and Trägårdh, 1994). Farber (1935) recognised that PV had potential for separating and concentrating protein and enzyme solutions, and used cellophane to concentrate very dilute protein solutions, simultaneously removing salts, glycerol and water.

The first known quantitative work on PV (Heisler *et al.*, 1956) separated a 50% v/v water/ethanol mixture in a cellophane bag suspended in a forced-draft oven at 45°C. Heisler *et al.* obtained a flux rate of 0.206 g/cm^2.hr (1.33 g/in^2.hr), and increased the water content in the permeate vapour to 66%. These researchers also separated benzoic acid, hydroquinone and citric acid from aqueous solutions.

A group in the petrochemical industry published the first literature on PV of organic/organic mixtures containing C_{6-9} alkanes, C_{6-7} alkenes, and C_6 (di)methyl-alkanes. Binning *et al.* (1958; 1961; 1962) laid the foundations for PV research and highlighted the potential for commercial processing of organic chemicals and hydrocarbons.

2.1.2 Primary applications

Pervaporation separation can be classified into three major fields: dehydrating aqueous–organic mixtures (Rapin, 1988; Deng *et al.*, 1991); removing trace volatile organic compounds from aqueous solution (Voilley *et al.*, 1988; Bengtsson *et al.*, 1989); and separating organic-organic (anhydrous) solvent mixtures (Cabasso *et al.*, 1974b; Feng and Huang, 1997). PV is especially suited for separating volatile organic compounds (Smitha *et al.*, 2004), so most of the recent PV research focuses on aqueous solutions.

Separating organic-organic mixtures using membranes has been extensively investigated over the past 40 or so years in an effort to find alternative separation processes for the fine-chemical and petrochemical industries. PV is a promising alternative to conventional energy-intensive technologies such as extractive or azeotropic distillation because it is economical, safe and 'clean' technology (Smitha *et al.*, 2004). PV is considered a basic unit operation for separating organic-organic liquid mixtures because it efficiently separates azeotropic and close-boiling mixtures, isomers and heat-sensitive compounds (Michaels *et al.*, 1962; Mulder *et al.*, 1982; Feng and Huang, 1997; Smitha *et al.*, 2004). Membranes for PV separation of the four major categories of organic-organic mixtures (Figure 2:02), can be organic and/or inorganic in nature (Smitha *et al.*, 2004).

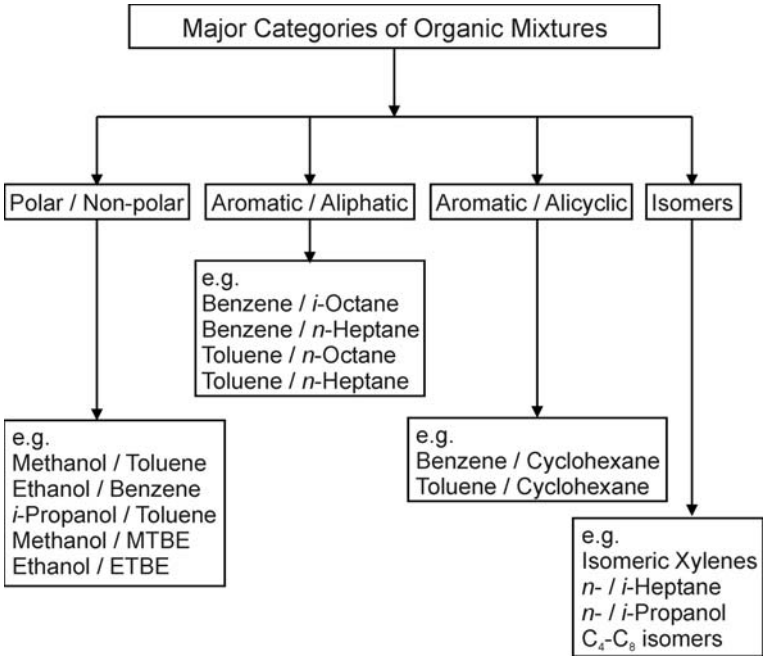

Figure 2:02 Classification of organic-organic pervaporation separation (Smitha *et al.*, 2004).

2.1.3 Alternative techniques

The requirements for technological or economic operation of the most common processing techniques for separating organic-organic mixtures are given in Table 2:01. Separating close-boiling organic-organic solvent mixtures by distillation or liquid-liquid extraction is difficult, as the components have very similar physical and chemical properties (Young, 1973).

Table 2:01 Processes for aromatic recovery (Villaluenga and Tabe-Mohammadi, 2000; Porter, 2001).

Process	Requirements for basic or economical operation
Azeotropic distillation	Requires high aromatic content (>90%)
Extractive distillation	Requires medium aromatic content (65–90%)
Liquid-liquid extraction	Requires low aromatic content (20–65%)
Crystallization	Distillative pre-separation (e.g., o-xylene and ethylbenzene separated from C_8 aromatic fractions)
Adsorption on solids	Continuous, reversible and selective adsorption

Because PV is based on sorption and diffusion properties of the feed components and membrane permselectivity rather than relative volatility, this process is especially attractive for azeotropes and close boiling point mixtures. For example, separating benzene (Bz) and cyclohexane (cHx) is a common and challenging process in the chemical industry, as there is only a 0.6°C difference in boiling points, and an azeotrope forms at 45% v/v cyclohexane. Conventional distillation produces a low purity product (85–98%), so azeotropic distillation

and extractive distillation are commonly used. However, these processes require addition of a third component, which increases the process complexity and cost (Villaluenga and Tabe-Mohammadi, 2000).

Adsorption is primarily used for aqueous-organic separations. However, PV is a better process when the organic components concentration is relatively high. The organic can be removed continuously so the process is not limited by adsorber capacity (Shao, 2003).

Systems combining PV membranes with traditional techniques (e.g., PV/distillation) have been used (Ishida and Nakagawa, 1985; Hömmerich and Rautenbach, 1998; Ferreira *et al.*, 2002). However, membrane performance is still the key factor limiting PV efficiency (Smitha *et al.*, 2004).

Essential oil folding

Raw essential oils such as cold-pressed citrus peel oils contain 89-98% terpene hydrocarbons, which oxidize easily and cause cloudiness in aqueous systems. The composition of such oils is usually altered via folding, a term used in the flavour industry to describe concentration of an essential oil. For example, reducing the volume to one-fifth produces a five-fold distillate. After folding, oils are enriched in the more desirable oxygenated components (aldehydes, alcohols, esters). Citrus peel oils produced by centrifugation during mechanical juice extraction, have a low aldehyde, alcohol and ester content and a high unstable terpene hydrocarbon content, and these typically sell for US$2.50–25/kg. In comparison, folded citrus essential oils with 5-95% oxygenates can sell for US$22–990/kg (Auerbach, 1995; Lotus Oils, 2005).

Essential oil folding is done primarily by vacuum distillation, or less commonly by solvent extraction (ethanol or CO_2). Such products may be thermally stressed, contain solvent residues, undesirable component ratios, or be too expensive. Terpenes can be removed from essential oils by adsorbing oxygenates onto a polar particulate solid followed by supercritical CO_2 or β-cyclodextrin extraction. However, these batch processes have limited terpene removal potential. PV is a low-temperature, solvent-free operation, with reduced oxidative degradation and controllable selectivity. It offers the perfumer or flavourist an entirely new product, with improved organoleptic properties (Auerbach, 1995).

2.1.4 Industrial applications

Separating purely organic mixtures by PV is a key challenge for industry (Jonquières *et al.*, 2002) and represents the least-developed application with the largest potential commercial impact (Drioli and Romano, 2001). Between 1984 when Gesellschaft für Trenntechnik (GFT) Co. produced the first commercial PV system, and 1996, over 63 industrial PV systems with capacities ranging from 1000 to 150,000 L/day (Figure 2:03) were commercialised (Roizard *et al.*, 1999; Drioli and Romano, 2001; Jonquières *et al.*, 2002). Twenty two units were for ethanol dehydration, 16 for iso-propanol dehydration and 12 were multi-functional units for organic solvent processing. A single non-dehydration unit recovers and recycles tetrachloroethylene in a dry-cleaning plant (Jonquières *et al.*, 2002).

(a)  (b) 

Figure 2:03 Typical pervaporation plants with a capacity of (a) a few kg per hour to (b) thousands of tonnes per year (Sulzer ChemTech, 2005).

Organophilic membranes have been developed more recently to remove organics from aqueous or gaseous effluents. Despite promising research on aroma recovery (Voilley *et al.*, 1988; Böddeker and Bengtson, 1990), there are few reports on using organophilic membranes for industrial PV of aqueous-organic mixtures, despite PV having low operating temperatures and minimal degradation of the high-value components (Smitha *et al.*, 2004).

Recent reviews of PV do not give any industrial applications for organic-organic separations (Johnson and Thomas, 1999; Villaluenga *et al.*, 2003). The first example of a large-scale application of PV for a purely organic mixture was for production of an octane enhancer for fuel blends (Chen *et al.*, 1989). Air Products and Chemicals, Inc. (PA, USA) used PV to separate methanol from methyl tert-butyl ether (MTBE) (Figure 2:04), in a skid-mounted

demonstration unit (Chen *et al.*, 1989; Kim *et al.*, 2000; Drioli and Romano, 2001; Smitha *et al.*, 2004).

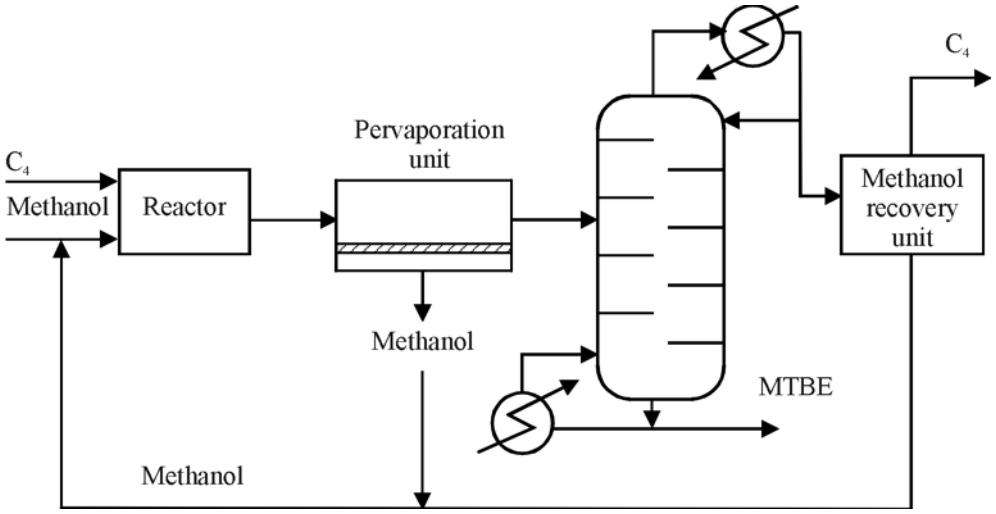

Figure 2:04 Pervaporation-enhanced MTBE production (Drioli and Romano, 2001).

GFT (now Sulzer Chemtech) commercialised a similar process using PV to synthesise 8.5 t/day of methyl ester while continuously removing methanol (Jonquières *et al.*, 2002). Membranes used in this application were developed to extract alcohols from alcohol / ether / hydrocarbon mixtures for purifying ethyl tert-butyl ether (ETBE), another fuel octane enhancer. A pilot scale hybrid distillation/PV process at the French Petroleum Institute gave 10-30% energy savings over the traditional method for purifying ETBE, and enabled commercialisation of the first organoselective membranes (PERVAP® 2256 1 and PERVAP® 2256 2), which are currently produced by Sulzer Chemtech for removing methanol or ethanol from purely organic mixtures (Roizard *et al.*, 1999; Jonquières *et al.*, 2002).

A Texaco-sponsored process analysis showed PV could be used to purify dimethyl carbonate, which forms an azeotrope containing almost 70 wt.% methanol (Shah and Bartels, 1991). Coupling PV with distillation broke the azeotrope and the subsequent mixture was injected onto a lower distillation plate. This hybrid process substantially reduced capital and operating costs. Although membrane replacement costs are significant, operating costs are only 40% that of conventional azeotropic distillation, mainly because the process pressure required are lower (Jonquières *et al.*, 2002).

Many researchers state that commercial application of organic-organic PV is limited by the lack of a range of stable, high-performance membranes (Johnson and Thomas, 1999; Cunha *et al.*, 2002; Villaluenga *et al.*, 2003). The primary problems needing to be solved are

degradation of membrane performance and loss of membrane integrity due to swelling (Yoshida and Cohen, 2003). Improved membrane stability under relatively harsh conditions (Feng and Huang, 1997) are most likely to be solved by synthesising new polymers, modifying existing polymers, and polymer blending (Johnson and Thomas, 1999).

2.1.5 Industrial patents

A patent search can help evaluate a process' potential for industrial growth and commercial importance (Smitha *et al.*, 2004). The number of registered European and USA/Canadian PV related patents peaked in the early 1990s (Figure 2:05). Jonquières *et al.* (2002) provide a detailed list of patents.

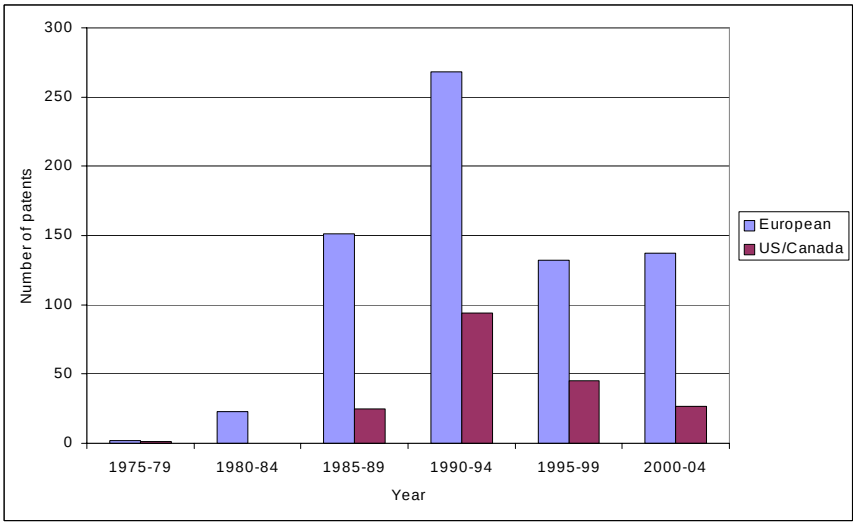

Figure 2:05 Patents associated with pervaporation (CIPO, 2005; EPO, 2005; USPTO, 2005).

These patents fall into four aspects of membrane separation processes; process development, module development, membrane development and separation applications (Jonquières *et al.*, 2002). European researchers focussed relatively evenly on all four aspects but American researchers worked mainly on separation applications (Figure 2:06). The present research falls into the membrane development category.

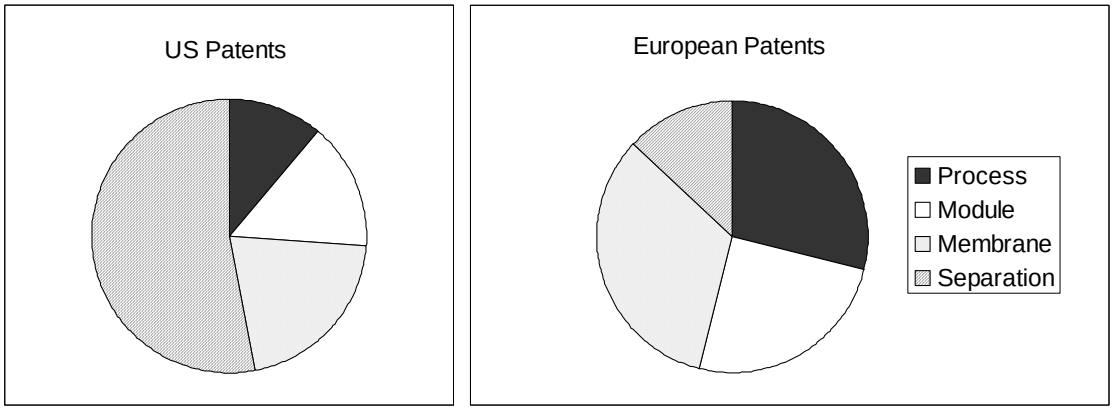

Figure 2:06 Different fields developed in pervaporation depicted by European/US patents (Jonquières *et al.*, 2002; Smitha *et al.*, 2004).

Several industrial companies (e.g. Texaco, Hoechst, etc.) active in developing PV in 1990–1995 have stopped their research, citing the great difficulty in profitably industrialising and commercialising PV processes (Jonquières *et al.*, 2002).

2.2 Pervaporation theory

Polymer films used in PV have a nonporous selective layer, and do not function by a molecular sieving action or convective flow. Binning *et al.* (1961) were the first to use the "solution-diffusion" model to describe PV through a homogenous polymeric membrane. Overall mass transport through the membrane can be represented by three steps:

- Solution of liquid in the membrane surface in contact with the liquid charge mixture;
- Migration (diffusion) through the body of the membrane ;
- Vaporization of the permeating material at the downstream interface where permeate is immediately swept away.

2.2.1 Solution-diffusion model

The solution-diffusion model is a semi-empirical or phenomenological model originally developed by Graham in 1866 to describe gas permeation through rubber septa. This model is also used for reverse osmosis, gas separation and PV (Lipnizki *et al.*, 1999).

A component's sorption rate is related to the total energy required to dissolve it in the polymer. The component with the lowest energy requirement is preferentially sorbed into the membrane polymer. Migration through the membrane depends on feed components,

membrane polymer and process parameters. Typical chemical potential (μ), pressure (p), and activity gradient (a) profiles through a membrane (Figure 2:07) show that pressure change from feed to permeate has a negligible effect on mass transfer (Lipnizki *et al.*, 1999).

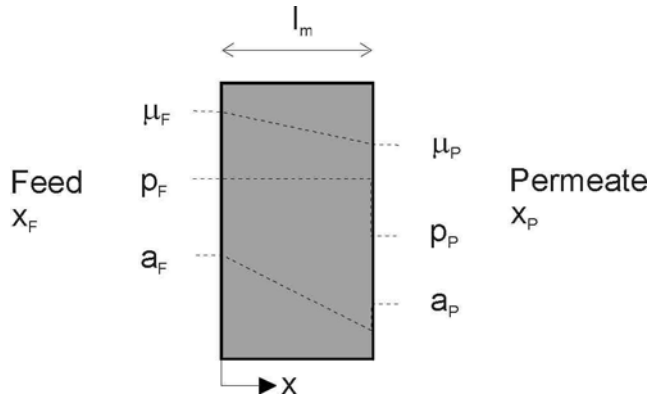

Figure 2:07 Schematic diagram of the solution-diffusion model (Lipnizki *et al.*, 1999).

Transport parameters will depend on whether the retentate is liquid or gaseous. In liquid permeation, the permeating liquid can dissolve in the polymer membrane to give a swollen "solution" of polymer and permeating organic compounds. However, a "dry" membrane exists in gas permeation. Permeation rate in liquid permeation is independent of the pressure differential across the membrane because of the large concentration gradient. However, liquid and gas permeation both follow Fick's first law of diffusion, where the steady-state rate is inversely proportional to membrane thickness (Binning *et al.*, 1961).

$$q = \frac{D(C_2 - C_1)}{L} \qquad \text{(Eqn. 2:1)}$$

where q is the amount of liquid permeating a unit area of membrane in unit time, L is membrane thickness, D is diffusion coefficient and $C_2 - C_1$ is concentration differential across the membrane.

Binning *et al.* (1961) proposed that a “solution phase zone” exists in PV. The “solution phase zone” makes up the major portion of the membrane film, plus a smaller “vapour phase zone”, where the permeating material is vaporising (Figure 2:08). Binning *et al.* (1961) theorised that liquid moves rapidly within the solution phase, and between the liquid feed phase and the solution phase; with most of the selectivity occurring at the interface between the solution phase and the vapour phase. The permeating species slowly diffuses through the vapour phase and is the rate-controlling step in the process. Because selectivity is not a function of

membrane thickness, some researchers suggest that the unswollen fraction of the skin layer (vapour phase) controls permselectivity (Binning *et al.* 1961, 1974; Néel, 1991).

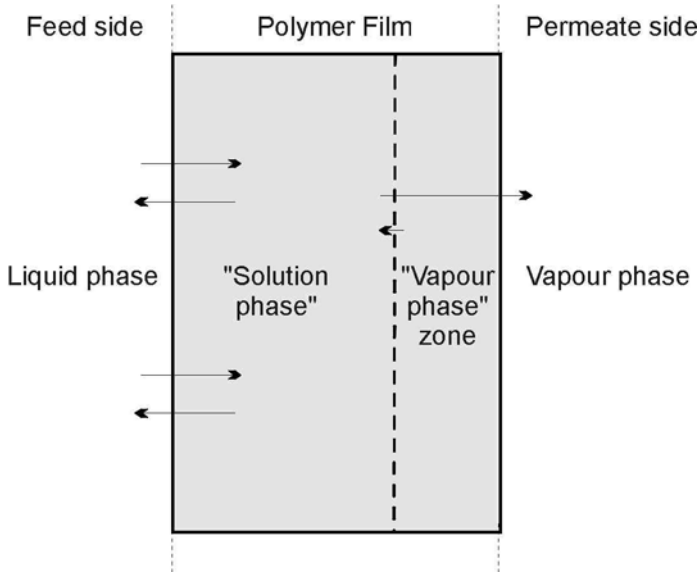

Figure 2:08 Polymer membrane under liquid permeation conditions with a solution phase zone and vapour phase zone (Binning *et al.*, 1961).

2.2.2 Driving force

A difference in chemical potential (due to partial pressure or activity) between feed and permeate side of the membrane is the driving force in PV (Lipnizki *et al.*, 1999). Feed components have different sorption and diffusion rates through the membrane, which govern selectivity and permeation rate (Qariouh *et al.*, 1999; Villaluenga and Tabe-Mohammadi, 2000).

2.2.3 Selectivity

Selectivity (or separation factor, α) can be used to express the separation capability of a PV membrane for a binary mixture of components *i* and *j* (Smitha *et al.*, 2004). Overall selectivity is the product of sorption selectivity, α_S, and diffusion selectivity, α_D (Villaluenga and Tabe-Mohammadi, 2000):

$$\alpha_{ij} = \frac{x_{p,i} / x_{p,j}}{x_{f,i} / x_{f,j}} = \alpha_D * \alpha_S \qquad \text{(Eqn. 2:2)}$$

where $x_{p,i}$ and $x_{p,j}$ are mole fractions of the preferential and secondary permeants respectively in the permeate, and $x_{f,i}$ and $x_{f,j}$ are the corresponding mole fractions in the feed.

Selectivity can vary from unity (no selective permeation) to infinity, and is affected by membrane/component solubility, feed hydrodynamic conditions, permeate resistance due to elevated partial pressures, and changes in diffusion rate due to membrane swelling (Smitha *et al.*, 2004). Membrane selectivity (especially in organic/organic separations with components of comparable size) is mainly governed by α_S due to the chemical interaction between permeant molecules and the membrane. Therefore, choosing a membrane with appropriate affinity is a crucial factor in PV (Villaluenga and Tabe-Mohammadi, 2000).

2.2.4 Membrane affinity

A polymer with higher affinity for one feed component gives greater selectivity. However, if the affinity is too high, the membrane is excessively swollen by the component, loses its integrity and therefore its selectivity. Consequently, it is important to suppress or control the degree of swelling by crosslinking or other methods (Villaluenga and Tabe-Mohammadi, 2000).

The effects of α_S and α_D on benzene and cyclohexane separations have been studied extensively (Inui *et al.*, 1998a; Uragami *et al.*, 1998; Villaluenga and Tabe-Mohammadi, 2000; Wang *et al.*, 2000; Ren *et al.*, 2001; Kao *et al.*, 2002). Benzene's smaller size, collision diameter, and planar shape, are believed to enhance its diffusivity (Table 2:02). There are contradictory views on whether α_S or α_D dominates overall PV selectivity, based largely on the molecules and membranes involved. Huang and Lin (1968) reported that permeation and separation of benzene/cyclohexane was significantly influenced by their molecular size. Inui *et al.* (1997b) showed that membrane selectivity of aromatic/cyclohexane mixtures decreased with increasing molecular size of aromatic hydrocarbons.

However, most experimental evidence indicates that benzene/cyclohexane separation is governed mainly by sorption selectivity due to chemical interaction between benzene molecules and the membrane (Tanihara *et al.*, 1994; Sun and Ruckenstein, 1995; Inui *et al.*, 1997a; Yamasaki *et al.*, 1997; Inui *et al.*, 1998b; Wang *et al.*, 1998). The hydrogen bonding component (δ_H) of benzene HSP is stronger than that of cyclohexane (Table 2:02), allowing greater interaction with free polar groups in a membrane (Villaluenga and Tabe-Mohammadi, 2000).

Table 2:02 Molar volume, collision diameter, and solubility parameter of organic components (Villaluenga and Tabe-Mohammadi, 2000).

Solvent	Molar volume (cm^3/mol)	Collision diameter (nm)	Solubility parameters ($MPa^{½}$)			
			δ_D	δ_P	δ_H	δ_{Total}
Benzene	89.4	0.526	18.4	0.0	2.0	18.6
Cyclohexane	108.7	0.606	16.8	0.0	0.2	16.8

Yamasaki *et al.* (1997) found that retention time of organics in a column containing Poly(vinyl alcohol) (PVA) was 1.5x longer for benzene than for *n*-hexane and cyclohexane, due to the stronger interaction between benzene and PVA. Tanihara *et al.* (1994) showed that the α_S did not affect overall membrane selectivity. Sun and Ruckenstein (1995) showed that swelling of different membranes was mainly due to sorption of benzene rather than cyclohexane.

It appears that when a liquid mixture contains molecules of very different sizes, then α_D dominates, and when they are similar sized, α_S dominates. Because benzene and cyclohexane have similar sizes (Table 2:02), chemical affinity is a more appropriate factor to use for membrane selection. Ideal membranes for separating an organic-organic mixture such as benzene/cyclohexane, need polar groups to facilitate benzene sorption, a rigid molecular structure that resists swelling helps retain the membrane's integrity (Villaluenga and Tabe-Mohammadi, 2000).

2.2.5 Flux rate

Component permeate fluxes are commonly obtained using the mass transfer resistance-in-series model (Karlsson and Trägårdh, 1993a; Feng and Huang, 1997). Overall permeate flux (J_k) for component k, where $k = i$ or $k = j$ for a binary feed is defined by:

$$J_k = \frac{C_{f,k} - H_k C_{p,k}}{R_{ov,k}} \qquad \text{(Eqn. 2:5)}$$

where $C_{f,k}$ and $C_{p,k}$ are component feed and permeate concentrations, H_k is a dimensionless equilibrium partition coefficient (i.e. C_k^{liq}/C_k^{vap}) and $R_{ov,k}$ is the overall component mass transfer resistance (Smitha *et al.*, 2004).

Under typical PV conditions, total permeate pressure is much lower than feed vapour pressures, and it is reasonable to assume that $C_{p,k} \approx 0$ or that $C_{f,k} >> H_k C_{p,k}$ (Mulder, 1991).

2.3 Organic-organic separations

Organic-organic liquid separations are commonly classified by the categories polar/non-polar, aromatic/alicyclic, aromatic/aliphatic, and isomeric mixtures.

2.3.1 Polar/non-polar solvent mixtures

Smitha *et al.* (2004) summarised performance of various membranes for separating polar/non-polar solvents such as alcohols/alkanes and alcohol/ether mixtures. The first demonstrations of polar/non-polar PV separations using cellulose membranes were done in the 1950s (Heisler *et al.*, 1956), but laboratory scale applications for removing organics from diluted organic liquid streams were studied in the 1960's (Binning *et al.*, 1961) using hydrophobic membranes made from polyethylene (PE) and polypropylene (PP). However, these membranes had low selectivities for polar/non-polar organic mixtures, primarily because they did not have any functional groups to create differential interactions between the components being separated (Smitha *et al.*, 2004).

A PTFE film grafted with N-vinylpyrrolidone gave good selectivity for separating polar/non-polar mixtures such as methanol/toluene, but fluxes were poor (Aptel *et al.*, 1976). Most membranes used in polar/non-polar separations were cellulose based (CA, CTA, CAB, CAP). The polar (-OH) groups in the cellulose structure attract the polar component (methanol or ethanol) and retard permeation of the non-polar component (benzene, toluene, MTBE etc.). Polar/non-polar separations are generally done between 25-70ºC, with the greatest number clustered around 50ºC.

Most PV membranes have experimental and/or industrial fluxes of 1–10 $kg.\mu m.m^{-2}.h^{-1}$, and selectivities of 5–20 (Villaluenga and Tabe-Mohammadi, 2000). Usually selectivity is inversely related to flux, but occasionally good flux occurs with exceptional selectivity. For example, methanol/toluene (5-90%) separated using a cellulose membrane had a flux greater than 15 $kg.\mu m/m^2.h$ and a selectivity of $\alpha_{MeOH/Tol} = 1200$ (Mandal and Pangarkar, 2002b).

Smitha *et al.* (2004) report two exceptional membranes with infinite selectivity: when separating methanol/MTBE (67-95%) a PIC membrane of SA and chitosan had a flux > 2.4 $kg.\mu m.m^{-2}.h^{-1}$ and a CAB and CAP blend had a flux of 1.41 $kg.\mu m.\ m^{-2}.h^{-1}$ when separating

Ethanol (5%)/ETBE. These two separations show promise for industrial scale up providing the membranes are stable during long-term use.

2.3.2 Aromatic/alicyclic mixtures

Potential applications of PV for separating aromatics/alicyclic separations include removing cyclohexane from benzene/cyclohexane mixtures formed in benzene, toluene and xylene production plants, and removing aromatics from the feedstock of ethylene plants to enhance their production capacities (Smitha *et al.*, 2004). Benzene/cyclohexane (Bz/cHx), one of the most common aromatic/alicyclic mixtures, is also the most difficult to separate. Many researchers have assessed PV properties of membrane materials for this separation (Cabasso *et al.*, 1974b; Rautenbach and Albrecht, 1980; Suzuki and Onozato, 1982; Terada *et al.*, 1982; Sun and Ruckenstein, 1995; Inui *et al.*, 1997b; Uragami *et al.*, 1998). Smitha *et al*. (2004) summarised some of the membranes for PV of aromatic/alicyclic mixtures.

Martin *et.al.*, (1961) used modified cellulose ester for their membrane, by blending it with 20 wt.% polyphosphonate ester. The feed contained 50 wt.% Bz/cHx and the permeate had 73 wt.% Bz, giving moderate selectivity ($\alpha_{Bz/cHx}$ = 2.7) and a flux of 1 kg/m^2.h. When membrane thickness is included, the flux was 100 kg.μm/m^2.h (Smitha *et al.*, 2004). Cabasso *et al.* (1974b), increased the membrane blending ratio using 50 wt.% polyphosphonate ester. A permeate of 90 wt.% Bz was produced from a feed of 50 wt.% Bz, giving a selectivity of $\alpha_{Bz/cHx}$ = 9 and fluxes of 1.6–2.0 kg.m^{-2}.h^{-1}. This highlights that tailoring a membrane can considerably increase selectivity and flux.

Smitha *et al.* (2004) report that operating temperatures for aromatic/alicyclic separations are usually between 25-80ºC. One outstanding Bz/cHx process run at 160ºC with an inorganic zeolite membrane (Nikolakis *et al.*, 2001) had higher selectivity ($\alpha_{Bz/cHx}$=160) and flux (561 kg.μm.m^{-2}.h^{-1}) than other membranes used to separate this organic mixture.

The grafted MA-g-HEMA membrane studied by Terada *et al.* (1982) gave exceptional selectivity (∞) and a moderate flux (7.4 kg.μm/m^2.h). Luo *et al.* (1997) also obtained very good selectivity ($\alpha_{Bz/cHx} > 10^4$) with a blended membrane; however the flux was very modest (0.16 kg.μm.m^{-2}.h^{-1}).

2.3.3 Aromatic/aliphatic hydrocarbons

Separating aromatic-aliphatic hydrocarbon mixtures was first investigated in a European project (Rautenbach & Albrecht, 1980). Little further research was reported until the mid 1980s when Brun *et al.* (1985) investigated separating benzene/n-heptane mixtures using elastomers. This research stimulated interest in elastomeric membranes and their blends (Smitha *et al.*, 2004).

Smitha *et al*.(2004) summarized the performance of a variety of aromatic/aliphatic separations published by the major researchers in this field (Suzuki and Onozato, 1982; Brun *et al.*, 1985; Hao *et al.*, 1997; Wang *et al.*, 1999; Roizard *et al.*, 2001; Cao and Henson, 2002; Cunha *et al.*, 2002; Matsui and Paul, 2002; Matsui and Paul, 2003). Most aromatic/alicyclic separations are carried out between 25-70ºC. Highest selectivities were produced using plasma-grafted membranes to separate benzene/*n*-hexane ($\alpha_{Bz/Hx}$ = 210); however, flux rates were low at 0.9 kg.μm.m^{-2}.h^{-1} (Wang *et al.*, 1999). Higher flux rates (20-1000 kg.μm.m^{-2}.h^{-1}) were achieved using an ionically crosslinked copolymer membrane to separate toluene (50%)/*i*-octane, with moderate to good selectivities ($\alpha_{Tol/i\text{-}oct}$ = 2.5-13.0) (Matsui and Paul, 2002; Matsui and Paul, 2003).

2.3.4 Isomers

Mulder *et al.* (1982) used thin membranes of cellulose esters treated with an organic solvent to separate isomeric xylenes. Relatively good fluxes but low selectivities were achieved. Since the 1980s a variety of membranes have been used to extract isomeric components such as xylene isomers, and 1º, 2º or 3º alkanes and alcohols (Funke *et al.*, 1997; Gump *et al.*, 1999; Wegner *et al.*, 1999; Chen *et al.*, 2000; Gump *et al.*, 2000; Nair *et al.*, 2001; Schleiffelder and Claudia, 2001). The use of PVA membranes for purifying mixed xylenes on an industrial scale has been limited by the very small separation factors (Smitha *et al.*, 2004).

Wessling *et al.* (1991) used dense homogeneous polyethylene (PE) membranes for PV of aromatic C_8-isomers. The mass transport rate across the membrane increased for in the order *o*-xylene < ethylbenzene < *m*-xylene < *p*-xylene and the flux of the components depended strongly on the downstream pressure.

Inorganic zeolite membranes (silicates of alumina) have become popular for separating alkane isomers in the last 5-10 years (Wegner *et al.*, 1999; Flanders *et al.*, 2000). Sulzer Chemtech commercialised lab-scale systems with ceramic membranes (modules Pervap® SMS) and this process could be industrialised within the next few years (Jonquières *et al.* 2002).

Separating aromatic isomers continues to be an active research area, largely because current separation methods are both complex and energy intensive (Smitha *et al.*, 2004).

2.3.5 Miscellaneous separations

Smitha *et al.* (2004) summarised a number of miscellaneous organic/organic separations including organic/chlorinated hydrocarbon, alkane/alkene, and alcohol/ketone mixtures etc.

Dutta and Sikdar (1991) used a composite PGSA/Teflon membrane to separate methanol and carbon tetrachloride with good flux rates (60 $kg.\mu m.m^{-2}.h^{-1}$) and selectivity ($\alpha = 14.6$). High selectivities permeation characteristics ($\alpha > 34$) were also obtained at high temperatures (86-236°C) using a silicate zeolite membrane for separating heptane/octane/benzene (Funke *et al.*, 1997). However, components in essential oils tend to be thermo-labile so high temperature membranes are of limited potential use.

Aqueous separations of flavour and aroma compounds commonly found in essential oils (e.g., linalool) have been studied (Baudot and Marin, 1997; Charbit *et al.*, 1997; Lomascolo *et al.*, 1999; Beauchêne *et al.*, 2000; Souchon *et al.*, 2002). Molina *et al.* (1997) separated water-ethanol-linalool, a mixture frequently found in the wastes of essential oil industries. Ferreira *et al.* (2001) studied separating fusel oils (*n*-propanol, *i*-butanol, *n*-butanol, *i*-amyl alcohol, ethyl acetate, linalool) from ethanol/water mixtures produced in a commercial distillery. Removing aroma components from aqueous beverage solutions (Karlsson and Trägårdh, 1994, , 1996) such as wine (Schäfer *et al.*, 1999; Vaz Freire *et al.*, 2001), fruit juice (Bengtsson *et al.*, 1989; Sampranpiboon *et al.*, 2000; Peng, 2004), tea (Kanani *et al.*, 2003), and other foodstuffs such as dairy products (Baudot and Marin, 1996) have also been studied.

Paris *et al.* (2004) separated aqueous mixtures of synthetically produced linalool (racemic mixture of S- and R-linalool) using a PDMS membrane and achieved a flux of 250 $g.h^{-1}.m^{-2}$

but with very little enrichment of the *R*-enantiomer ($\alpha_{R\text{-Lool/S-Lool}}$ = 1.2-1.3). Paris *et al.* (2004) reported studies separating equimolar limonene and α-pinene mixtures.

Auerbach (1995) examined the folding of citrus peel oils using hybrid ultrafiltration, reverse osmosis, dialysis and PV. However this research used water to extract oxygenated oil components from the citrus peel oil, which were subsequently removed from the aqueous solution using PV (Auerbach, 1995). To date, no literature has been published with on organic/organic essential oil separations using PV.

2.4 Membrane structure and materials

Work on membrane separations began in the early 1960s, using membrane materials such as dense metals, zeolites, polymers, ceramics and biological materials. Of these, polymers are the most widely used material (Smitha *et al.*, 2004). Several different polymer membrane structures are commonly used today, including porous, dense and asymmetric membranes. Selecting a good membrane requires a sound knowledge of membrane structures. Much of the following discussion is based on the excellent review by Smitha *et al*. (2004).

2.4.1 Membrane morphology

Membranes used for laboratory scale organic mixture separation are generally homogeneous and symmetric (Figure 2:09 a). These are easy to cast and will directly give the intrinsic separation properties of the polymer. However, to attain commercial viability, membranes need to be prepared in asymmetric or composite form. These two morphologies give a thin effective separation layer, enabling high flux while maintaining the desired mechanical strength of the membrane.

Asymmetric membranes have a thin dense layer on top of a porous support layer of the same material (Figure 2:09 b). They are generally prepared by a phase inversion technique - a homogeneous polymer solution is cast as a thin film or spun as a hollow fibre and immersed in a non-solvent bath after a brief evaporation time in air. The membrane is formed by precipitating polymer when the solvent is replaced by a non-solvent.

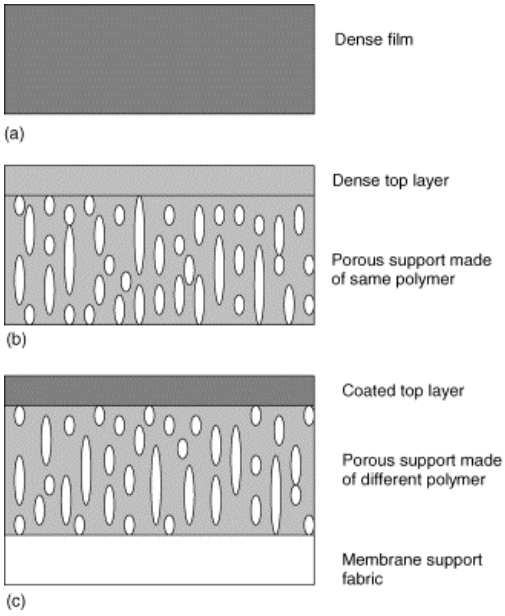

Figure 2:09 Schematic of three different membrane morphologies (Néel, 1991).

Composite membranes consist of a porous support layer with a thin dense skin layer on top (Figure 2:09 c). The skin is usually a different polymer material from the support layer. Composite membrane structures minimize membrane cost by reducing the quantity of expensive high-performance material used. In principle, composite membranes allow the properties of the dense separating layer and the porous support layer to be optimised individually, and to a greater extent, than in the phase inversion process.

2.4.2 Membrane formation

Although researchers' interest in synthesizing polymer membranes for different applications has existed for about a century, major developments in preparing membrane materials were made only relatively recently as a result of advances in synthetic polymer technology (Lipnizki *et al.*, 1999). The phase inversion technique for forming membranes was initially explored by Mulder *et al.* (1983). Subsequently, researchers obtain greater permeabilities by reducing the thickness of the effective separation layer (Geng and Park, 1994; Yeom *et al.*, 1996; Ray *et al.*, 1997; Cunha *et al.*, 1999; Ray *et al.*, 1999a; Smitha *et al.*, 2004). Modern polymers have better thermal and mechanical properties than the natural polymers of old, as well as good selectivity and flux.

In 1982/1983, GFT developed the 'composite membrane' for dehydrating ethanol, which had three layers: a very thin layer of crosslinked poly(vinyl alcohol) (PVA) on top of porous

polyacrylonitrile (PAN) support, which was further backed by even more porous non-woven membrane support fabric. This membrane is also suitable for separating organic mixtures. Most inorganic polymer composites rely on physical attachment of the polymer to the inorganic substrate, followed by cross-linking. These composites are stable even when contacted by liquid in which the native polymer is completely soluble. Composite membranes made from inorganic polymers have significantly improved the effectiveness of organic-organic separations.

The main advantage of ceramic membranes reinforced with glass or other fibres is their thermal stability at high temperatures. Hence, they find wide applications in catalytic membrane reactors (CMR), and separating organic liquid mixtures that can withstand high temperature processing.

Polymer alloy or blended membranes are commonly used for PV of organic-organic liquid mixtures such as Bz/cHx. Blending creates new polymeric materials that combine the properties of two homopolymers. The composition of the blend affects the physical, mechanical and permeation properties of the resultant polymer (Johnson and Thomas, 1999). Alloy membranes, such as those used in Bz/cHx separation, are commonly prepared by mixing a benzene-soluble polymer with a benzene-non-soluble one. The insoluble polymer forms the backbone of the polymeric membrane, while the soluble one provides affinity for benzene.

Membrane selectivity is enhanced by techniques such as cross-linking, graft-polymerization, microphase separation, concentrated emulsion polymerization, and copolymerisation (Villaluenga and Tabe-Mohammadi, 2000). Sun and Ruckenstein (1995) produced an emulsion polymerised membrane with selectivity of $\alpha_{Bz/cHx} = 25$ at a flux of ~2 kg.μm/m^2.h.

Novel materials can be produced by modifying polymers through chemical reaction, radiation, plasma treatment, or a combination of any of these methods. In these membranes, specific groups are introduced to the bulk polymer or to the surface of polymer membrane (Johnson and Thomas, 1999).

Several studies examine other types of membranes for organic-organic separations including different degrees of "R-group" addition to a polymer backbone (Inui *et al.*, 1998b), and the

use of Ag(I) ions to facilitate transport in a PVA membrane (Bryant *et al.*, 1997). Darkow *et al.* (1994) synthesized polyacrylonitril-co-butadien-co-styrene-co-diaryltetrazolyl (ABSV) membrane, a new type of co-polymer with a photosensitive moiety. The functionalisation and cross-linking were initiated by photo-irradiation. The photochemical treatment enhanced permselectivity of the membrane, but the separation factor was still relatively low ($\alpha = 2.46$).

Commercially available polymeric membranes have not been used for industrial organic-organic separations largely because membrane performance decreases due to swelling and loss of membrane integrity (Feng and Huang, 1997). To improve membrane stability, researchers are extensively modifying membranes (cross-linking or blending) for various separation applications, based on the mixture to be separated (Ishihara and Matsui, 1987; George *et al.*, 1999; Ren *et al.*, 2001; Roizard *et al.*, 2001; Matsui and Paul, 2002; Wang *et al.*, 2002).

2.4.3 Membrane modification

A membrane should have both a high flux and a high selectivity. However, an increase in flux is usually accompanied by a decrease in selectivity. Therefore, membrane performance has to be adjusted to achieve optimum performance for a given separation (Johnson and Thomas, 1999). Membrane chrystallinity, the degree of cross-linking, blending, grafting, and copolymerisation can all affect polymers separation characteristics and membrane stability.

Crystallinity

Highly crystalline polymers do not dissolve easily in many organic solvents, primarily due to a lack of flexible groups, which prevent a high degree of swelling. The crystallites act as physical cross-links keeping the polymer tightly packed. Because dissolution generally occurs in the amorphous part of the polymer, the degree of crystallinity has large influence on dissolution of the feed into the membrane. Highly crystalline polymers have lower permeability than amorphous polymers.

In polymers of type $(---CH_2---CHR---)_n$ the size of side group (R) plays an important role in predicting polymer crystallinity. Generally, polymers such as PVDF, PE (LDPE, HDPE), PP and PS can be used for organic mixture separation because they are crystalline when the side group chains are isotactic or syndiotactic in nature (Smitha *et al.*, 2004).

Membrane density

Yamasaki *et al.* (1997) studied the effect of membrane density on selectivity for separating Bz/cHx. They obtained a selectivity of $\alpha_{Bz/cHx} = 10$ for an asymmetric PVA membrane compared to $\alpha_{Bz/cHx} = 3$ for an homogeneous PVA membrane. The differences were attributed to the difference in density of the skin layer. The asymmetric membrane probably had denser polymer packing, resulting in smaller free volume for diffusion of permeating molecules. Therefore, sorption selectivity dominated overall selectivity. Because benzene has greater affinity towards PVA, overall selectivity increased with increasing polymer density (Villaluenga and Tabe-Mohammadi, 2000).

Cross-linking

There are two reasons to cross-link a polymer when making membranes; to make the polymer insoluble in the feed mixture, and to decrease the degree of swelling a polymer undergoes. A good example of this is the chemically cross-linked PVA top layer of the GFT composite membrane (Spitzen *et al.*, 1987), which has excellent resistance to many solvents.

Cross-linking can be carried out in three main ways; via chemical reaction using a compound to connect two polymer chains, by irradiation, and by physical cross-linking. The degree of cross-linking must be thoroughly controlled. It is particularly difficult to ensure controlled cross-linking for composite membranes, which are produced by a coating-evaporation technique and chemical cross-linking only occurs during the evaporation period. Here, definite cross-linked polymer networks of an appropriate chemical nature are produced by "physical" cross-linking. Exxon obtained promising results for separating aromatics and saturates using physical cross-linking, with membranes made of multi-block copoly-condensates comprising alternate flexible (soft) and rigid (hard) sequences (Koenitzer, 1990).

However, excessive cross-linking can make the polymer membrane brittle; a loss in dimensional stability will reduce its suitability as a pervaporation membrane (Smitha *et al.*, 2004).

Blending

A mixture of polymers not covalently bonded is called a polymer blend. This is an ideal technique for separating mixtures with components containing very different functional groups such as aqueous/organic separations. Optimum blending-ratios can be determined by

mixing various amounts of hydrophilic polymer with a hydrophobic polymer and measuring the permeability and selectivity (Park *et al.*, 1994; George *et al.*, 1999).

There are two types of polymer blends used in thin film membrane production: homogeneous blends, where two polymers are miscible on a molecular scale for all compositions, and heterogeneous blends, in which two polymers are not totally miscible. In the latter, domains of one polymer are distributed within the matrix of the other polymer. Many researchers believe that only homogeneous blends have potential as membrane materials for PV because heterogeneous blends will not give enough mechanical strength in thin membranes. The properties of a membrane containing two different polymers can be optimised to achieve the best chemical stability and separation characteristics.

Grafting

In grafting, oligomeric chains are irregularly attached by chemical reaction or irradiation as side chain branches to the main polymer chain. If molecules to be grafted contain a functional group that can react with a functional group on the polymer, chemical grafting can occur. Grafting by irradiation is a versatile technique for modifying insoluble polymer films.

Polymers with good chemical resistance can be made into films by melt extrusion/calendering followed by irradiation-based grafting. Aptel, Neel and co-workers (Aptel *et al.*, 1972, 1974), Ellinghorst *et al.* (1987), Ulbricht and Schwarz, (1997), and Yanagishita *et al.* (2002) researched grafting films by irradiation. Base polymers such as PVDF, PVF, PTFE, PAN, and PI were grafted with monomers such as pyrrolidone, pyridine, vinyl acetate, acrylic acid, imidazole, methacrylate, and benzophenone.

Copolymerisation

Copolymerization involves covalently bonding two polymers to produce a membrane with increased mechanical stability. Copolymers with block and random repeat units can be formed by this technique, however the degree of crystallinity is an important property. Random copolymers might be fully amorphous while grafted copolymers have some crystallinity. Membranes made of random copolymers cannot be used for PV as the membrane needs some crystallinity to show preferential sorption for one of the organic components (Tanihara *et al.*, 1995; Smitha *et al.*, 2004).

2.4.4 Developing new membrane materials

Membrane flux and selectivity are key factors in pervaporation mass transport. The aim in developing new pervaporation membranes is either to increase flux, keeping selectivity constant and/or higher selectivities at constant flux. There are three approaches in membrane development; developing completely new polymers, functionalizing membrane polymers, or integrating adsorber agents into polymers (e.g., zeolite).

The objective of this thesis was to use Hansen solubility parameters to scout for potential homogeneous membrane materials suitable for PV of organic liquid mixtures containing essential oil components. The permeation properties of these membranes can later be improved by polymer modification or producing asymmetric or composite membranes.

2.5 Factors affecting membrane performance

Specific characteristics of the feed components, the membrane, and process operating parameters influence overall PV performance. These factors include trans-membrane pressure, process temperature, feed composition and concentration, concentration polarization, feed turbulence, membrane thickness and the materials the membranes are made from (Binning *et al.*, 1961; Cabasso, 1983; Néel, 1991; Mathys *et al.*, 1997; Miranda and Campos, 1999; Villaluenga and Tabe-Mohammadi, 2000; Miranda and Campos, 2001a; Matsui and Paul, 2002; Yoshida and Cohen, 2003; Smitha *et al.*, 2004).

Table 2:03 Factors influencing pervaporation separation characteristics.

	Condition that induces:	
Factor	Major Influence	Minor Influence
Feed pressure	-	• 20 atm
Permeate pressure	• $P_p > 0.3\ P^o$ permeant • $P_p \approx > 10$ kPa	• $P_p < 0.3\ P^o$ permeant • $P_p \approx < 10$ kPa
Process temperature	• Close to polymer melting point • Termolabile product	• Close to normal working temp for polymer
Feed composition and concentration	• One component very attracted to polymer	• Components less attracted to polymer
Concentration polarization or fouling	• Presence of particulates or cells	• 'Clean' organic liquid mixtures
Feed turbulence	-	• Sub-turbulent flow rates
Membrane thickness	• All thicknesses	-
Membrane materials	• All membrane materials	-

Table 2:03 shows a brief summary of the degree of influence (major/minor) these factors have on PV.

2.5.1 Pressure differential

Pressure differential between the feed and permeate side of the membrane is directly related the activity of the components at the permeate side. At pressure differentials close to the vapour pressure of the liquid, permeate pressure strongly influences the pervaporation characteristics (Dutta and Sikdar, 1991; Smitha *et al.*, 2004).

Permeate and feed pressure

Increasing downstream permeate pressure decreases both selectivity and flux of a polar/non-polar PV separation (Figure 2:10).

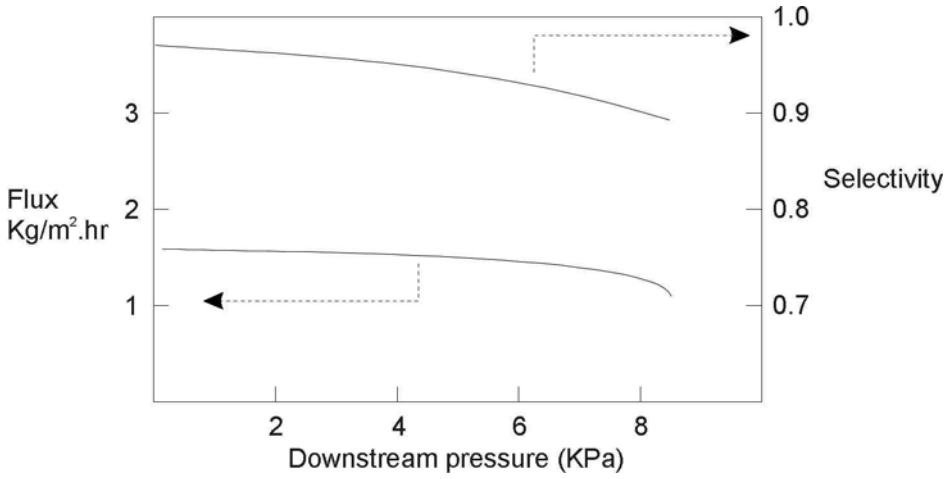

Figure 2:10 Effect of pressure on pervaporation of ethanol/benzene mixtures (Smitha *et al.*, 2004).

Permeation of n-heptane was found to be practically constant between permeate pressures of 2.66 – 66.6 kPa (equivalent to pressure differentials ranging from 35 to 98 kPa). The molecular concentration in the liquid feed phase was much greater than the vapour permeate phase, so the concentration gradient ($C_2 - C_1$ in Eqn. 2:1) was not affected by these changes in permeate pressure (Binning *et al.*, 1961).

However, other researchers have found that partial vapour pressure of a component on the permeate side, affects its permeation rate significantly (Figure 2:11). Therefore, downstream

vapour pressure should be kept as low as economically feasible to maximize the driving force for the permeation (Wijmans and Baker, 1995; Feng and Huang, 1997).

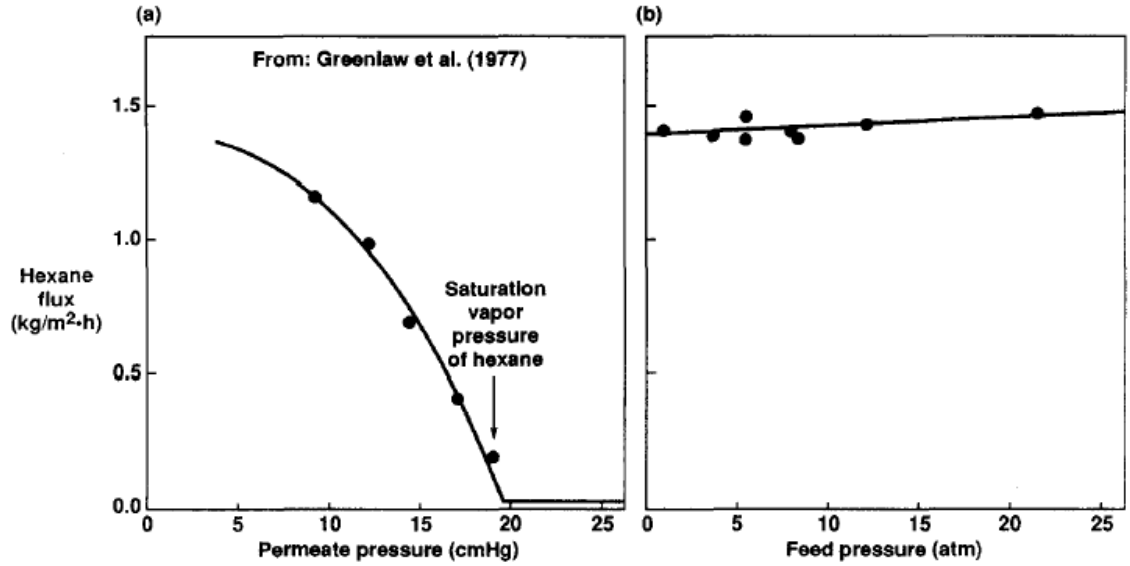

Figure 2:11 Effect of feed and permeate pressure on flux of hexane through a rubbery pervaporation membrane (Wijmans and Baker, 1995), 5 cmHg ≈ 6.6 kPa.

Flux through the membrane is independent of feed pressure up to 2026 kPa (20 atm) (Figure 2:11 b), but extremely sensitive to permeate pressure (Figure 2:11 a). Note that the pressure range referred to in Figure 2:10 is < 10 kPa, and in Figure 2:11 a where pressure is <10 cmHg (13.3 kPa) the flux rate levels off. Hwang and Kammermeyer (1984) stated that so long as the downstream pressure is less than 30% of the permeating species vapour pressure, the flux rate would remain within 90% of the flux obtained at full vacuum ($P_p/P^o = 0.3$ where P_p is permeate pressure and P^o is the vapour pressure of the liquid).

There are conflicting opinions about the influence of feed pressure on PV permeation. Dutta and Sikdar (1991) state that the maximum trans-membrane pressure gradient is obtained at zero permeate pressure (full vacuum), so any permeate pressures higher than this will mean that the feed pressure can influence PV characteristics (Dutta and Sikdar, 1991; Smitha *et al.*, 2004). However, many other researchers state that feed pressure has an insignificant effect on PV permeability and selectivity (Binning *et al.*, 1961; Feng and Huang, 1997; Villaluenga and Tabe-Mohammadi, 2000). Binning *et al.* (1961) found that altering feed pressure between 101 – 810 kPa (1 – 8 atm) using nitrogen, had no effect on permeability or selectivity.

2.5.2 Process temperature

Process temperatures affect both PV membrane selectivity and permeant flux.

Effect of temperature on selectivity

In most cases, increasing process temperature causes a small decrease in selectivity (Villaluenga and Tabe-Mohammadi, 2000). Huang and Lin (1968) found that selectivity for 50:50 benzene and cyclohexane decreased from 1.632 at 25ºC to 1.439 at 45ºC, as shown in Figure 2:12. Note the x-axis units are inverse temperature.

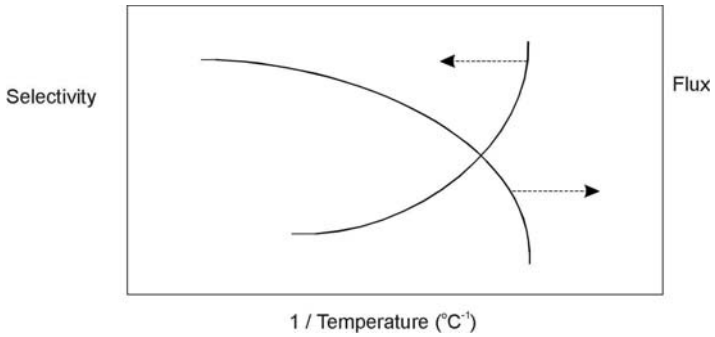

Figure 2:12 Effect of temperature on flux and selectivity of benzene/cyclohexane mixtures (Villaluenga and Tabe-Mohammadi, 2000; Smitha *et al.*, 2004).

Effect of temperature on flux

Many researchers show that increasing the temperature increases membrane permeability and decreases selectivity (Kucharski and Stelmaszek, 1967; Cabasso *et al.*, 1974a; McCandless *et al.*, 1974; Acharya *et al.*, 1988; Inui *et al.*, 1999; Villaluenga and Tabe-Mohammadi, 2000). Binning *et al.* (1961) found that flux rate approximately doubled with a 20ºC increase in temperature.

Several researchers showed that temperature has an Arrhenius type effect on PV membrane permeability (Huang and Lin, 1968; Cabasso *et al.*, 1974a; Acharya *et al.*, 1988; Inui *et al.*, 1999; Villaluenga and Tabe-Mohammadi, 2000; Smitha *et al.*, 2004):

$$Q_i = Q_i^0 \exp\left\{-\frac{E_p}{RT}\right\} \quad \text{or} \quad J = J_0 \exp\left\{\frac{E_p}{RT}\right\} \qquad \text{(Eqn. 2:8)}$$

where Q_i^0 is a constant, E_p is activation energy for permeation, R is the universal gas constant, and T is absolute temperature.

Theoretical explanations

Sun and Ruckenstein (1995) explained that temperature had two effects on the membrane (Villaluenga and Tabe-Mohammadi, 2000):

- Increasing polymer chain mobility, which facilitated diffusion of both components.
- Weakening the interaction between the preferentially attracted molecule and the membrane, which lowered its sorption.

Huang and Lin (1968) also described how increasing the temperature increased agitational energy or motion of the polymer chains. At lower temperatures, permeation based on diffusional cross section (size) of the permeating molecules is restricted. As agitational energy of the polymer chains increases, there are larger gaps in the amorphous regions of the membrane, so larger molecules that had previously been restricted can permeate. This increases flux and decreases selectivity (Huang and Lin, 1968).

Cabasso (1974a) found that the sorption rate of benzene also depended on the thermal history of the membrane. Sorption increased with decreasing temperature, and reversing the direction also reversed sorption behaviour. However, when the temperature increased from low values, sorption increased again, until the starting temperature of the first experiment was reached. Reversing the temperature direction at this point did not reverse sorption behaviour, but caused it to increase along the same curve as in the first experiment. Acharya *et al.* (1988) also realized that flux was higher when cooling than when heating the feed. Their observations can be explained by the 'temperature history effect' proposed by Cabasso *et al.* (1974a).

2.5.3 Feed concentration and composition

In theory, PV can be used to separate any liquid mixture in all concentration ranges (Johnson and Thomas, 1999). However, it is primarily used for removing or recovering the minor component in organic/organic azeotropic, close-boiling point, or isomeric mixtures (Mulder *et al.*, 1982; Blume *et al.*, 1990; Böddeker *et al.*, 1990).

Permselective properties of PV membranes are determined by sorption and diffusivity of the permeating components in the membrane. Because both sorption and diffusion phenomena depend on composition of the liquid mixture, membrane permeation characteristics are usually strongly influenced by feed composition (Johnson and Thomas, 1999).

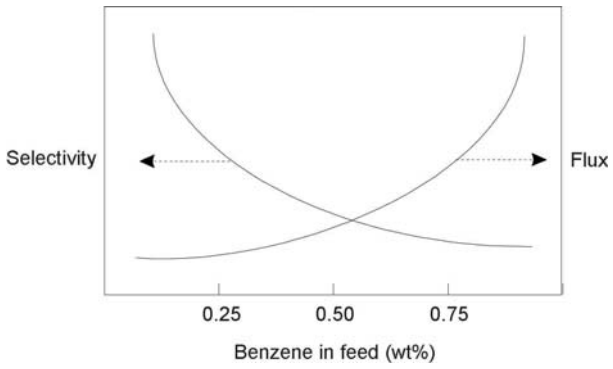

Figure 2:13 Effect of feed concentration on organic–organic pervaporation of benzene–cyclohexane mixture (Villaluenga and Tabe-Mohammadi, 2000; Smitha *et al.*, 2004).

Figure 2:13 shows that permeability increases and selectivity decreases sharply, with increasing benzene content of the feed. The decline in selectivity is explained by the plasticizing effect of benzene on the membrane. As benzene content increases, the membrane swells and the relaxed polymer chains allow greater permeation of cyclohexane (Villaluenga and Tabe-Mohammadi, 2000).

Huang and Lin (1968), studied the effect of feed composition and temperature on flux of binary mixtures through polyethylene (PE). They observed the feed components gave "permeation enhancement" and "permeation depression" effects. The flux of 50 wt% benzene/n-hexane was over twice that of the flux calculated from the ideal single component rates. This permeation enhancement was due to the complimentary plasticizing actions of both components. Conversely, in a 50 wt% 2,2-dimethyl butane/cyclohexane feed, the presence of 2,2-dimethyl butane decreased the flux of cyclohexane when compared to that of the pure component. Huang and Lin (1968), stated this was due to steric hindrance caused by the bulky molecular volume of 2,2-dimethyl butane, which was greater than any plasticizing action on the PE membrane.

The effect of feed concentration on membranes permeability and selectivity has also been studied by McCandless *et al.* (1974), Suzuki and Onozato (1982), Acharya *et al.* (1988), Enneking *et al.* (1996), Tanihara *et al.* (1994; 1995), Inui *et al.* (1997b; 1997c; 1998b), and Ray *et al.* (1997).

Effect of molecular size, shape, and chemical nature

The first two steps of the permeation process involve dissolution of molecules into the polymer membrane then diffusion of these molecules through the membrane. Differences in either solubility or diffusivity give preferential permeation. Solubility depends primarily on differences in the chemical nature of the permeating species whereas diffusivity is determined largely by the size and shape of these molecules and the degree the diffusing species aggregate within the polymer (Huang and Lin, 1968).

Binning *et al.* (1961) used several pure hydrocarbons to study the effect of size, shape and chemical nature on permeation through a PV membrane. The flux of a homologous series of normal paraffins through a polymer film under the standard conditions decreased with the number of carbon atoms. Johnson and Thomas (1999) attributed this phenomenon to decreased diffusivity with increased penetrant size. Thus even if solubility increases, the decrease in diffusivity reduces overall flux. These researchers also found that the degree of membrane swelling increased with penetrant size.

Hexane isomers were used to investigate the effect of molecular shape on flux. They found that the more linear a molecule is, the faster its flux. The straight chain *n*-hexane permeated more than three times faster than the singly branched methyl-pentanes and about a hundred times that of the doubly branched 2,2-dimethyl butane (Binning *et al.*, 1961).

Binning *et al.* (1961) also found that chemical nature had a significant effect. By observing the relative permeability of hydrocarbon pairs of similar size and shape they found that the permeability of 1-hexene (an olefin with one double bond) was about three times that of *n*-hexane (equivalent paraffin) despite having the same number of carbon atoms. Molecular shape dominates in chemically similar components but size and shape has little influence on permeability when differences in chemical or solubility characteristics are very large. Binning *et al.* (1961) found that when there were considerable differences in molecular size, shape and chemical nature (e.g., benzene and methanol), solubility was the main factor determining membrane selectivity.

In summary the following three general trends were observed (Huang and Lin, 1968):

- In binary permeation of two species of a homologous series, the lower molecular weight species permeates preferentially.

- Molecules with smaller diameter will permeate faster than their bulkier counterpart.
- Shape and size effects predominate for chemically similar molecules. However, molecules with large differences in chemical nature are affected more by parameters such as solubility, than shape and size.

2.5.4 Concentration polarization

The components in a binary liquid have individual permeation rates through a semi-permeable membrane. The less-permeable component will concentrate in the boundary layer at the membrane surface and adversely affect permeation rate. This effect is called concentration polarization (CP) (Bhattacharya and Hwang, 1997; Smitha *et al.*, 2004). Some researchers have concluded that CP does not play a very significant role in PV of organic-water mixtures (Psaume *et al.*, 1988; Karlsson and Trägårdh, 1993b). However, Jiang *et al.* (1997) found that CP can be significant for concentrated organic-organic solutions (e.g. 2–4 wt% methanol/triethylene glycol dimethyl ether), especially for thin composite membranes.

Feed turbulence

The most common method of reducing CP, and therefore improving the mass transfer, is to promote turbulence at the surface of the membrane (Wijmans *et al.*, 1996; Ferreira, 1998). The membrane unit used in the current study has a conical shaped flow distributor (also called an impinging jet) to minimise CP (Miranda and Campos, 2001a). Feed flows through a circular nozzle, impinges the membrane and is forced to flow radially outwards. Flow is confined by the conical shape of the impinging jet, which extends from the nozzle to a short distance above the membrane surface (Figure 2:14).

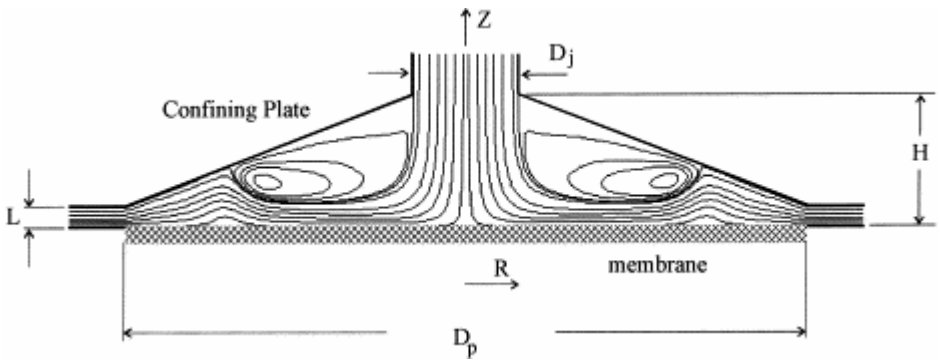

Figure 2:14 Membrane unit impinging jet flow distributor with laminar flow pattern (Re = 860) (Miranda and Campos, 2001b).

Miranda & Campos (1999) found that the critical Reynolds number to obtain turbulent flow in this conical flow distributor was approximately *Re* = 1600. Turbulent flow minimises the stagnant zones which can occur as the feed flows over the membrane surface, thereby improving mass transfer.

2.5.5 Membrane material

The chemical nature of the polymer used in the membrane, and the presence of plasticizers and solvents, influences permeation rate and separation (Binning *et al.*, 1961). Membranes containing polar groups tend to preferentially permeate polar feed components (and vice versa for non-polar membranes) (Sweeny and Rose, 1965; Huang and Lin, 1968). This is discussed further in Chapter 3.

Chemical and thermal stability of the films in the presence of the feed under operating conditions are also important characteristics. Some thin polymer films are much more stable and selective under permeation conditions than others, depending on their solubility in the feed components (Binning *et al.*, 1961).

2.5.6 Membrane thickness

Permeation rate is inversely proportional to membrane thickness but selectivity is said to be independent of thickness in the range considered practical for commercial use. Binning *et al.* (1961) established a linear inverse relationship between flux and film thickness (0.8- 1.9 mm), yet selectivity of the *n*-heptane / iso-octane mixture (50 Vol%) was essentially the same at all four membrane thicknesses. For film thicknesses that could be produced in 1961, Binning *et al.* (1961) felt that PV could still retain selectivity and rapid permeation rates even when operating with very thin films (800 μm). Modern polymer membranes can be as thin as 10-35 μm (Smitha *et al.*, 2004), and modern literature makes little mention of membrane thickness affecting selectivity.

2.5.7 Membrane swelling

If sorption dominates over diffusion in a PV separation, membrane swelling can occur (Sun and Ruckenstein, 1995). Swelling will change both flux and selectivity (Smitha *et al.*, 2004), and the degree of membrane swelling must be suppress or controlled (Villaluenga and Tabe-

Mohammadi, 2000), because swelling decreases membrane performance, and causes loss of membrane integrity (Feng and Huang, 1997).

A trade-off between sorption and swelling is needed. For preferential permeation to occur, there must be a high degree of chemical affinity between one component and the membrane. However, if affinity is too great, the membrane will swell and lose integrity. Thus, a membrane suitable for an organic-organic separation such as Bz/cHx, must possess both polar groups to facilitate benzene sorption, and a rigid molecular structure resistant to swelling to maintain membrane integrity (Villaluenga and Tabe-Mohammadi, 2000).

Baddour *et al.* (1964) found that osmotic stresses during swelling fragmented and disoriented the crystalline structure of their PE membranes. Crystallization and or stress relaxation caused steady-state flux to decrease after the rearrangement of chain segments in the swollen state. Cross-linking the polymer membrane strands is the primary method to overcome rearrangement of polymer chain segments due to swelling (Smitha *et al.*, 2004).

2.5.8 Membrane fouling

Deposition of impermeable substances in the feed, on the membrane surface is called fouling. Fouling is less a problem in PV than in other membrane separation processes like reverse osmosis, electrodialysis and nanofiltration; and as such is usually caused by scale formation rather than clogging or blocking of pores. Membrane fouling reduces flux and ultimately makes the membrane ineffective. It can be minimised by using a highly turbulent flow regime, ceaning the membrane semi-continuously, or by filtering the feed before PV (Smitha *et al.*, 2004):

2.5.9 Summary

The primary factors influencing selectivity and flux of permeants through a PV membrane include: feed component size, shape and chemical nature; membrane materials, thickness, and degree of swelling; process temperature and pressure; feed composition and concentration. Permeation through a PV membrane involves three primary steps: solution of the liquid feed mixture in the film surface; migration of feed components through the body of the film; and vaporization of the permeating material at the downstream interface where permeate is immediately removed (Binning *et al.*, 1961). The primary influence on this process is

molecular affinity between the polymer membrane and permeating molecules. If permeants cannot adsorb onto the membrane surface (e.g., one repelled by the membrane), they cannot begin to diffuse through the membrane to the permeate.

The scope of PV process variables that can be studied include the influence of feed composition and concentration, upstream and downstream pressures, feed and permeate temperatures, membrane thicknesses and swelling (Binning *et al.*, 1961), feed streams turbulence over membrane surfaces (Miranda and Campos, 1999), membrane concentration polarization or fouling (Miranda and Campos, 2001a), and performances of membrane materials (Cabasso, 1983; Néel, 1991; Mathys *et al.*, 1997; Matsui and Paul, 2002; Yoshida and Cohen, 2003).

2.6 Membrane material selection

Selecting membrane materials for PV is often done by trial and error. This is time consuming and the best membrane may not be found due to the limited number of membranes tested. A more rational method would match the physico-chemical properties of the membrane material with the components of the liquid to be separated. This is done simplistically for common PV applications such as organic liquid dehydration or waste-water treatment by choosing hydrophilic or hydrophobic membranes. However, hydrophobicity is not a major distinguishing factor for components in an organic/organic mixtures so a more comprehensive approach is required.

2.6.1 Membrane selection procedures

Three aspects are important when selecting polymers for a separation: the polymer should have high chemical resistance (compatibility), sorption capacity, and good mechanical strength in the solution. It should also interact preferentially with one of the components being separated (Sridhar *et al.*, 2000). Generally it is more economical to preferentially transport the component with the smallest weight fraction across the membrane. Koops and Smolders (1991) recommend that potential membrane materials be identified by: (1) literature search, (2) properties of the mixture, and (3) chemical and thermal stability of polymer.

Literature search

A literature search will identify prior research for PV separation of the mixture under study. Problems occur if the exact mixture has not been previously studied or if very few membranes have been identified. Most membranes reported in the literature were selected by trial and error, so the number of polymers tested may have been limited, which may have lead to the use of less than optimal membrane materials.

Feed mixture properties

Membrane selection for aqueous/organic separations has been dominated by choices between 'organophilic' or 'hydrophilic' membranes. However, choosing between these two membranes does not always work and very few investigations have dealt with the criteria for an ideal membrane. Selecting membranes for PV of compounds with widely differing polarity is relatively easy. Thus, silicone rubber membranes are often chosen for removing non-polar organics from water; and polyvinyl alcohol or similar hydrophilic membranes are commonly used for dehydrating organics. Hydrophilic membranes are also effective for separating relatively polar organics such as methanol from non-polar organics such as pentane. Finding a suitable polymeric membrane with good selectivity and flux for compounds of similar polarity is difficult, and the selection criteria may include complex thermodynamic considerations (Ray *et al.*, 1999a).

Membrane stability

Membranes need to be stable in terms of permeability and selectivity under standard operating conditions for extended periods. Membrane stability is vital in organic/organic separations, and is primarily affected by the chemical, mechanical, and thermal properties of the membrane (Feng and Huang, 1997).

2.6.2 Comparing alternate polymer selection theories

A parameter that can classify functional group interactions between solvents and polymers would be a valuable practical aid in predicting separations. This would provide a framework for selecting polymer membranes rather than choosing at random (Mandal and Pangarkar, 2002a). Hildebrand solubility parameter, Flory-Huggins interaction parameter, gas chromatography, solvatochromic polarity parameters, UNIQUAC method, and Hansen solubility parameters are all potential candidates for assisting in membrane selection.

Hildebrand solubility

Although many different methods are available to assess polymer-solvent interactions, there has been a strong tendency to use the simplistic Hildebrand solubility parameter δ_{total} (Hildebrand and Scott, 1964) to select membrane materials (Mandal and Pangarkar, 2002a; Price and Shillcock, 2002). However, it is difficult to determine accurate δ_{total} for polymers, and this method works only for a limited number of simple, low molecular weight, a-polar liquid mixtures without hydrogen bonding (Cabasso, 1983; Ghosh *et al.*, 1987; Mandal and Pangarkar, 2003; Hansen, 2004a).

Flory-Huggins interaction

Mandal and Pangakar (2002a) used the Hildebrand-Scott solubility parameter and the Flory–Huggins interaction parameters (χ_{12}) to predict sorption characteristics of a membrane material. They found that the lower the interaction parameter value, the higher the interaction or affinity the solvent has for a membrane. (Mandal and Pangarkar, 2003). Park *et al.* (1998), who originally made use of the Flory–Huggins interaction parameter, found that PV is dominated by preferential sorption, and that diffusion is of minor importance in this separation. However, this parameter still requires experimental sorption/swelling studies on a polymer-by-polymer basis, so is of limited use for predicting the properties of novel membrane materials. In addition to this limitation, Hansen and Smith (2004) stated that the χ parameter is readily predicted using the Hansen (2000) relative energy difference (RED) parameter.

Gas Chromatography

Feng and Huang (1997) proposed the use of inverse gas chromatography (I-GC) for predicting selective permeation. Here, polymer materials are modified into beads, packed into a long tubular column and analysed via probe solvents under gas chromatography conditions. Making the beads was the limiting factor in this method. As well as the complexity of forming tiny uniform-sized beads from a wide range of polymer materials, the process of converting the membrane polymer into beads can modify polymer characteristics, therefore defeating the objective of quantifying the differences in interaction between membrane polymers and permeating solutes in the vapour phase.

Roberts *et al.* (2000) used gas chromatography (GC) retention data to describe the interaction or retention of compounds on a GC stationary phase. The higher the retention index, the

larger the interaction between a solute and the stationary phase. Because partitioning in GC is similar to that in a membrane, Roberts *et al.* (2000) felt these indices could indicate interactions between polymers and solution components. They used this method to select membranes for separating ketones and alcohols from hydrocarbons. Although this method may predict solubility of solutes in a material, it does not provide relative diffusion rates. However, this method warrants further investigation.

A more promising method called Thin Layer I-GC was proposed by Huang *et al*. (2001). This method could directly study the partitioning of solvent probes against the polymer materials in the flat sheet form, without the need to modify the thin film polymer into beads. However, temperatures required to obtain good peak shape for the large solvent molecules (>150°C) used in the current model PV solution (linalool and linalyl acetate), were far above the upper working temperatures (50-95°C) of most of the polymers (Goodfellow, 2002), so this method was subsequently discontinued.

Solvatochromic polarity parameters

Spectrophotometric changes observed when solvents are introduced to solvatochromic dyes showed potential in quantifying polar interactions between solvents and polymers (Reichardt, 1988; Rose-Pehrsson and Krech, 1995). The corresponding polarity parameters reflect the intensity of solute/solvent interactions (Kosower, 1958; Abboud *et al.*, 1977; Hubert *et al.*, 1995; Rose-Pehrsson and Krech, 1995; Jonquières *et al.*, 1996; Feng and Huang, 1997). However, impregnating solvatochromic dye into a wide variety of polymers to be tested was impractical (Hubert *et al.*, 1995), negating its potential for selecting novel polymer membrane materials.

UNIQUAC

The universal quasi-chemical activity coefficient (UNIQUAC) (Heintz and Stephan, 1994) is another pre-screening tool for selecting membranes materials for aqueous/organic separations. Ferreira *et al.* (2001) used a semi-empirical equation that relates the enrichment factor to the molecular structure of the permeants and the feed conditions. However, this model does not account for molecular size, so the tendency for small molecules to permeate through a membrane more quickly than larger molecules is not predicted. Lue *et al.* (2004) reported low correlation between experimental and UNIQUAC predicted values for organic/organic mixtures.

Hansen Solubility Parameters

Solubility parameters proposed by Hansen (1969) are an ideal means of quantifying the affinity between a polymer membrane and any given solute, and hence predict the selective permeation through the membrane. Hansen solubility parameters (HSP) have significant potential for identifying novel membrane materials for PV fractionation (Feng and Huang, 1997), based on the concept that preferential sorption is the prerequisite to preferential permeation (Mulder *et al.*, 1985; Wenzlaff *et al.*, 1985; Mulder and Smolders, 1986). Hansen solubility parameters are able to quantify the relationship between the polymer and solvent/solute. Analyses by Mulder *et al.* (1982), Cabasso (1983), Lloyd and Meluch (1985), Lee *et al.* (1987), Yamaguchi (1992; 1993), Jonquières *et al.* (1996), Ray *et al.* (1997; 1999b), Wang *et al.* (2001), Buckley-Smith & Fee (2002b), Mandal and Pangarkar (2003) and Pal *et al.* (2005), have shown that HSP have great potential for selecting pervaporation membrane materials.

Conclusion

Preliminary reading and investigations indicated three potential membrane selection techniques that warranted further investigation: inverse gas chromatography (I-GC), solvatochromic polarity parameters and Hansen solubility parameters (HSP). The I-GC method quantifies interactions between polymer and solutes in the vapour phase, the solvatochromic method quantifies relationships between polymer and solutes in the liquid phase; and HSP collated from empirical and theoretical data have the potential to predict inter-atomic/molecular interactions between polymer and solutes.

Hansen solubility parameters were finally chosen as the membrane selection method because HSP showed the most promise to identify a novel membrane material for successfully separating a solution that has never been studied before. Once experimental work on homogeneous membranes has been completed, this method may be used further to find compatible polymers for copolymer membranes that have superior permeation characteristics as well as chemical and physical stability and mechanical strength.

2.7 Hansen solubility parameters

Solubility parameters are an attempt to quantify the chemist's “rule of thumb” that “like dissolves like” and extend the rule to encompass “like seeks like” (Hansen, 2004a). These

parameters follow the rule that if the parameters of two different materials are sufficiently close, then they should be mutually soluble. In terms of non-soluble or only partly soluble systems, the "like seeks like" rule means that those components or segments of components with similar energies will tend to aggregate with their own kind (Orme *et al.*, 2002; Hansen, 2004a).

In the late 1960s, Hansen studied miscibility relations between polymers and solvents and he quickly concluded that liquids with widely different solubility parameters tend to be immiscible and vice versa (although numerous other factors affect this phenomenon, including polymer crystallinity, molecular weight, and choice of solvent). These broad and general statements are typical of the observations one makes when considering solvent/polymer interactions from a solubility parameter point of view (Hansen, 1969; Croll and Stöver, 2003).

In addition to miscibility relationships between polymers and solvents, HSP concepts can be used to interpret relations involved in liquid-liquid miscibility, polymer-polymer compatibility, adsorption onto solid surfaces, dispersion phenomena, solubility of inorganic as well as organic materials in organic liquids, and "salting in" phenomena. Since the phenomena of solution, adsorption, and dispersion are vital to these situations, the general principles developed are easily applied to other systems. The first step in applying these principles is to characterize the polymeric material by a solubility parameter study, which traditionally involved contacting the material with numerous, well-chosen solvents under conditions relevant to a given problem, and observing what happens. When the energy properties of the material are similar to those of a given solvent, it will dissolve, swell, or adsorb on the material (Hansen, 1969).

Since all solvents that have properties in common with the material being studied are also similar to each other, a suitable presentation of solvent properties will yield regions of interaction for the material and a physical characterization of polymer energy properties in terms of solvent energy properties. The nature of the material itself does not have much influence, as long as differences in its physical behaviour with various organic solvents can be detected (Hansen, 1969).

2.7.1 Origin of Hansen solubility parameters

Hansen solubility parameters have their roots in the research by Hildebrand and Scott in 1950 (Hansen, 2004a). Using solubility parameter to predict sorption selectivity lies in "The Regular Solution Theory", and was based on the energy required to vaporize the molecule and to expand the vapour to ideal gas state (Mandal and Pangarkar, 2003).

2.7.1.1 Hildebrand parameter

The solubility parameter (δ_H) defined by Hildebrand and Scott (1950) measured "cohesive energy density", or the strength of the intermolecular forces (cohesive energy) holding molecules together in the liquid phase (Mandal and Pangarkar, 2002b; Price and Shillcock, 2002). The Hildebrand value for low molecular weight liquids is calculated via the heat of vaporisation (ΔH_{vap}), and molar volume (V = density / molecular weight = cm^3/mol)) (Orme *et al.*, 2002):

$$\delta_H^2 = \frac{\Delta H_{vap} - RT}{V} = \left(\frac{\Delta E}{V}\right) = \left(\frac{(E_{coh})_{total}}{V}\right) \qquad \text{(Eqn. 2:09)}$$

The cohesive energy of a material is the amount of energy to separate the constituent atoms or molecules to an infinite distance; hence, it is a direct measure of the attraction its atoms or molecules have for one another. Thus, $(\Delta E_{coh})_{total}/V$ indicates the amount of total energy required to vaporise a unit volume of the liquid (Hancock *et al.*, 1997; Mandal and Pangarkar, 2002b). However, since polymers tend to degrade rather than evaporate, they do not have a ΔH_{vap}. Consequently, their δ_H is usually determined using solvent/non-solvent correlation information (Orme *et al.*, 2002) using enthalpy of mixing (ΔH) instead of ΔH_{vap}.

Dissolving an amorphous polymer in a solvent is governed by the free energy of mixing (ΔG) (Pal and Pangarkar, 2005):

$$\Delta G = \Delta H - T\ \Delta S \qquad \text{(Eqn. 2:10)}$$

where ΔS is entropy of mixing.

For mutual solubility of two components, ΔG should be negative so that the mixing process will occur spontaneously (Mandal and Pangarkar, 2002b). Because dissolution of a high-molecular-weight polymer is always connected with a modest increase in ΔS, enthalpy (sign and magnitude of ΔH) determines the sign of ΔG. Enthalpy of mixing (ΔH) can be correlated to the solubility parameter (δ) (Mandal and Pangarkar, 2002b; Pal and Pangarkar, 2005):

$$\Delta H = \varphi_1 \varphi_2 V_1 (\delta_1 - \delta_2)^2 \qquad \text{(Eqn. 2:11)}$$

where φ_1 and φ_2 are volume fractions of the solvent and solute respectively, and V_1 is molar volume of the solution. Since ΔS is positive, ΔH must be reduced as much as possible to ensure a more negative ΔG. Hence, for higher affinity between the polymer and the penetrant, $\Delta\delta$ should be as small as possible (Mandal and Pangarkar, 2002b; Pal and Pangarkar, 2005). When δ_1 is equal to δ_2, ΔG is always less than zero and the components are miscible in all proportions. In general, the difference must be small for miscibility over the entire volume fraction range (Pal and Pangarkar, 2005).

The concept of the Hildebrand parameter was originally developed for simple liquid mixtures. To extend the principles to more complex situations, several approximations and assumptions are required. To apply solubility parameter theories to ideal gases and organic solids, gases are treated as hypothetical liquids whilst solids are treated as super-cooled liquids (Hancock *et al.*, 1997).

The Hildebrand parameter works well for low molecular weight non-polar solvents and polymers. However, a single parameter cannot adequately describe solubility behaviour when polar and hydrogen-bonding solvents are included in the system. HSP address this problem by using three parameters to describe solubility behaviour (Orme *et al.*, 2002; Mandal and Pangarkar, 2003). For example, while the Hildebrand parameters for xylene and propyl acetate are identical, their HSP emphasise the higher dipolar and hydrogen bonding ability of the ester (Croll and Stöver, 2003).

2.7.1.2 Division of inter-molecular forces

Cohesive energy is the net effect of all the inter atomic/molecular interactions including Van der Waals interactions, covalent bonds, ionic bonds, hydrogen bonds, electrostatic interactions, induced dipole and permanent dipole interactions (Hancock *et al.*, 1997). The total cohesive energy (E_{total}) that holds a liquid together is approximated by the sum of the energy required to overcome atomic dispersion (London) forces (E_d), forces between permanent dipoles of adjacent molecules (polar interaction) (E_p), and to break hydrogen bonds (exchange of electrons, proton donor/acceptor) between molecules (E_h) (Hansen, 1969; Hansen, 2000; Mandal and Pangarkar, 2002b).

$$E_{total} = E_d + E_p + E_h \qquad \text{(Eqn. 2:12)}$$

Dividing this equation by the molar volume of a solvent gives (Hansen, 1969);

$$\frac{E}{V} = \frac{E_d}{V} + \frac{E_p}{V} + \frac{E_h}{V} \qquad \text{(Eqn. 2:13)}$$

or, alternatively written;

$$\delta_t^2 = \delta_d^2 + \delta_p^2 + \delta_h^2 \qquad \text{(Eqn. 2:14)}$$

where δ_t (total solubility parameter) should be identical to δ_H (Orme *et al.*, 2002) and $\delta_t = (E / V)^{½}$ = (cohesive energy density)^{½} (Hansen, 1969).

Thus, HSP is made up of three individual parameters:

Dispersion	Polar	Hydrogen bonding
$\delta_d = (E_d / V)^{½}$	$\delta_p = (E_p / V)^{½}$	$\delta_h = (E_h / V)^{½}$

Units for these parameters were traditionally (cal/cc.)^{½} (Hansen, 1969), but more recently units of (J/cm^3)^{½} or (MPa)^{½} have been used (Hancock *et al.*, 1997).

Although Hansen's (1967) study focused on solubility of a polymer in a solvent rather than a solute into a polymer (as found in membrane systems), the underlying theory of cohesive energy and HSP being a qualitative measure of the inter-atomic/molecular interactions is of primary importance (Feng and Huang, 1997). However, if the solute is too soluble in the polymer, the membrane is likely to disintegrate, or the desirable solute may 'stick' to the polymer (Schrodt *et al.*, 1961). Thus, a trade-off will be necessary as chemical and thermal stability of the polymer membrane becomes an important issue (Koops and Smolders, 1991).

2.7.2 Calculation of the solubility parameter

The solubility parameter concept is fundamentally sound because it is based on well-defined and correct principles. It uses the so-called geometric mean of interactions in two pure liquids to estimate the interaction between the unlike molecules in their mixtures. The use of the geometric mean has been shown experimentally (using hundreds of HSP correlations for solubility, surface phenomena, etc.), to represent data correctly. This is true not only for non-polar interactions, but also for permanent dipole–permanent dipole and hydrogen bonding between the molecules (Hansen, 2004a).

Modern Hansen solubility parameters can be derived by numerous empirical and theoretical methods, including actual dissolution experiments, and correlations such as group contribution, sublimation, vaporisation, inverse gas chromatography, polymer swelling, partition coefficients, calorimetry and surface tension (Mulder *et al.*, 1982; Rey-Mermet *et al.*, 1991; Yamaguchi *et al.*, 1993; Hansen, 2000).

2.7.2.1 Calculating solvent HSP

Numerical values for the component parameters were originally determined in the following way. First, the dispersion force for a particular liquid was calculated using the homomorph method. The homomorph of a polar molecule is the non-polar molecule most closely resembling it in size and structure (n-butane is the homomorph of n-butyl alcohol). The Hildebrand value for the non-polar homomorph (being due entirely to dispersion forces) was assigned to the dispersion component value (δ_d) of the polar molecule. This δ_d squared value was then subtracted from the square of the Hildebrand (δ_H) value of the liquid. The remainder (δ_a) was designated as a value representing the total polar interactions of the molecule ($\delta_a = \delta_p^2 + \delta_h^2$). Through trial and error on numerous solvents and polymers, Hansen separated the polar value into polar and hydrogen bonding component parameters best reflecting empirical evidence displayed by dipole moments (Burke, 1984).

Modern HSP for solvents are primarily determined from their refractive index (δ_d), dipole moment (δ_p) and group contribution methods (δ_h) (Yamaguchi *et al.*, 1992).

2.7.2.2 Calculating polymer HSP

Hansen solubility parameters for polymers were traditionally obtained by an indirect method which involved placing the relevant material in contact with many (>40), well-chosen solvents under conditions relevant to a given problem. When the energy properties of the material are similar to those of a given solvent, it will dissolve, swell, or adsorb onto the material (Hansen, 1969).

Thus, is can be seen that Hansen parameters are concerned with the magnitude and nature of energies holding a unit volume of a solvent or material together (cohesion), rather than the strength of a particular type of bond (Hansen, 1969).

Hansen (1969) found that plotting so a unit distance on the δ_d axis is twice that along the δ_p and δ_h axes, yields essentially spherical interaction regions (Figure 2:15). The coordinates at the centre of the solubility sphere located by the three component parameters (δ_d, δ_p and δ_h); coupled with a radius, characterizes a material. Researchers identified that solvents for the polymer lay within the sphere (radius of interaction, R_o) and non-solvents lay outside the sphere (Hansen, 1969; Burke, 1984; Frank *et al.*, 1999).

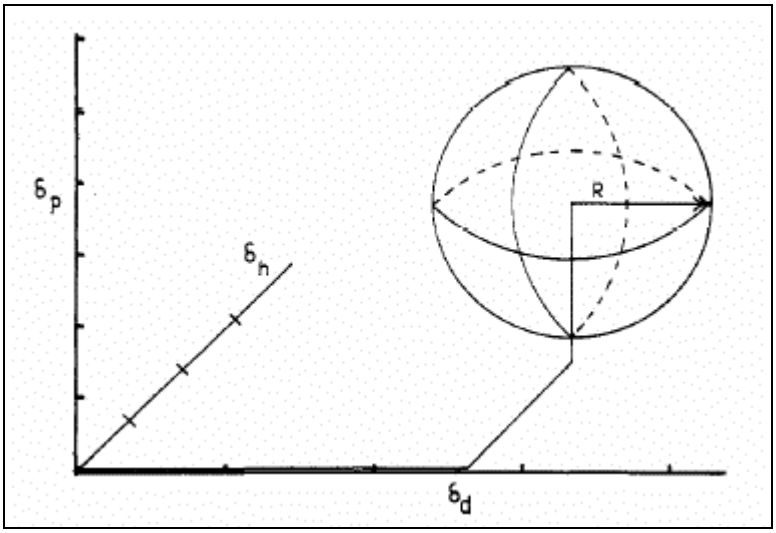

Figure 2:15 Typical volume of interaction (Hansen, 1969).

2.7.2.3 Numerical representation of HSP

Although *n*-hexane, cyclohexane and benzene have the same number of carbons; *n*-hexane has the smallest dispersion component of the first series of molecules shown in Table 2:04. The polarity parameter for *n*-hexane, cyclohexane and benzene is zero, but increases for toluene which has a methyl group that distorts the spread of π electrons in the unsaturated ring and gives toluene a slightly polar charge ($^S\delta_p = 1.4$). Phenol, with its alcohol group, has the highest polar contribution to its cohesive energy. The hydrogen-bonding component also increases steadily from *n*-hexane through to phenol.

The homologous series of alcohol molecules demonstrates that dispersion increases with increasing molecular weight and number of carbons. The polar and hydrogen bonding components decrease as carbon chain length increases because the solitary alcohol group has less influence on overall properties of the molecule.

Table 2:04 Published Hansen solubility parameters for solutes and polymers (Macrogalleria, 1996; Hansen, 2000; ChemFinder, 2002).

Solute/Polymer	Structure	δ_d	δ_p	δ_h	R_o
n-Hexane		14.9	0.0	0.0	-
Cyclohexane		16.8	0.0	0.2	-
Benzene		18.4	0.0	2.0	-
Toluene	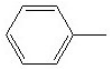	18.0	1.4	2.0	-
Phenol	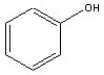	18.0	5.9	14.9	-
Methanol		15.1	12.3	22.3	-
Ethanol		15.8	8.8	19.4	-
Propanol		16.0	6.8	17.4	-
Cellophane (CPN)	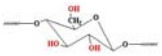	16.1	18.5	14.5	9.3
Nylon (PA)	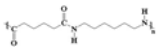	16.0	11.0	24.0	3.0
Teflon (PTFE)	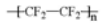	17.1	8.1	1.3	4.7

Teflon is considered a low polarity polymer, because it has low dipole interactions and limited opportunity for hydrogen bonding between molecular chains. Both cellophane and nylon contain oxygen groups and hence have significant polar and h-bonding components. The large R_o value for Cellophane (a naturally occurring cellulose-based polymer), indicates that solvents over a wider range of solubility parameters can solubilise it.

To determine if a solute lies within the solubility sphere of a polymer, its position from the centre of the polymer solubility sphere must be less than the radius of interaction for the polymer (Eqn. 2:15) (Burke, 1984; Hansen, 2000).

$$\Delta\delta_{(S-P)} = [4({}^{S}\delta_d - {}^{P}\delta_d)^2+({}^{S}\delta_p - {}^{P}\delta_p)^2+({}^{S}\delta_h - {}^{P}\delta_h)^2]^{½} \quad \text{(Eqn. 2:15)}$$

where;

$\Delta\delta_{(S-P)}$ = distance between solute and centre of solubility sphere

${}^{S}\delta$ = Hansen parameter for solvent

${}^{P}\delta$ = Hansen parameter for polymer

The constant (4) in the first term of Equation 2:15 creates a spherical volume of solubility by doubling the δ_d axis (Burke, 1984).

The difference between the solubility parameters of a polymer and a liquid, $\Delta\delta$, indicates their affinity. The smaller $\Delta\delta$ is, the greater the affinity between polymer and liquid (Villaluenga *et al.*, 2003). This method avoids relying on graphic representations of solubility behaviour allows numerical values to be used solely (Burke, 1984).

Relative energy difference

The RED number, calculated from the difference in HSP of the materials involved, is frequently used as a single parameter to evaluate the compatibility of the solute and polymer.

$$RED = \Delta\delta_{(S\text{-}P)}/R_o \qquad \text{(Eqn. 2:16)}$$

RED is zero for a perfect match of two materials values, and progressively higher RED numbers indicate decreasing compatibility (Hansen, 2004b). If the RED is less than unity (i.e., radius is larger than HSP difference), then the polymer should be soluble in the solvent. The solubility of methanol and benzene in polymers such as Cellophane, nylon and Teflon are shown in Table 2:05.

Only methanol is soluble in nylon (RED < 1.0). However, methanol is close to the edge of the solubility sphere of Cellophane (RED ≈ 1.0), and benzene is close to the perimeter of Teflon's solubility sphere, indicating potential attraction between these solvents and polymers even though dissolution is unlikely.

Table 2:05 Predicting polymer solubility in benzene and methanol (Hansen, 2000).

	Benzene			Methanol		
	$\Delta\delta_{(S\text{-}P)}$	RED	Solubility	$\Delta\delta_{(S\text{-}P)}$	RED	Solubility
Cellophane (CPN)	22.07	2.37	No	10.16	1.09	No
Nylon (PA)	24.68	8.23	No	2.80	0.93	Yes
Teflon (PTFE)	7.69	1.64	No	21.79	4.64	No

HSP correlations can also be based on a given amount of swelling or uptake rather than complete solubility. In this case, RED = 1 indicates compatibility at the amount used to separate the "good" solvents from "bad" ones (Hansen, 2004b).

Graphical presentation of HSP

Traditionally graphical representations of Hansen parameters were defined on three-dimensional Cartesian coordinates. These three dimensional Hansen parameters are reasonably accurate for predicting solubility behaviour because precise values for all three component parameters are used, and concise because the entire solubility volume for a polymer can be indicated by four terms rather than one set of parameters and a radius (Burke, 1984). However many people have difficulty in graphically presenting and/or understanding the data in three dimensions.

Hansen's three dimensional volumes can be presented in two dimensions by plotting a cross-section through the centre of the solubility sphere on a graph using only two of the three parameters (most commonly δ_p and δ_h). A two-dimensional presentation sacrifices some of the accuracy and conciseness for a system that clearly and easily illustrates the relative positions of many materials.

Predicting whether a polymer is soluble in a binary solvent mixture is possible mathematically but is more easily accomplished by seeing whether a line drawn between the two solvents passes through the area of solubility for the polymer (Burke, 1984). As an example, the volumes of solubility for Cellophane, Nylon and Teflon; and a variety of solvents are plotted using the polar component parameter and the hydrogen bonding component parameter (Figure 2:16). In this plot, methanol can be seen inside the R_o of Nylon, and on the periphery of the Cellophane solubility sphere; whereas ethanol appears outside the solubility spheres of all three polymers.

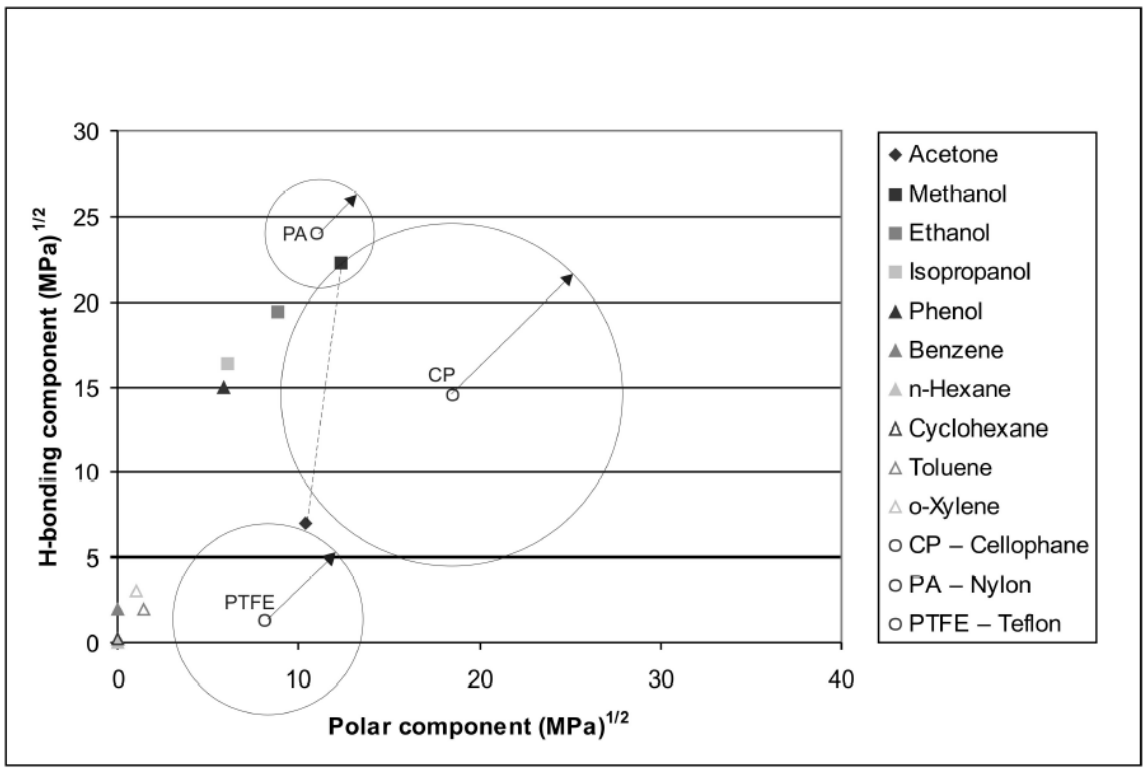

Figure 2:16 Solubility parameters for some polymers and solvents as a function of δ_p and δ_h.

Several researchers have used this graphical presentation to describe HSP (Hansen, 1969; Yamaguchi *et al.*, 1993); while others combine the dispersion and polar components to obtain δ_v (Jonquières *et al.*, 1996; Jou *et al.*, 1999; Orme *et al.*, 2002), :

$$\delta_v = (\delta_d^2 + \delta_p^2)^{½} \qquad \text{(Eqn. 2:17)}$$

Displaying a three-dimensional parameter using only two dimensions can be misleading. In the two dimensional plot (Figure 2:16), a binary mixture of methanol and acetone appears to be soluble in cellophane whereas using the combined parameter (δ_v) shows clearly that these solvents are outside the solubility sphere for cellophane (Figure 2:17).

Despite being more difficult to visualise trends occurring, the numerical method is a more thorough method of determining solubility interactions between polymers and solvents than simplified graphical presentations.

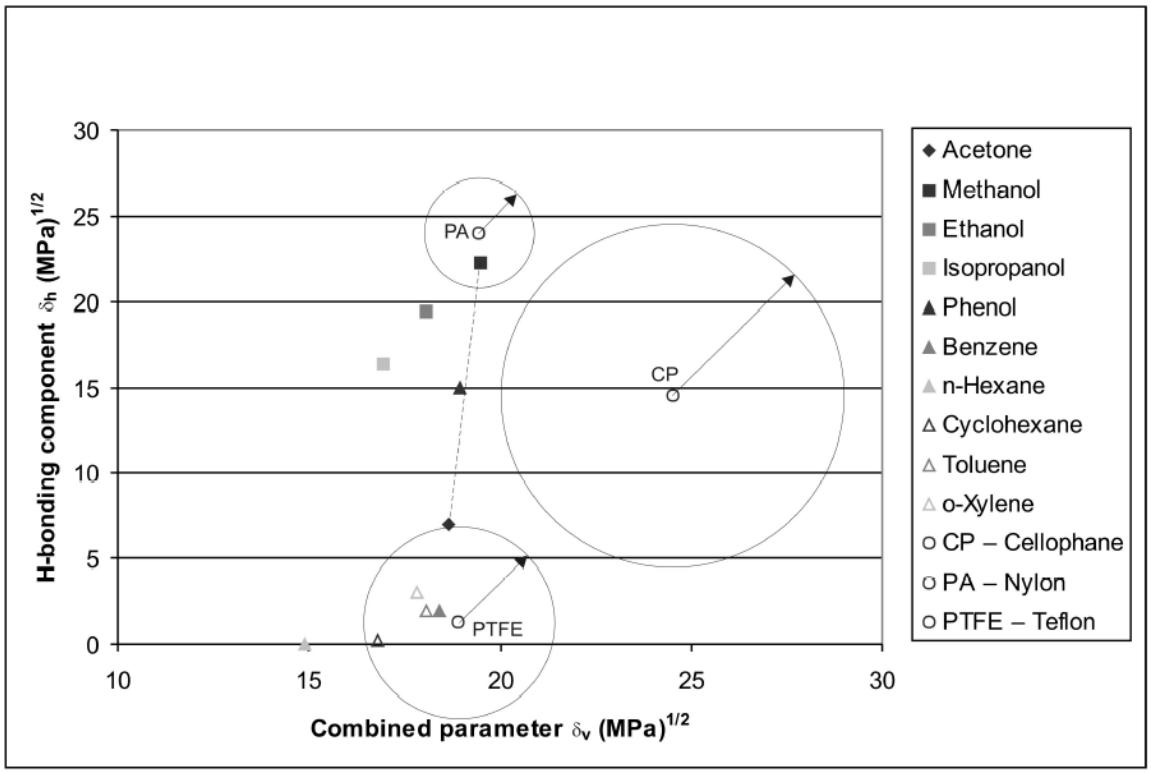

Figure 2:17 Solubility parameters as a two dimensional plot of δ_h and the combined parameter $\delta_v = (\delta_d^2 + \delta_p^2)^{½}$.

2.7.3 Variation within published HSP

Hansen (2000) acknowledges there may be local variations in HSP of some polymers, especially if they are not homopolymers. This is because absorbed solvents tend to locate in regions with similar solubility parameter; clustering around chemical groups that may be different from the bulk polymer, around additives, or localise around one species of a copolymer. Crystalline regions within a polymer are also unlikely to contain solvent.

Consistency between manufacturers

A gap in the literature was observed regarding the consistency of HSP values within a polymer species. Where multiple entries existed in the literature for polymers with the same functional groups, the statistical variation of HSP data collated from Hansen's (2000) and Mulder (1982) was analysed using an Excel spreadsheet. Polymers displayed in Figure 2:18 included Cellulose acetate (CA), Cellulose acetobutyrate (CAB), Polyamide (PA), Polycarbonate (PC), Polyethylene (PE), Poly(ether imide) (PEI), Poly(ether sulphone) (PES), Poly(methyl methacrylate) (PMMA), Polypropylene (PP), Polystyrene (PS), Polysulphone (PSU), Poly(tetrafluoro ethylene) (PTFE), Polyurethane (PUR), Poly(vinyl alcohol) (PVA),

Poly(vinyl chloride) (PVC). Figure 2:18 indicated that values for the dispersive parameter (δ_d) had the least statistical variation (average standard error of ± 0.6 $MPa^{½}$).

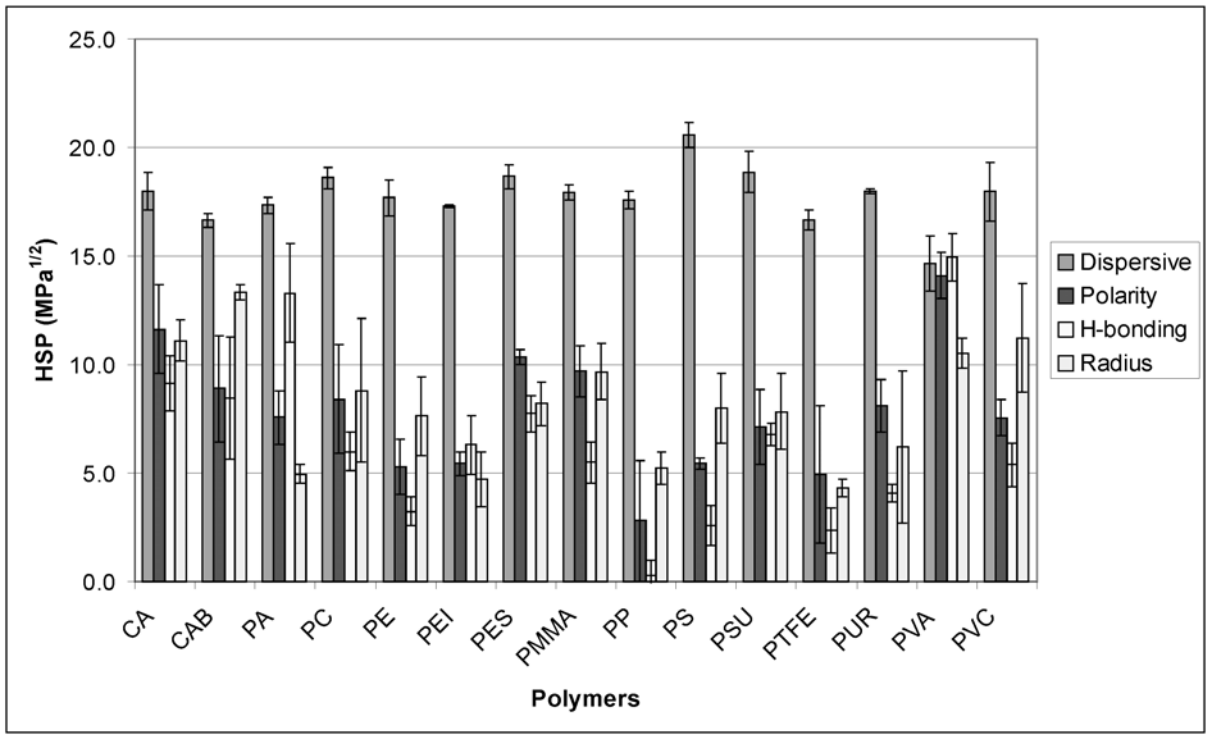

Figure 2:18 Degree of variation in Hansen Solubility Parameters for common polymers. Error bars show standard error of the mean.

The polar (δ_p) and H-bonding (δ_h) parameters had an average standard error of ± 1.5 $MPa^{½}$, and ± 1.1 $MPa^{½}$, respectively for the polymers studied. This degree of variation is likely due to differing manufacturing practices, and the presence of processing residues and additives such as plasticizers, compounding agents, and dyes commonly used.

The parameters for PC, PTFE, and PUR had the largest variation for all parameters, however this is probably due to the small sample sizes (n=2), compared to PE (n=11), PMMA (n=9), CA (n=8), and PA (n=6). The variability for Nylon was expected as this subset was calculated for polymer repeating units PA 6, PA 6-6, PA 11 and PA 12.

The variability of HSP for polyethylene (PE) (Figure 2:19) is likely due to different manufacturing processes, degree of cross-linking, crystallinity, density, polymerization times and chain length; or additives such as plasticizers, colourants, stabilisers, and crosslinking agents (Zhang and Drioli, 1995). High density polyethylene (HDPE) has a published polarity of zero (Figure 2:19), compared to low density polyethylene (LDPE), and other polyethylene

polymers where the density was not given (Hansen, 2000). Of particular interest, the component parameters (δ_d, δ_p, and δ_h) and solubility radius of 'R HDPE/LDPE' mixed density polymer is intermediate between LDPE and HDPE.

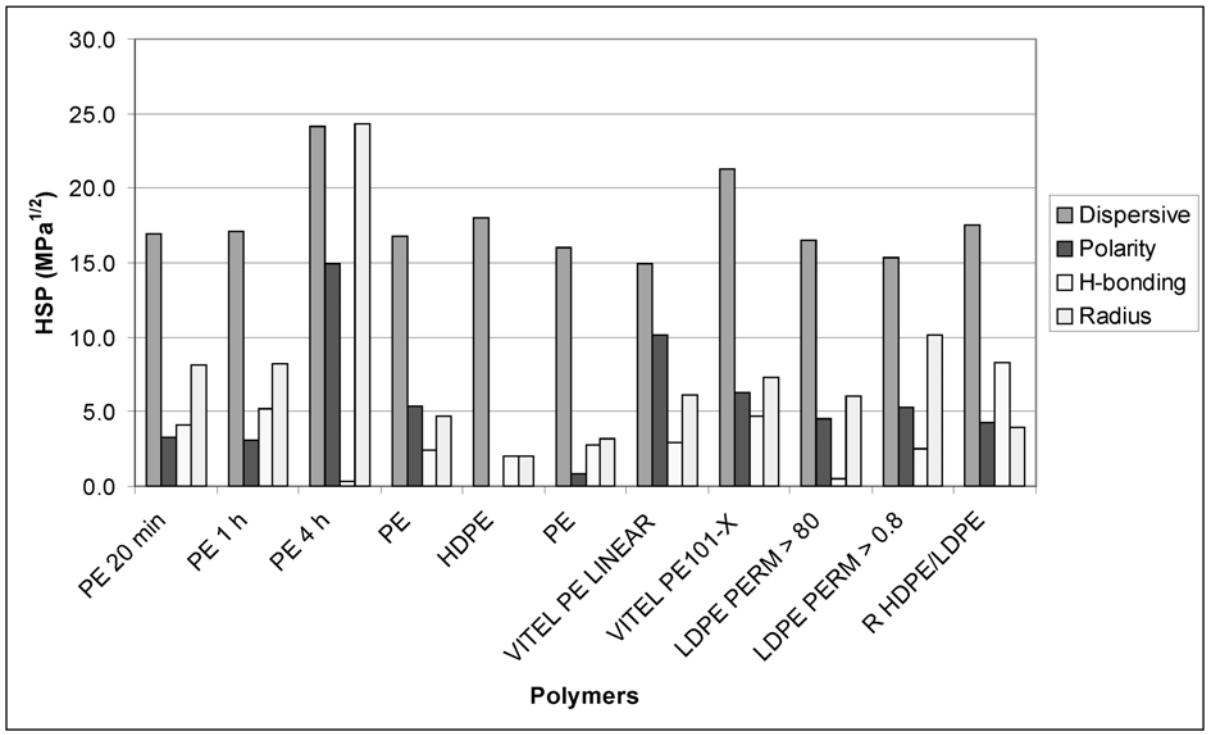

Figure 2:19 Variation in Hansen solubility parameters for polyethylene polymers (Hansen, 2000).

The largest variation was seen in the radius of the solubility sphere. The very high R_o value for "PE 4h" (Figure 2:19), implies that its solubility sphere is more than twice the diameter of any other PE polymers, and is soluble in a very large number of solvents.

2.7.4 Consistency between different methods of data collection

Several authors note that the methods used to obtain HSP produce different values (Rey-Mermet *et al.*, 1991; Jonquières *et al.*, 1996; Hancock *et al.*, 1997).

Solute HSP calculation

Rey-Mermet *et al.* (1991) analysed the HSP values obtained by various methods (Table 2:06). Variation in the total solubility parameter of materials are common when calculated by different methods (Hancock *et al.*, 1997).

Table 2:06 Solubility parameters of caffeine obtained by various methods ($MPa^{½}$).

Method	**Dispersion (δ_d)**	**Polarity (δ_p)**	**H-bonding (δ_h)**	**Total (δ_t)**
IGC [#]	17.0	11.7	17.0	26.7
Solubility [#]	20.1-20.6	7.2-13.9	10.5-18.6	26.6-28.7
Solubility *	19.5	10.1	13.0	
Partition [#]	21.4	3.8	8.3	23.3
Calorimetry [#]	17.3	13.7	13.4	25.8
Group Contribution [#]	20.0	14.3	13.3	28.0
Mean:	19.4	10.7	13.4	26.4
Std. Dev:	1.7	3.9	3.5	1.8

(Hancock *et al.*, 1997)[#], (Hansen, 2004b)*

The values calculated by group contribution are within one standard deviation of the mean of values obtained by the various methods (Table 2:06). The traditional solubility method appears to be the most reliable and the partition method the least reliable method of obtaining HSP.

Polymer HSP calculation

Several methods have been used to obtain the solubility parameters of polymer materials (Table 2:07), including swelling in solvents, viscosity, refractive indices, dipole moments, group contribution and the traditional method of solubility analysis. Solubility parameters calculated from swelling data are generally considered to be accurate to within 5% (Van Krevelen, 1990). By comparison, solubility parameters calculated by group contribution methods have an accuracy of approximately 10% (Jonquières *et al.*, 1996).

Dipole moment data is rarely available for polymer materials and the polarity values obtained by this method were much lower than those obtained by solubility analysis. The dispersive component value calculated from the refractive index was similar to the value obtained by solubility analysis. Values obtained by swelling experiments were also similar.

It is important to minimise errors associated with determining the solubility parameters of solutes/solvents and polymers by direct and indirect methods. Wherever possible, more than one method should be used to determine the HSP of a polymer and predictions of material properties or interactions should ideally be supported by other analyses (Hancock *et al.*, 1997). If the solubility method is not an option due to time constraints or the vast array of potentially toxic solvents that must be tested (>40), the next best option is to average HSP from the most reliable methods listed in Tables 2:06 and 2:07.

Table 2:07 Effect of methodology on solubility parameters ($MPa^{½}$) of poly(methyl acrylate) cited in Yamaguchi, (1992).

Calculation Method	Dispersion (δ_d)	Polarity (δ_p)	H-bonding (δ_h)	Total (δ_t)
Swelling [a]				20.8
Swelling *	18.0	9.0	4.9	20.7
Viscosity [b]				20.7
Refractive index [d]	17.1			
Dipole moment [d]		1.5		
Group contribution [c, e]	16.9	5.8	8.6	19.8
Solubility #	17.2-18.6	5.5-10.5	2.9-7.5	18.7-22.7
Mean:	17.6	6.5	6.0	20.6
Std. Dev:	0.8	3.5	2.6	1.4

[a]Mangaraj *et. al.* (1963a); [b]Mangaraj *et. al*. (1963b); [c]Small (1953); [d]Ahmad (1982); [e]Koenhen & Smolders (1975); cited in Yamaguchi (1992). * Yamaguchi (1992) calculated by swelling experiments where solvents that swelled the membrane >42% were classified as soluble. # Hansen (2000) collated for PMMA.

2.7.5 HSP assumptions, limitations and restrictions

Several authors have expressed reservations in using solubility parameters to predict polymer-solvent interactions (Mulder and Smolders, 1986; Lee *et al.*, 1987; Feng and Huang, 1997). These authors stated that solubility parameter theory is based on the assumptions of regular solution theory, and deviations from ideal behaviour (e.g. changes in volume on mixing) must be allowed for. Problems with HSP often occur in aqueous systems, which are highly hydrogen bonded, and with charged ionic species (e.g. salt forms). Solids and gases are approximated as liquids in the extended solubility parameter approach, and deviations from ideal behaviour can occur (Hancock *et al.*, 1997).

Solubility parameter approaches require several key assumptions and have some specific limitations and restrictions. These include diffusion-dominated systems, interference of competitive solutes in multi-component systems, the relationship between intermolecular attraction and distance from the centre of the solubility sphere, and the importance of entropy in polymer/solvent systems.

Diffusion dominated systems

The size and shape of the solute molecule effects diffusion, permeation, and equilibrium in a polymer/solvent system (Hansen, 2000). Smaller and more linear molecules diffuse more rapidly than larger more bulky ones (Hansen, 2000).

If diffusion dominates the separation process, the solubility parameter approach may be misleading (Feng and Huang, 1997). The extra weighting on the dispersive component of the solubility parameter calculation ($\Delta\delta_{(S-P)}$) (see Eqn 2:15), may allow for this (Hansen, 2000), however, some researchers alter this weighting factor (Zellers *et al.*, 1996b). An analysis of HSP dispersion values (Figure 2:20) shows that the average polymer dispersion value is higher ($^{P}\delta_d = 18.6 \pm 2.5$) than that of small solvents such as such as methanol ($^{S}\delta_d = 15.1$) or water ($^{S}\delta_d = 15.5$). The increased distance separating the polymer and the low molecular weight solute may induce an error in predicting selective permeation.

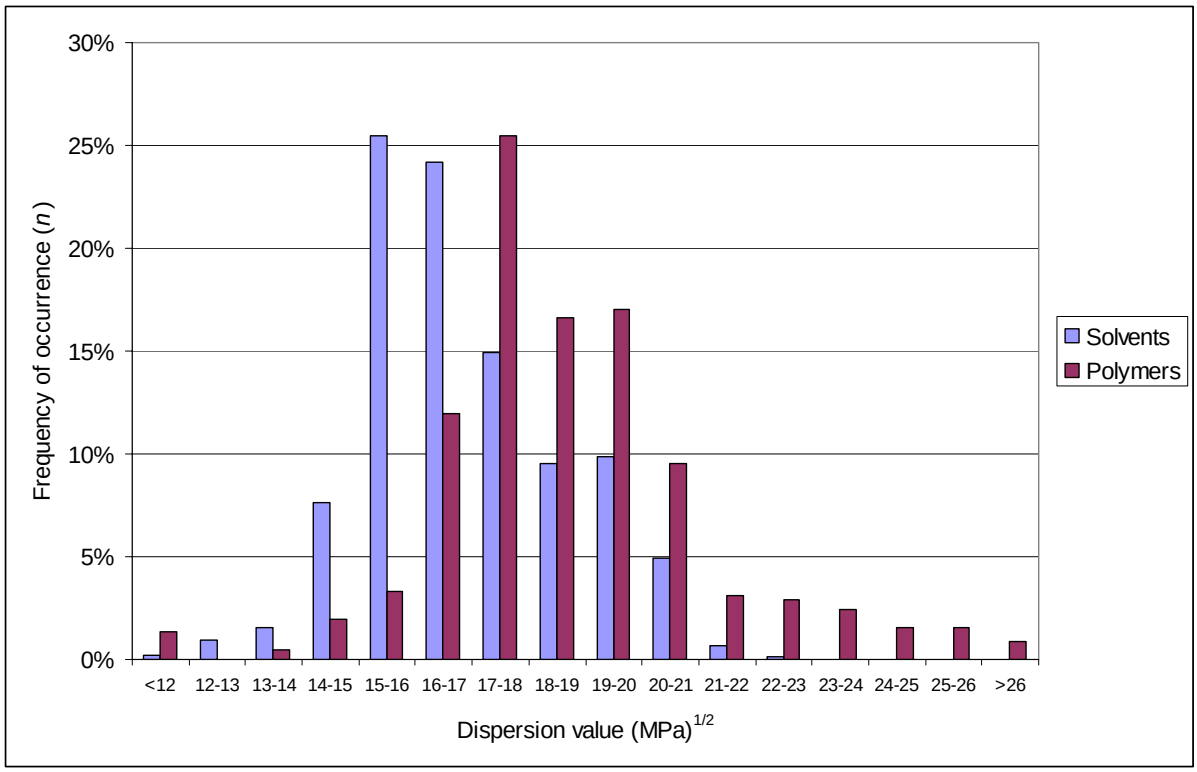

Figure 2:20 Distribution of solvent and polymer dispersion component values. Data collated from Hansen (2000).

The solution diffusion model of PV transport indicates that the solvent must adsorb onto the membrane surface before it can diffuse through the membrane and be swept away in the permeate. HSP methodology may underestimate the absorption of smaller molecules onto a polymer, especially in PV where a small solute is paired with a much larger one. In these cases, the ability of a polymer to preferentially permeate one molecule due to its affinity may be overridden by the ability of a small molecule to diffuse through the polymer. HSP is better for predicting selective permeation of comparable-sized, higher molecular weight molecules through the polymer membrane.

Pure substances and multi-component mixtures

Solute permeation in the presence of another solute can be quite different to permeation of a single species. Solubility parameters predict the affinity of solvents and polymers from the properties of pure substances and ignore the presence of competitive solutes (Mulder and Smolders, 1986; Lee *et al.*, 1987). As these competitive solutes can alter selectivity and flux in PV membranes, the reliability of HSP permeation predictions in ternary systems may be questioned. When comparing a polymer's affinity for each component in a system, the one with greatest affinity should preferentially adsorb and permeate through the membrane.

It is possible to use Hansen's tie-line method examine polymer solubility in a binary solvent mixture. Mixtures of miscible materials have intermediate solubility parameters, and multi-dimensional solubility parameter maps can be used to determine the compatibility of multi-component mixtures (Hancock *et al.*, 1997).

A simple two-dimensional plot using δ_p and δ_h can be used to solve practical problems. The nonpolar cohesion parameter, δ_d, cannot always be neglected, however noncyclic solvents used in practical situations tend to have similar dispersion parameters regardless of structure.

For example neither xylene nor n-butanol individually dissolves a high molecular weight epoxy as both solvents are outside the solubility sphere (Figure 2:21), and have very different HSP characteristics (Hansen, 2000). The tie-line for HSP of xylene and n-butanol crosses the solubility sphere, indicating that some combinations of these two solvents will dissolve Epoxy resin. This observation is reinforced by calculating the three-dimensional HSP (Table 2:08).

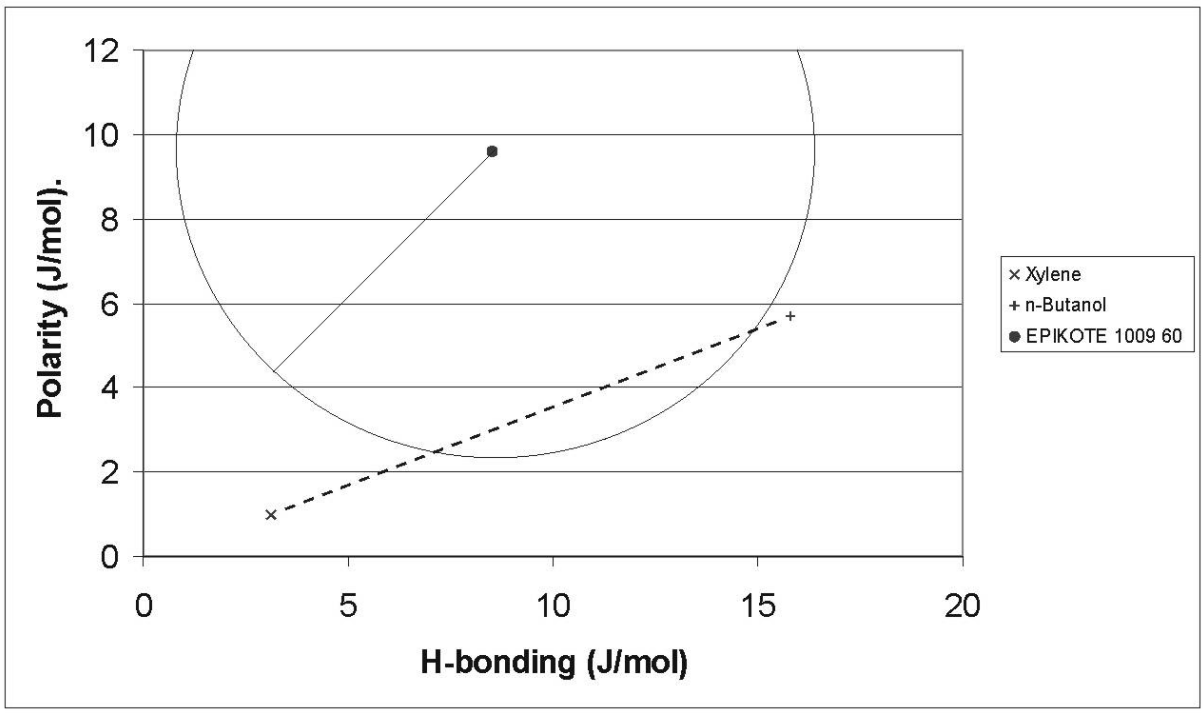

Figure 2:21 Two-dimensional plot of Hansen solubility parameters for xylene/*n*-butanol, and Epoxy resin polymer (Epikote).

Table 2:08 Hansen solubility values for Epoxy resin in pure solvents and 50 wt% xylene/*n*-butanol mixtures (Hansen, 2000).

Polymer/Solvent	δ_d (J/mol)	δ_p (J/mol)	δ_h (J/mol)	Radius (J/mol)	$\Delta\delta_{(S-P)}$ ($MPa^{1/2}$)	RED ($MPa^{1/2}$)
Epikote 1009 60	17.0	9.6	8.5	7.6		
Xylene	17.6	1.0	3.1		10.2	1.35
n-Butanol	16.0	5.7	15.8		8.5	1.12
50 wt% xylene/*n*-butanol	16.8	3.4	9.5		6.3	0.83

The RED for 50 wt% xylene/*n*-butanol is less than unity, indicating that this mixture has greater affinity for the polymer than the pure components. This phenomenon, easily accounted for in HSP terms, may explain the trends observed in PV where flux of a solvent mixture is greater than the flux of the components. Feed composition affects the degree of membrane swelling and consequently the rate solute can permeate through a membrane. Huang and Lin (1968) reported that the permeation rate for 50 wt% benzene/*n*-hexane (x_B = 50) was significantly higher than when the feed has pure benzene (x_B = 100) or pure *n*-hexane (x_B = 0) (Figure 2:22).

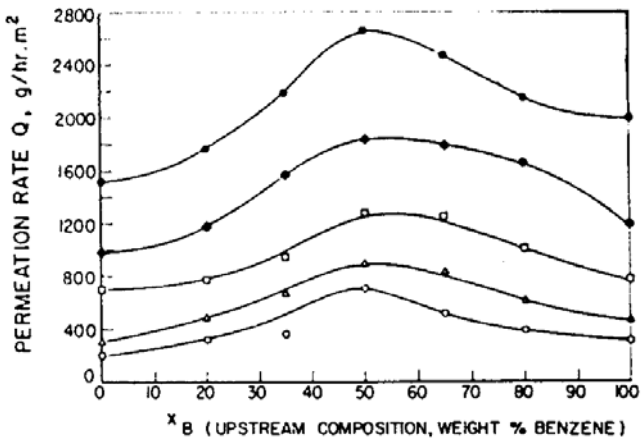

Figure 2:22 Effect of feed composition and temperature on permeation rate of benzene / n-hexane through an LDPE membrane(Huang and Lin, 1968). Temperatures: 45°C (●), 40°C (♦), 35°C (□), 30°C (Δ), 25°C (○).

HSP can predict the effect of composition on permeation rate. Figure 2:23 illustrates why a 50:50 mixture of benzene and *n*-hexane permeates through the LDPE membrane faster than the pure components.

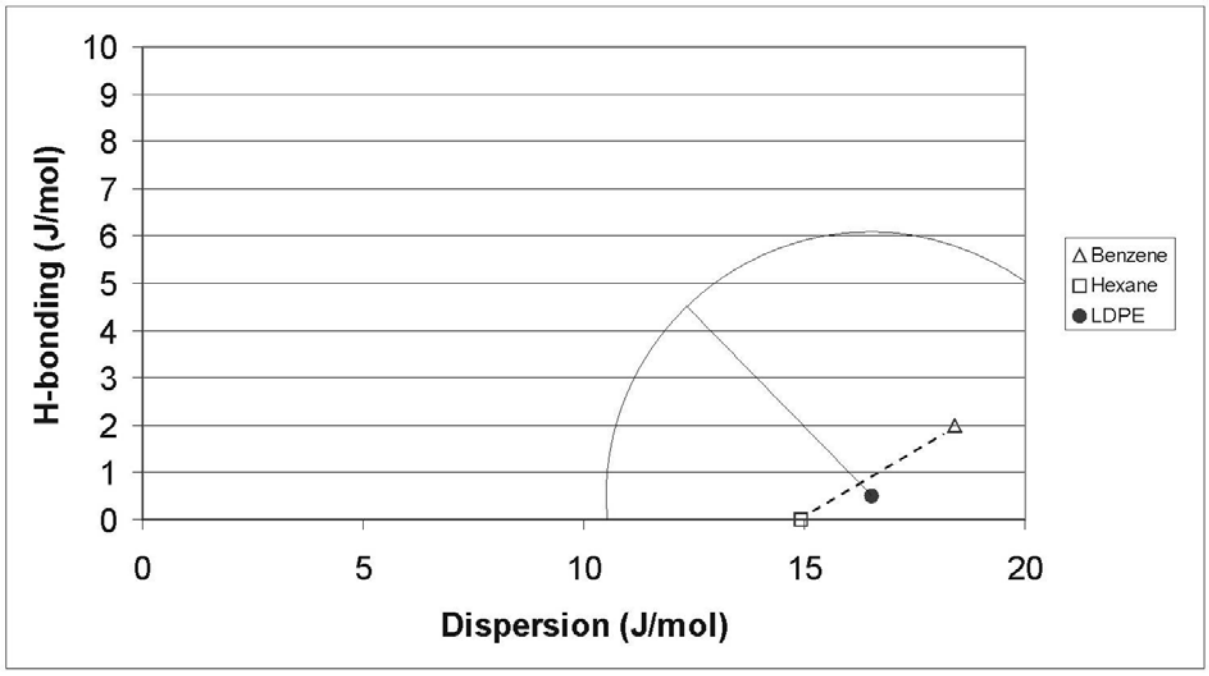

Figure 2:23 Two-dimensional plot of Hansen solubility parameters; Dispersion and H-bonding parameters for benzene and *n*-hexane, in conjunction with Low Density Polyethylene polymer.

The solubility parameters for the 50 wt% mixture are mid-way in the tie-line between the pure components. This mid-point is significantly closer to the polymers HSP than either pure

component, and thus has greater affinity for the membrane. The polymer is therefore more likely to swell which loosens the polymer structure, allowing more solute to permeate.

Two-dimensional visualisations can occasionally be deceptive. A more accurate analysis would include the third dimension (polarity) and calculate the RED between polymer and solute (Table 2:09). Benzene and *n*-hexane are both near the boundary of the solubility sphere, (RED = 0.91 and 0.92 respectively) close to unity. In comparison, the δ_d, δ_p and δ_h values of a 50 wt% mixture, places the solubility parameter ($\Delta_{(S-P)}$), well inside the LDPE solubility sphere with an RED of 0.68.

Table 2:09 Hansen solubility values for low density Polyethylene, benzene and *n*-hexane (Hansen, 2000).

Polymer/Solvent	δ_d (J/mol)	δ_p (J/mol)	δ_h (J/mol)	Radius (J/mol)	$\Delta\delta_{(S-P)}$ ($MPa^{½}$)	RED ($MPa^{½}$)
LDPE PERM > 80	16.5	4.5	0.5	6.0		
Benzene	18.4	0.9	2.0		5.4	0.91
n-Hexane	14.9	0.0	0.0		5.5	0.92
50:50 mixture	16.65	0.45	1.0		4.1	0.68

When HSP are examined more closely, hexane had zero polarity and hydrogen bonding parameters (see Table 2:09), whereas benzene had ${}^{S}\delta_p = 0.9$ and ${}^{S}\delta_h = 2.0$ which are closer to the moderate polarity values for LDPE. Thus LDPE and benzene have higher affinity for each other than do hexane and the polymer. Theoretically, one would expect the preferentially attracted component to be preferentially adsorbed to the membrane surface where it can migrate through the membrane and be swept away into the permeate collection vessel.

Huang and Lin (1968) also found that membrane selectivity decreased as concentration of the preferentially permeating benzene increased (Figure 2:24), this was probably due to a loosening of the structure allowing more of the less attractive component to permeate also.

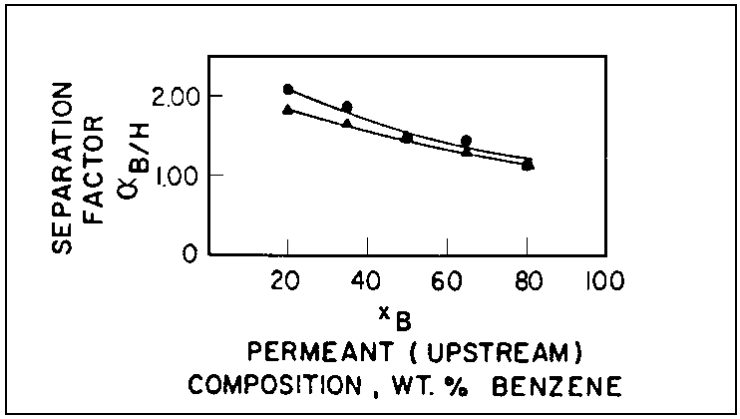

Figure 2:24 Separation of benzene/n-hexane mixture at 25°C (▲) and 45°C (●) (Huang and Lin, 1968).

Centre of Solubility Sphere

Zellers *et al.* (1996b) mistakenly challenged the commonly-held belief of an inverse relationship between the distance (in 3D-HSP space) between a given polymer and solvent and their mutual solubility or interaction strength. Their data for weight gain when butyl rubber was immersed in various solvents was logarithmically related to the 3D-HSP distance of butyl rubber and the solvent (Figure 2:25). Irrespective of the presence of misclassified solvents within the solubility sphere, a logarithmic relationship exists between the degree of swelling and proximity to the polymers HSP (centre of solubility sphere).

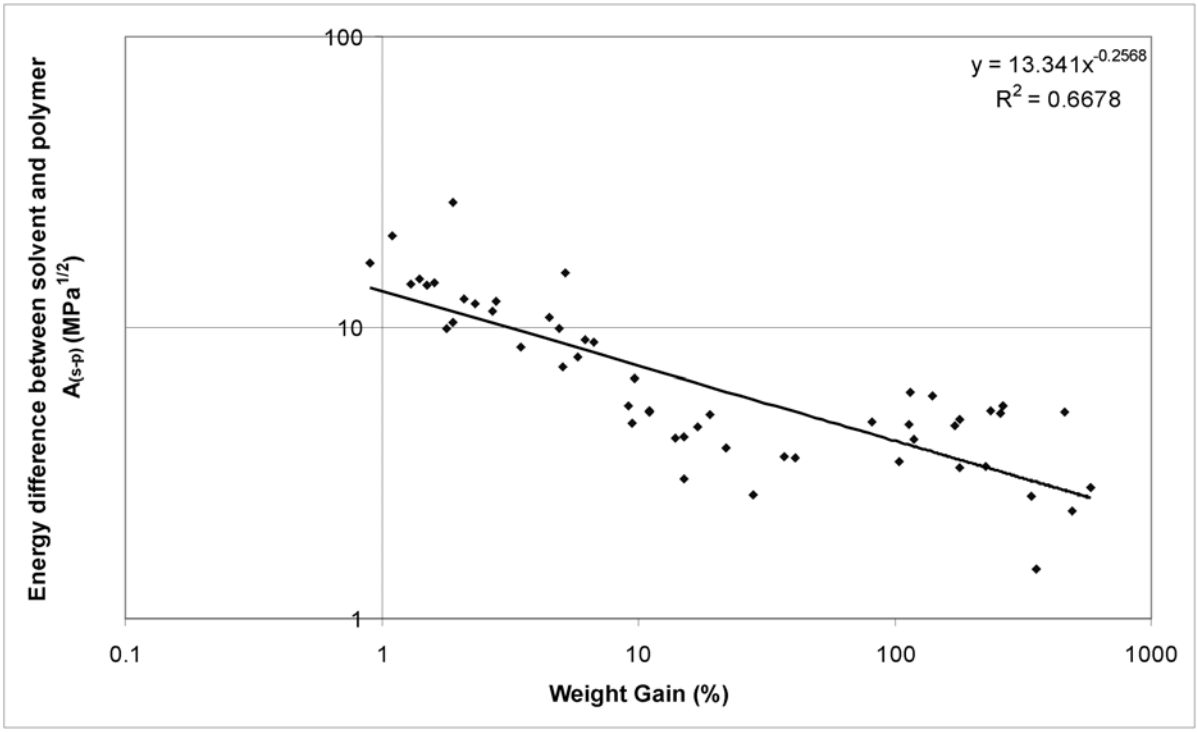

Figure 2:25 Logarithmic plot of 3D-HSP difference ($A_{(s-p)}$) and immersion-test weight gain for solvents in butyl rubber (Zellers *et al.* (1996b) data re-analysed).

The greatest correlation occurs between HSP and the weight gain of the less efficient solvents. The coefficient of determination rises from $R^2 = 0.67$ to 0.80 when only data for the polymers absorbing less than its own weight of solvent (<100%) are used.

Van Krevelen (1990) also showed an inverse relationship between interaction strength and the distance in 3D-HSP space separating polystyrene and solvents (Figure 2:26). These results also supports the practice of using swelling data to determine HSP of polymers.

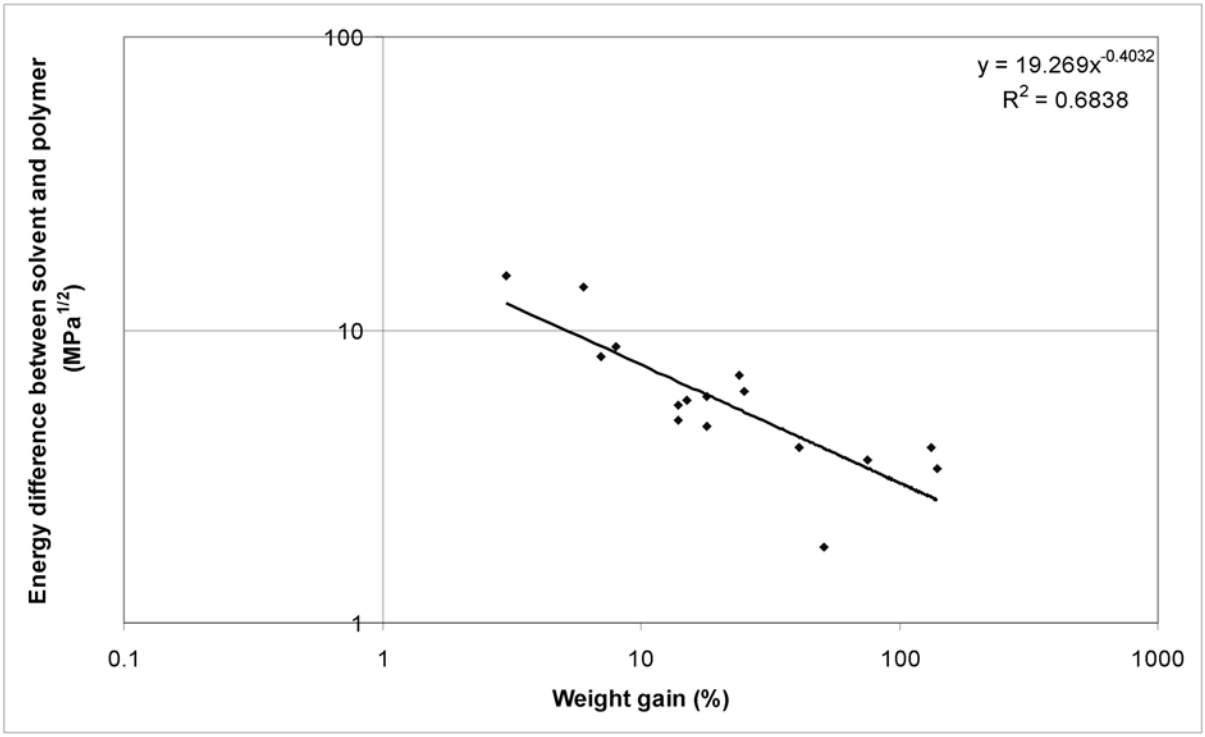

Figure 2:26 Logarithmic plot of Van Krevelen (1990) data for solubility of polystyrene in various solvents (δ_v x δ_h, where $\delta_v = (\delta_d^2 + \delta_p^2)^{0.5}$).

Entropy of mixing

Mulder *et al.* (1982) and Lee *et al.* (1987) identified some limitations for predicting selectivity from solubility parameter theory. Solubility parameter theory only accounts for direct contact energies between components (Rey-Mermet *et al.*, 1991; Rudolf *et al.,* 1995). Thus, only energetic contributions in the mixing process were included in the theory; entropic effects are disregarded (Mulder *et al.*, 1982; Lee *et al.*, 1989). As a polymer dissolves, it becomes molecularly disperse, or more disordered, during the mixing process (Horst and Wolf, 2005) and entropy increases. Although polymer dissolution is not the objective in PV membranes, membrane swelling does occur and increases the entropy of mixing. The

changes in mixing volumes, coil expansion, and chain rigidity (Anastasiadis *et al.*, 1988) are not accounted for in solubility parameters, which are based primarily on the attractive forces between molecules.

Hansen solubility parameters do not include kinetic effects on diffusion rates or other free volume considerations (Hansen, 2000). Heat increases the size of the solubility sphere due to an increase in disorder (entropy) of the system. The more disordered a system, the less it matters how dissimilar the solubility parameters of the components are. Since entropy is also affected by the number of elements in a system (more elements = more disorder), lower molecular weight polymers (many small molecules) will have larger solubility spheres than higher molecular weight polymer (few, large molecules) (Burke, 1984). All these effects could contribute to the degree of variation in polymer species HSP.

However, because complete dissolution of the membrane is not the objective, the fact that HSP do not account for entropic effects does little to detract from their usefulness in membrane material selection, and predicting selective permeation properties.

H-bonding donor/acceptor

Stavroudis and Blank (1989) consider that one of the weaknesses of the Hansen solubility parameters was that assigning a solitary hydrogen bonding parameter eliminated an important detail in the nature of hydrogen bonding. "For hydrogen bonding to occur there must be both a proton (hydrogen) donor site (e.g., an O-H group) and an acceptor site (for example, the electron pairs zipping about an oxygen atom, C=O, in a ketone)." Some molecules, for example chloroform, possess a donor site and no acceptor; others, like methyl ethyl ketone (MEK), have an acceptor without a donor. Stavroudis and Blank (1989) thought that a single number cannot represent both cases.

However, Hansen (2000) felt that proton donor and acceptor phenomena were adequately accounted for via the polarity and hydrogen bonding parameters for these molecules. Classifying the acid or base character leads to the generality that acidic molecules have higher δ_H, while basic molecules generally have higher δ_P (Hansen, 2004a). For example, cyclohexane has very low polarity parameters ($\delta_h = 0.2$ and $\delta_p = 0.0$); the proton-donating cyclohexanol has a very high hydrogen-bonding component ($\delta_h = 13.5$) and a moderate-to-low polar component ($\delta_p = 4.1$); and the proton-accepting cyclohexanone has moderate

polarity (δ_p = 6.3) and hydrogen bonding (δ_h = 5.1) parameters (Table 2:10). These HSP values highlight the influence of induced dipoles and uneven distribution of electrons in cyclohexanone, which can attract another molecule with the opposite induced charge.

Table 2:10 Effect of proton donor/acceptor on Hansen solubility parameters of various compounds (Hansen, 2000; ChemFinder, 2002).

Solvent	Structure	δ_d	δ_p	δ_h	Mol.Vol.
Cyclohexane		16.8	0.0	0.2	108.7
Cyclohexanol	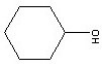	17.4	4.1	13.5	106.0
Cyclohexanone	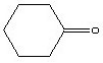	17.8	6.3	5.1	104.0
Glycerol	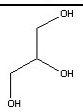	17.4	12.1	29.3	73.3
Ethylene glycol	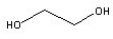	17.0	11.0	26.0	55.8
1,3-Butanediol	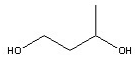	16.6	10.0	21.5	89.9
Nitromethane		15.8	18.8	5.1	54.3
Acetonitrile		15.3	18.0	6.1	52.6
γ-Butyrolactone		19.0	16.6	7.4	76.8

Compounds with multiple hydrogen bond donor sites such as glycerol, ethylene glycol and other multi-ols have very high h-bonding parameters (Table 2:10). Hydrogen bond acceptor compounds such as nitromethane, acetonitrile, and other lactones have very high polar contributions to HSP.

In addition to δ_P and δ_H having different values for acidic/alkaline molecules, the environment (e.g. pH) can change the charge (acidic = positive and basic = negative). However, HSP do not change with pH, giving the solubility parameter a robustness for determining solubility and affinity, that would be absent in more complex model (Hansen, 2004a).

Additives and manufacturing processes

Hansen (2000) was concerned about the reliability of solubility parameters if residual solvent from the formation process or other common polymer additives such as plasticizers, pigments, adhesion promoters, dispersion aids, surfactants, fire retardants, heat and light stabilizers, antioxidants, anti-static agents etc., remained in the polymer (Hansen, 2004b). Such additives affect polymer HSP, thus a polymer species manufactured by a different company could have a different HSP value.

Usefulness of Data

Cabasso (1983) felt the accuracy of the Hansen solubility parameter left much to be desired. However, although the calculated values for δ_d, δ_p, and δ_h are sometimes only crude estimations of the relevant forces and interactions, their shortcomings do not eliminate their usefulness completely. The solubility parameter theory is convenient to use and a useful first estimate of interaction phenomena (Mulder *et al.*, 1982; Lee *et al.*, 1987; Yamaguchi *et al.*, 1993). Hansen solubility parameters have been used to predict interactions between polymers and solutes with 95% accuracy in well over 400 cases in the paint industry (Hansen, 1967). In the least accurate correlation observed, nearly 82% of the solvents within the solubility sphere could dissolve the polymer (PVDC). Usually, 93-99% of the solvents within solubility sphere of a given polymer, can dissolve that polymer (Hansen, 2000).

Most exceptions tend to occur at the boundary of the solubility sphere, especially if the solvents have large molecular weights. Temperature can also influence whether solvents at the boundary of the radius of interaction are inside or outside the solubility sphere. Difficulties also occur where the polymer has very high HSP values. A lack of appropriate, high HSP solvents with which to carry out solubility testing, can made it difficult to accurately predict the centre of the solubility sphere (Hansen, 2000).

2.7.6 Sorption vs diffusion

Pervaporation is generally described by the solution–diffusion model. Sorption is a thermodynamic phenomenon and the concept of solubility parameter allows differentiation between sorption of different compounds in a given polymer. The diffusion coefficient, is generally governed by a molecule's size, shape and mass. A component with high sorption and diffusivity values will have a very high PV selectivity for this component. If one of these is low, the overall selectivity can be relatively poor. For instance, Dagaonkar *et al.* (1998)

showed that organophilic membranes with high sorption selectivity for the piperazines, selectivity favoured water in an alkyl piperazines–water separation due to the low diffusion coefficient of alkyl piperazine. Piperazines are much bulkier than water and therefore diffuse through the membranes far more slowly (Ray *et al.*, 1999a). Most components in organic liquid mixtures such as essential oils have similar molecular size, so sorption should dominate the separation process.

2.7.7 Affinity but not dissolution

Membrane integrity for PV is critical for process success. Even minor imperfections in the membrane's selective layer significantly decrease selectivity. Polymer membranes that deteriorate on contact with organic solvents, are unsuitable for PV separations.

To decrease the likelihood of membrane failure during processing, polymers from the periphery of the desired feed component solubility sphere should be chosen. This means a trade-off between polymer-permeant proximity (attraction) and polymer stability. Billmeyer (1984) suggested, as a good first approximation and in the absence of strong interactions such as hydrogen bonding, that solubility can be expected if the difference in polymer-solvent HSP is less than 3.5-4.0. This gives a rough estimate of how far apart solute and membrane polymer should ideally be in 3-dimensional HSP space (3-D HSP).

2.7.8 Use of HSP in pervaporation

Several researchers have used the relationship between solubility parameters and polymer/solvent affinity to analyse pervaporation. Many separation mixtures ranging from aqueous-organic, organic-organic, and halogen-containing mixtures have been studied.

Aqueous/organic mixtures

The solubility parameter approach to selecting appropriate membranes has previously been applied to aqueous/organic separations, with mixed success. Lee *et al.* (1989), separated aqueous solutions of ethanol and found that the solubility parameter approach did not always work (Lee *et al.*, 1989; Feng and Huang, 1997). Diffusivity rather than the solubility of the permeants had a major effect on the PV performance (Qariouh *et al.*, 1999). Yoshikawa *et al.* (1986) reported a better correlation between PV selectivity and the δ_h component for separating ethanol/water mixtures by synthetic polymers (Jonquières *et al.*, 1996).

Nijhuis *et al.* (1993), used a wide range of homogeneous elastomeric membranes to remove volatile organics from water. They used the solubility parameters and glass transition temperatures to relate elastomer permeation and sorption data with the chemical and physical nature of the elastomers. Unnikrishnan *et al.* (1997) attributed the differences in permeability of the organic component through the membrane, to the degree of unsaturation and the presence of steric side groups.

However, membranes for PV removal of water from rocket fuels (hydrazine and MMH) have been successfully selected using Hansen's solubility parameters and the Flory–Huggins interaction parameter (Ravindra *et al.*, 2000; Sridhar *et al.*, 2000). Mandal *et al.* (2002a), also successfully predicted selective dehydration of a mixture of methoxy-propanol/water using polyacrylonitrile (PAN) copolymer membranes and observed increasing selectivity for water as the co-monomer solubility parameter increased and approached the HSP of water.

Orme *et al.* (2002) used Hansen solubility parameters to characterize the effect of blending pendant groups with differing solvent compatibility onto a phosphazene heteropolymer (HPP) backbone. Selective permeation of alcohol over water (water/isopropanol, and water/methanol) in PV, depended on the proximity of solvent HSP and copolymer HSP. Orme *et al.* (2002) also stated that HSP could determine the applicability of phosphazene heteropolymers for novel separations, and could be used to further tailor the copolymer by designating the pendant group distribution.

Because irregular predictions for aqueous/organic mixtures are obtained with solubility parameter methods, several authors propose that the method is used only to indicate relationships between selectivities and solubility parameters (Jonquières *et al.*, 1996).

Halogenated hydrocarbons

Lee *et al.* (1987) found that the surface thermodynamics (preferential sorption) approach was better for predicting selectivity of halogen mixtures in dilute aqueous-organic mixtures, than the solubility parameter approach. They also observed that Hansen's solubility parameters were unable to predict the pervaporation characteristics of aqueous chloroform mixtures (Lee *et al.*, 1989). Diffusivity (due to difference in atomic size) may have more of an impact than solubility in separating halogen mixtures.

Jou *et al.* (1999) successfully chose a PVAC polymer for PV of trichloroethylene (TCE) and chloroform from aqueous solutions. They chose this polymer because of its high affinity for TCE and chloroform, and low affinity for water in 3-D HSP space.

Organic/organic mixtures

Binning *et al.* (1961) and Sweeny and Rose (1965) identified the link between separation potential and physicochemical properties of both the feed components and polymer membrane material (Cabasso, 1983). Mulder *et al.* (1982) realised that solubility of the penetrant in the membrane, i.e. the interaction between polymer and penetrant, can be described qualitatively by solubility parameter theory. They then took the next logical step and evaluated the solubility parameter concept for predicting permeation behaviour of isomeric xylenes within cellulose ester membranes.

Cabasso (1983) used Hansen solubility parameters to select and prepare asymmetric "alloy" membrane materials of compatible polymers for specific organic separations. He obtained high separations for organic/organic mixtures by matching the chemical affinity of tailored membranes and one of the permeating components. For example, polyphosphonate is soluble in methanol while cellulose acetate is not, so an alloy of these two polymers will not dissolve in methanol but can be an effective membrane for selective permeation of methanol from methanol/hexane. Cabasso (1983) was able to validate this theory.

Yamaguchi *et al.* (1992) took the inverse approach and successfully used Hansen parameters to identify the organic mixtures their composite membrane (MA/HDPE) could separate. They simplified the selection theory by studying only soluble/insoluble mixtures for their membrane and then tailored their membrane (creating a copolymer) to a specific separation mixture using HSP (Yamaguchi *et al.*, 1993). Yamaguchi *et.al.* (1993) also simplified determining polymer solubility coefficients by using only eight solvents (benzene, cyclohexane, carbon tetrachloride, acetone, methanol, ethanol, 2-propanol, and water) rather than the usual 54.

Jonquières *et al.* (1996) successfully correlated PV selectivity of ethanol/ ethyl-tertiary-butyl-ether (ETBE) separated by various poly(urethane imides) (PUI) and interaction selectivity, which they derived from the solubility parameters of the different species involved.

Calculating the HSP for their block copolymer PUI membranes only required knowledge of the chemical structure of the soft segment (PEG, PCL, PTMG, PPG, or PCD) to predict selectivity of the corresponding PUI. Other correlation methods such as the geometric mean of the polymer solubility parameter using volume fraction (Froehling *et al.*, 1976), vectorial distance between HSP with (Zellers, 1993; Hansen, 2000) and without (Huang and Rhim, 1991) various weighting factors, and vectorial addition, subtraction and ratio methods (Sferrazza and Gooding, 1988; Jonquières *et al.*, 1996; Mandal and Pangarkar, 2003) did not successfully predict the separation of ethanol-ETBE by various polymers.

Ray *et al.* (1997) studied the PV of benzene and cyclohexane using acrylonitrile copolymer membranes, and tailored their membrane using HSP of monomers (styrene, methyl methacrylate, and vinyl acetate) in the copolymer, relative to the HSP of benzene and cyclohexane. Permeation selectivity for benzene for these membranes followed the trend of their relative HSP solubilities when monomer concentration was low (3% in acrylonitrile). In a later study on methanol/MTBE separation (Ray *et al.*, 1999a), the monomers (hydroxyl ethyl methacrylate, methacrylic acid, and vinyl pyrrolidone) attached to the copolymer acrylonitrile membrane were chosen on the basis of their solubility parameter values relative to methanol. Because the membrane and methanol had comparable solubility parameter values (δ_d, δ_p, δ_h, and δ_t) the membranes had much greater sorption for methanol than MTBE. The difference in molecular size may also have significantly influenced this separation process; methanol (molecular diameter = 2.82 Å) being much smaller than MTBE (mol. diam. = 4.94 Å). A subsequent study of methanol/ethylene glycol separation (Ray *et al.*, 1999b) further reinforced that the permeation selectivity of each membrane followed the same trend as their HSP solubilities.

Unnikrishnan *et al.* (1997) observed that natural rubber (NR) membranes exhibited permselectivity toward *n*-hexane in an acetone/*n*-hexane system, and realised it was because the total solubility parameter values (δ_t) of the preferentially permeating component and the membrane were similar (NR δ_t = 16.2; *n*-hexane δ_t = 14.9; acetone δ_t = 20.3). Wang *et al.* (2000; 2001) found that permselectivity of binary mixtures of benzene-hexane and benzene-cyclohexane was primarily due to the solubility of these permeants in the glassy polyamide copolymer membrane. Mandal and Pangarkar (2003) used Hansen parameters and Flory–Huggins interaction parameters to evaluate separation potential of isopropyl alcohol, benzene and toluene mixtures in a variety of hydrophilic polymer PV membranes. Pal *et al.* (2005)

used the solubility parameter concept to select appropriate membranes for preferential permeation of methanol from toluene. The backbone of the copolymer membrane was polyacrylonitrile, and five different monomers (acrylonitrile with maleic anhydride, acrylic acid, methacrylic acid, methyl methacrylate, and styrene) were selected by their proximity to methanol (polar) in HSP space with respect to toluene (non-polar).

2.8 Summary

Of the three major pervaporation separations; dehydrating organic liquids, removing trace organics from aqueous streams, and organic-organic mixture separations; the latter has been the least developed industrially. Despite being a promising alternative to conventional separation techniques, which are energy intensive and far less eco-friendly than pervaporation, this process has not become widespread for organic-organic separations, primarily due to the lack of commercially-available high-performance membranes. Literature indicates that pervaporation is suitable for separating a wide variety of organic liquid mixtures including polar/non-polar, aromatic/alicyclic, aromatic/aliphatic, and even isomeric components.

Solution-diffusion is believed to be the primary model for transport through a pervaporation membrane. It requires sorption of feed components in the membrane before diffusion can occur. Hansen solubility parameters (HSP) are believed to be a good first estimate of this initial step, and has potential for selecting membrane materials for specific organic-organic separations. Most researchers have used this relationship merely to explain interaction phenomena observed between different membranes. Other researchers have used HSP to identify compatible polymers for improving stability of membranes in specific separations; to tailor copolymer membranes for specific separations; or to propose potential uses for the polymer membrane.

Using HSP to select novel membrane materials has recently regained attention after this method was presented at an international membrane society conference (Buckley-Smith & Fee, 2001). This thesis uses a model solution of lavender essential oil components (linalool and linalyl acetate in ethanol) to validate the use of HSP values for predicting preferential permeation in organic-organic PV separation.

Chapter

3

Selection of Membrane Materials & Calculation of Hansen Solubility Parameters

This chapter details the accuracy of HSP in predicting selective permeation of a wide variety of organic feed solutions, and how HSP were used to select suitable PV membrane materials for the current study. Hansen solubility parameters for the solutes and polymers used in this study were calculated using group contribution, physical and electrical properties, swelling experiments and literature values.

3.1 Predicting selective permeation

Much of this section is based on work presented at conference by the author (Buckley-Smith and Fee, 2002b).

Selectivity data from literature sources were collected for the membrane materials including: Cellulose acetate (CA), Cellulose aceatate butyrate (CAB), Cellophane (CPN), Cellulose tripropionate (CTP), Acrylonitrile butadiene rubber (NBR), Polyamide (PA), Polyethylene (PE), Poly(etherimide) (PEI), Polypropylene (PP), Poly(tetrafluoroethylene) (PTFE), Polyurethane (PUR), Poly(vinyl alcohol) (PVA), Poly(vinyl chloride) (PVC), Poly(vinylidene chloride) (PVDC), Poly(vinylidene fluoride) (PVDF), and Poly(styrene acrylic acid) (Sty-AA) (Carter and Jagannadhaswamy, 1964; Mulder *et al.*, 1982; Brun *et al.*, 1985; Knight *et al.*, 1986; Koops and Smolders, 1991; Cunha *et al.*, 1999). These polymers were quoted in literature as having successfully separated organic/organic mixtures by pervaporation. Solutes separated included; *n*-hexane, cyclohexane, benzene, toluene, xylene isomers, *n*-heptane, acetone, methanol, ethanol, isopropanol, methyl acetate, ethyl acetate, ethylene glycol, and chlorinated hydrocarbons; carbon tetrachloride, chloroform and trichloroethylene (Table 3:01). Feed solutions for these separations were made up of organic/organic mixtures of concentrations ranging from 20:80 solutions to 50:50 weight percent.

Hansen solubility parameters were collated from Hansen (2000) and Mulder (1982) for the above polymers and solutes. As the exact polymers produced by the appropriate manufactures were not always available in Hansen's (2000) data, equivalent materials were selected on the basis of equivalent chemical structure (not calculated via group contribution).

The solubility of each solute in its respective polymer was calculated using Eqn. 2:15 (Burke, 1984; Hansen, 2000) on an Excel™ spreadsheet, then compared with the radius of interaction

(Eqn. 2:16) to see how similar the solute was to the polymer (in 3-D HSP space), and determine wheather the preferentially permeating solute was within the solubility sphere.

Table 3:01 Details of organic/organic PV experiments from literature.

Polymer	Composition in Feed (A/B in wt.%)	Flux ($kg/m^2.hr$)	Selectivity ($\alpha_{A/B}$)	Reference
CA 1,2,3	p-xylene/o-xylene (50:50)	-	1.00	ϕ
CAB 171	p-xylene/o-xylene (50:50)	-	1.34	ϕ
CAB 272	p-xylene/o-xylene (50:50)	-	1.36	ϕ
CPN	chloroform/acetone (30:70)	-	0.88	β
CPN	carbon tetrachloride/chloroform (40:60)	-	1.68	β
CPN	methanol/ethylene glycol (50:50)	-	6.50	β
CTP	p-xylene/o-xylene (50:50)	-	1.30	ϕ
NBR	n-heptane/benzene (50:50)	-	0.13	α
PA	chloroform/trichloroethylene (30:70)	-	0.82	β
PE	benzene/isopropanol (60:40)	1.10	1.46	β
PE	benzene/methanol (40:60)	1.10	2.15	β
PE	benzene/phenol (50:50)	0.70	9.00	δ
PE	cyclo-hexane/n-heptane (60:40)	0.38	0.91	δ
PE	chloroform/acetone (30:70)	-	0.95	β
PE	carbon tetrachloride/acetone (20:80)	-	1.43	β
PE	carbon tetrachloride/chloroform (60:40)	-	1.11	β
PE	carbon tetrachloride/ethyl acetate (60:40)	2.3	0.99	β
PE	ethanol/toluene (50:50)	-	0.20	ε
PE	n-hexane/n-heptane (50:50)	-	1.20	ε
PE	n-heptane/toluene (40:60)	1.37	0.71	χ
PEI	benzene/n-hexane (60:40)	0.90	9.10	χ
PP	benzene/cyclo-hexane (50:50)	4.57	1.43	δ
PP	benzene/methanol (60:40)	0.72	2.40	δ
PTFE	chloroform/acetone (30:70)	-	0.76	β
PUR	benzene/n-hexane (50:50)	3.20	4.60	χ
PVA	benzene/n-hexane (60:40)	0.003	3.00	χ
PVC	methanol/ethylene glycol (50:50)	-	8.92	β
PVDC	chloroform/acetone (30:70)	-	0.95	β
PVDC	chloroform/trichloroethylene (40:60)	-	1.12	β
PVDF	p-xylene/ethyl benzene (50:50)	0.50	1.15	δ
Sty-AA	benzene/cyclo-hexane (50:50)	6.33	3.00	χ

Literature source for separation information: α = Brun *et al.* (1985); β = Carter and Jagannadhaswamy (1964); χ = Cunha *et al.* (1999); δ = Koops & Smolders (1991); ε = Knight *et al.* (1986); ϕ = Mulder *et al.* (1982).

3.1.1 Results and discussion

Figure 3:01 shows the relationship between selectivity and solubility for organic solutes in the various polymers. In this graph a selectivity of $\alpha_i > 1$ (see vertical dotted line) means that the membrane is more selective towards the component, and a selectivity of $\alpha_i < 1$ means the membrane preferentially permeates the other component in the system. Note how the

separation of benzene and cyclo-hexane in PP has selectivity of 1.43 (x-axis) for benzene, and the inverse of this (0.7) gives selectivity for cyclo-hexane.

RED numbers less than 1.0 $MPa^{½}$ indicates high affinity between polymer and solute. Values greater than 1.0 $MPa^{½}$ indicate progressively lower affinities.

Thus again for the benzene/cyclo-hexane - PP system, both solutes are within the solubility sphere of PP (RED < 1), however benzene is closer to zero (y-axis) and therefore more similar to PP (lower relative energy difference). This is illustrated in Figure 3:01 by the small arrows in the lower left hand quadrant.

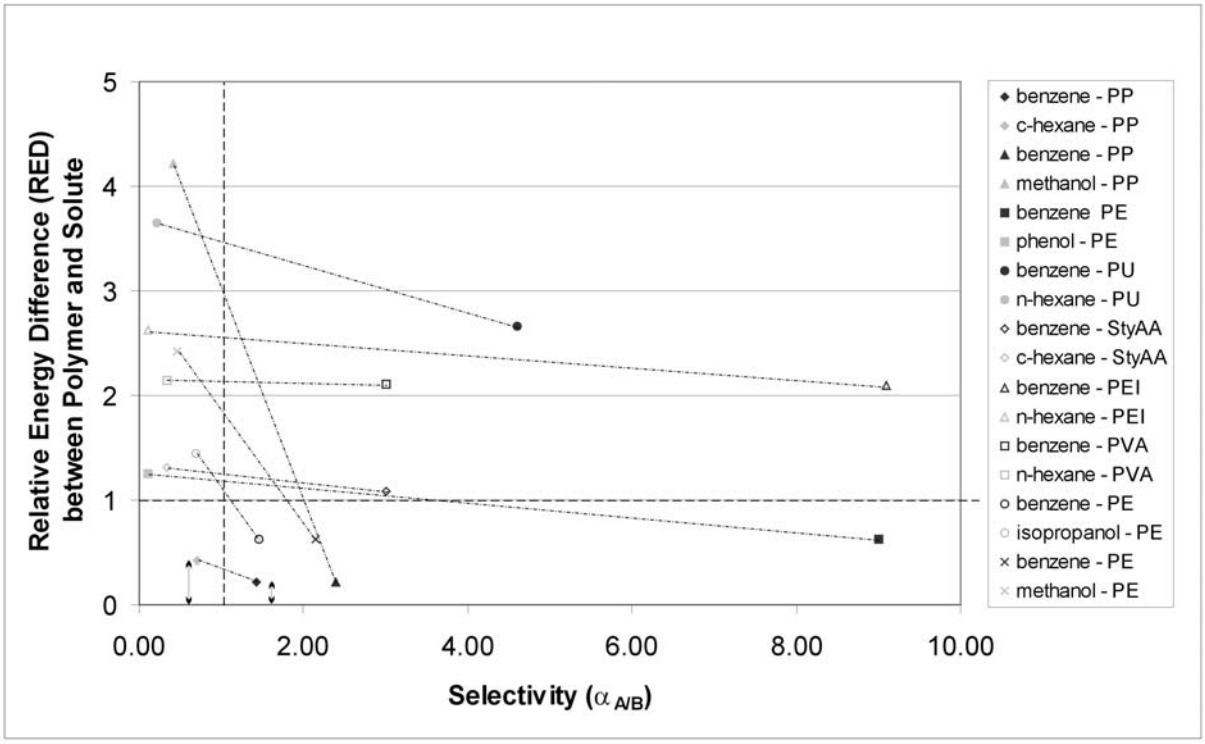

Figure 3:01 The relationship between Hansen Solubility Parameters and Selectivity of Membrane Materials for Benzene/organic mixtures (Carter and Jagannadhaswamy, 1964; Koops and Smolders, 1991; Cunha *et al.*, 1999).

The relationship between Hansen Solubility Parameters and Selectivity is emphasised in Figure 3:02 which displays data from the pervaporation of alcohol/organic systems. The negative slopes shown on the diagram linking pairs of solutes within a system indicate that as a general rule, preferential permeation occurs when a solute is very attracted to the polymer. In this case, solutes that lie within or bordering the solubility sphere of the polymer, will permeate through the membrane preferentially over solutes that lie at a considerable distance

from the edge of the solubility sphere. This trend appears to be particularly prominent where the solute mixture contains components of significantly different polarity and hydrogen bonding. Table 3:02 shows that the alcohols contain significantly higher ${}^{S}\delta_p$ and ${}^{S}\delta_h$ than their alkane counterparts from Figure 3:02.

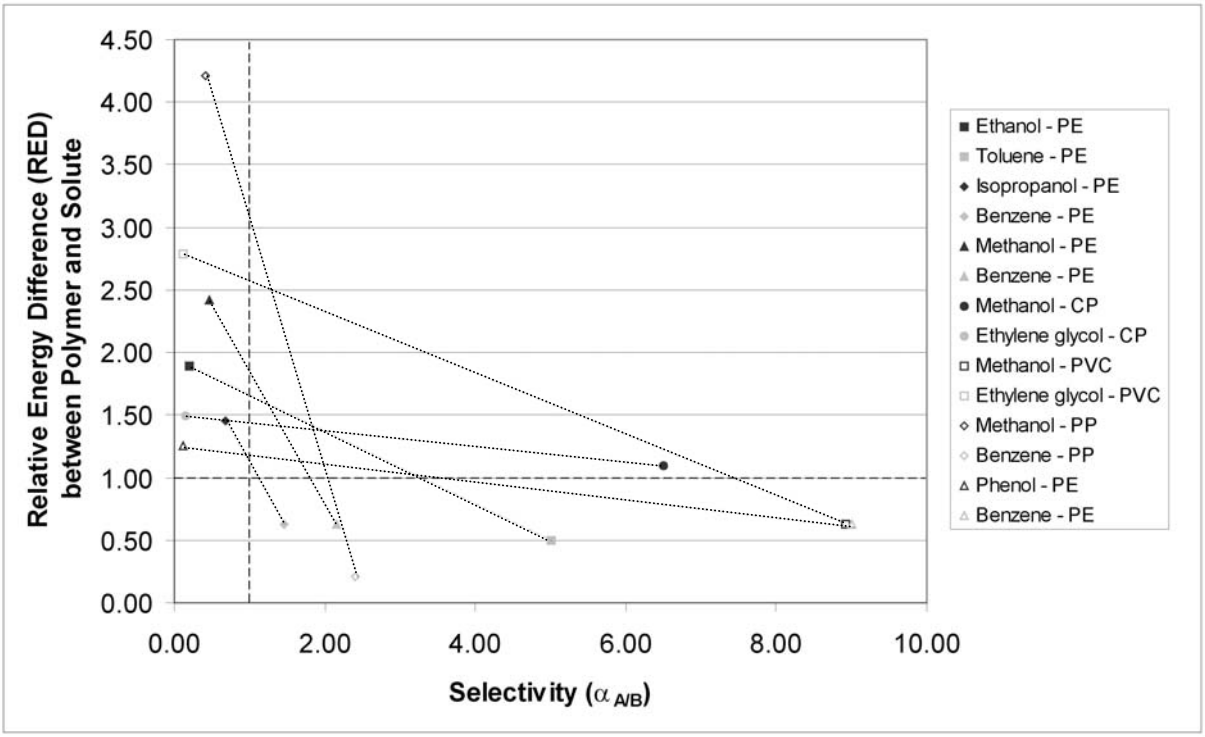

Figure 3:02 The relationship between Hansen Solubility Parameters and Selectivity of Membrane Materials for Alcohol/organic mixtures (Carter and Jagannadhaswamy, 1964; Knight *et al.*, 1986; Koops and Smolders, 1991).

Table 3:02 Hansen solubility parameters for alcohol/organic solutes (Hansen, 2000).

Solute	${}^{S}\delta_d$	${}^{S}\delta_p$	${}^{S}\delta_h$	M_r
Acetone	15.5	10.4	7.0	58.07
Benzene	18.4	0.0	2.0	78.11
1,3-butadiene	14.8	2.8	5.6	54.09
Carbon tetrachloride	17.8	0.0	0.6	153.82
Chloroform = Trichloromethane	17.8	3.1	5.7	119.38
Cyclohexane	16.8	0.0	0.2	82.15
Ethanol	15.8	8.8	19.4	46.07
Ethyl acetate	15.8	5.3	7.2	88.11
Glycol = Ethylene glycol	17.0	11.0	26.0	62.07
n-Heptane	15.3	0.0	0.0	100.20
n-Hexane	14.9	0.0	0.0	86.18
Isopropanol = Propan-2-ol	15.8	6.1	16.4	60.10
Isobutylene	14.5	2.0	1.5	56.11
Methanol	15.1	12.3	22.3	32.04
Methyl acetate	15.5	7.2	7.6	74.08

Table 3:02 continued…

Phenol	18.0	5.9	14.9	94.11
Trichloroethylene	18.0	3.1	5.3	131.39
Toluene	18.0	1.4	2.0	92.14
o-Xylene	17.8	1.0	3.1	318.50
m-Xylene	17.8	0.8	2.7	318.50
p-Xylene	17.8	0.0	2.7	318.50

For example, phenol and benzene have polarity parameters ($^{S}\delta_p$) of 5.9 and 0.0 J/mol respectively; and hydrogen bonding values ($^{S}\delta_h$) of 14.9 J/mol for the alcohol and 2.0 J/mol for the alkene.

This difference is reflected in the RED values (Figure 3:02) for Polyethylene (PE) which happens to be a polymer of moderate polarity ($^{P}\delta_p$ = 3.1 J/mol) and hydrogen bonding ($^{P}\delta_h$ = 5.2 J/mol). Thus the phenol solute is more attracted to the polymer, and preferentially permeates through this membrane. Figure 3:03 shows graphically how the solute benzene is within the solubility sphere for PE, and phenol outside.

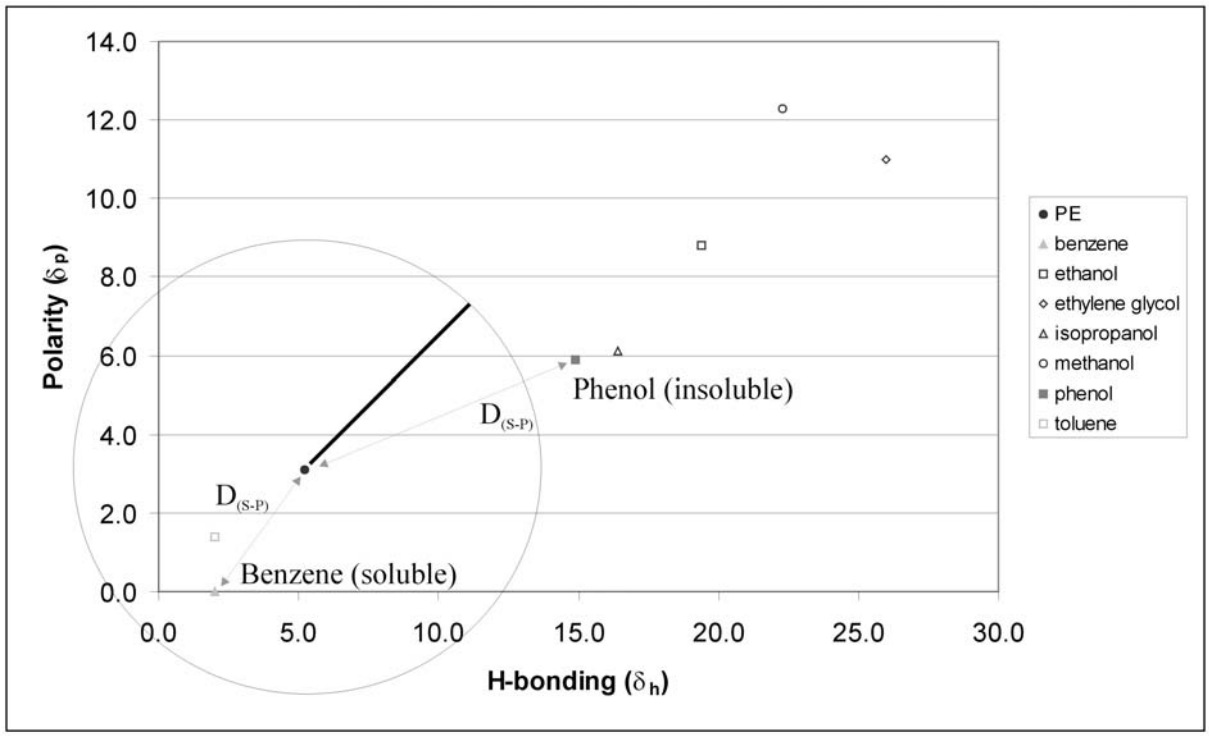

Figure 3:03 Two dimensional plot of Hansen Solubility Parameters for various polymers and solutes.

Figure 3:04 shows the relationship within systems containing alkane/organic mixtures. The majority of alkane/organic systems follow the trend mentioned previously, where a reduced

difference in relative energy between solute and polymer gives permeation of that particular component in preference to the other component in the system.

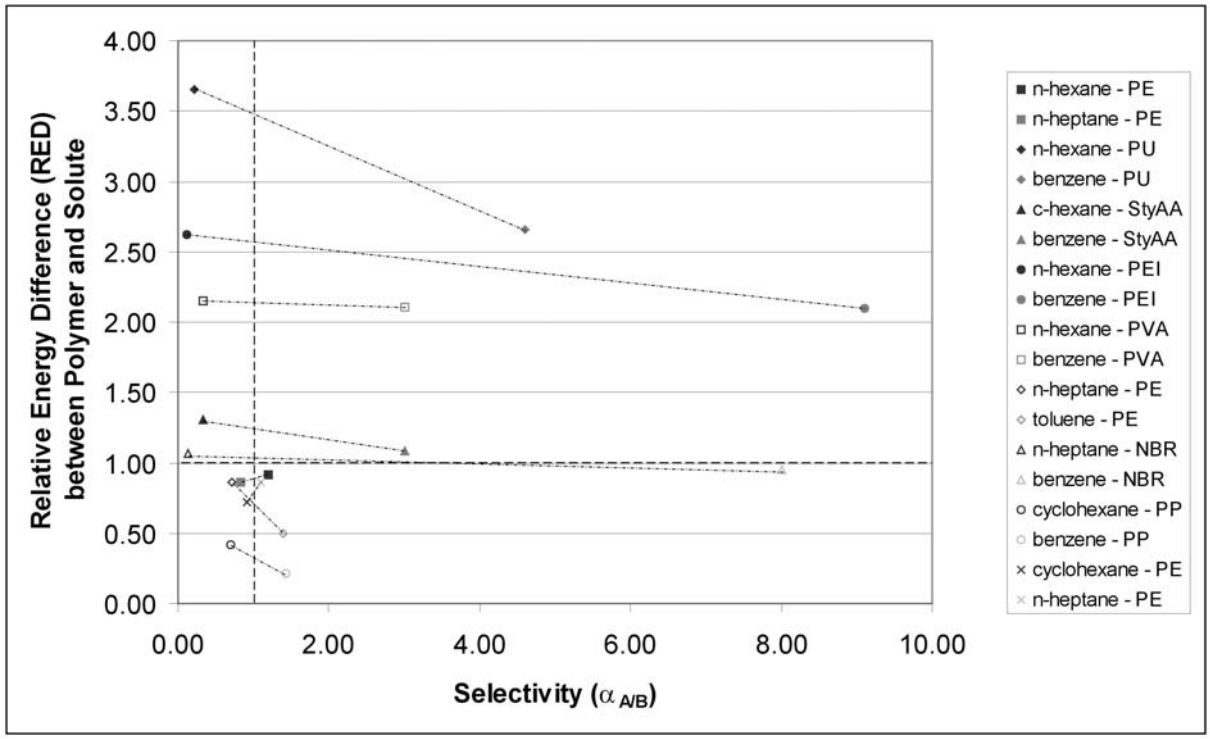

Figure 3:04 The relationship between Hansen Solubility Parameters of Membrane Materials for Alkane/organic mixtures (Knight *et al.*, 1986; Koops and Smolders, 1991; Cunha *et al.*, 1999) (Brun *et al.*, 1985).

Where the difference between components within a system is sterically and physico-chemically very small, this trend does not continue (Figure 3:05). Xylene isomers differ only in the position of the dimethyl groups protruding from the benzene group (see Figures 3:06 a & b). Unexpectedly, the CAB and CTP polymers displayed in Figure 3:05 preferentially permeate p-xylene. The p-xylene isomer has lower polarity (δ_p= 0.0 J/mol), than o-xylene (δ_p= 1.0 J/mol), and when compared to these membranes, which have significantly higher polar forces (6.5 and 6.3 J/mol respectively) than both the isomers, one would expect o-xylene (being most similar) to be attracted to the membranes, and thus preferentially permeate.

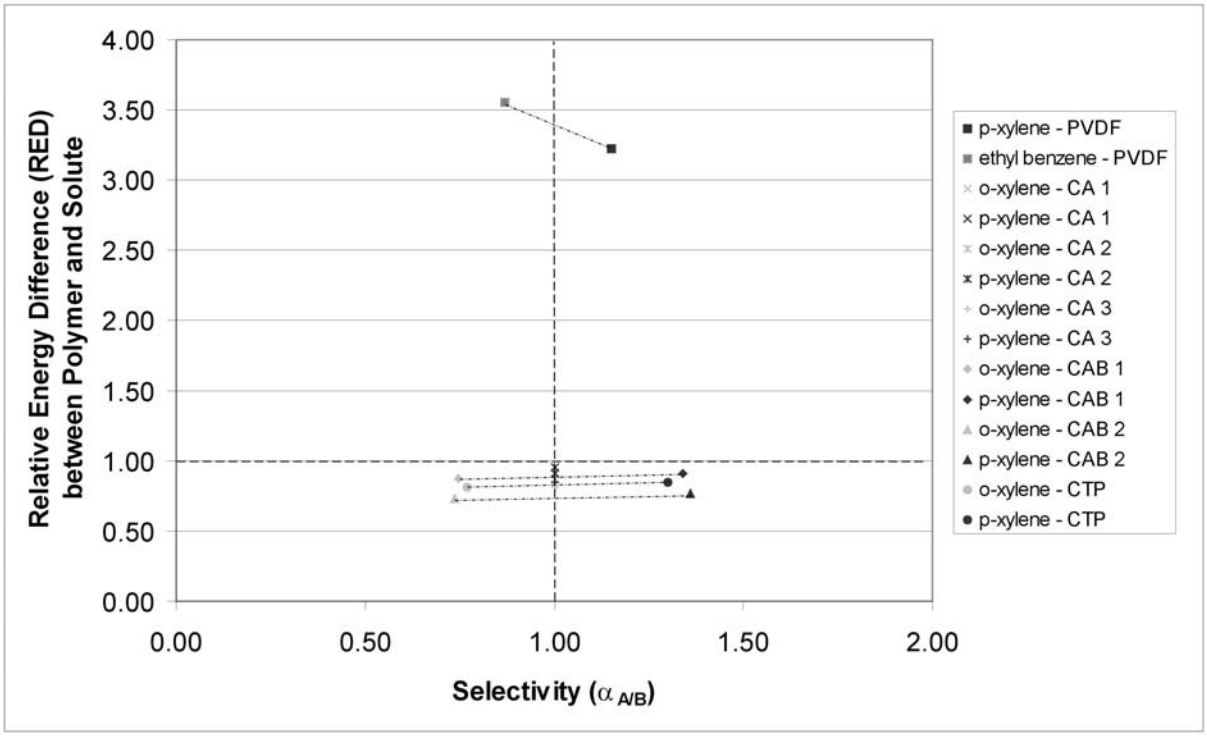

Figure 3:05 The relationship between Hansen Solubility Parameters of Membrane Materials for Xylene/organic and Xylene isomer mixtures (Mulder *et al.*, 1982).

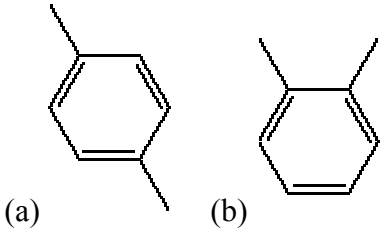

Figure 3:06 Xylene isomers (a) p-xylene (b) o-xylene (ChemFinder, 2002).

There also appears to be a break in the trend when the pervaporation system is made up of components containing halogens. The chlorinated hydrocarbons shown in Figure 3:07, illustrate this point graphically. Where a large difference between the polymer and chlorinated hydrocarbon is predicted by the Hansen solubility parameters, low selectivity is expected; however this is not the case for all halogenated systems, especially where the two separating components are both halogenated.

The cellophane system containing chloroform and acetone behaves as expected, however the chloroform and carbon tetrachloride separation does not. Where acetone is more attracted to cellophane, it preferentially permeates in respect to chloroform; but where carbon

tetrachloride is further out of the solubility sphere than chloroform, one would not expect it to preferentially permeate (Figure 3:07 below).

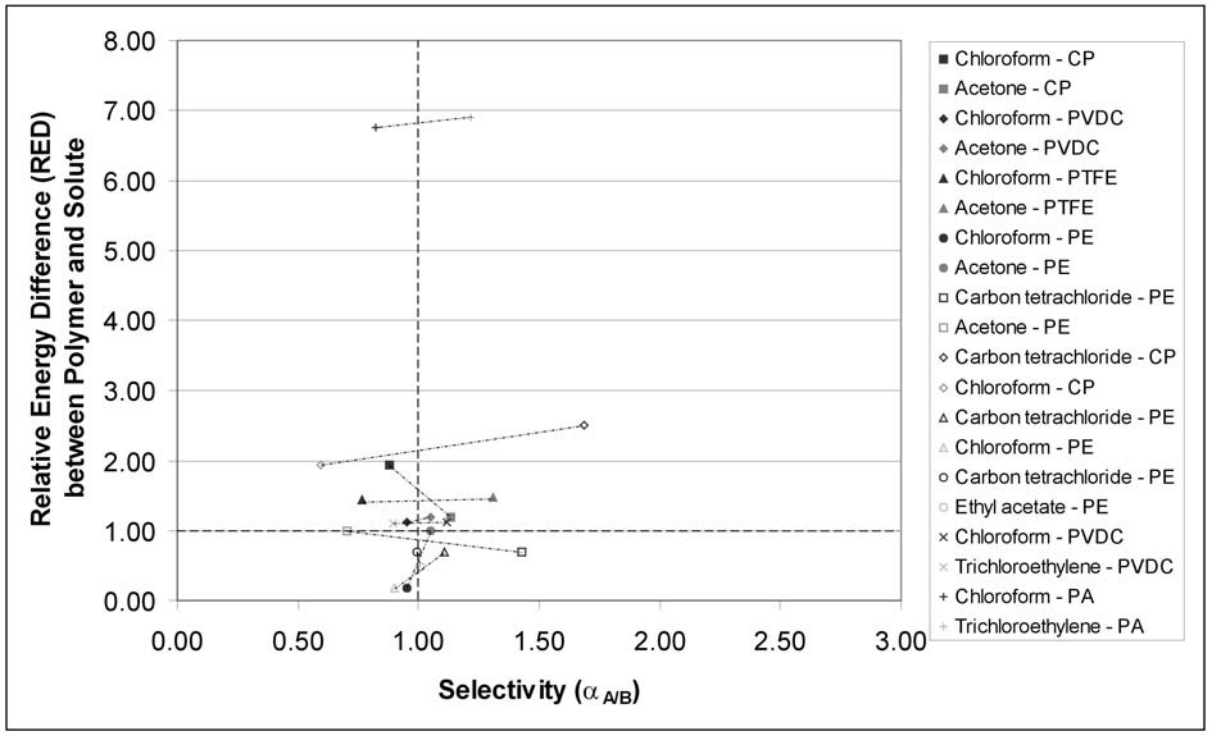

Figure 3:07 The relationship between Hansen Solubility Parameters of Membrane Materials for Chlorinated hydrocarbon/organic mixtures (Carter and Jagannadhaswamy, 1964).

An explanation proposed by Lloyd and Meluch (1985) could explain the inconsistencies seen in Figures 3:05 and 3:07. They theorised that the solute with the greatest similarity to the membrane (RED close to zero), was so attracted to the membrane that its transport was restricted ("immobilization" within the membrane), causing the other component to be preferentially permeated. This theory has some merit, although it becomes an unlikely explanation for solute mixtures that lie a significant distance outside the solubility sphere of the membrane.

Another plausible explanation that can be offered for the inability of Hansen solubility parameters to predict the separation of halogenated species, is that chloroform, carbon tetrachloride and trichloroethylene have relatively large molecular weights (Table 3:02), which makes them vulnerable to exclusion outside the solubility sphere despite their apparent attraction to the membrane material.

Lee et al. (1989) also studied the separation of aqueous solutions of ethanol and chloroform, and found that the solubility parameter approach does not always work for these components (Lee *et al.*, 1989; Feng and Huang, 1997). However, no such problem arose in Buckley-Smith & Fee's (2001) study of chloroform/aqueous solutions. In the 2001 study, Hansen solubility successfully predicted preferential permeation of chloroform in aqueous solutions when separated using NBR, SBR, LDPE and silicone Pervaporation membranes. They also successfully predicted that PVA membranes would preferentially permeate water rather than chloroform.

Feng & Huang (1997) stated that where diffusion dominates the separation process, the solubility parameter approach may be misleading. Separation of ethanol/water and halogen/halogen mixtures may be one such case where diffusivity has more of an impact on separation than solubility. Hansen (2000) states that the size and shape of the solute molecule has an important effect on diffusion, permeation, and attainment of equilibrium. Hansen (2000) goes on to say that smaller and more linear molecules diffuse more rapidly than larger bulkier ones. The extra weighting on the dispersive component of the solubility parameter distance ($D_{(S-P)}$) calculation, may account for this factor to a limited extent, but other aspects such as kinetic effects on diffusion rates or other free volume considerations are not accounted for thermodynamically in Hansen solubility parameters.

Another potential reason for the lack of correlation between HSP and halogen permeation could be the afore mentioned issue raised by Stavroudis and Blank (1989) regarding the lack of a dual H-bonding donor/acceptor parameter (Section 2.7.5). They felt that Hansen solubility parameters needed a proton donor component and a proton acceptor component to fully describe molecules with mobile electrons. This may be at the root of the problems with the chlorinated hydrocarbons, especially chloroform.

3.1.2 Potential for predicting separation characteristics

Aside from the halogenated permeation systems, the results studied in this paper are relatively internally consistent for organic/organic separations. The general trend for the organic mixtures is to have good selectivity for the desired organic when the solute and polymer are very similar.

Where the difference in hydrogen bonding and polarity parameters was significant (i.e., alcohol/alkene separations), the Hansen solubility parameters successfully matched the selectivity seen in practical experiments. This is consistent with literature published previously by the author for aqueous/organic separations (Buckley-Smith and Fee, 2001), where aqueous mixtures of n-hexane, cyclohexane, benzene, toluene, styrene, chloroform, and n-butyl acetate were successfully predicted using Hansen solubility parameters. Also seen in the same paper, was the inability of the Hansen solubility parameter to predict the separation characteristics of ethanol/water mixtures. This is also likely to be due to the physico-chemical similarity of these components hydrogen bonding and polarity parameters.

Yamaguchi *et al.* (1992) successfully used Hansen parameters to enable identification of organic mixtures their composite membrane could separate. They simplified the selection theory by studying only soluble/insoluble mixtures for their polymer membrane.

This current study went one step further and successfully predicted the permeation characteristics of mixtures where the components were soluble/insoluble (one component inside the solubility sphere and one outside), insoluble/insoluble (RED > 1, both outside the solubility sphere) and soluble/soluble (RED < 1, both inside the solubility sphere) in their respective membranes (see Figures 3:01, 3:02 and 3:04) (Buckley-Smith and Fee, 2002b).

Thus, in spite of the limitations identified with the separation of halogenated/organic mixtures, the solubility parameter approach appears to be a convenient method to use as a first estimate in the selection of polymer membrane materials, especially in the separation of organic compounds with significantly different functional groups (i.e., alcohol versus alkene).

3.1.3 Conclusions

Hansen Solubility Parameters have significant potential as a method of predicting which polymers would preferentially permeate desired solutes.

The Hansen solubility parameter approach successfully predicted the separation characteristics of the majority of benzene/organic, alcohol/alkene, and alkane/organic solutions.

The Hansen solubility parameter approach was unable to consistently predict the separation characteristics of halogenated/organic and xylene isomer mixtures.

3.2 Selecting membrane materials

The HSP of components in the model solution being studied were identified and compared with a database of known polymer HSP to identify those on the boundary of the solubility sphere. Much of this section was presented at various conferences by the author (Buckley-Smith and Fee, 2001, , 2002b, 2002a).

Composition of lavender essential oil

Lavender essential oil is extracted from the flowers of three species of lavender, true lavender (*Lavandula angustifolia*), spike lavender (*L. latifolia*), and lavandin (hybrid *L. angustifolia* × *L. latifolia*). The steam distilled essential oil of true lavender can contain up to 65% of the linear molecules linalool and linalyl acetate; which are components used widely in the perfume industry (Table 3:03). Spike lavender oil is dominated by small compact bi-cyclic molecules such as camphor, fenchone, cineole, and pinene in addition to linalool (Bienvenu, 1995; Akgün *et al.*, 2000). These molecules have comparable size ($C_{10} - C_{15}$) but their size and shape may influence their PV permeation characteristics.

Table 3:03 Effect of species on lavender essential oil composition (Bienvenu, 1995; Akgün *et al.*, 2000; ChemFinder, 2002).

Component	Structure	Concentration (%)		
		true lavender	lavandin	spike lavender
Ketone				
Camphor $C_{10}H_{16}O$	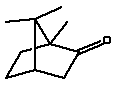	0.5-1	4-11	10-45
Fenchone $C_{10}H_{16}O$	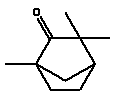	-	-	30-35
Ether/Ester				
1,8-Cineole $C_{10}H_{18}O$	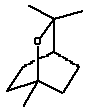	1-2	5-10	20-30
Linalyl acetate $C_{12}H_{20}O_2$	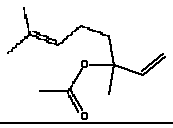	30-45	20-30	<1

Table 3:03 continued…

Alcohol				
Linalool $C_{10}H_{18}O$	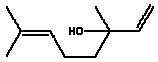	30-49	30-40	40-50
Alkene				
Caryophyllene $C_{15}H_{24}$	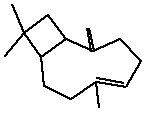	3-12	-	-
Ocimene $C_{10}H_{16}$	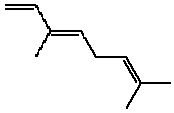	2.5-6	-	-
α-Pinene $C_{10}H_{16}$	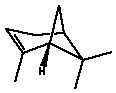	-	-	1-3

3.2.1 HSP of lavender oil components

The Beerbower method for group contributions to partial solubility parameters described in Hansen (2000) was used to calculate the HSP for oil components (Table 3:04). Because there was no data for 4- and 9-membered rings, the value for the 4-membered ring in caryophyllene was assumed to be equivalent to a 5-membered ring, and its 9-membered ring was assumed to be equivalent to the group contribution of a combined 5- and a 6-membered ring (Figure 3:08).

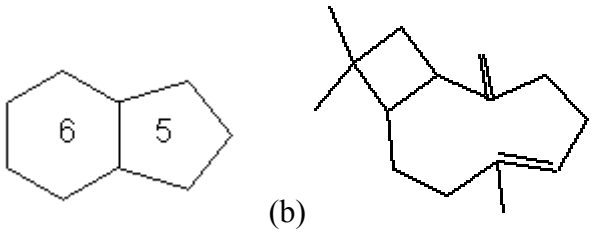

Figure 3:08 Substituting (a) 5- & 6-membered rings for the (b) 9-membered ring in caryophyllene.

The bi-cyclo nature of camphor and fenchone were assigned the group contribution of 5- & 6-membered rings, and the values for cineole and pinene were assigned two 6-membered rings. The remainder of their molecular structure were assigned the contributions for various alkane, alkene, alcohol, ketone, ester and ether components.

Table 3:04 Calculated HSP for lavender essential oil components (Hansen, 2000; Buckley-Smith and Fee, 2002a; ChemFinder, 2002), CAS numbers obtained from the World Wide Web (ChemFinder, 2002).

Solute	CAS No.	HSP ($MPa^{½}$)			M_r (a.m.u.)
		δ_d	δ_p	δ_h	
Ketone					
Camphor	[76-22-2]	17.5	5.2	4.7	152.24
Fenchone	[1195-79-5]	17.1	5.1	4.6	152.24
Alcohol					
Linalool	[78-70-6]	16.3	4.4	11.2	154.25
Ether/Ester					
1,8-Cineole	[470-82-6]	15.9	3.9	3.4	154.25
Linalyl acetate	[115-95-7]	14.3	1.5	6.2	196.29
Alkene					
Caryophyllene	[87-44-5]	16.9	1.2	3.6	204.35
Ocimene	[13877-91-3]	15.6	2.2	5.2	136.24
α-Pinene	[7785-26-4]	16.2	1.0	3.1	136.24

Of the lavender oil components, camphor has the highest dispersive HSP (δ_d = 17.5 $MPa^{½}$), and linalyl acetate the lowest (δ_d = 14.3 $MPa^{½}$). The ketones have the highest polar component (δ_p = 5.1, 5.2 $MPa^{½}$) and pinene the lowest (δ_p = 1.0 $MPa^{½}$). There is a large range in the values for hydrogen bonding compared to the polar and dispersive components, linalool has a very high value (δ_h = 11.2 $MPa^{½}$) linalyl acetate an intermediate value (δ_h = 6.2 $MPa^{½}$) and pinene the lowest (δ_h = 3.1 $MPa^{½}$). Thus hydrogen bonding may be the most important factor for selecting polymers to separate the major components in this oil.

3.2.2 Comparison with polymers

Hansen solubility data for polymers were collated from Hansen (2000) and Mulder (1982) and stored in an Excel™ spreadsheet. The solubility of lavender oil components in 458 polymers was then calculated using Eqns. 2:15 and 2:16 to determine the three-dimensional similarity between solute and polymer (RED). An "If" statement in the spreadsheet identified whether the solute was inside the solubility sphere of each polymer.

= IF ("RED"< 1.0, TRUE, FALSE) (Eqn 3:1)

The TRUE/FALSE values for each solute were then evaluated to see which polymers were selectively soluble for one component but none of the others. For example, the following identifies those selective for camphor:

= IF (AND('camphor' = TRUE, 'fenchone'=FALSE, 'linalool' = FALSE, 'cineole' =FALSE, 'linalyl acetate' = FALSE, 'ocimene'=FALSE, 'pinene'=FALSE, 'caryophyllene'=FALSE), TRUE, FALSE)

The results were then compared with a spreadsheet of polymer abbreviations (Macrogalleria, 1996; MatWeb, 2002; Plastics USA, 2005) to identify the composition of likely membrane materials.

3.2.3 Results and discussion

Twenty four potential polymer materials were identified as preferentially soluble for linalool and four polymers were preferentially soluble for camphor (see Table 3:05). Although other components in lavender essential oil were soluble in many polymers, no polymers were identified with preferential solubility.

Table 3:05 Number of polymers calculated to have total or preferential solubility for lavender essential oil components.

Component	Total Soluble polymers	Preferentially Soluble
Ketone		
Camphor (x_{camph})	349	4
Fenchone (x_{fench})	338	0
Alcohol		
Linalool (x_{lool})	254	24
Ether/ester		
1,8-Cineole (x_{cine})	238	0
Linalyl acetate (x_{lyl})	87	0
Alkene		
Ocimene (x_{ocim})	185	0
Caryophyllene (x_{cary})	216	0
α-Pinene (x_{pine})	169	0

The following polymers were preferentially soluble for linalool: Lytron (maleic anhydride-styrene copolymer), Epoxy resins, Acrylamide, Barex 210 CR-Styrene (methacrylate / acrylonitrile / styrene co-polymer), Cellnit (cellulose nitrate), Mowital B60H (polyvinyl butyral), Polyamide (PA11, PA6, Versamid), Phenolic (phenol-formaldehyde polymers), POMH / POMC (polyoxymethylene homo/co-polymer), PVA (poly vinyl alcohol), Shellac (natural resin/wax), and VBE / MA / MAC (methyl acrylate copolymer).

The following polymers were preferentially soluble for camphor: acetal homopolymer (polyoxymethylene, POM), FEP (copolymer of tetrafluoroethylene and hexafloropropylene), Furan (furfuryl alcohol based polymer), and Styron (Polystyrene).

When essential oil components were grouped by functional group, further polymers showed preferential solubility. The ketones camphor and fenchone were preferentially soluble in 29 polymers: Celanese (acetal copolymer), Alloprene (chlorinated rubber), MAA/EA/ST (methyl methacrylate copolymer), Mylar PET (poly(ethylene terephthalate) or Polyester), NR (natural rubber), PC (polycarbonate), PEI (poly(ether imide)), Pliolite (cyclized rubber), PSU (polysulfone), PUR (polyurethane rubber), PBT (poly(butylene terephthalate)), Polyaldehyde, Styrene copolymers, Teflon (poly(tetrafluoroethylene) - PTFE), VDC/AA (poly(vinylidene chloride) acrylic acid copolymer), V-lit (poly(vinyl chloride) - PVC), and V-lite (polyvinyl chloride co-vinyl acetate – PVC-PVAC). The cyclic alkenes were only preferentially soluble in PP (polypropylene).

The calculated RED values indicated that the following polymers would selectively permeate linalyl acetate but not linalool: BR (polybutadiene rubber), BR-STY (polybutadiene styrene rubber), C-flex (polyisoprene, IR), CTFE (chlorotrifluoroethylene), Lutonal (polyvinyl ethers), P-lite (cyclized rubber), EPDM (ethylenepropylenediene), and Silicone (poly(dimethyl siloxane)). These polymers were reduced further to those commercially available from Goodfellow Cambridge Ltd., UK (2002).

3.2.4 Chemical and thermal stability

The thermal and chemical stability of the selected polymers (Goodfellow, 2002) was used to further analyse the potential of each polymer as a membrane material (Table 3:06). These included Cellulose acetate (CA), High density polyethylene (HDPE), Low density polyethylene (LDPE), Polyamide (PA), Poly(butylene terepthalate) (PBT), Polycarbonate (PC), Poly(ether sulphone) (PES), Poly(ether imide) (PEI), Polyimide (PI) Poly(methyl methacrylate) (PMMA), Poly(oxy methylene) (POM), Polypropylene (PP), Poly(phenylene sulphide) (PPS), Polysulphone (PSU), Poly(tetrafluoro ethylene) (PTFE), Poly(vinyl chloride) (PVC), Polystyrene (PS).

Linalool, the most abundant component in lavender oil, is an alcohol. All polymers in Table 3:06 except PI, have a fair to good rating for alcohol, which indicates that linalool should not

cause these membrane materials to disintegrate. No thermal and chemical stability data were available for esters (e.g. linalyl acetate), so the resistance of each polymer to ketones was assumed to be similar. Ketones (camphor, fenchone + linalyl acetate) are also the next largest group of components in lavender oils. Polymers: CA, PC, PES, PEI, PMMA, PSU, PVC, and PS are unsuitable as they have a "poor" rating for ketones and could disintegrate under PV conditions. The polymers LDPE, PMMA, and PS had "poor" resistance to greases and oils (i.e., alkanes/alkenes). These polymers may disintegrate under operating conditions. However, caryophyllene, ocimene and α-pinene are very minor components in lavender oil and should not significantly effect membrane stability.

Table 3:06 Chemical & thermal resistance of various polymers (Buckley-Smith and Fee, 2002a; Goodfellow, 2002).

Polymer	Alcohols	Aromatic Hydrocarbons	Greases and oils	Ketones	Upper working Temp (°C)
CA	fair	good	good	**poor**	55-95
HDPE	good	fair/**poor**	fair	good	55-120
LDPE	good	**poor**	**poor**	good	55-90
PA 11	fair	good	good	good	70-130
PA 6,6	good	good	good	good	70-130
PBT	good	good	good	good	120 +
PC	good	**poor**	fair/good	**poor**	115-130
PES	good	fair	good	**poor**	180-220
PEI	good	**poor**	good	**poor**	170-200
PI	**poor**	good	good	good	250-320
PMMA	fair	**poor**	**poor**	**poor**	50-90
POM	good	good	good	good/fair	80-120
PP	good	fair	fair	good	90-120
PPS	good	good	good	good	200-260
PSU	good	fair	good	**poor**	150-180
PTFE	good	good	good	good	180-260
PVC	fair	**poor**	fair	**poor**	50-75
PS	good	**poor**	**poor**/good	**poor**	50-95

The performance ratings of some membranes in Table 3:06 were verified experimentally by immersion in pure solvents. PS and PMMA disintegrated within hours of contact with lavender oil, whereas LDPE did not.

Operating temperatures in PV can range from 15°C – 137°C, but most processes operate at or near room temperature (Koops and Smolders, 1991). All polymers mentioned in Table 3:06 should not undergo significant thermal degradation, provided membrane operating conditions are kept below 50°C.

Based on lavender oils being made up of primarily alcohols and ketones, and the availability of polymers from Goodfellow (2002) the selection procedure indicated that; CA, HDPE, PA 6,6, PBT, POM, PP, and PTFE would be the best membrane materials to trial.

3.2.5 Relative energy difference

The further a components HSP is from the boundary of the solubility sphere, the less attracted it will be to the polymer and the least likely to permeate the membrane. If far enough away, the component may even be repulsed by the membrane.

Normally, the smaller the relative energy difference, the more soluble the polymer/solute combination and the more likely the membrane will disintegrate. It is expected that membrane/solute combinations which border the solubility sphere for the polymer (RED ≈ 1.0) will preferentially permeate the desired component yet not be so soluble that the membrane disintegrates, this is especially important if the solute is the predominant component in the organic liquid mixture.

The polymers selected in this study had moderate solubilities because the polymer had to be soluble for one component and none of the others. The distance each solute is from the centre of each polymer's solubility sphere is shown in Figure 3:09. PE and PUR have extremes of RED for the various lavender oil components; PE and PTFE had very low affinity for linalool, linalyl acetate and ketones, compared with high affinity for alkenes such as ocimene, with the RED for PTFE and ocimene being will inside the solubility sphere. However, as only a small proportion of lavender oil components are alkene's, PTFE is less likely to disintegrate and more likely to preferentially permeate these components.

PA 12 and PA 6,6 are the polyamide derivatives with the most promise for selective permeation as well as chemical stability. All PA's have preferential affinity for linalool; however linalool is well inside the solubility spheres of PA 11 and PA 6, so these polymers are likely to disintegrate when pervaporating lavender oil.

Polymers from FEP – PUR (Figure 3:09) have selective affinity for ketones. However, PC, NR, PETP, PET and PEI all have $RED_{camphor} \approx 0.5$, implying the polymer will disintegrate if the feed solution has a high ketone content such as in spike lavender essential oil (Bienvenu,

1995). The remainder (FEP, POMH, PFA, STY, PBT, PSU, PES, CBR and PUR) have selective affinity between 0.5 and 1.0 and are less likely to disintegrate.

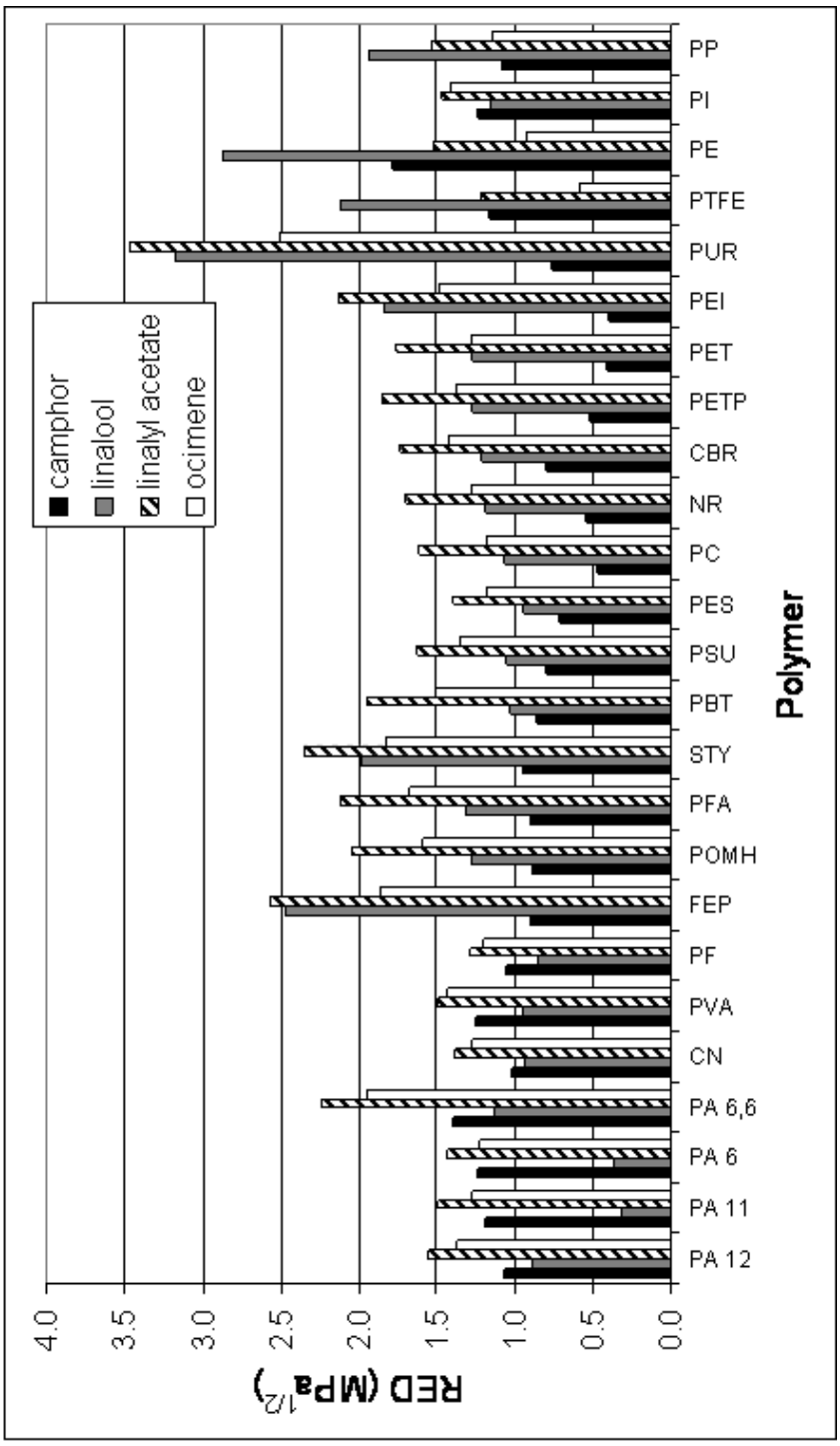

Figure 3:09 Relative energy differences between polymers and essential oil components (Hansen, 2000). Abbreviations listed in glossary.

3.2.6 Conclusions

The following homogeneous polymers were identified using Hansen solubility parameters to most likely selectively separate lavender essential oil components under PV conditions:

Selective for:	**Polymer:**
● linalool	Epoxy, CN, PVB, PA, PF, PVA
● ketone	POMH, FEP, PS, Cl R, PET, NR, PC, PEI, PSU, PUR, PBT, PTFE, PVC
● alkenes	PP
● linalyl acetate but not linalool[#]	BR, IR, CTFE, PVE, PDMS

[#](excluding other components from calculation)

Of these polymers, only a selected few were available from Goodfellow (2002):

Selective for:	**Polymer:**
● linalool	PA 6,6.
● ketone	POMH, PS, PC, PEI, PSU, PBT, PTFE, PVC
● alkenes	PP
● linalyl acetate but not linalool	nil.

This list was reduced still further based upon chemical and thermal stability (Goodfellow, 2004):

Selective for:	**Polymer:**
● linalool	PA 6,6.
● ketone	POMH, PSU, PBT, PTFE,
● alkenes	PP
● linalyl acetate but not linalool	nil.

3.2.7 Recommendations

This selection process indicated that polymers such as PA 6,6, POMH, PSU, PBT, PTFE, and PP had the greatest potential for selective permeation. Once obtained they coule be tested for chemical resistance to lavender essential oils, then used under PV conditions to assess selective permeability. If a wider variety of membranes was desired, polymers with borderline stability could be included (PS, PC, PEI, PVC). As it is known that the membrane manufacturing process can affect HSP and membrane performance, if polymers do not selectively permeate as expected, membranes from a different supplier could also be tested.

3.3 Calculating HSP by group contribution

As solubility parameters (δ_d δ_p and δ_h) are available for only a limited number of solvents and polymers, a method to predict these quantities is valuable. Accurate prediction of solubility parameter components from the chemical structure is difficult because the interaction of different structural groups producing overall polar and hydrogen-bonding properties do not obey simple rules. Despite this, several useful prediction methods based on molecular structure have been proposed proposed by Van Krevelen and Hoftyzer (1976), Hoy (1985), and Beerbower (1984). The following is a brief summary of these methods, more detailed information can be obtained from their respective references.

Table 3:07 shows the properties and structural formula of linalool and polyamide 6,6, which are used as examples in the following explanations.

Table 3:07 Structural, physical and electrical properties of linalool and poly(amide 6,6).

Property	**Solvent** ♥	**Polymer** ♠
Common name	linalool	poly(amide 6,6)
Scientific name	2,6-Dimethylocta-2,7-dien-6-ol	poly(hexamethylene adipamide)
CAS number	[78-70-6]	
Molecular structure	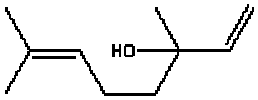	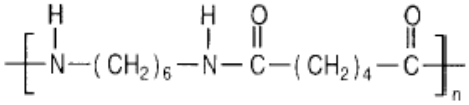
Formula	$C_{10}H_{18}O$	$-[C_{12}H_{22}O_2N_2]_n-$
Molecular weight	154.2516 g /mol	226.3 g /mol
Density	0.868 g /cm^3	1.14 g /cm^3
Molar volume	177.7 cm^3 /mol	198.52 cm^3 /mol
Boiling point	199 °C	-
Refractive Index	1.463	1.53

♥(ChemFinder, 2002), ♠(Goodfellow, 2002)

3.3.1 The Hoftyzer and Van Krevelen method

The Hoftyzer-Van Krevelen (1976) group contribution method is traditionally used to calculate the HSP for solvents but can also be applied to polymers by using the molar mass of the repeating unit, the polymer chain length does not need to be known (Van Krevelen and Hoftyzer, 1976; Jonquières *et al.*, 1996).

Solubility parameter components can be predicted using the following equations (Van Krevelen, 1990) to calculate the dispersion, polar and h-bonding components:

$$\delta_d = \frac{\Sigma F_{di}}{V} \qquad \delta_p = \frac{\sqrt{\Sigma F_{pi}^2}}{V} \qquad \delta_h = \sqrt{\frac{\Sigma E_{hi}}{V}} \qquad \text{(Eqn. 3:01)}$$

which are found in Table 3:08. For a more detailed explanation see Van Krevelen (1990).

Table 3:08 HSP calculation for linalool using the Hoftyzer-Van Krevelen method.

Structural groups	No. groups (N)	N*F_{di}	N*F^2_{pi}	N*E_{hi}
– CH_3	3	1,260	0	0
>CH_2	2	540	0	0
>C<	1	-70	0	0
=CH_2	1	400	0	0
=CH–	2	400	0	0
=C<	1	70	0	0
– OH	1	210	250,000	20,000
	Sum:	2,810	250,000	20,000
	δ_d	δ_p	δ_h	δ_t
HSP:	15.8	2.8	10.6	19.2

Table 3:09 shows an example of how HSP are calculation for polymers by the Hoftyzer-Van Krevelen method (Eqn. 3:01).

Table 3:09 HSP calculation for poly(amide 6,6) using the Hoftyzer-Van Krevelen method.

Structural groups	No. groups (N)	N*F_{di}	N*F^2_{pi}	N*E_{hi}
>CH_2	10	2700	0	0
-CO-	2	580	2371600	4000
-NH-	2	320	176400	6200
		3600	2548000	10200
	δ_d	δ_p	δ_h	δ_t
HSP:	18.1	8.0	7.2	21.1

3.3.2 The Hoy method

The Hoy method for calculating HSP is more complex than the Hoftyzer-Van Krevelen method. The solubility parameter components for linalool and polyamide (Table 3:11 and 3:11) were predicted from group contributions using the equations in Table 3:10. For more information regarding this method of HSP calculation see Van Krevelen (1990).

Table 3:10 Equations used to calculate HSP by Hoy's method (1985).

Formulae	Solvents	Polymers
Additive molar functions	$F_t = \Sigma N_i F_{t,i}$ $F_p = \Sigma N_i F_{p,i}$ $V = \Sigma N_i V_i$ $\Delta_T = \Sigma N_i \Delta_{T,i}$	$F_t = \Sigma N_i F_{t,i}$ $F_p = \Sigma N_i F_{p,i}$ $V = \Sigma N_i V_i$ $\Delta_T^{(P)} = \Sigma N_i \Delta_{T,i}^{(P)}$
Auxiliary equations	$(T_b/T_{cr}) = 0.567 + \Delta_T - (\Delta_T)^2$ $\text{Log}\ \alpha = 3.39(T_b/T_{cr}) - 0.1585 - \text{log}V$	$n = 0.5/(\Delta_T^{(P)})$ $\alpha^{(P)} = 777(\Delta_T^{(P)}) / V$
HSP calculations	$B = 277$ $\delta_t = (F_t + B) / V$ $\delta_p = \delta_t((1/\alpha)(F_p / (F_t + B)))^{½}$ $\delta_h = \delta_t((\alpha - 1) / \alpha)^{½}$ $\delta_d = (\delta_t^2 - \delta_p^2 - \delta_h^2)^{½}$	$B = 277$ $\delta_t = (F_t + (B/n)) / V$ $\delta_p = \delta_t((1 / \alpha^{(P)})(F_p / (F_t + (B/n))))^{½}$ $\delta_h = \delta_t((\alpha^{(P)} - 1) / \alpha^{(P)})^{½}$ $\delta_d = (\delta_t^2 - \delta_p^2 - \delta_h^2)^{½}$

Table 3:11 HSP calculation for linalool using the Hoy method.

Structural groups	No. groups (N)	$N*F_{t,i}$	$N*F_{p,i}$	$N*V_i$	$N*\Delta_{T,i}$
$-CH_3$	3	910.5	0	64.65	0.069
$>CH_2$	2	538.0	0	31.10	0.040
>C<	1	65.5	0	3.56	0
$=CH_2$	1	259.0	67	19.17	0.018
=CH–	2	498.0	119	26.36	0.036
=C<	1	173.0	63	7.18	0
– OH	1	500.0	500	12.45	0.082
	Sum:	2944.0	749	164.47	0.245
		δ_d	δ_p	δ_h	δ_t
	HSP:	14.0	7.7	11.3	19.6

Table 3:12 HSP calculation for poly(amide 6,6) using the Hoy method.

Structural groups	No. groups (N)	$N*F_{t,i}$	$N*F_{p,i}$	$N*V_i$	$N*\Delta_{T,i}^{(P)}$
$>CH_2$	10	2690	0	155.5	0.200
-CO-	2	1076	1050	34.6	0.080
-NH-	2	736	736	22.0	0.055
	Sum:	4502	1786	212.1	0.335
		δ_d	δ_p	δ_h	δ_t
	HSP:	15.7	12.3	9.5	22.1

The Hoy method was the most straight-forward for calculating HSP for polymers and solvents using an Excel spreadsheet. It was less confusing as to which groups applied in appropriate situations (especially for ether and carboxyl groups, and aromatic rings). However, calculating values for polymers such as PE, PP and PTFE was complicated by the unusual $\Delta_T^{(P)}$ values which corrected for non-ideality.

3.3.3 The Beerbower method

Hansen (2000) recommended the Beerbower method for calculating HSP via group contribution. The equation used for this calculation was:

$$\delta_x = \left[\frac{\Sigma \Delta V \delta_x^2}{\Sigma \Delta V} \right]^{1/2} \qquad \text{(Eqn. 3:02)}$$

Example calculations for calculating HSP values of linalool and poly(amide) are shown below in Tables 3:12 and 3:13 respectively. The instructions in Hansen (2000) were unclear, which created some confusion for calculating the HSP of ketones and esters. For more detailed information regarding this method of HSP calculation, refer to Hansen (2000).

Table 3:13 HSP calculation for linalool using the Beerbower method (J/mol).

Structural groups	No. groups (N)	N∗ΔV	N∗ΔV δ_D^2	N∗ΔV δ_P^2	N∗ΔV δ_H^2	N∗ΔV δ_T^2
– CH_3	3	100.5	14121.0	0.0	0.0	14121.0
>CH_2	2	32.2	9874.2	0.0	0.0	9874.2
>C<	1	-19.2	1464.4	0.0	0.0	1464.4
=CH_2	1	28.5	3556.4	104.6	753.1	4309.5
=CH–	2	27.0	7322.0	150.6	1506.2	8619.0
=C<	1	-5.5	3347.2	251.0	753.1	4309.5
– OH	1	10.0	7405.7	2928.8	19455.6	29790.1
	Sum:	173.5	47090.9	3435.1	22468.1	72487.8
			δ_d	δ_p	δ_h	δ_t
	HSP:		16.5	4.4	11.4	20.5

Table 3:14 HSP calculation for Poly(amide 6,6) using the Beerbower method (J/mol).

Structural groups	No. groups (N)	N∗ΔV	N∗ΔV δ_D^2	N∗ΔV δ_P^2	N∗ΔV δ_H^2	N∗ΔV δ_T^2
$>CH_2$	10	161.0	49371.2	0.0	0.0	49371.2
-CO-	2	21.6	655.1	5811.1	6694.4	34727.2
-NH-	2	9.0	9623.2	836.8	6276.0	16736.0
	Sum:	191.6	59649.5	6647.9	12970.4	100834.4
			δ_d	δ_p	δ_h	δ_t
	HSP:		17.6	5.9	8.2	22.9

3.3.4 Results of group contribution calculation of HSP

The HSP parameters for selected solvents and polymers, obtained by the various group contribution methods are summarised in Table 3:15.

Table 3:15 HSP values calculated by various methods ($MPa^{½}$).

	Dispersion (δ_d)	Polarity (δ_p)	H-bonding (δ_h)	Total (δ_t)
Linalool				
Hoftyzer-Van Krevelen method	15.8	2.8	10.6	19.2
Hoy method	14.0	7.7	11.3	19.6
Beerbower method	16.3	4.4	11.2	20.5
Kanani (2003)	16.5	2.8	10.6	19.8
Mean	**15.7**	**4.4**	**10.9**	**19.7**
Linalyl acetate				
Hoftyzer-Van Krevelen method	15.7	2.2	5.7	16.8
Hoy method	15.1	7.9	7.4	18.6
Beerbower method	14.3	1.5	6.2	15.7
Mean	**15.0**	**3.9**	**6.4**	**17.0**
Polyethylene				
Hoftyzer-Van Krevelen method	17.7	0.0	0.0	17.7
Hoy method	18.0	0.0	0.0	18.0
Beerbower method	17.5	0.0	0.0	17.5
Mean	**17.7**	**0.0**	**0.0**	**17.7**
Solubility data (Hansen, 2000)	17.7	5.3	3.2	18.7
Poly(amide 6,6)				
Hoftyzer-Van Krevelen method	18.1	8.0	7.2	21.1
Hoy method	15.7	12.3	9.5	22.1
Beerbower method	17.6	5.9	8.2	22.9
Mean	**17.1**	**8.7**	**8.3**	**22.0**
Solubility data (Hansen, 2000)	17.2	9.9	16.5	25.8

Table 3:15 Continued...

	Dispersion (δ_d)	Polarity (δ_p)	H-bonding (δ_h)	Total (δ_t)
Polycarbonate				
Hoftyzer-Van Krevelen method	15.9	2.5	6.2	17.2
Hoy method	14.9	11.6	11.0	21.9
Beerbower method	9.6	7.4	5.1	18.6
Mean	**13.5**	**7.2**	**7.4**	**19.2**
Solubility data (Hansen, 2000)	18.6	8.4	6.0	21.3
Poly(ether imide)				
Hoftyzer-Van Krevelen method	15.6	11.3	9.8	21.6
Hoy method	11.3	18.2	13.8	25.5
Beerbower method	18.9	10.8	11.3	24.5
Mean	**15.3**	**13.4**	**11.6**	**23.9**
Solubility data (Hansen, 2000)	17.3	5.4	6.3	19.2
Poly(ether sulfone)				
Hoftyzer-Van Krevelen method	18.0	2.8	5.4	19.0
Hoy method	15.3	11.4	9.9	21.5
Beerbower method	-	-	-	-
Mean	**16.7**	**7.1**	**7.7**	**20.3**
Solubility data (Hansen, 2000)	18.7	10.3	7.7	22.7
Polyimide				
Hoftyzer-Van Krevelen method	18.0	13.3	9.9	24.5
Hoy method	11.4	17.9	13.2	25.0
Beerbower method	19.1	10.3	10.9	24.3
Mean	**16.2**	**13.8**	**11.3**	**24.6**
Solubility data (Hansen, 2000)	24.3	19.5	22.9	38.7
Poly(methyl methacrylate)				
Hoftyzer-Van Krevelen method	17.0	5.8	9.1	20.2
Hoy method	13.6	9.3	10.3	19.4
Beerbower method	15.1	12.6	8.0	20.3
Mean	**15.2**	**9.2**	**9.1**	**20.0**
Solubility data (Hansen, 2000)	17.9	9.7	5.5	21.1
Polypropylene				
Hoftyzer-Van Krevelen method	16.5	0.0	0.0	16.5
Hoy method	16.7	0.0	0.0	16.7
Beerbower method	16.4	0.0	0.0	16.4
Mean	**16.5**	**0.0**	**0.0**	**16.5**
Solubility data (Hansen, 2000)	17.6	2.8	0.3	17.8
Poly(tetrafluoro ethylene)				
Hoftyzer-Van Krevelen method	16.3	0.0	0.0	16.3
Hoy method	-	-	-	-
Beerbower method	8.4	11.9	0.0	20.3
Mean	**12.4**	**5.9**	**0.0**	**18.3**
Solubility data (Hansen, 2000)	16.7	5.0	2.4	17.6

Kanani (2003) calculated linalool HSP by Van Krevelen group contribution method.

The values obtained (Table 3:15) by the various group contribution methods do not always agree well with the values obtained from solubility data. Van Krevelen (1990) considered that

the Hoftyzer-Van Krevelen and Hoy algorithmic methods have similar accuracy (10%), and recommended that both methods should be used and the results averaged. The means in Table 3:15 are an average of the Hoftyzer-Van Krevelen, Hoy and Beerbower methods, which can be compared against the solubility study data provided in Hansen (2000).

The average HSP values calculated often varied by more than 10% from the values obtained in solubility experiments. Thus, group contribution is probably the least reliable method to calculate HSP values, especially considering that different manufacturers use different additives in their manufacturing processes.

3.4 Calculating HSP from physical and electrical properties

Relationships exist between physical properties of a molecule, and HSP. The dispersive component δ_d, is correlated to the refractive index (n); the polar component δ_p, is correlated with the dipole moment (μ); and the hydrogen bonding component δ_h, with the hydrogen bonding number (Δv) (Van Krevelen, 1990; Yamaguchi *et al.*, 1992). However, as this kind of data is not always available solvents and polymers, it can be of limited practical use.

3.4.1 Dispersive component

The HSP δ_d component and refractive index of solvents are directly related. Solvents (♦) used to show this correlation in Figure 3:10 included: benzene, cyclohexane, carbon tetrachloride, acetone, methanol, ethanol, and propan-2-ol. Polymers (■) included: polyethylene, polyamide, polycarbonate, poly(ether sulphone), polyimide, poly(methyl methacrylate), polypropylene and poly(tetrafluoro ethylene).

The correlation between refractive index and published δ_d values for solvents and polymers were similar.

Solvent	$\delta_d = 19.9n - 11.4$	$R^2 = 0.99$	(Eqn. 3:03)
Polymer	$\delta_d = 19.4n - 11.2$	$R^2 = 0.51$	(Eqn. 3:04)

Because there were no published δ_d values for the polymers used in this study (manufactured by Goodfellow), δ_d values were obtained using their refractive index values and Eqn. 3:03 (Table 3:16).

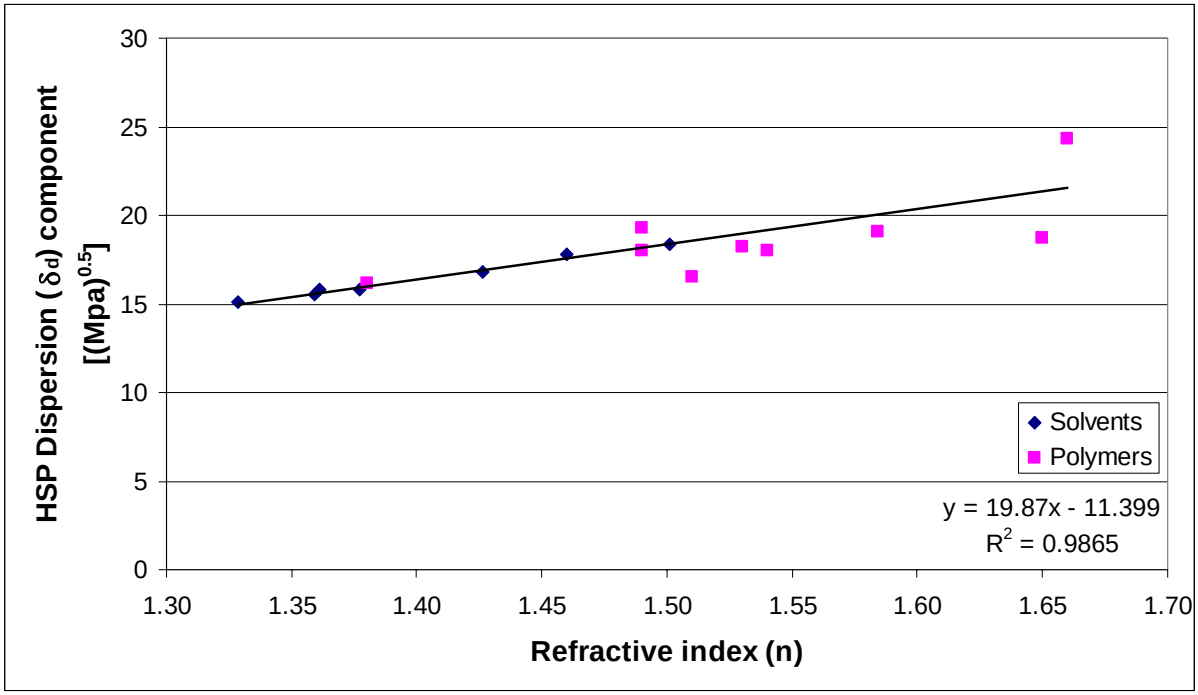

Figure 3:10 Relationship between refractive indices (from Goodfellow (2002) and ChemFinder (2002)) and HSP dispersive component (from Hansen, 2000).

Table 3:16 Dispersion HSP component of polymers calculated from the refractive index supplied by manufacturer.

Polymer	Refractive index♠ (n)	Calculated Dispersion (δ_d)	Published values♥ (δ_d)
HDPE	1.54	19.2	18.0
LDPE	1.51	18.6	15.3
PA	1.53	19.0	17.2
PC	1.584	20.1	18.6
PEI	-	-	17.3
PES	1.65	21.4	18.7
PI	1.66	21.6	24.3
PMMA	1.49	18.2	17.9
PP	1.49	18.2	17.6
PTFE	1.38	16.0	16.7

Key: ♠Goodfellow (2002), ♥ Hansen (2000).

Refractive index more accurately predicts δ_d for the polymers used in this study than both literature values and group contribution methods, because they directly relate to the polymers properties as stated by the manufacturer, rather than generic assumptions about polymer species.

3.4.2 Polar component

The polar HSP component of solvents is correlated with their dipole moment (Figure 3:11). This dataset includes dipole moments of the solvents: carbon tetrachloride, chloroform, acetone, methanol, ethanol, propan-1-ol, propan-2-ol, butanol, benzene, toluene, phenol, diethyl ether, dimethyl ether, methyl ethyl ether, anisole, acetaldehyde, formaldehyde, ethylene glycol (Weast, 1988).

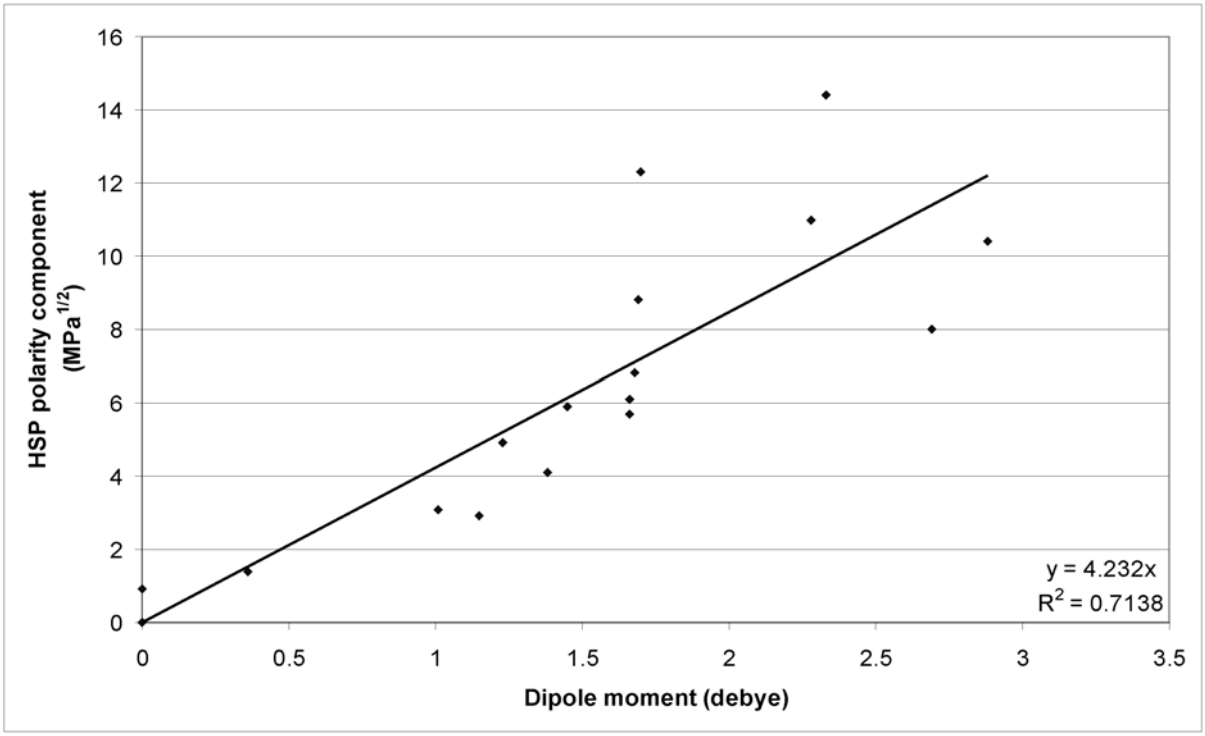

Figure 3:11 Relationship between dipole moments (Weast, 1988) and HSP polar componet (Hansen, 2000), of various solvents.

Hansen derived the following equation to calculate δ_p from dipole moment:

$$\delta_p = 37.4(\mu) / V^{½} \qquad \text{(Eqn. 3:04)}$$

where μ = dipole moment (Debye),

and V = molecular weight/density (cm^3/mol)

The data obtained when using this equation for various solvents agrees with Hansen's (2000) solubility data (Figure 3:12) for the majority of solvents ($R^2 = 0.8546$).

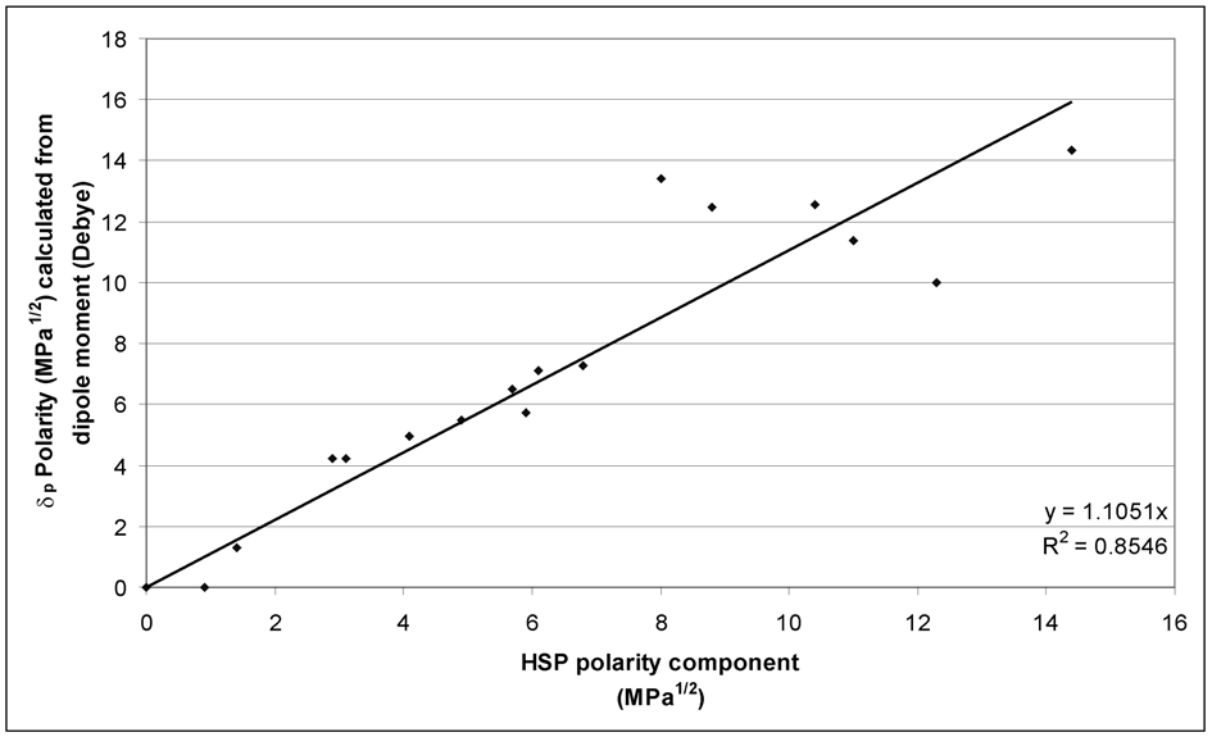

Figure 3:12 Solvent HSP polar component calculation using Hansen's (2000) equation in comparison with solubility values (Hansen, 2000), (Weast, 1988).

Because dipole moments were not available for polymer materials used in this study, Eqn. 3:04 could not be used directly. However, the dipole moment can be calculated using the dielectric constant and the refractive index (via the Masotti-Debye equation, Eqn. 3:05), if polymer molecular weights (M_r) are known:

$$\left(\frac{M_r}{\rho}\right)\left(\frac{\varepsilon-1}{\varepsilon+2}\right)-\left(\frac{M_r}{\rho}\right)\left(\frac{n^2-1}{n^2+2}\right)=P_o=\left(\frac{4\pi N}{3}\right)\left(\frac{\mu^2}{3kT}\right) \qquad \text{(Eqn. 3:05)}$$

where; ρ = density, ε = dielectric constant, n = refractive index, P_o = electric polarizability, N = Avogadro's number, μ = dipole moment, k = Boltzman constant, and T = temperature.

In the absence of polymer molecular weights, the published dielectric constants (Goodfellow, 2002) for the polymers used in the experiments, were used to determine the polarizability, which in turn was used to calculate the HSP polar component.

Calculating polarizability

When an insulating material is subjected to an electric field, an electric dipole is induced. The magnitude of the dipole depends on the strength of the applied field and a characteristic of the substance, known as polarizability. The magnitude of the polarizability (P_o), of a dielectric material is related to the dielectric constant (ε) (Seymour and Carraher, 1988):

$$P_o = \frac{3(\varepsilon - 1)}{4\pi(\varepsilon + 2)} \qquad \text{(Eqn. 3:06)}$$

Figure 3:13 shows the relationship between dielectric data published by Goodfellow (2002) and HSP polar component δ_p for equivalent generic polymer species (Hansen, 2000). These polymer species include: ABS, CA, CAB, CTFE, E-CTFE, FEP, HDPE, LDPE, PA 6,6, PA 11, PA 12, PBT, PC, PEI, PES, PETP, PI, PMMA, POM, PP, PPO, PS, PTFE, PVC, PVDC, and TPX.

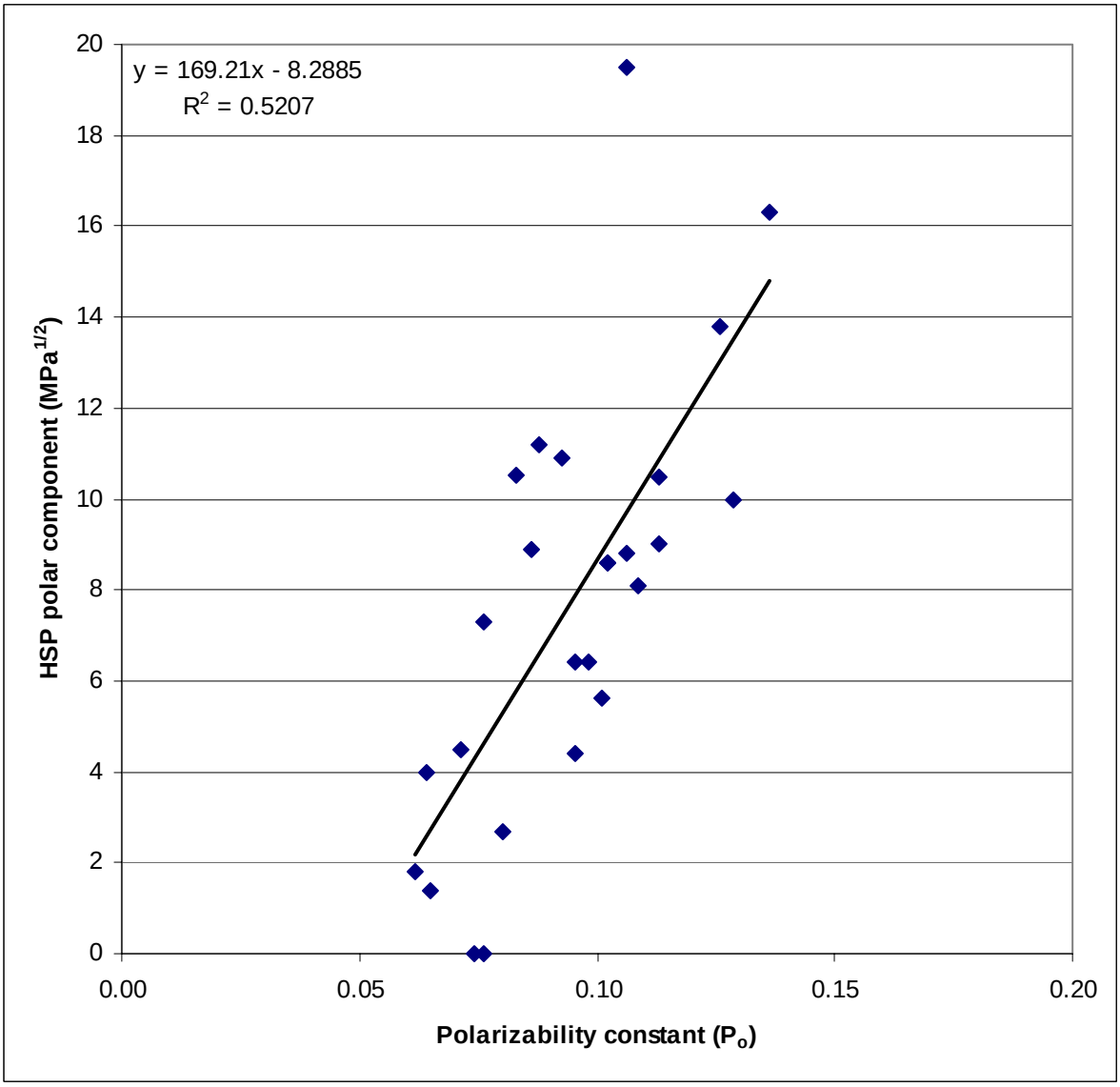

Figure 3:13 Relationship between polarizability constant and δ_p for various polymer species.

Although the correlation coefficient in Figure 3:13 was low ($R^2 = 0.52$), this is most likely due to the use of generic HSP for the 26 polymer species used to determine this equation. If

the outlier value for PI (δ_p = 19.5) is removed from the dataset, the correlation coefficient improves to R^2 = 0.60 and the equation becomes $\delta_p = 157.17P_o - 7.5527$. When viewed in conjunction with other methods of determining δ_p, this degree of variation does not detract significantly from the usefulness of this correlation to determine specific δ_p for the polymers used in this study. Because PI is included in the dataset in Table 3:17, the equation used to calculate the polar HSP component was $\delta_p = 169.21P_o - 8.2885$ (Figure 3:13).

Table 3:17 Calculation of polar HSP component of Goodfellow (2002) polymers from dielectric constants provided in technical data supplied by manufacturer.

Polymer	Dielectric constant (ε)	Polarizability constant (P_o)	Calculated Polarity (δ_p)
HDPE	2.35	0.0741	4.2
LDPE	2.275	0.0712	3.8
PA	3.4	0.1061	9.7
PC	2.9	0.0926	7.4
PEI	3.7	0.1131	10.8
PES	3.1	0.0983	8.3
PI	3.4	0.1061	9.7
PMMA	2.6	0.0830	5.8
PP	2.4	0.0760	4.6
PTFE	2.05	0.0619	2.2

Further investigation based on swelling properties of actual polymers may contribute to a better understanding of polymer δ_p.

3.4.3 Hydrogen bonding component:

The hydrogen bonding parameter was originally found by subtracting the polar (E_p) and dispersion (E_d) energies of vaporization from the total energy of vaporization ($E = \Delta H_{vap} - RT$). This is still widely used if reliable data for $E = E_d + E_p + E_h$ are available. When such data are not available, the group contribution techniques are the best method for determining δ_h (Hansen, 2000).

3.5 Calculation of HSP by membrane swelling experiments.

Traditionally, HSP for polymers were determined graphically. The degree a polymer dissolved when immersed in 40-45 well chosen solvents was noted, and the HSP of soluble and insoluble solvents were then plotted. The centre of a circle around the soluble solvents

(Figure 3:14) was designated the 3D-HSP coordinates for the polymer. The boundary between solvents/non-solvents is most important in determining the centre of the sphere and consequently the HSP of the polymer (Hansen, 2000).

However, if the number of solvents available to test polymer solubility is small, better results are obtained by measuring the degree of swelling or solvent uptake (Hansen, 2000).

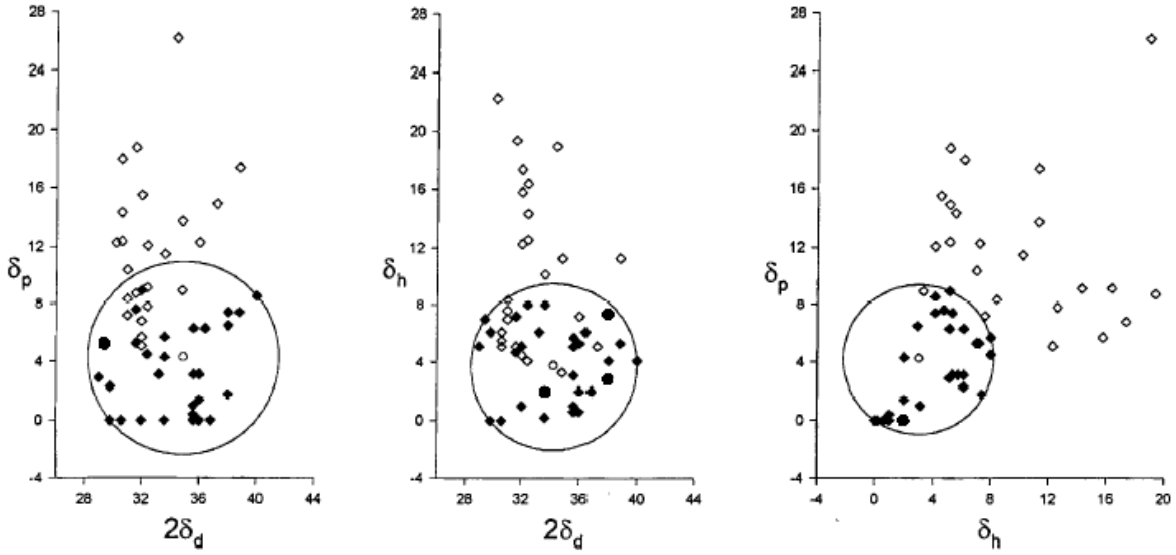

Figure 3:14 Graphical method for determining HSP of polymers (δ_d= 17.3, δ_p =4.3, δ_h = 3.4) (Zellers *et al.*, 1996a).

Yamaguchi *et.al.* (1992; 1993) simplified determining polymer solubility coefficients by using only eight solvents (benzene, cyclohexane, carbon tetrachloride, acetone, methanol, ethanol, 2-propanol, and water) rather than the 54 proposed by Hansen (2000) for solubility experiments. The solvents chosen have a broad range of values for the component parameters (Table 3:18), allowing the affinity between the selected polymers and solvents to be correlated effectively.

Table 3:18 HSP parameters of solvents used in Yamaguchi *et.al.* (1993) experiments.

Solvent	δ_d	δ_p	δ_h	Molar vol.
benzene	18.4	0.9	2.0	89.4
cyclohexane	16.8	0.0	0.2	108.7
carbon tetrachloride	17.8	0.0	0.6	97.1
acetone	15.5	10.4	7.0	74.0
methanol	15.1	12.3	22.3	40.7
ethanol	15.8	8.8	19.4	58.5
2-propanol	15.8	6.1	16.4	76.8
water	15.5	16.0	42.3	18.0

Measuring solubility

Yamaguchi *et al.* (1993) methodology was used to measure solubility coefficients of the membrane materials HDPE, LDPE, PA 66, PC, PEI, PES, PI, PMMA, PP and PTFE (Goodfellow UK, Ltd.), in the following eight AR grade solvents: benzene (Scharlau, 99.8%), cyclohexane (Unilab, 95%), carbon tetrachloride (May & Baker, 99.8%), acetone (Univar, 99.5%), methanol (Univar, 99.5%), ethanol (Univar, 99.5%), 2-propanol (Univar, 99.5%), and water (distilled).

Polymer samples were cut into 16 x 16 mm pieces using a metal ruler and sharp blade. The length and width of these samples were then measured using manual calipers (Mitutoyo, ±0.02 mm), the thickness measured (average of six points) using a digital micrometer (Mitutoyo, ±0.001 mm), and weighed on a microbalance (Mettler, ±0.1 mg). Duplicate polymer samples were immersed in 15 mL of each solvent, and equilibrated in an oven at 25°C for two days. Samples were removed from the solvent using tweezers on one corner of the sample, then excess solvent was removed by wiping the surfaces on a piece of filter paper that had been previously soaked in the same solvent. The swollen membrane was weighed immediately (Mettler, ±0.1 mg). Weight decreased due to evaporation, so measurements were recorded at 5-10 second intervals over one minute. The weight was then plotted against time and extrapolated to give the initial weight at time zero.

The degree of solubility was expressed in terms of the solubility coefficient *S* (g of solvent/g of dry membrane) (Yamaguchi *et al.*, 1993):

$$S = \frac{\left(\frac{\Delta W}{\rho_1}\right)}{\left(\frac{\Delta W}{\rho_1} + \frac{1}{\rho_2}\right)} \qquad \text{(Eqn. 3:08)}$$

where ΔW is weight of organic liquid dissolved in the membrane (g of solvent/g of dry membrane) and ρ_1, ρ_2 are density of liquid and dry membrane respectively.

Yamaguchi *et.al.*, (1992) used a critical value to define polymers as soluble ($S_c > 0.42$) or insoluble ($S_c < 0.42$). Other researchers use different uptake criterion (10, 25, 50, 100 and 200%) to define solubility / insolubility, and hence the size of the polymer solubility sphere (Zellers *et al.*, 1996a).

Zellers *et.al.* (1996b) proposed that a weighted average of weight gain (affinity) for polymers soaked in a range of organic solvents, be used to calculate the HSP values (Eqn. 3:09). The weighting factor is the product of solvent molar volume (V = mol/cm^3) and fractional uptake of the solvent (g solvent / g polymer) obtained by immersion testing:

$$\delta_{d2,p2,h2} = \frac{\sum_{i=1}^{n} u_i V_{li}^{z} \delta_{(d1,p1,h1)i}}{\sum_{i=1}^{n} u_i V_{li}^{z}} \qquad \text{(Eqn. 3:09)}$$

where u_i is fractional uptake of solvent *i* expressed in terms of weight or volume and *n* is total number of solvents tested. The exponential term *z* allows for adjustment of the weighting of the solvent molar volume.

Solubility coefficient

Data from the sorption experiments are shown in Table 3:19. Where a solvent completely disintegrated/dissolved the polymer, a value of 1 was assigned. Values above Yamaguchi *et al.*'s (1992) critical level of $S_c = 0.42$ are indicated in bold. Yamaguchi *et al*. (1992) considered that this experimental methodology had a standard error of 10%.

PMMA had the lowest chemical resistance ($S = 1$) and disintegrated in benzene, carbon tetrachloride and acetone. HDPE, which has the smallest radius of interaction ($R_o = 2.0$) in Hansen (2000) data, was one of the most "soluble" polymers. This HDPE (Goodfellow UK, Ltd.) had HSP values closer to the published values (Hansen, 2000) of generic polyethylene polymers rather than the high density polyethylene HSP values.

Table 3:19 Sorption ($S = (\Delta W / \rho_1) / (\Delta W / \rho_1 + 1 / \rho_2)$) results of membranes at 25°C.

	Bz	Chx	CCl_4	AcO	MeOH	EtOH	PrOH	H_2O
HDPE	**0.83**	**0.86**	**0.80**	**0.64**	**0.55**	**0.80**	**0.68**	**0.75**
LDPE	**0.56**	**0.57**	**0.52**	0.29	**0.44**	**0.45**	**0.50**	0.34
PA 66	**0.47**	0.38	**0.45**	0.28	0.38	**0.49**	**0.56**	0.34
PC	**1**	**0.47**	**0.62**	**0.92**	**0.54**	**0.63**	**0.63**	**0.44**
PEI	0.41	**0.47**	0.36	**0.59**	**0.52**	**0.53**	**0.54**	0.27
PES	**0.55**	**0.57**	0.31	**1**	**0.47**	**0.55**	**0.56**	0.35
PI	**0.50**	**0.55**	0.28	0.40	**0.42**	**0.48**	**0.56**	0.41
PMMA	**1**	**0.46**	**1**	**1**	**0.57**	**0.61**	**0.60**	0.18
PP	**0.79**	**0.67**	**0.63**	**0.58**	**0.46**	**0.63**	**0.63**	**0.58**
PTFE	0.38	**0.57**	0.40	0.37	0.38	**0.47**	**0.56**	0.01

Bz = benzene, Chx = cyclohexane, CCl_4 = carbon tetrachloride, AcO = acetone, MeOH = methanol, EtOH = ethanol, PrOH = propan-2-ol, H_2O = water.
Bold values are $S_c > 0.42$. Polymers which disintegrated were assigned a value of $S = 1$.

PC and PP also had $S > 0.42$ in all solvents tested. Thus HDPE, PC and PP should have very large solubility spheres. The samples of HDPE, PP and PC were 10.5, 17.0 and 20.0 μm thick respectively, compared with 26.1 – 51.8 μm thick for the other polymers tested (Figure 3:15). The thinness of the membrane may have decreased the accuracy of the measurements, and hence the predicted HSP values. PTFE and PI deviate from the trend (Figure 3:15) because they are much more dense than the other polymers tested.

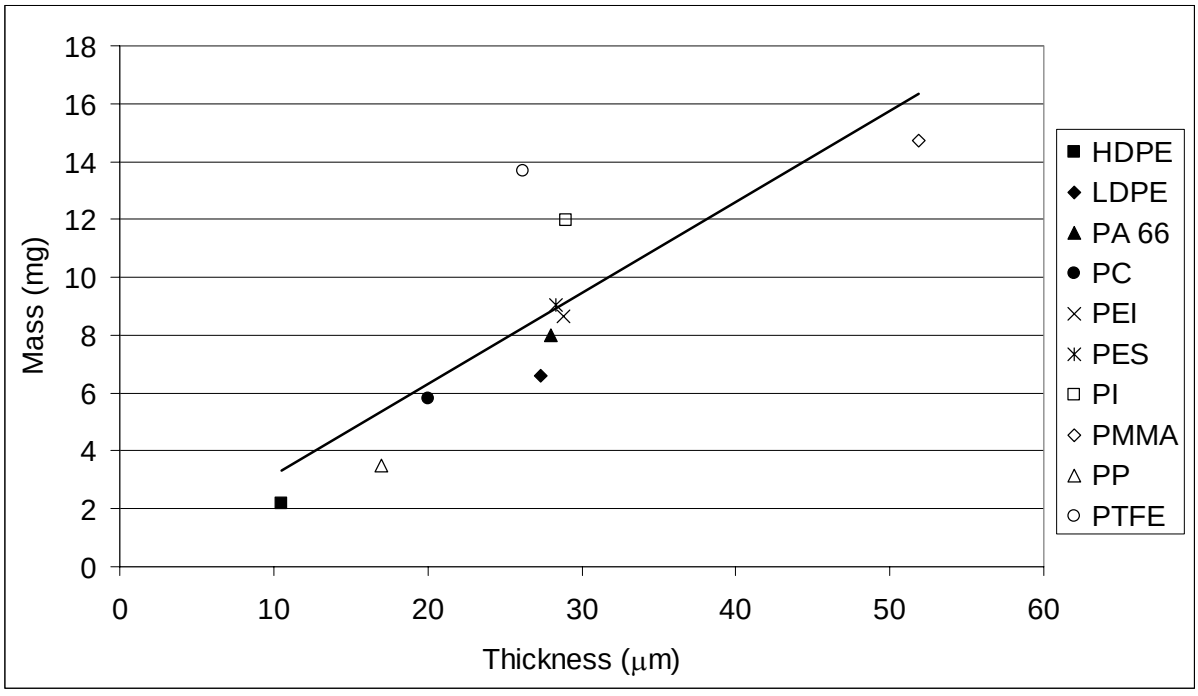

Figure 3:15 Thickness and mass of 16x16 mm polymer samples used in membrane swelling experiments.

Immersion testing

Where the polymer completely dissolved, u_i was assigned a value of 10 (Eqn. 3:09). The polymers HDPE and PC absorbed the most solvent without disintegrating (Table 3:20).

Table 3:20 Amount of solvent absorbed by polymer membranes at 25°C (g solvent/g polymer).

	Bz	Chx	CCl_4	AcO	MeOH	EtOH	PrOH	H_2O
HDPE	5.10	5.52	7.64	1.65	1.15	3.81	1.97	3.47
LDPE	1.27	1.17	1.96	0.36	0.71	0.74	0.92	0.57
PA 66	0.77	0.46	1.28	0.30	0.46	0.74	0.97	0.49
PC	10.00	0.64	2.48	8.11	0.87	1.26	1.29	0.73
PEI	0.55	0.63	0.80	1.04	0.79	0.83	0.86	0.34
PES	0.92	0.90	0.61	10.00	0.61	0.84	0.88	0.47
PI	0.59	0.63	0.41	0.36	0.38	0.49	0.68	0.46
PMMA	10.00	0.65	10.00	10.00	1.05	1.23	1.18	0.21
PP	4.30	2.10	3.47	1.43	0.86	1.76	1.79	1.81
PTFE	0.29	0.55	0.56	0.24	0.26	0.38	0.54	0.01

Results of HSP calculated using Zellers *et al.*'s (1996b) method are given in Table 3:21. The accuracy of this method is limited by the number of solvents used in the analysis. Ideally, 27 solvents should be used, but as few as 13 can be used (Zellers *et al.*, 1996b).

Table 3:21 HSP of polymers calculated by the weighted average method using the immersion test data (Zellers *et al.*, 1996a).

Polymer	δ_d ($MPa^{½}$)	δ_p ($MPa^{½}$)	δ_h ($MPa^{½}$)	δ_t ($MPa^{½}$)
HDPE	17.1	2.6	5.3	18.1
LDPE	17.1	2.8	6.0	18.3
PA 66	16.9	3.7	7.9	19.0
PC	17.1	4.4	5.2	18.4
PEI	16.5	5.1	8.7	19.3
PES	16.0	8.0	7.4	19.4
PI	16.7	4.1	8.3	19.1
PMMA	17.2	3.6	4.0	18.0
PP	17.1	3.0	6.0	18.4
PTFE	16.8	3.4	6.7	18.4

Water is not generally recommended as a test liquid for obtaining HSP parameters (Hansen, 2000). However, solvents with high hydrogen-bonding were needed in the current research, so water was included as one of the solvents.

3.6 Comparison of the different methods for calculating HSP

The effect of the methodology for calculating the HSP of the polymers used in the current research are summarised in Table 3:22. The average of all the methods of determining HSP for each polymer HSP is displayed.

Table 3:22 HSP of polymers calculated by various methods.

	Dispersion (δ_d)	Polarity (δ_p)	H-bonding (δ_h)	Total (δ_t)
Polyethylene - HDPE				
Literature (Hansen, 2000)	18.0	0.0	2.0	18.1
Group contribution	17.7	0.0	0.0	17.7
Refractive index	19.2	-	-	-
Dielectric constant	-	4.2	-	-
Swelling experiments	17.1	2.6	5.3	18.1
Average	**18.0**	**1.7**	**2.4**	**18.0**
Polyethylene - LDPE				
Literature (Hansen, 2000)	15.9	4.9	1.5	16.7
Group contribution	17.7	0.0	0.0	17.7
Refractive index	18.6	-	-	-
Dielectric constant	-	3.8	-	-
Swelling experiments	17.1	2.8	6.0	18.3
Average	**17.3**	**2.9**	**2.5**	**17.6**
Poly(amide 6,6)				
Literature (Hansen, 2000)	17.2	9.9	16.5	25.8
Group contribution	17.1	8.7	8.3	22.0
Refractive index	19.0	-	-	-
Dielectric constant	-	9.7	-	-
Swelling experiments	16.9	3.7	7.9	19.0
Average	**17.6**	**8.0**	**10.9**	**22.3**
Polycarbonate				
Literature (Hansen, 2000)	18.6	8.4	6.0	21.3
Group contribution	13.5	7.2	7.4	19.2
Refractive index	20.1	-	-	-
Dielectric constant	-	7.4	-	-
Swelling experiments	17.1	4.4	5.2	18.4
Average	**17.3**	**6.9**	**6.2**	**19.6**
Poly(ether imide)				
Literature (Hansen, 2000)	17.3	5.4	6.3	19.2
Group contribution	15.3	13.4	11.6	23.9
Refractive index	-	-	-	-
Dielectric constant	-	10.8	-	-
Swelling experiments	16.5	5.1	8.7	19.3
Average	**16.4**	**8.7**	**8.9**	**20.8**

Table 3:22 continued…

	Dispersion (δ_d)	Polarity (δ_p)	H-bonding (δ_h)	Total (δ_t)
Poly(ether sulfone)				
Literature (Hansen, 2000)	18.7	10.3	7.7	22.7
Group contribution	16.7	7.1	7.7	20.3
Refractive index	21.4	-	-	-
Dielectric constant	-	8.3	-	-
Swelling experiments	16.0	8.0	7.4	19.4
Average	**18.2**	**8.4**	**7.6**	**20.8**
Polyimide				
Literature (Hansen, 2000)	24.3	19.5	22.9	38.7
Group contribution	16.2	13.8	11.3	24.6
Refractive index	21.6	-	-	-
Dielectric constant	-	9.7	-	-
Swelling experiments	16.7	4.1	8.3	19.1
Average	**19.7**	**11.8**	**14.2**	**27.5**
Poly(methyl methacrylate)				
Literature (Hansen, 2000)	17.9	9.7	5.5	21.1
Group contribution	15.2	9.2	9.1	20.0
Refractive index	18.2	-	-	-
Dielectric constant	-	5.8	-	-
Swelling experiments	17.2	3.6	4.0	18.0
Average	**17.1**	**7.1**	**6.2**	**19.7**
Polypropylene				
Literature (Hansen, 2000)	17.6	2.8	0.3	17.8
Group contribution	16.5	0.0	0.0	16.5
Refractive index	18.2	-	-	-
Dielectric constant	-	4.6	-	-
Swelling experiments	17.1	3.0	6.0	18.4
Average	**17.4**	**2.6**	**2.1**	**17.6**
Poly(tetrafluoro ethylene)				
Literature (Hansen, 2000)	16.7	5.0	2.4	17.6
Group contribution	12.4	5.9	0.0	18.3
Refractive index	16.0	-	-	-
Dielectric constant	-	2.2	-	-
Swelling experiments	16.8	3.4	6.7	18.4
Average	**15.5**	**4.1**	**3.0**	**18.1**

Based on the principle of Hansen solubility parameters that polymers and solvents in close proximity to each other in 3D-HSP space, have high affinity for each other, the data obtained shows that solvents with:

- high δ_d, δ_p, and δ_h parameters will be most attracted to polyimide;
- moderate δ_d, δ_p, and δ_h will be attracted to polymers such as polycarbonate or PMMA;
- low δ_p, and δ_h parameters should be most attracted to polyethylene or polypropylene.

After investigating the various different methods for determining HSP, it was concluded that the polymer swelling method was better than the solubility method as it was simple, time efficient and used a far lower number of potentially toxic solvents. If electrical data are available for polymers, the refractive index method is a very good method of determining δ_d, and although there was low correlation for the dielectric constant method, this too should give good relative δ_p values within a set of polymers. Possibly the least accurate method of determining HSP was the group contribution method, as it made a large number of assumptions based on generic polymer species, and took no account of individual variations due to manufacturing process and additives.

Chapter 4

Materials & Methods

This chapter provides a detailed reference list of materials and equipment used in this research and discusses the experimental procedures used in pervaporation experiments. Data analysis procedures and mass balance analyses are Appendices 1 and 2.

4.1 Materials list

Solvents

All organic solvents used were AR grade.

Acetone (Univar, 99.5%), Benzene (Scharlau, 99.8%), Cyclohexane (Unilab, 95%), Carbon tetrachloride (May & Baker, 99.8%), Ethanol (Univar, 99.5%), Linalool (Aldrich, 97%), Linalyl acetate (Aldrich, 97%), Methanol (Univar, 99.5%), 1-Octanol (Sigma, 99%), Propan-2-ol (Univar, 99.5%), Water (distilled), Liquid nitrogen (University of Waikato).

Polymers

All polymers shown in Table 4.01 were purchased from Goodfellow Cambridge Ltd.

Table 4.01 Details of polymer materials used for PV and solubility experiments. *(Mathias, 2004; Robello, 2004).

Polymer Film	Structure *	Details	Thickness	Manufacturer code
Polyamide (PA 6,6)	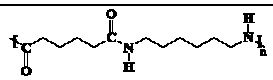	Nylon 6,6,	0.025 mm	LS214545 JV, AM321025/1
Polycarbonate (PC)	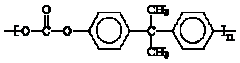	Yellow Makrofol N® isotropic cast	0.020 mm	LS214545 JV, CT301210/2
Polyetherimide (PEI)	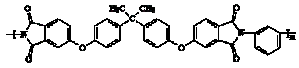	Clear amber	0.025 mm	LS214545 JV, EI311025/1
Polyethersulphone (PES)	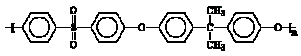	Clear amber	0.025 mm	LS236146 JV, SU301025/3
Polyethylene, Low Density (LDPE)	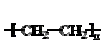	Clear	0.025 mm	LS214545 JV, ET311126/2
Polyethylene, High Density (HDPE)		Clear	0.010 mm	LS214545 JV, ET321010/1
Polyimide (PI)	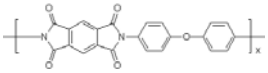	Black Kapton MTB®	0.025 mm	LS214545 JV, IM301213/1
Polymethylmethacrylate (PMMA, Acrylic)	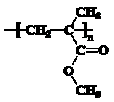	Impact modified	0.050 mm	LS236146 JV, ME301200/1
Polypropylene (PP)	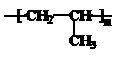	Clear - Biaxially oriented	0.015 mm	LS236146 JV, PP301150/1
Polytetrafluoroethylene (PTFE)	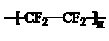	Clear	0.015 mm	LS236146 JV, FP301200/6

4.2 Equipment list

Pervaporation equipment

Water bath (± 0.2°C, Julabo F25, Germany)

2-L Feed tank (designed by P Ewart, built by the University of Waikato workshop staff).

Feed pump (Ismatec Reglo-Z, Switzerland)

Membrane cell (built by University workshop: diameter 210 mm, height 90 mm)

Stainless steel tubing with hot water pipe lagging insulation and Swagelock fittings

Thermocouples (0-100°C, unknown origin)

Pressure transmitter (-1 - 0 bar, Alexander Wiegand GmbH & Co.)

Vapour flow monitor (Top-Trak™ Series 820, Sierra Instruments, The Netherlands)

Vacuum pump (Edwards RV3, England)

Gas Chromatograph with Flame Ionisation Detector, and 1-mL gas sampling valve (GC-FID, Perkin Elmer Autosystem XL, Australia), Carrier gas: Nitrogen (Instrument Grade), Flame gases: Air (Instrument Grade), Hydrogen (Instrument Grade), Valve actuator gas: compressed air, Chromatography column: Medium polarity, Perkin Elmer PE-5 megabore column (0.53mm i.d. x 25m long x 1.5µm film thickness) or Alltech AT-5 column (0.53mm i.d. x 30m long x 1.5µm film thickness).

Cold traps (purpose built 500mL, University glassblower)

Computers, Electronics & Software

Computer (Pentium III, manufactured by Dell Co., USA containing Microsoft™ Windows ’98 operating system, Microsoft Office 2000)

Process control and data acquisition (Labview™ software, version 5.1 from National Instruments Co., USA)

GC-FID control (Turbochrom Navigator software, Perkin Elmer, USA)

Data monitoring of temperature probes, pressure transmitter and flow meter (LittleStar™ control board, Z-World Engineering, USA)

Miscellaneous equipment

Microbalance (Mettler AG204 Microbalance, grams to 4 d.p.)

Balance (Mettler BB2440 Balance, ±0.01g)

Micrometer (Mitutoyo 293-766-30 digital micrometer, mm to 3 d.p.)

Callipers (Mitutoyo analogue Vernier callipers, 8262611)

Cold trap grease (Glisseal™)

Positive displacement pipettes (Gilson: 10 μL, 250 μL)

Air displacement pipette (Gilson: 1000 μL)

Timer (Electronic clock timer, Model 870A, China)

Volumetric flask (2000mL,)

Volumetric cylinders (10mL, 50mL, 100mL, 500mL, 1000mL)

4.3 Pervaporation equipment

This PV setup consists of a membrane module with a synthetic polymer film, a feed delivery system, a vacuum pump for permeate removal and a permeate condensation system (Figure 4:01).

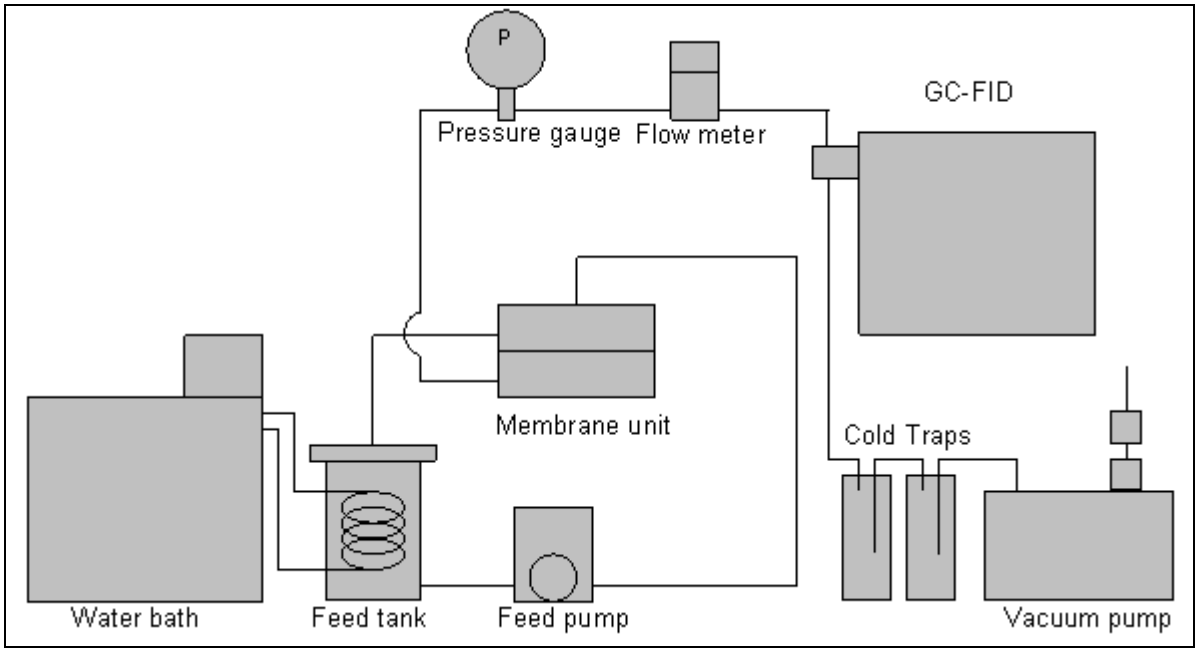

Figure 4:01 Schematic representation of pervaporation equipment.

Feed temperature was regulated by circulating water through heat exchanger coils in the feed tank. Feed solution was pumped from the feed tank to the top of the membrane cell (Figure 4:02 a). The solution then flowed over the surface of the polymer membrane, and retentate returned to the feed tank. Permeate molecules were volatilised from the downstream side of the membrane under vacuum conditions, and transported through the GC-FID equipment to cold traps where they were condensed using liquid nitrogen (Figure 4:02 b).

Process control and data acquisition was carried out using Labview software. Temperature, pressure and flow data from a 10 second interval were averaged and recorded in a text file during the run. Labview also controlled the automated sampling interval of the Gas Chromatograph (GC-FID) using a gas sampling valve (GC-GSV), set to inject 1 mL of permeate vapour under vacuum conditions at 1-hour intervals for a 44-hour run.

(a) 

(b) 

Figure 4:02 Pervaporation system; (a) Feed tank, liquid pump and membrane unit; (b) cold traps and vacuum pump.

4.3.1 Feed tank

The 2-L feed tank (Figure 4:03 and 4:04) was purpose built by the University of Waikato workshop from recycled stainless steel. All external surfaces of the tank were lagged (insulated) (Figure 4:04 a and b). The lid was sealed using an O-ring and a pressure gauge and pressure release valve were mounted on the lid (Figure 4:04 c).

In designing the feed tank, the volume was deemed a compromise between maintining an infinitely large volume during processing, and the expense of feed components. Two litres was deemed sufficiently large that changes in feed composition during processing would be below GC-FID detection limits.

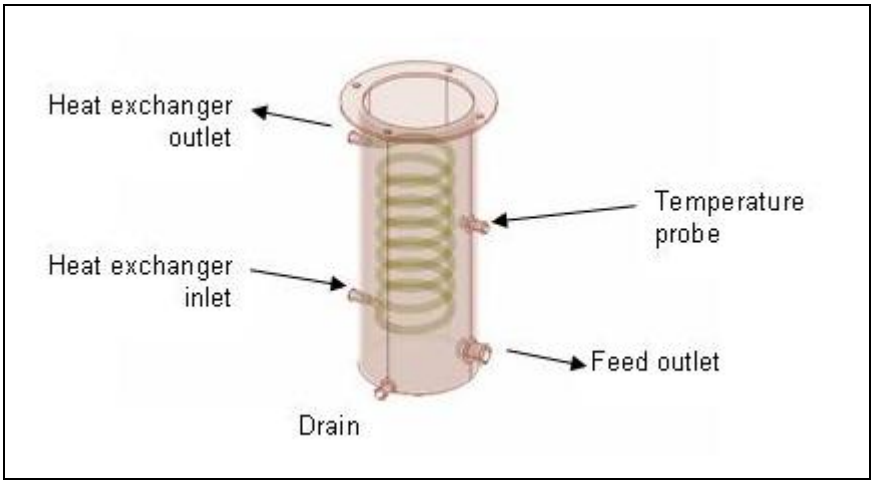

Figure 4:03 Schematic of feed tank; diameter 110 mm, height 240 mm.

(a)

(b)

(c)

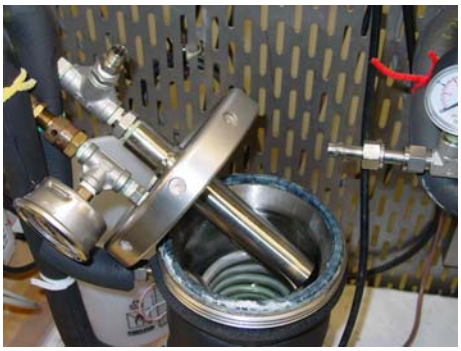

Figure 4:04 Feed tank connected to waterbath with (a) insulation, (b) lid exposed, and (c) showing interior heat exchanger coils.

4.3.2 Membrane cell

The stainless steel membrane cell (diameter 210 mm, height 90mm) was designed by Mr. Dinglei He (He, 2000) and Prof. Jim Dickson (McMaster University in Ontario, Canada) and built by the University of Waikato workshop staff (Figure 4:05).

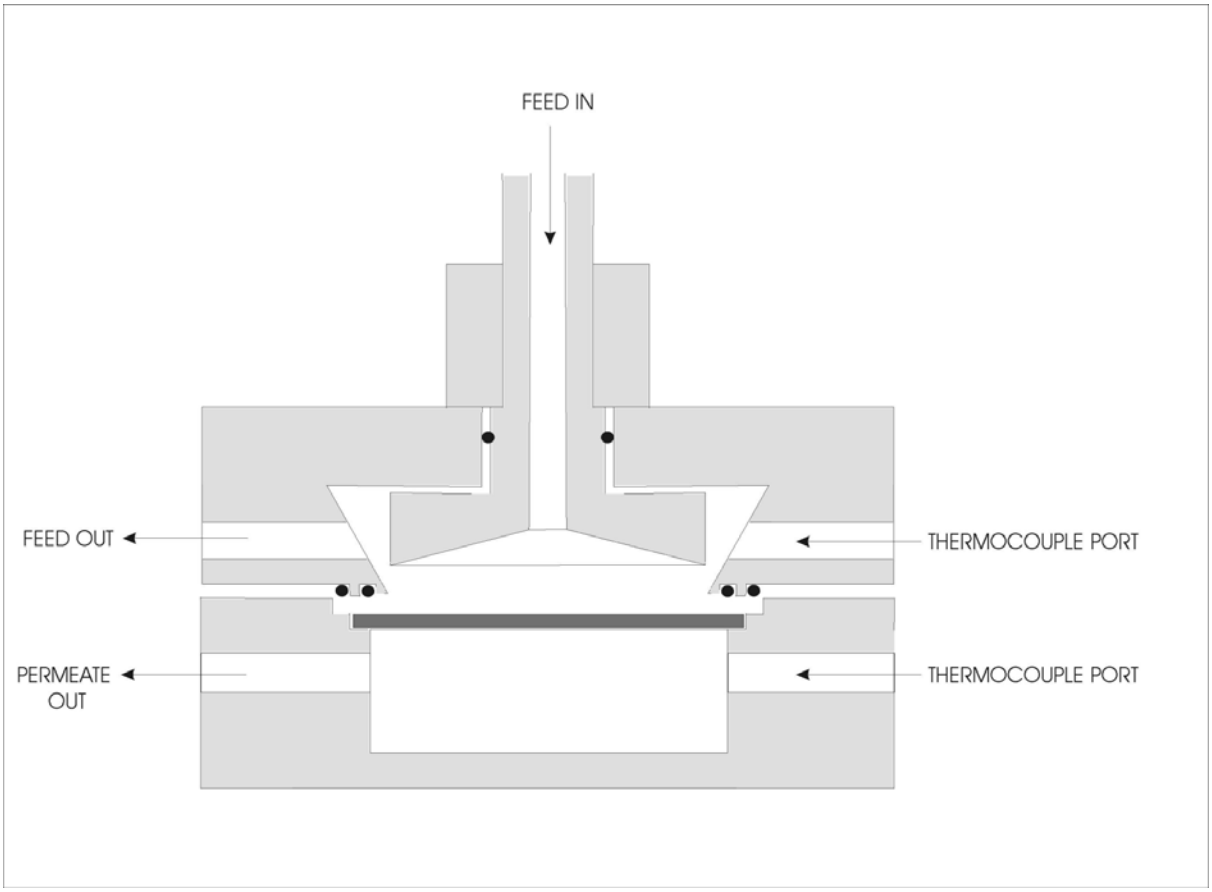

Figure 4:05 Schematic of membrane unit, (●) O-ring seals.

Dimensions for the membrane unit impinging jet (Figure 4:06) were: D_j = 8.73 mm, H = 11.36 mm, L = 1.36 mm, D_m =99.74 mm. The height (L) of the membrane units impinging jet can be altered to affect the flow characteristics of the feed over the membrane surface.

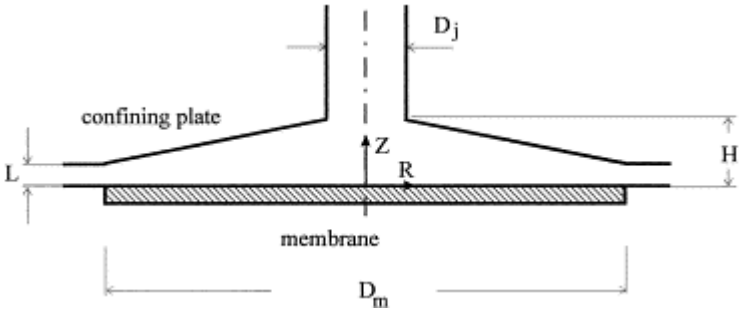

Figure 4:06 Schematic representation of membrane cell impinging jet (Miranda and Campos, 2001a)

The lower section of the membrane unit had a perforated support plate and wire gauze mesh (Figure 4:07). Thin film membranes need to be supported (to prevent perforation) without inhibiting vapor permeate removal on the downstream side. The wire mesh screen on a perforated plate worked satisfactorily. It also removed the possibility of organic molecules being attracted to the support, which would hinder permeation and evaporation into the permeate stream. Other researchers (Sweeny and Rose, 1965) used filter paper on a screen and perforated plate.

(a) 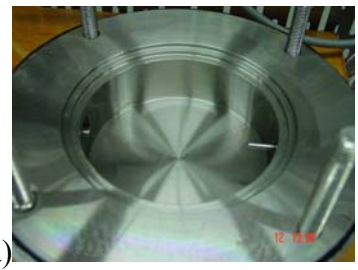 (b)  (c) 

Figure 4:07 Membrane unit (a) permeate chamber, (b) perforated plate, (c) wire gauze.

The upper section of the membrane unit contained O-ring seals (Figure 4:08). The rim of the perforated plate, and plate recesses were lubricated with Glisseal^{TM} before the unit was put together for each run.

(a) 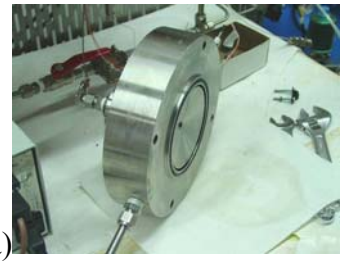 (b) 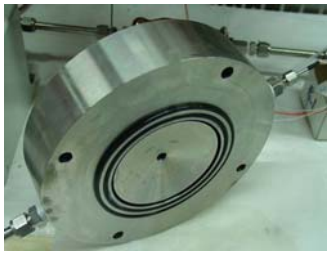 (c) 

Figure 4:08 Membrane unit (a) feed flow distributor, (b) two O-rings, (c) assembled.

Membrane

A 126 mm diameter circular template was used to cut each membrane. The effective membrane area was 0.012469 m^2. Membranes were pre-soaked in feed solution for a minimum of 48 hours to minimise the time to reach steady-state. The dry and wet weight (x6 microbalance measurements), thickness (x6 random digital micrometer measurements) and diameter across four quadrants (calipers) were measured for each membrane.

The pre-soaked membranes were placed on the upper section of the membrane unit. A pulley was used alignin the upper section over the lower section of the unit. The unit was then bolted together and the in/outlet lines connected. The entire membrane unit and feed lines were covered in insulation.

A vacuum was then applied before adding any feed as this procedure has been said to reduce membrane failure (Sweeny and Rose, 1965).

4.3.3 Feed recirculation

Feed was recirculated feed at approximately 804 mL/min (calibrated manually) from the feed tank to the top of the membrane cell, and back to the feed tank. At the end of each PV run, feed lines were purged using compressed air controlled via Labview.

4.3.4 Cold traps

The 500 mL cold traps were built by S Newcombe, the University of Waikato glassblower (Figure 4:09). Vapour was sucked from the permeate side of the membrane, through the GC-GSV and into the cold trap. To prevent permeate condensing inside the glass inner tube and blocking the vacuum pump flow, the cold traps were aligned so that vapour entered the main body of the trap, vapour condensed on the walls, then uncondensed gasses were drawn up through the inner glass tube and into the subsequent trap (Figure 4:09 a). All cold traps were greased with Glisseal^{TM} and weighed, then connected to the GC-GSV and vacuum pump, placed in thermos flasks, evacuated, then surrounded with liquid nitrogen. Any remaining air was sucked up the inner tube and through into the subsequent cold trap prior to the vacuum pump. Two cold traps in series were used to ensure all vapour was collected and no solvent entered the vacuum pump. Liquid nitrogen was replenished at 10-15 hr intervals throughout a PV run.

(a) 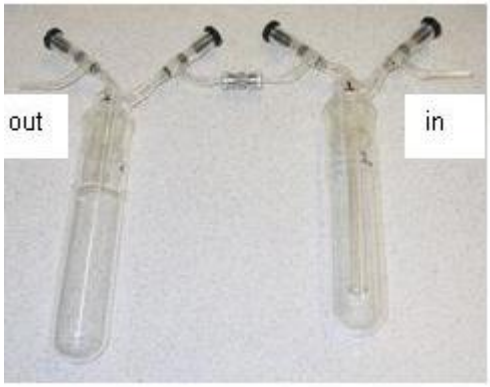

(b) 

Figure 4:09 (a) Cold traps, (b) in thermos flasks with liquid nitrogen.

At the end of a run, cold trap valves were closed and disconnected from the vacuum lines. Cold traps were then removed from the liquid nitrogen and placed in a plastic container and allowed to return to room temperature. Any condensation on the outside was wiped off and the vacuum released. The cold trap was re-weighed to determine the amount of permeate inside. The vapour condensed in the cold trap could later be analysed manually by GC-FID.

4.3.5 Vacuum pump

The vacuum pump had a Swagelock vacuum isolation valve and a one-way Swagelock valve on the pump inlet to prevent pump oil backflowing into the cold traps during a power outage. There was an oil vapour trap on the vacuum pump outlet to recycle pump oil during continuous runs. The vacuum pump was run for 1 hour before every process start-up. Once the cold traps and vacuum lines were connected, a vacuum was created in the PV system by opening isolation valves sequentially, from the vacuum pump and working towards the membrane unit.

4.3.6 Data acquisistion

Process control and data acquisition was carried out using Labview^{TM} software. The GC-FID was controlled by Turbochrom Navigator software. Process data from temperature probes, pressure transmitter and flow meter (Figure 4:10) were acquired by a LittleStar control board and recorded by Labview^{TM}. At the start of each run, LittleStar was zeroed. Initial system conditions were recorded manually including: water bath temperature, permeate pressure, vacuum flow rate, atmospheric pressure, impinging jet height for flow distributor, feed

solution concentration, cold trap filled with liquid nitrogen and feed recirculation pump speed.

Thermocouples were placed in the feed tank and on both the feed and permeate sides of the membrane unit (Figure 4:10). Water bath temperature was controlled by Labview^{TM} software. Normal operating temperatures during various polymer membrane pervaporation runs was 35°C. Thermocouples and water bath temperature were calibrated using a Precision Thermometer (F150, Automatic Systems Laboratory, England).

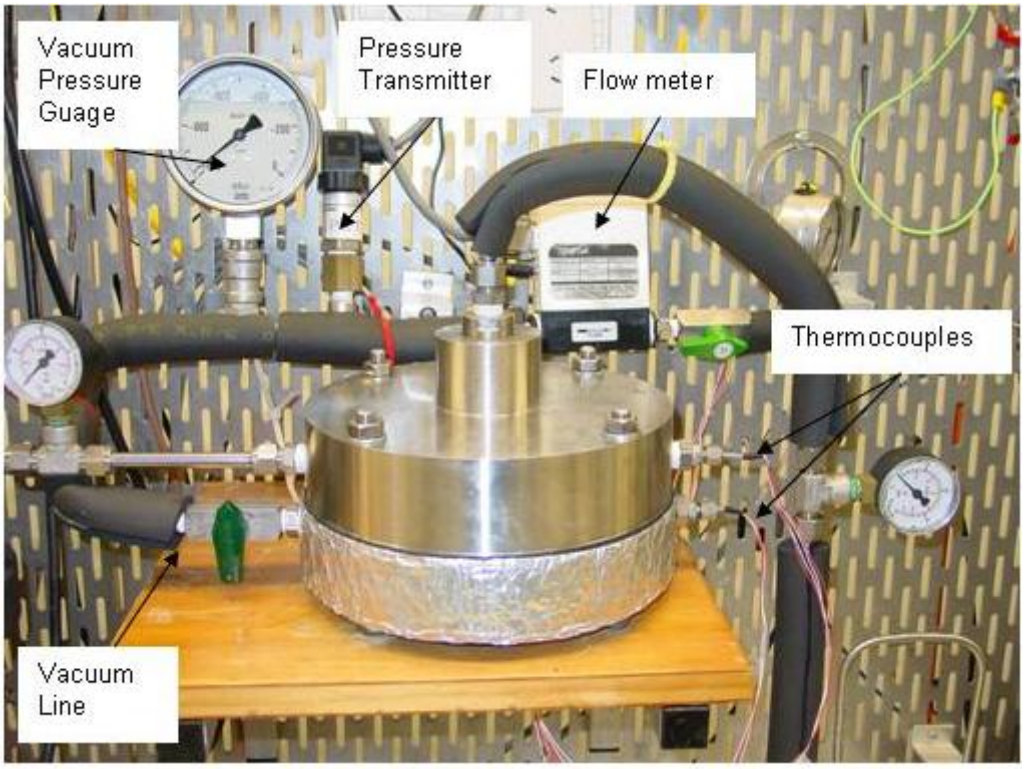

Figure 4:10 Process monitoring instruments.

The pressure and process flow data was transmitted to the computer via RS-232 cables. The pressure transmitter output was calibrated using a mercury manometer (Chemistry Dept., University of Waikato). The flow meter had been factory calibrated and was periodically zeroed online. Standard conditions for the Top-Trak^{TM} mass flow meter ($sccm_{(EtOH)}$) calibration were 21°C and 760 mmHg (Sierra Instruments Inc., 1994). Adjustment factor for solvent vapour content as per manufacturers instructions was incorporated in the Labview data acquisition (see Appendix 1).

4.3.7 GC-FID standard operating conditions

Permeate vapour and liquid feed concentrations were analysed with a Gas Chromatograph equipped with a flame ionisation detector (GC-FID) and gas sampling valve (GSV) (Figure 4:11). Real-time sampling of permeate vapour was desired so steady-state conditions could be monitored throughout each PV run. The GC-FID operating conditions for analyses are shown in Table 4:01.

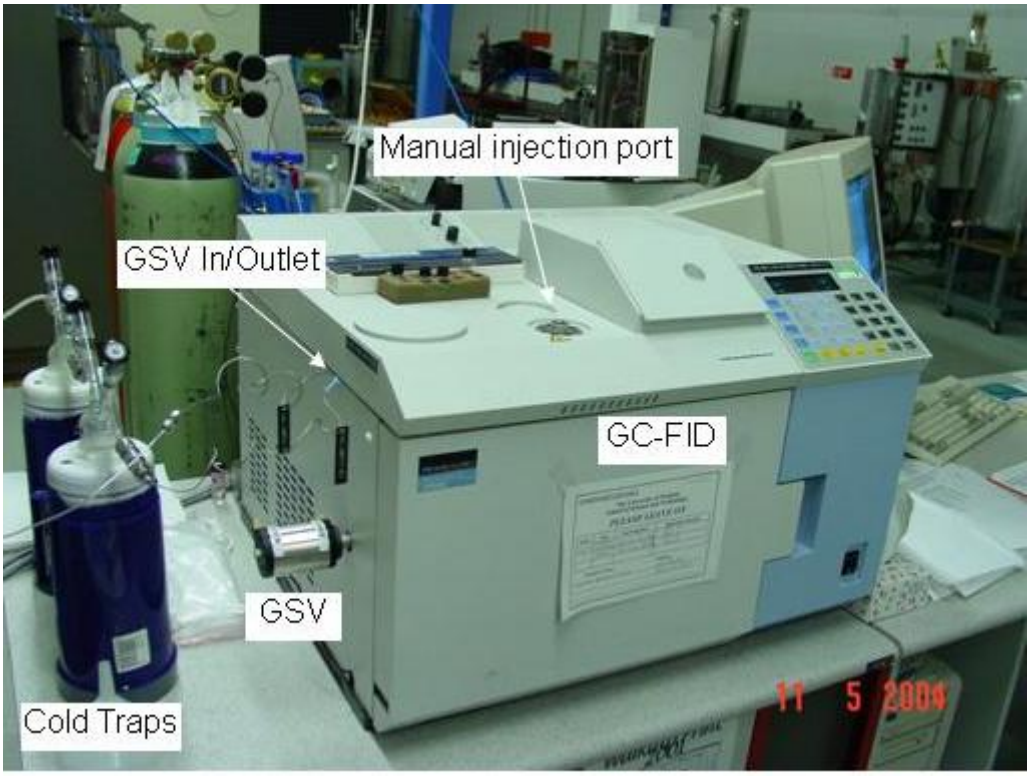

Figure 4:11 Perkin Elmer GC-FID and gas sampling valve with cold traps.

Liquid GC-FID injections

Manual feed injections were done before and after each PV run. Feed and membrane pre-soak solutions were diluted in ethanol and octanol internal standard was added. The GC-FID was set up with the appropriate TurboChrom^{TM} method and carrier (N_2), actuator (compressed air) and FID (H_2, dry air) gases (Table 4:02). The solvent solution was injected manually using a 0.1 μL syringe (Supelco SGE) into the manual injection port (Figure 4:11).

Table 4:02 GC-FID operating conditions for standard analyses.

GC-FID conditions	Vapour injections	Manual liquid injection
Injection volume	1.0 mL	0.01 µL
Dilution	Nil	50 µL/1000µL
Internal standard	Nil	2.5 µL/1000µL octanol
Vapour sampling loop pressure	Recorded by pressure transmitter	Bypassed
Injector temperature	140°C	250°C
GC oven temperature	hold at 70°C for 1 min, ramp at 5°C/min to 140°C, ramp at 45°C/min to 300°C, hold at 300°C for 2 min.	Same
Column	Medium polarity Perkin Elmer PE-5 megabore column (0.53 mm i.d. x 25 m long x 1.5 µm film thickness) or Alltech AT-5 column (0.53 mm i.d. x 30 m long x 1.5 µm film thickness)	Same
Carrier gas	Nitrogen Flow rate 8 mL/min	Same
Detector	FID	Same
Detector temperature	300°C	Same
Range	1	Same
Attenuation	PE: -5 (32x)	Same

Gas Vapour Sampling

GC-FID analysis of the permeate vapour occurred under the same conditions as for manual sample injections, except the sample was transferred onto the column by a 1 mL gas sampling valve (GSV) at 140°C. The GSV actuator was driven by compressed air, and the temperature was controlled by an external oven with a maximum temperature of 175°C. Under normal operation, the GSV is in the OFF position. At pre-set intervals, it switches to the ON position and delivers a 1 mL vapour sample to the GC-FID column.

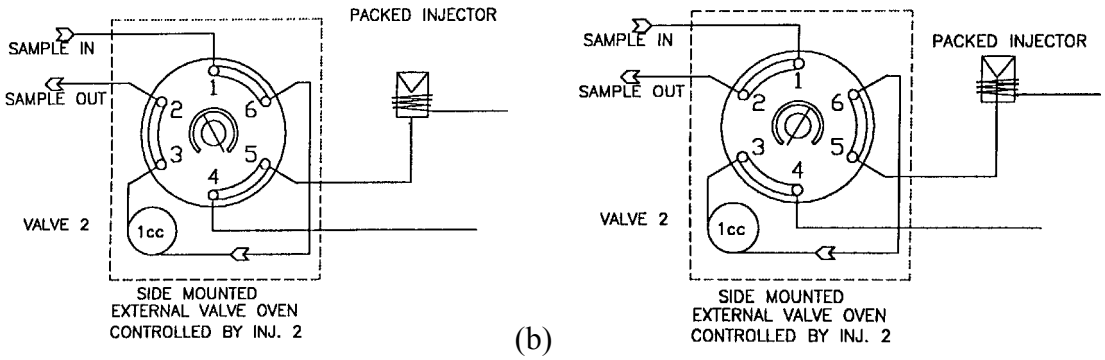

Figure 4:12 Schematic of gas sampling valve designed by Perkin Elmer, in (a) ON and (b) OFF positions.

Each GC-FID sequence was controlled and recorded with Turbochrom Navigator™ software. The auto-sampling interval for the GC-GSV was typically set at 01:00:00 (hourly) using Labview™ software and the GC-GSV initially sampled at time zero. As soon as data acquisition started, the final valve between vacuum lines and membrane unit was opened. The permeate pressure was monitored to ensure the system had no leaks.

Peak areas of vapour samples were measured against liquid injections of internal standards.

4.4 Pervaporation process variables

Initial standard operating conditions for process variable experiments were:

- Feed temperature 20°C
- Vacuum pressure < 10 kPa
- Impinging jet height 1.36 mm
- Feed flow rate 804 mL/min
- Feed concentration 5% v/v linalool & linalyl acetate in ethanol
- Membranes un-soaked polyethylene membranes

To test the effect of temperature, triplicate experimental runs were done at: 20, 25, 30, 35, and 40°C. Vacuum pressure during process runs ranged from: 2 – 8 kPa. To test the effects of membrane unit impinging jet height, runs were carried out in triplicate at heights of: 0.36, 1.36, 2.36 and 3.36 mm. Feed flow rate was tested in duplicate over the range: 541 – 1328 mL/min. Concentration effects on PV flux and selectivity were tested using: 1.78 – 6.01 % v/v linalool & linalyl acetate in ethanol. The effect of pre-soaking the membrane for 48 hours prior to pervaporation was also examined.

4.4.1 Pervaporation of membrane materials

The standard PV operating conditions for investigating membrane characteristics were:

- Feed temperature: 35°C
- Vacuum pressure: < 10kPa
- Impinging jet height: 1.36 mm
- Feed flow Rate: 804 mL/min (20% capacity)
- Feed concentration: 5% v/v linalool & linalyl acetate, in ethanol
- Membranes: pre-soaked for 48 h in feed solution
  PA 66, PC, PE, PEI, PES, PI, PP, PTFE

Feed concentrations were monitored before and after every PV run, with no statistically significant differences found. Methods of analysis are in Appendix 1.

Chapter 5

Results: Pervaporation

5.1 Effect of process variables on pervaporation

Process variables such as permeate temperature, permeate pressure, feed flow rate, feed concentration, membrane unit impinging jet height, membrane thickness and pre-soaking of membranes, were analysed to determine their potential impact on pervaporation processing of a model solution. The intent was not to investigate these effects in-depth, but to determine the degree to which these process variables might affect membrane selection criteria (selectivity and permeate flow rate).

5.1.1 Permeate temperature

Generally, process temperatures have a significant effect on pervaporation selectivity and flux rate. An increase in temperature normally leads to increasing permeability and a subsequent small decrease in selectivity of membranes (Villaluenga and Tabe-Mohammadi, 2000). Following are the results of a series of experiments run on high-density polyethylene (HDPE) membranes, to determine the effects of process temperature on the separation of linalool and linalyl acetate in ethanol.

5.1.1.1 Temperatures studied

Pervaporation of 10 μm thick HDPE membranes was carried out offline at several different waterbath temperatures; 20, 25, 30, 35, and 40ºC. Runs of 20 hours duration were carried out under as close to identical conditions as possible, however some variation from run to run was inevitable. Steady-state permeate pressures were maintained at approximately 5 kPa or less for these offline sampling runs ($\widetilde{P}_p$: 0.88 – 5.28 kPa), averaging around $\widetilde{P}_p$ 3.30 kPa (± 1.44 kPa). Controllable variables such as membrane unit impinging jet height were kept at 1.36 mm, and the feed flow rate at ≈ 804 mL/min.

Figure 5:01 shows the system temperatures observed in runs of various waterbath temperatures, with the initial permeate temperature giving an indication of the ambient room temperature at the start of processing. Room temperature ranged from 17.6°C to 30.5°C, averaging around 22.7°C (± 3.38°C), making temperature control difficult. Control of system temperature was not ideal as it was achieved by control of the external waterbath temperature (see Figure 4:04), and heat losses varied with differing room temperatures.

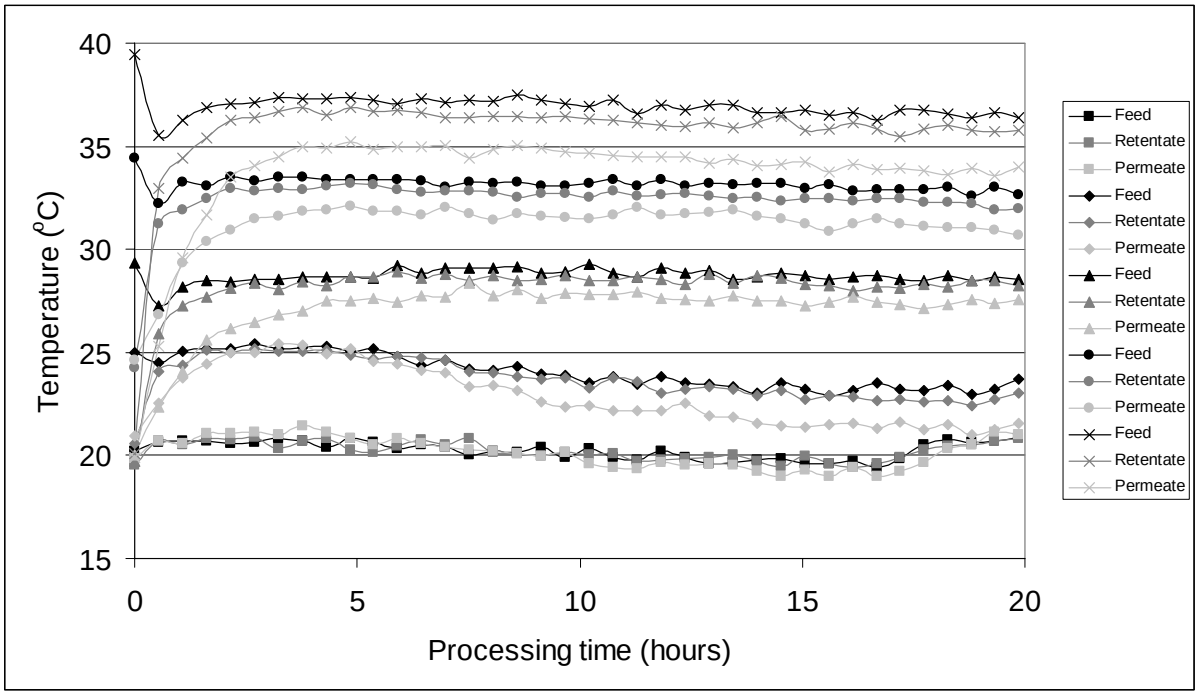

Figure 5:01 Process variables for pervaporation runs with waterbath temperature settings: ■ 20°C, ♦ 25°C, ▲ 30°C, ● 35°C, x 40°C.

Also note in Figure 5:01, the length of time required for the permeate temperature to reach approximately steady state (3-4 hours), especially for the higher temperature runs.

5.1.1.2 Composition and selectivity

Concentration of feed solutions at the start of processing were approximately 5% (±1%) linalool and linalyl acetate in ethanol. Analysis of permeate vapour composition and selectivity of the membrane was carried out from offline sampling of the condensate using GC-FID. Figure 5:02 shows a selectivity of $\alpha > 1.0$, which indicated that linalool was preferentially permeated through the majority of these 10 μm HDPE membranes.

Due to the size of standard error (error bars on Figure 5:02) for each dataset, there is no significant improvement in selectivity with increasing temperature for the range of temperatures studied here. It is possible to draw a horizontal line for selectivity ($\alpha \approx 1.2$) between $\widetilde{T}_p$ = 22-34°C, with only the 20°C runs showing no selective permeation of either feed component. There is low correlation between increasing selectivity with permeate temperature.

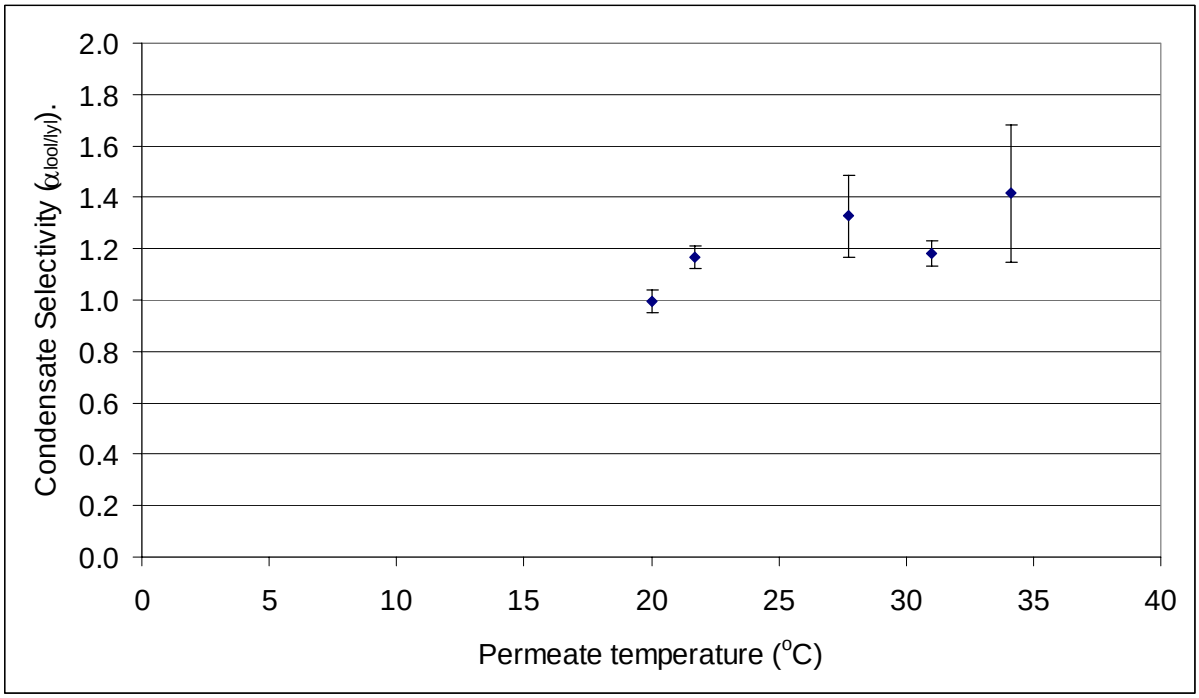

Figure 5:02 Selectivity of HDPE membranes at various processing temperatures.

5.1.1.3 Flow rate

The volume of condensate collected in cold traps is displayed in Figure 5:03, and represents an average of the flow of permeants throughout the entire process run.

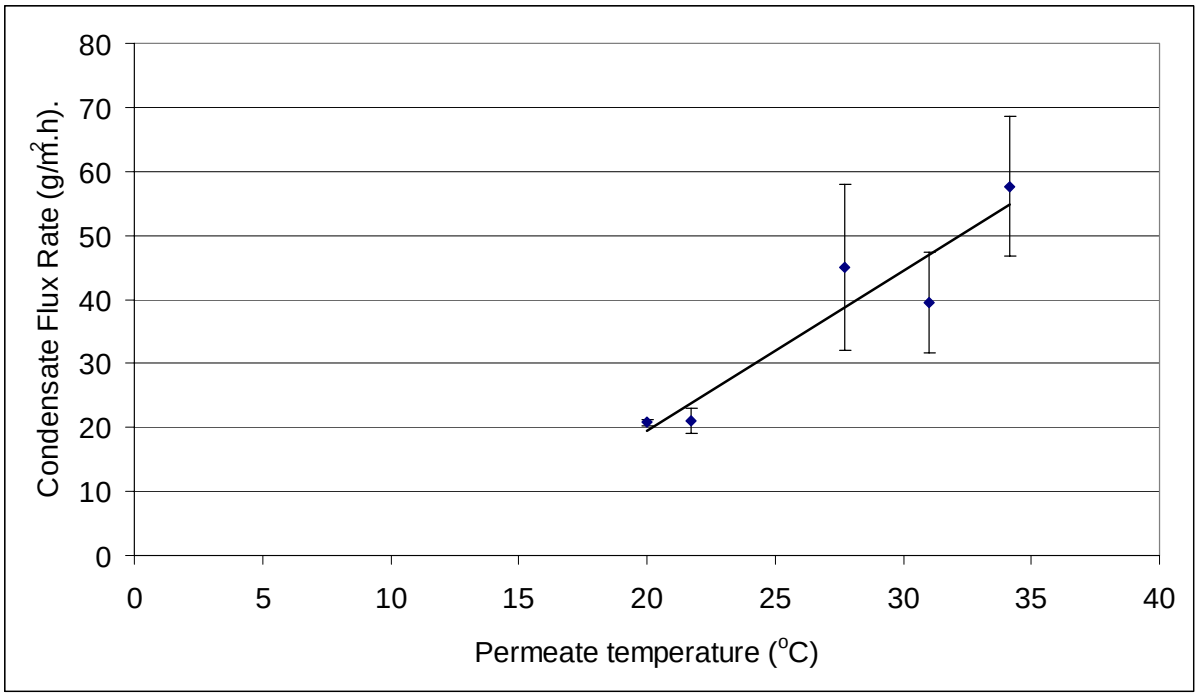

Figure 5:03 Correlation between permeate temperature and flow rate, calculated via volume of permeate condensate collected in cold traps.

There is a significant degree of variation (shown by standard error bars in Figure 5:03) in the volumes of condensate collected for these 10µm HDPE membranes. When viewed in combination with the increasing selectivity, this increase in flow rate is most likely to be due to a loosening of the polymer structure, rather than pinhole imperfections. One would expect selectivity to deteriorate if pinholes were present.

Intuitively one might expect greater flux rates to reduce the selectivity, but this was not observed in these pervaporation runs.

5.1.1.4 Online sampling analysis of temperature variation

Further experiments were carried out for various membranes using online sampling of permeate vapour. These identified that temperature variation of several degrees Celsius within an experiment does not significantly influence selectivity.

Despite the large variation (up to 4°C) in permeate temperatures (Figure 5:04), there appears to be little effect on the selectivity for these runs. Thus, process temperature variations of ± 2°C either side of the set temperature are acceptable and should not significantly influence selectivity.

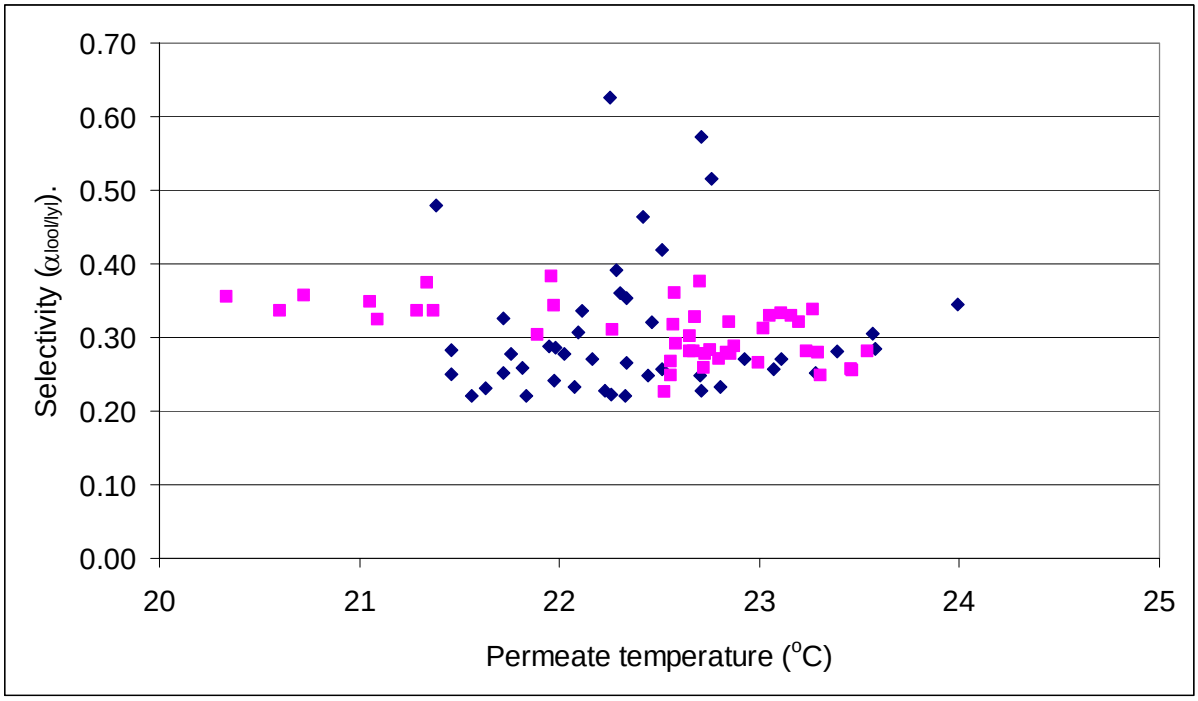

Figure 5:04 Effect of permeate temperature on the selectivity of a (♦) 31.5 µm and (■) 13.5 µm LDPE membrane.

The same can be said about the effects of temperature variation on permeate flow rate within a run Figure 5:05.

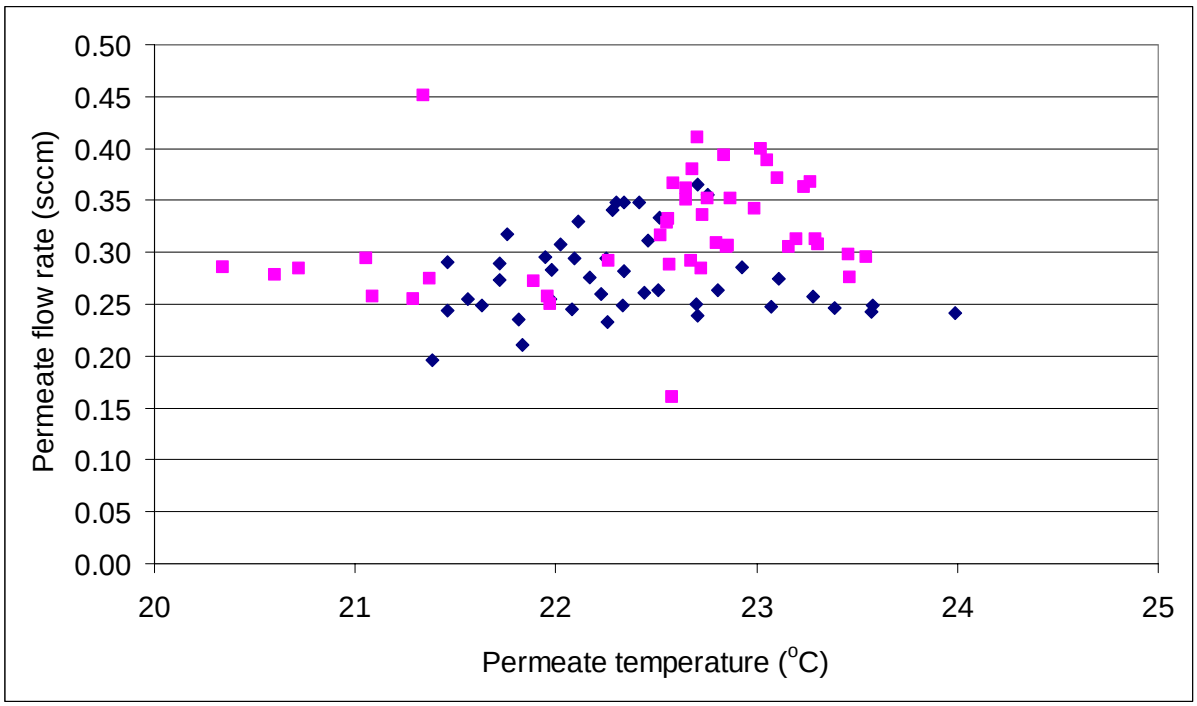

Figure 5:05 Effect of permeate temperature on the flow of permeate through (♦) 31.5 µm and (■) 13.5 µm LDPE membranes.

5.1.1.5 Alteration of temperature in continuous runs

Further investigation into the effects of temperature on pervaporation was carried out using online analysis of LDPE membrane performance under continuous operation. Temperatures were varied between 20-35 °C (permeate temp) and allowed to reach steady state (15-20 hours) before any temperature change was initiated (Figure 5:06 and 5:07).

Note the disparity seen between the feed and permeate temperatures when PV was operated at 35°C (ΔT_f-$T_p \leq 3.0$°C at steady-state). The design for temperature control was less than optimum, as the permeate chamber was indirectly heated by the waterbath via the feed stream. The temperature gap may have consequences for stability of permeation characteristics at higher temperatures. No significant correlation was noted between temperature and permeate flow rate, nor between temperature and selectivity at temperatures ranging from 20-35°C (Figures 5:08 and 5:09). However, selectivity deteriorated (tended towards $\alpha = 1.0$) over the course of both PV runs.

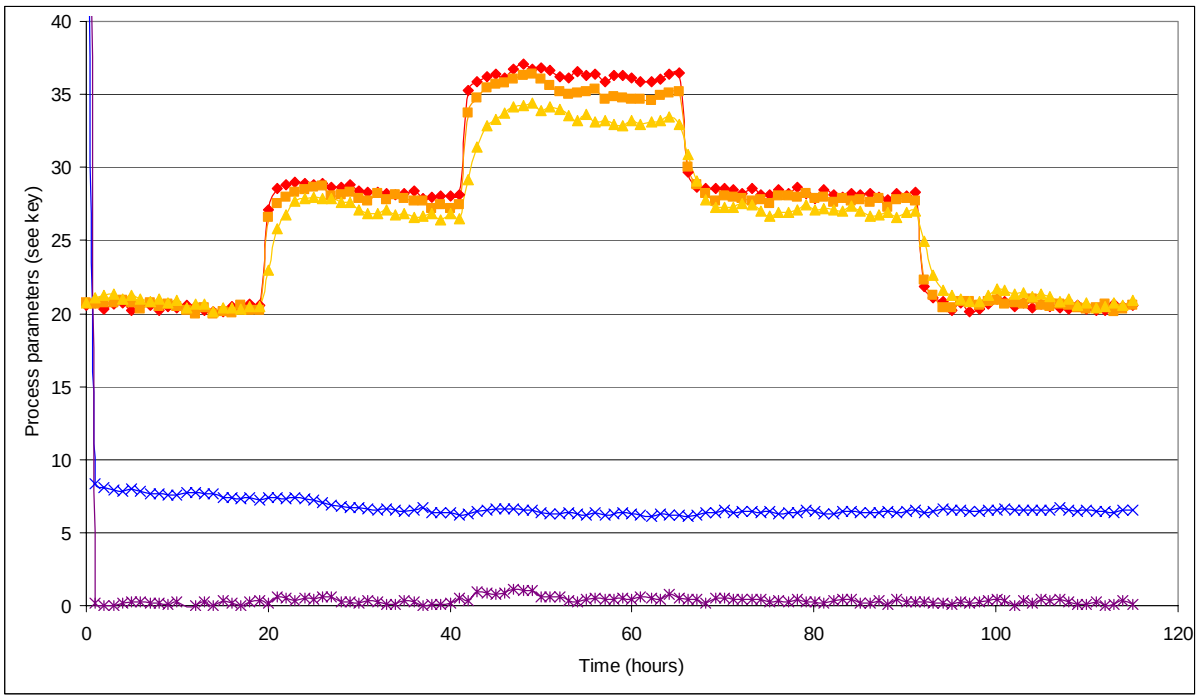

Figure 5:06 Process conditions for temperature variation under continuous operation of 27.7 µm LDPE membrane. Key: ♦ Feed tank temperature (°C), ■ Feed / Membrane temperature (°C), ▲ Permeate temperature (°C), x Vacuum pressure (kPa), ✳ Flow rate (sccm x10).

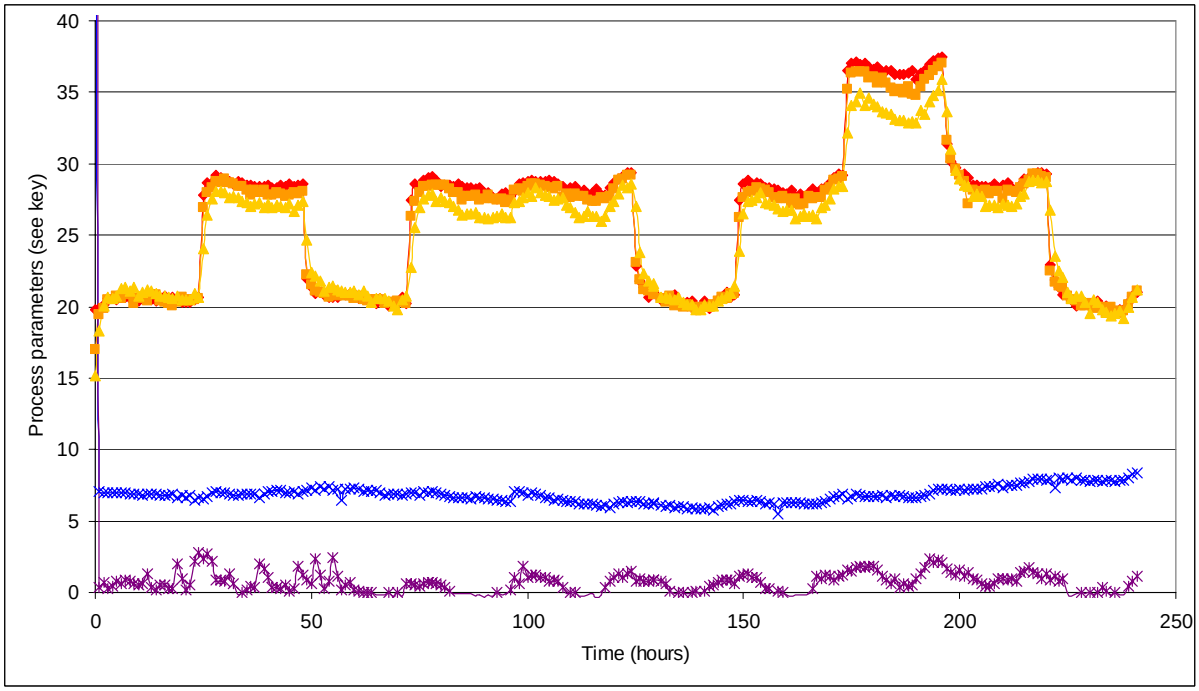

Figure 5:07 Process conditions for temperature variation under continuous operation of 26.3 µm LDPE membrane. Key: ♦ Feed tank temperature (°C), ■ Feed / Membrane temperature (°C), ▲ Permeate temperature (°C), x Vacuum pressure (kPa), ✳ Flow rate (sccm x10).

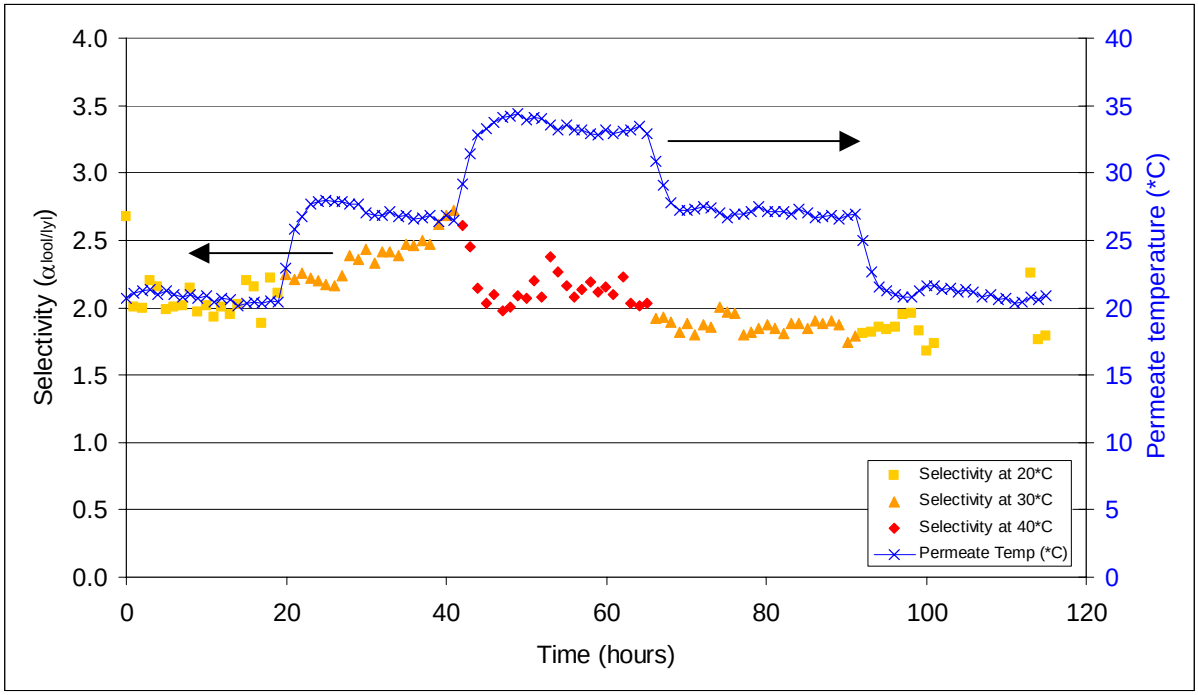

Figure 5:08 Selectivity of LDPE membrane (27.7 µm) with temperature variation under continuous operation.

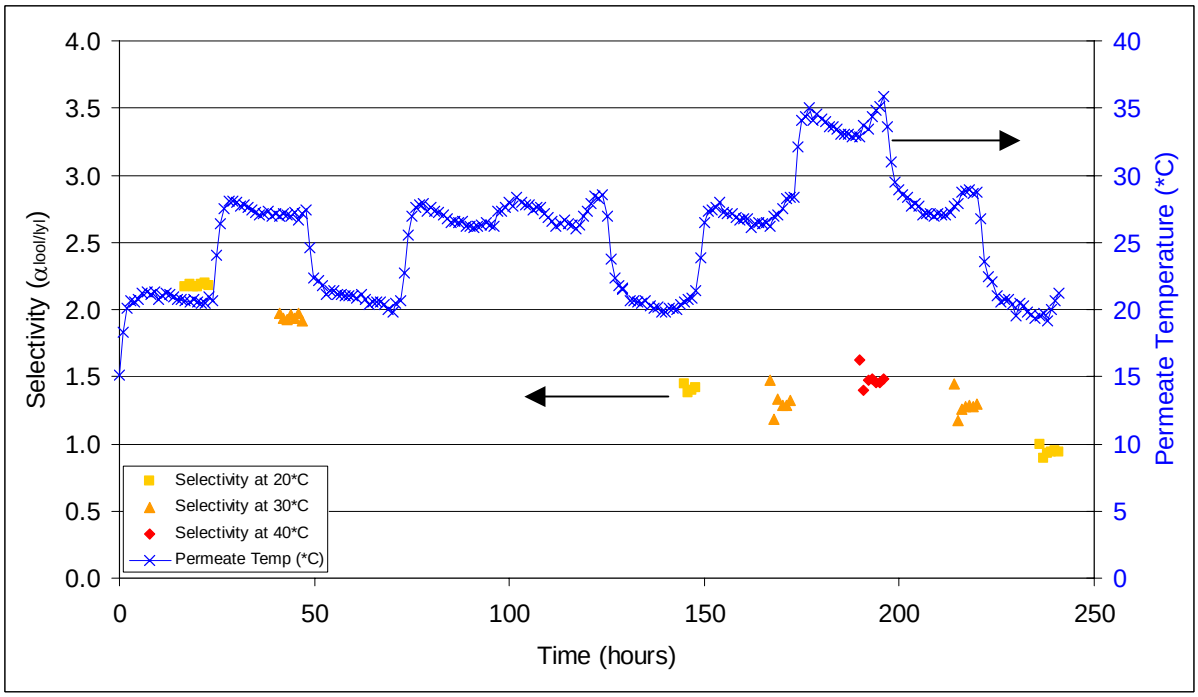

Figure 5:09 Selectivity of LDPE membrane (26.3 µm) with temperature variation under continuous operation.

Deterioration in selectivity can be observed clearly in Figure 5:09, with $\alpha \approx 1.0$ for the final series of online samples at 236 hours. The gap in selectivity sampling between 50-140 hours

(Figure 5:09) was due to equipment failure mid experiment. Subsequent sampling was initiated manually on the GC-FID at hourly intervals.

5.1.1.6 Summary

For offline sampling PV runs, temperature affected flux rate of HDPE membranes, but not selectivity, (however a significant degree of variation was observed in the scatter of datapoints). Normally selectivity declines with increasing temperature, as the increasing temperature loosens the polymer structure and lowers its ability to selectively restrict one of the components in the feed mixture, the increase in flux rate observed with increasing temperature is in agreement with this. In the range of permeate temperatures studied here (20-35°C), there was no significant increase in selectivity for linalool with increasing temperature.

Online sampling of LDPE membranes indicated that variation of up to 2°C during a process run is acceptable, and unlikely to significantly affect selectivity or flux rate. No significant trend was observed in selectivity of online permeate vapour when temperatures were varied from 20-35°C under continuous PV operation, however selectivity was observed to deteriorate over time.

5.1.2 Vacuum pressure

As the main driving force in pervaporation, the pressure differential between the feed and permeate sides of the membrane can have a significant influence on the permeation characteristics of a membrane. The objective of this series of experiments was to determine if the normal range of pressure variation seen in working pervaporation conditions (< 10 kPa) had a significant influence on permeate flow rate and selectivity of a membrane.

LDPE membranes (≈ 25 μm thick) were run under pervaporation conditions of T_p = 21.6°C ± 0.29°C, $\widetilde{P}_p$ < 10 kPa, membrane unit impinging jet height = 1.36 mm, feed flow rate of 804 mL/min, and a feed concentration ≈ 5% v/v linalool and linalyl acetate in ethanol. Pressure had a moderate effect on flow rates, but showed no significant influence on selectivity.

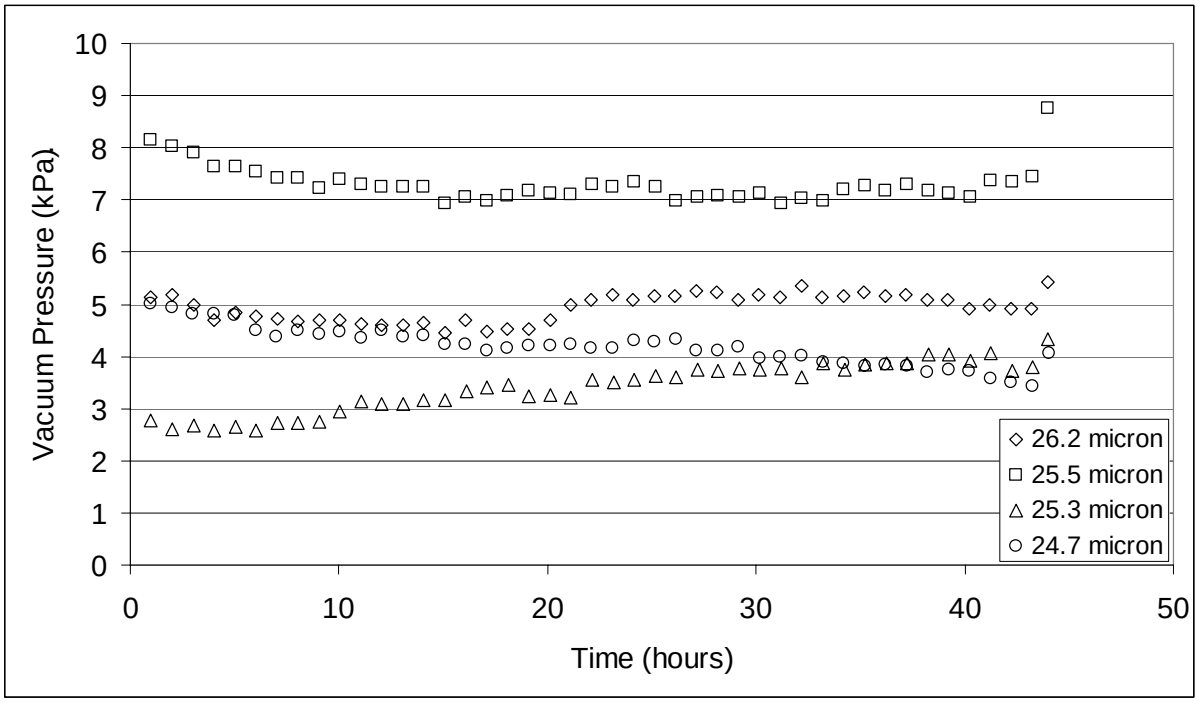

Figure 5:10 Real time permeate pressures of ≈ 25 μm LDPE membranes.

Despite significant variation in permeate pressures observed in Figure 5:10, steady-state selectivity in Figure 5:11 remains very constant. Thus when permeate pressure is maintained at less than 10 kPa, it has no significant influence on selectivity.

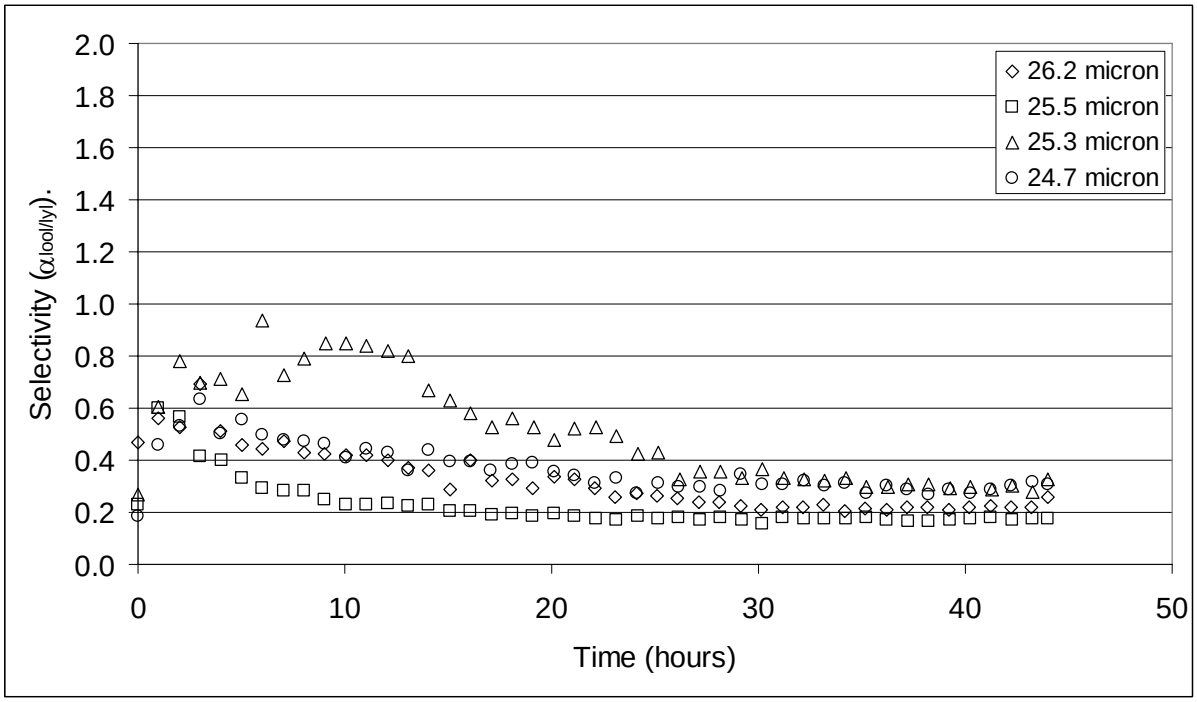

Figure 5:11 Real time selectivity from online sampling of permeate vapour of ≈ 25 μm LDPE membranes.

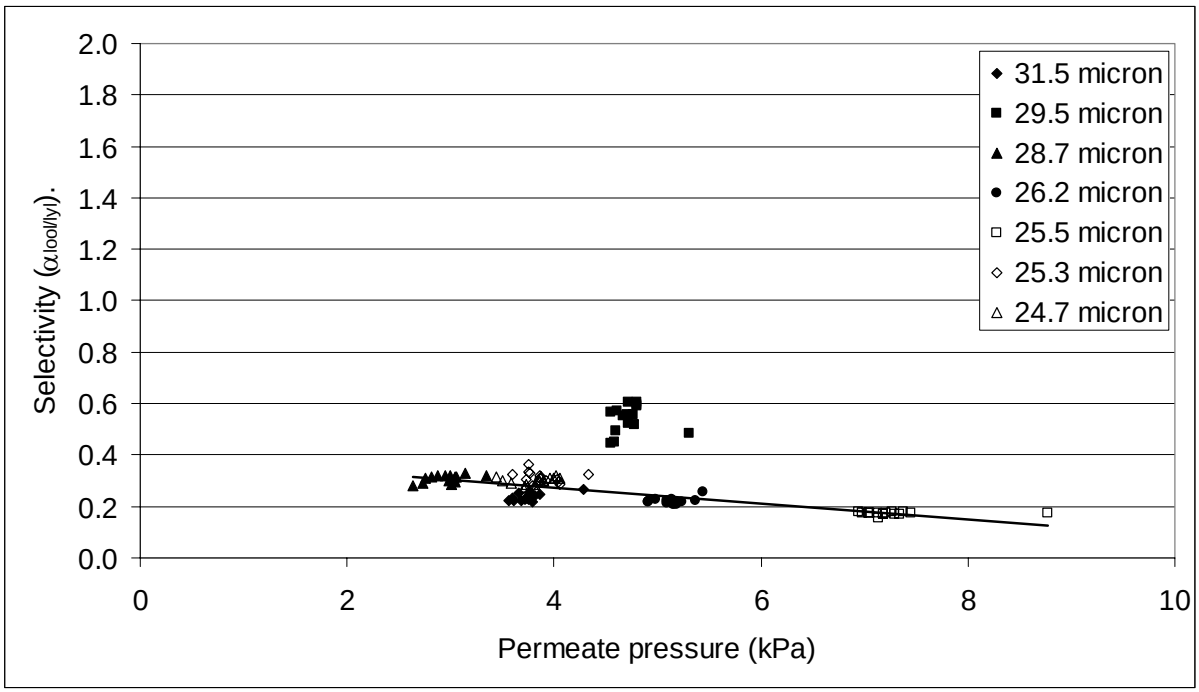

Figure 5:12 Effect of steady state permeate pressure on selectivity of LDPE membranes.

Figure 5:12 shows steady state pressure variations ranging from 2.64 – 8.77 kPa with a slight negative correlation between selectivity and pressure when data from the 29.5 μm run was excluded. As nothing exceptional occurred in the 29.5 μm run (temp, pressure, flux all normal), this particular membrane may have been behaving anomalously. The trend-line observed shows that as permeate pressure moves towards zero (the trans-membrane pressure differential increases), selectivity for linalyl acetate is improved (moves further from unity). The greater the pressure differential, the greater the driving force.

When observed as a whole, the preferential permeation of linalyl acetate remains relatively constant ($\widetilde{\alpha} = 0.30 \pm 0.11$) during steady-state operation period (30-45 hours), with relatively good reproducibility for all these runs.

However, pressure tended to have a negative influence on flow rate within any one run (Figure 5:13). As permeate pressure moved away from zero, trans-membrane pressure decreased, and the permeate flow rate tended to decrease. If the data from 25.5 and 25.3 μm runs was excluded, a definite 'inter-run' correlation between permeate flow rate and permeate pressure can be observed.

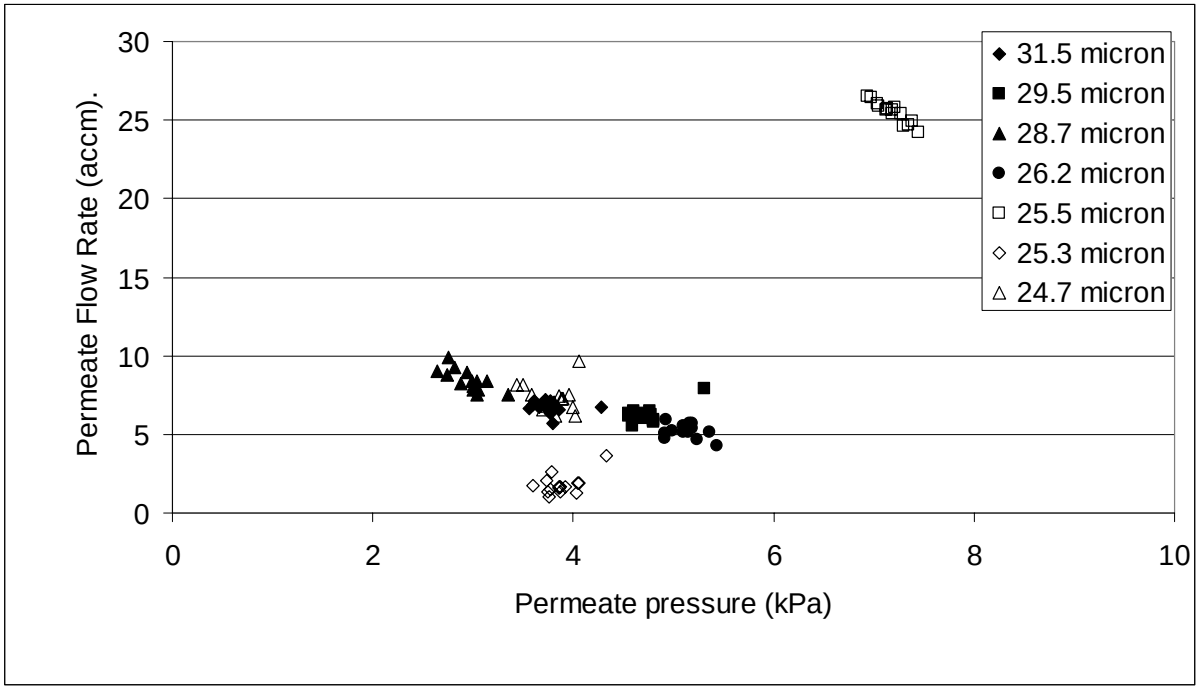

Figure 5:13 Effect of steady state permeate pressure on permeate flow rate (accm = actual cm^3/min).

The exceptionally high flow rate observed for 25.5 μm run may have been due to minor leaks in the vacuum lines, it is unlikely to be due to pinhole imperfections in the membrane, or imperfect seal between the polymer film and o-rings in the membrane unit, as selectivity was not affected. The extremely low permeate flow rate observed in the 25.3 μm run, may have been due to variation in cyrstallinity of the polymer material used in this membrane.

5.1.3 Membrane unit impinging jet height

The effect of the impinging jet height in the membrane unit was studied using HDPE membranes (10 μm thick). These experiments were run at $\widetilde{T}_p$ = 19.88°C ± 0.72°C, $\widetilde{P}_p$ < 10 kPa, feed concentrations ≈ 5% v/v linalool and linalyl acetate in ethanol, and a feed flow rate of 804 mL/min, membrane unit impinging jet height ranging from 0.36 to 3.36 mm. Impinging jet height had no detectable influence on selectivity, however permeate flow rate varied significantly with the height of the conical impinging jet from the membrane (see L, Figure 4:06). Figure 5:14 shows representative flow rates for each impinging jet height.

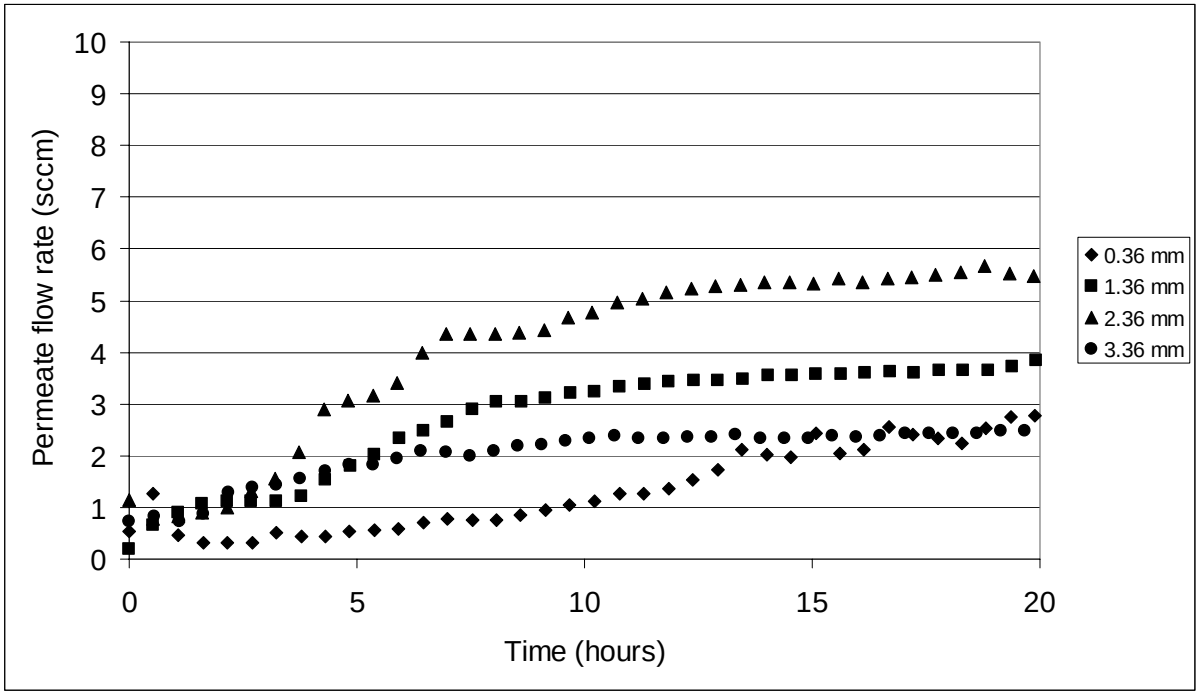

Figure 5:14 Permeate flow rates of HDPE membranes at impinging jet heights ranging from 0.36 mm to 3.36 mm.

Pervaporation runs with impinging jet heights of 1.36, 2.36 and 3.36 mm tended to reach their steady-state permeate flow rate between 5-10 hours processing time (10 μm HDPE), however an impinging jet height of 0.36 mm tended to take much longer to reach steady-state (15-20 hours), if at all in the allotted 20 hours processing time (Figure 5:14).

Adapter heights 1.36 and 2.36 tended to produce higher steady-state flow rates than 0.36 and 3.36 mm runs (Figure 5:15), however an impinging jet height of 1.36 mm had the highest reproducibility in the total volume of permeate collected in the cold traps (Figure 5:16), thus this setting was used in later experiments.

The most likely cause of membrane permeation rates reaching maxima between impinging jet heights of 1.36-2.36 mm, was the optimum turbulence necessary to reduce the thickness of the boundary layer. As the impinging jet moved further away from the the optimal height above the membrane surface, the flow characteristics over the surface will have changed, potentially causing stagnant zones and less than optimal permeation.

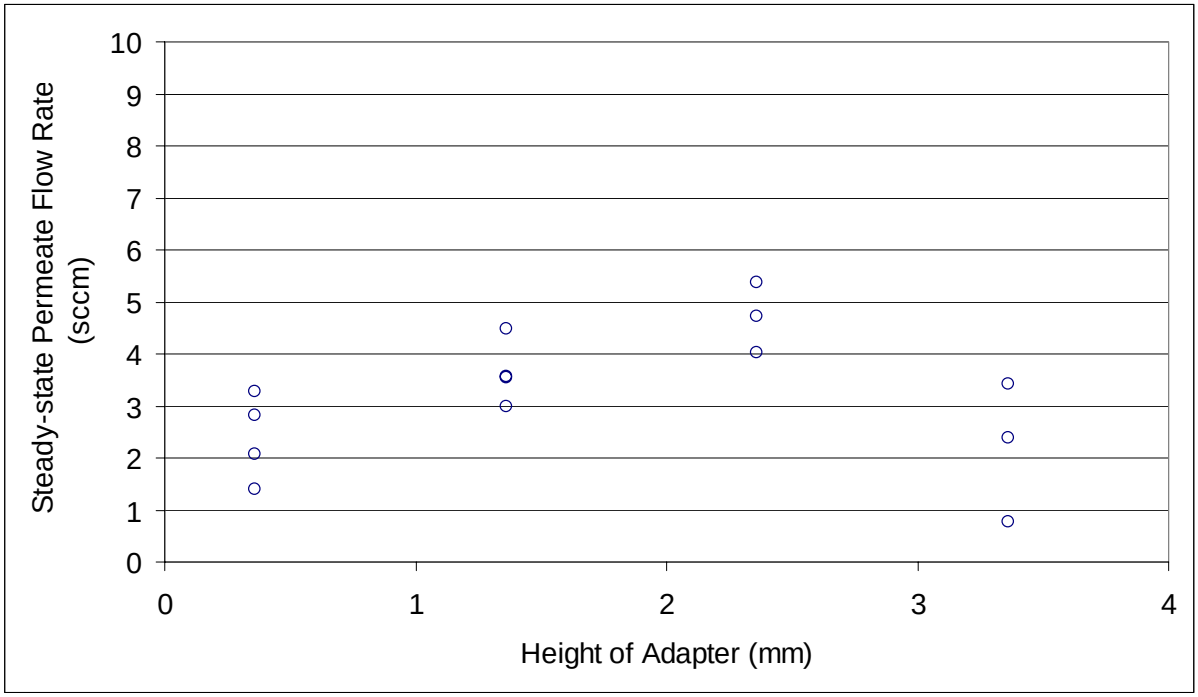

Figure 5:15 Effect of membrane impinging jet height (L) on steady-state permeate flow rate.

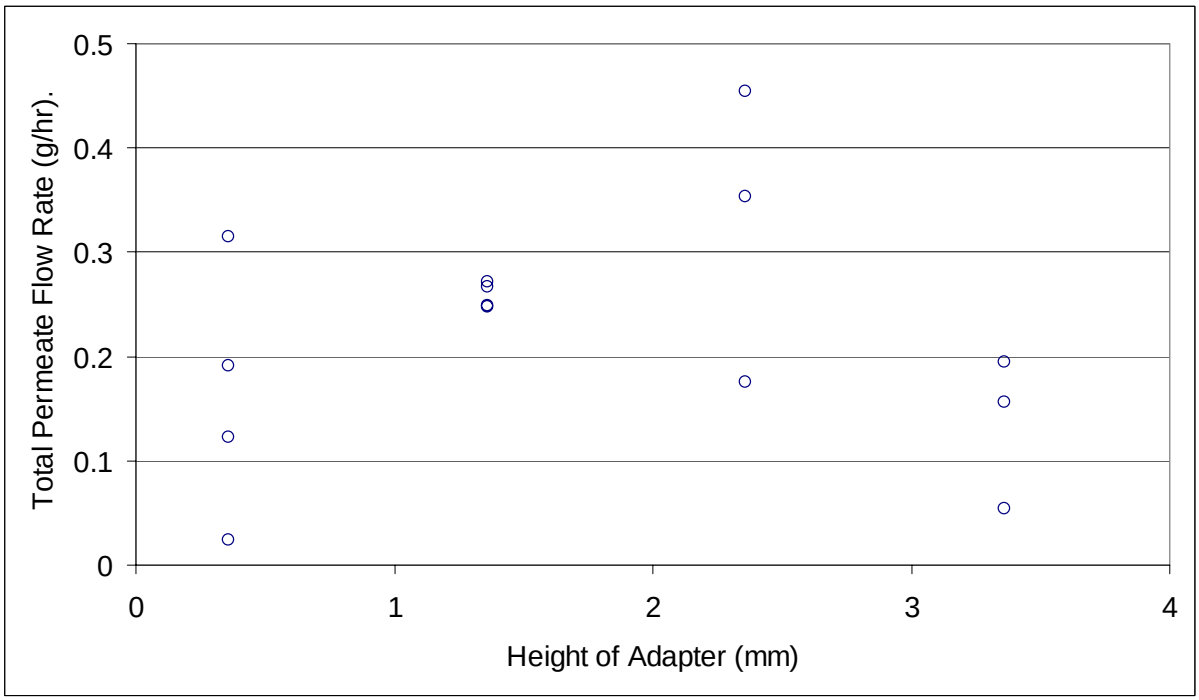

Figure 5:16 Effect of membrane impinging jet height (L) on the total permeate collected in cold traps.

5.1.4 Feed flow rate

Turbulence within a membrane unit is desirable to minimise the effects of fouling and concentration polarization in the boundary layer. Changes in the diameter of the flow distributor tube (Figure 5:17) can cause changes in the critical Reynolds number (*Re* = 2000). If a pipe converges, the critical Reynolds number required to achieve turbulence is higher, whereas divergence such as seen in the membrane unit flow distributor produces a lower value for Newtonian fluids (Massey, 1979). The divergence occurring at the flow distributor (impinging jet) increases the likelihood that feed flowing through the membrane unit will be turbulent.

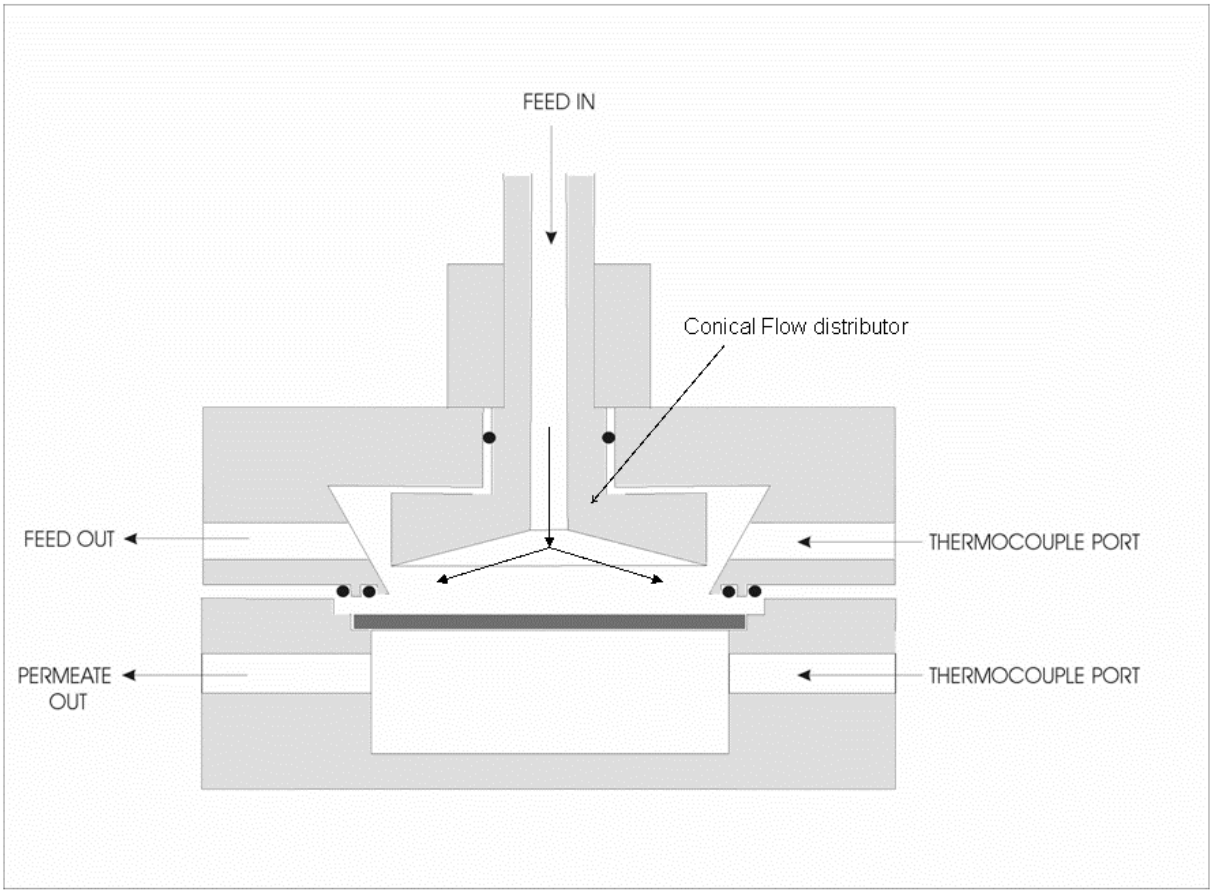

Figure 5:17 Schematic diagram of membrane cell (He, 2000).

The transition from laminar to turbulent flow regime within a conical membrane cell flow distributor was studied by Miranda & Campos (1999). They found that in a conical flow distributor, the critical value of jet Reynolds number was approximately *Re* = 1600.

Reynolds numbers were calculated to measure the turbulence at the Jet nozzle in the membrane unit (Miranda and Campos, 2001a).

$$\mathrm{Re} = \frac{\rho_o * V_j * D_j}{\mu_o} \qquad \text{(Eqn 5:1)}$$

where V_j is the average jet velocity at the nozzle exit, D_j the diameter of the jet, ρ_o and μ_o, the density and the viscosity of the feed solution. The density and viscosity were approximated to that of ethanol $\rho_{o\ EtOH}$ = 789 kg/m^3 and $\mu_{o\ EtOH}$ = 0.00119 kg/(m·s) at 20°C, and the jet diameter D_j = 0.00873 m. Linear flow rates were calculated from volumetric flow rate (m^3/sec) divided by the jet area = 5.986 x10^{-05} m^2 (see dimensions in Chapter 4, Figure 4:06).

At pump flow rate 804 ± 9 mL/min, flow at the jet nozzle gave an average Reynolds Number of 1691 (using linear Equations in Figures A2:01 and A2:03 from Appendix 2), close to the *Re* = 1600 recommended by Miranda & Campos (2001a).

The effect of feed flow rate on pervaporation was studied using HDPE membranes (10 μm thick). These experiments were run at $\widetilde{T}_p$ = 22.6°C ± 0.77°C, $\widetilde{P}_p$ < 10 kPa, membrane unit impinging jet height = 1.36 mm, feed concentrations ≈ 5% v/v linalool and linalyl acetate in ethanol, and a feed flow rate ranging from approximately 541– 1328 mL/min ($\pm_{max}$ 28 mL/min). The linear range for the pervaporation feed flow rate was calibrated manually *in-situ* using water, and was found to be between 378 – 1656 mL/min. Feed pump speeds below 378 mL/min were not reproducible, and speeds above 1656 mL/min were non-linear (see Appendix 2).

Despite the recommendation of Miranda & Campos (2001a), variation in the feed flow rate had no statistically significant effect on permeate flow rate (Figure 5:18) and selectivity (Figure 5:19) of the 10 μm HDPE membranes. This may be due to a large degree of scatter (standard deviation) in the results.

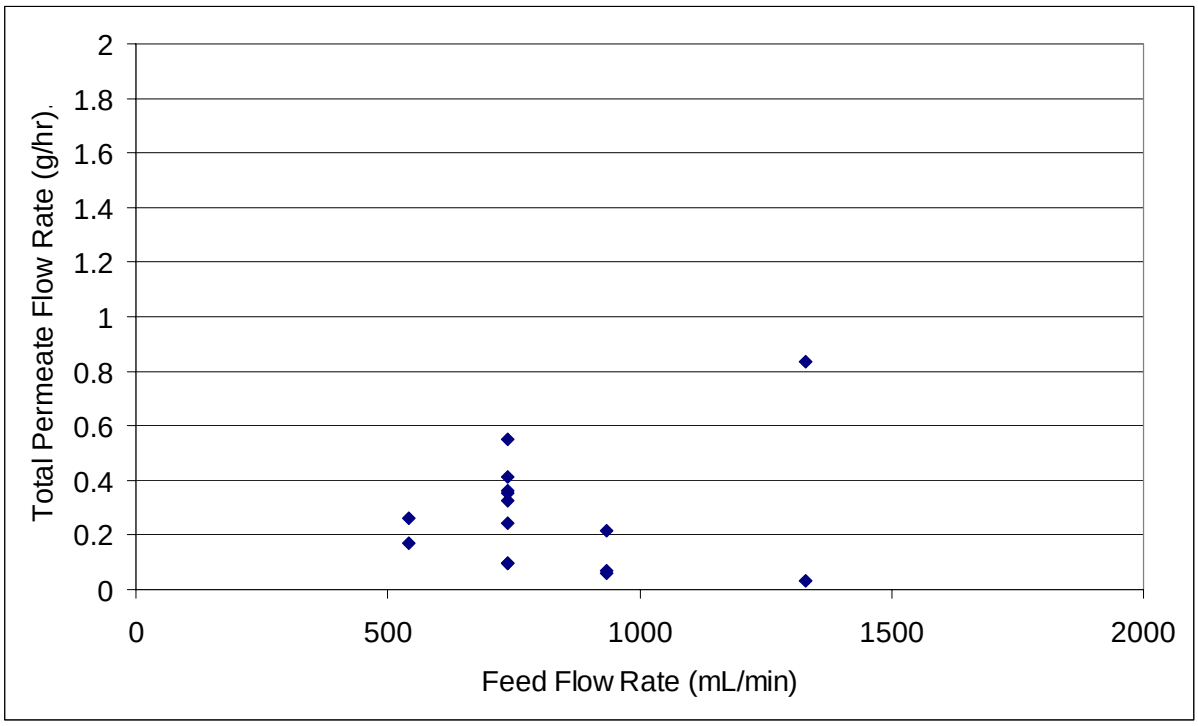

Figure 5:18 Permeate flow rate through HDPE (10 μm thick) membranes at varying feed flow rates.

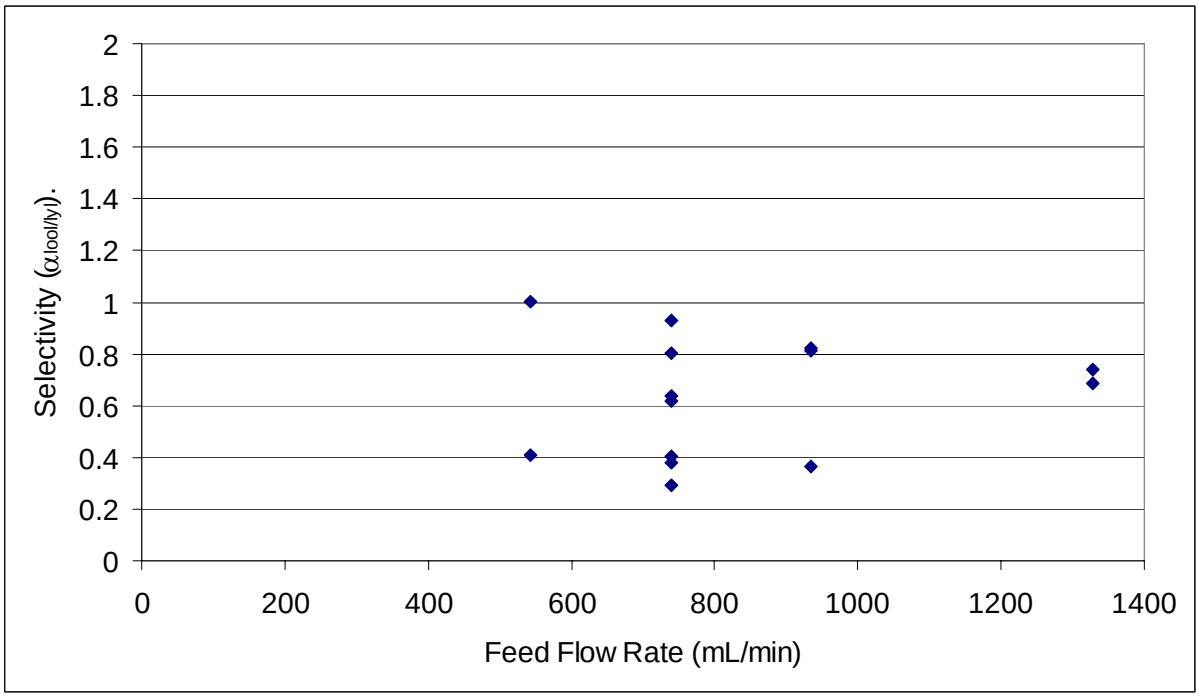

Figure 5:19 Selectivity of HDPE (10 μm thick) membranes at varying feed flow rates.

5.1.5 Concentration

The effect of feed concentration was studied using 10 μm HDPE membranes. These experiments were run at $\widetilde{T}_p$ = 30.87°C ± 0.84°C, $\widetilde{P}_p$ < 10 kPa, membrane unit impinging jet height = 1.36 mm, feed flow rate of 804 mL/min, and model solution feed concentrations ranging between 0.100 – 0.339 mol/L (1.78 – 6.01 % v/v) of linalool and linalyl acetate in ethanol.

Despite the general trend observed in Figure 5:20, there were no statistically significant differences between the mean selectivity at 0.1 mol/L and 0.3 mol/L runs. This is primarily due to the variation seen in data collected for the different feed concentration levels (selectivity $\alpha_{lool/lyl}$: $\overline{\alpha}_{0.10}$ = 0.94 ± 0.17 $\overline{\alpha}_{0.17}$ = 1.29 ± 0.26 and $\overline{\alpha}_{0.31}$ = 1.35 ± 0.27).

The lowest feed concentration runs clustered around a selectivity of 1.0 indicating that no selective permeation occurred through these HDPE membranes, whereas the higher concentration runs tended to show selective permeation for linalool.

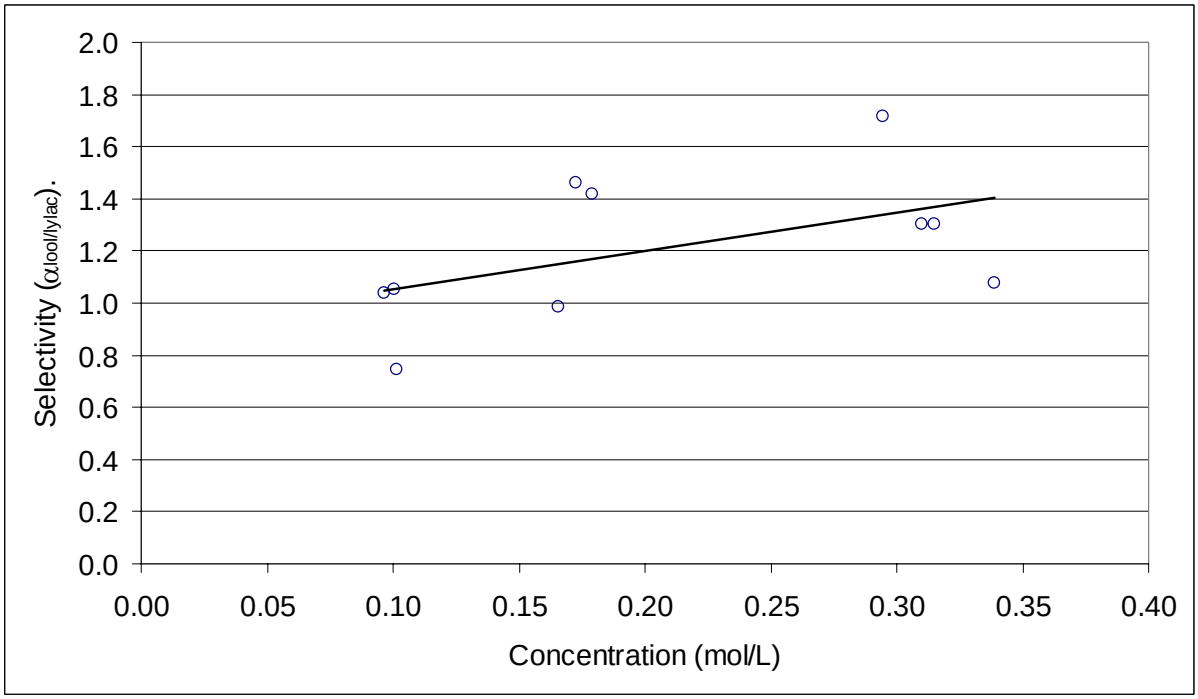

Figure 5:20 Effect of feed concentration on selectivity of 10 μm HDPE membrane.

There were also no statistically significant differences between the mean permeate flow rates at 0.1 mol/L and 0.3 mol/L runs (Figure 5:21) where; $\overline{Q}_{0.10}$ = 0.95 ± 0.31 g/h, $\overline{Q}_{0.17}$ = 0.47 ±

0.22 g/h, and $\overline{Q}_{0.31}$ = 0.49 ± 0.207 g/h for concentrations of 0.10, 0.17 and 0.31 mol/L respectively.

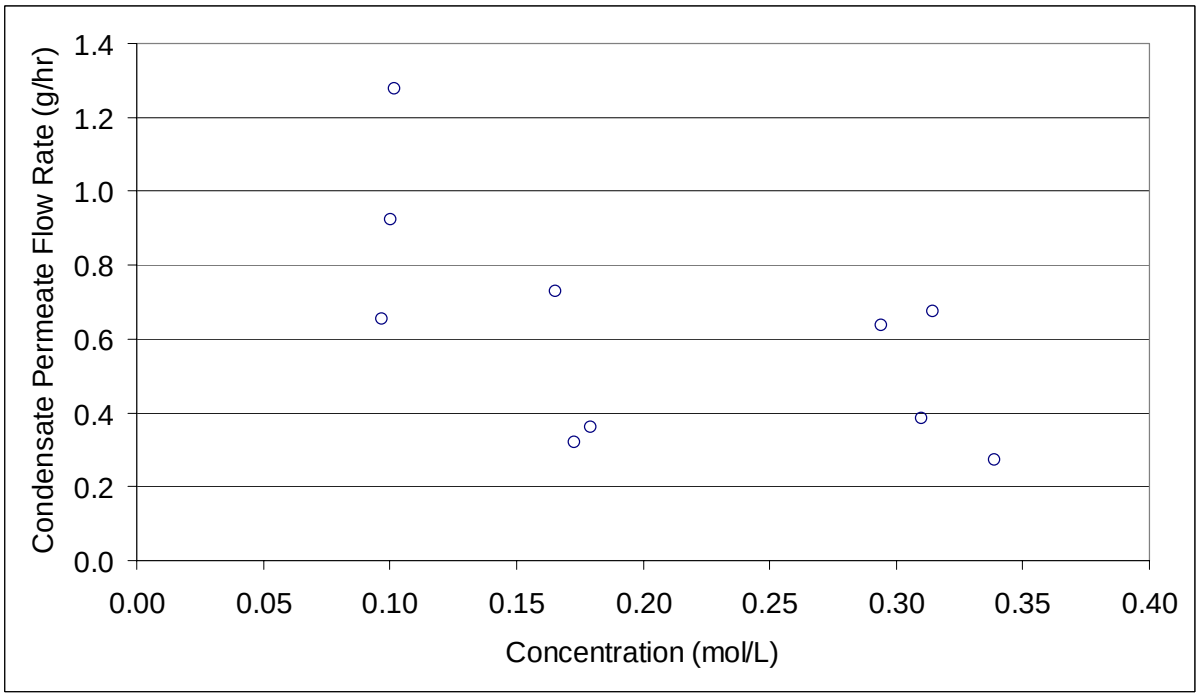

Figure 5:21 Effect of feed concentration on flow rate through 10 μm HDPE membrane.

It is possible that the higher permeate flow rates observed for the lowest concentration runs (0.1 mol/L linalool and linalyl acetate in ethanol) were due to the larger ethanol content. As ethanol is a significantly smaller molecule (M_r/ρ = 58.39 cm^3/mol) than linalool (177.1 cm^3/mol) or linalyl acetate (217.9 cm^3/mol), it follows that more ethanol is likely to permeate through the membrane. Also, a higher concentration of ethanol at the membrane interface would mean a larger proportion could permeate through the membrane less-hindered by the membranes attraction to linalool or linalyl acetate.

5.1.6 Pre-soaking

The effect of pre-soaking membranes was studied using 10 μm HDPE membranes. These experiments (Figures 5:22 and 5:23) were run at $\widetilde{T}_p$ = 23.0°C ± 0.33°C, $\widetilde{P}_p$ < 10 kPa, membrane unit impinging jet height = 1.36 mm, feed concentrations ≈ 5% v/v linalool and linalyl acetate in ethanol, and a feed flow rate of 804 mL/min.

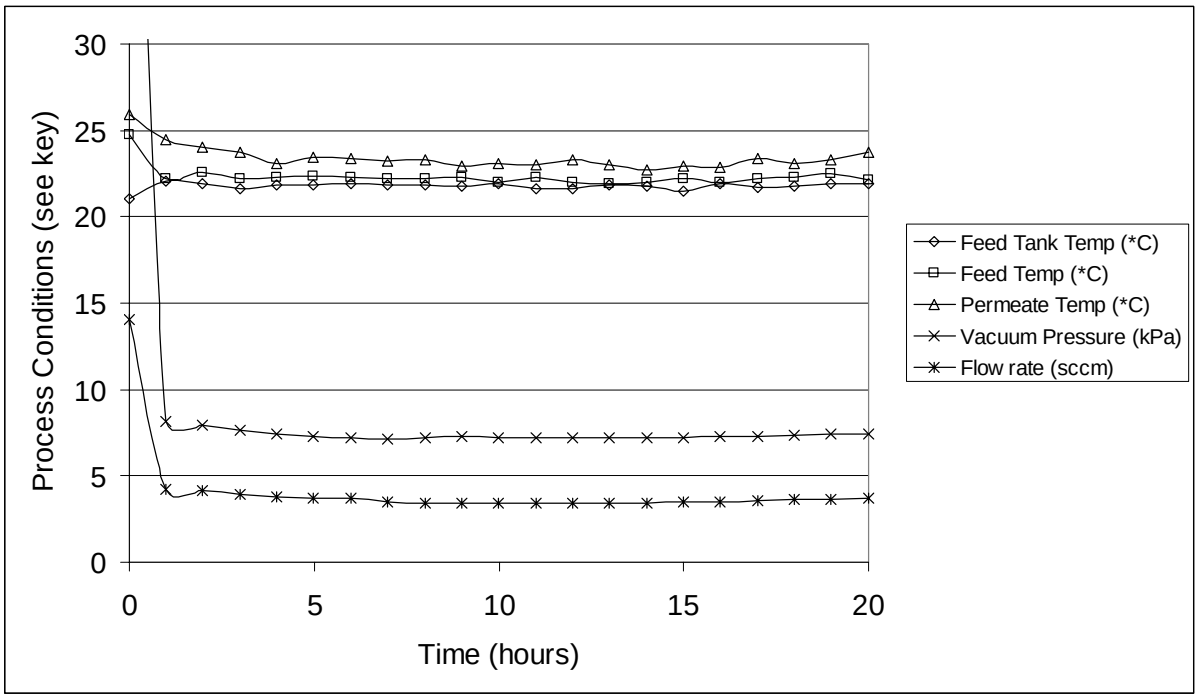

Figure 5:22 Process conditions for pervaporation of pre-soaked HDPE (031222) membrane.

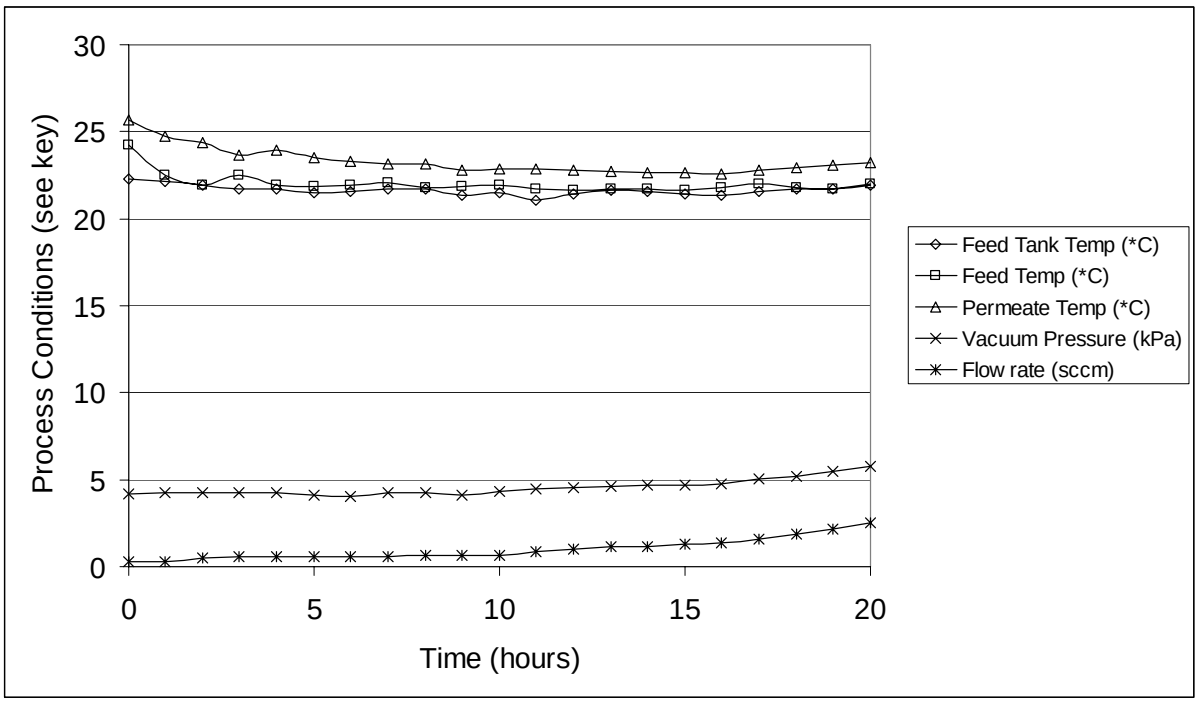

Figure 5:23 Process conditions for pervaporation of a dry start HDPE (031218) membrane.

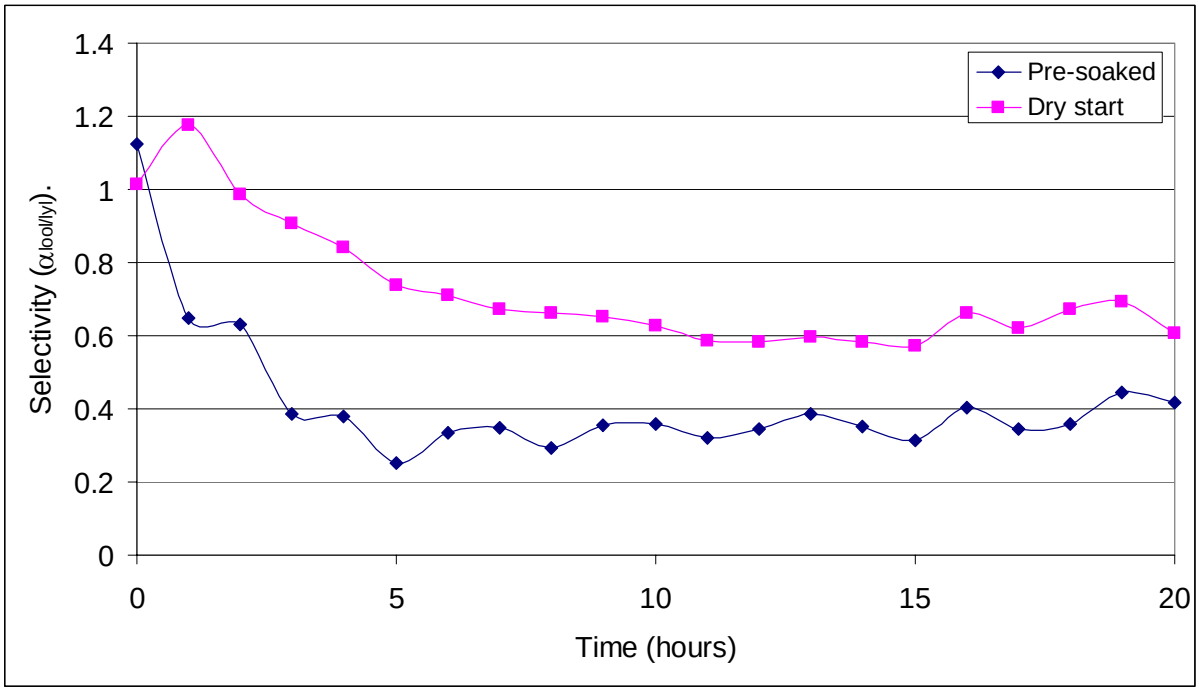

Figure 5:24 Selectivity of a pre-soaked and dry start 10 µm HDPE membranes.

Membranes which started pervaporation dry (Figure 5:24) tended to take longer to reach steady-state conditions than those which had been previously soaked in the feed solution. This trend held true for membranes of different thicknesses as well as different polymer structures, although the time taken to reach steady-state varied from polymer to polymer.

5.1.7 Membrane thickness

Membrane thickness has little effect on selectivity, but has an inverse relationship with flux rate (Binning *et al.*, 1961). A series of low density polyethylene (LDPE) membranes ranging in thickness from 11.3 to 31.5 µm were used to determine the influence of membrane thickness on separation of linalool and linalyl acetate in ethanol.

5.1.7.1 Representative process conditions

Pervaporation runs of 44 hours were carried out with conditions kept as constant as possible. Variations from run to run were inevitable, but fixed parameters included keeping the permeate pressure at $\tilde{P}_p$ < 10 kPa, processing temperatures at approximately 20°C, membrane unit impinging jet height = 1.36 mm, feed flow rate of 804 mL/min, and a feed concentration

≈ 5% v/v linalool and linalyl acetate in ethanol. Figure 5:25 shows process conditions for a typical pervaporation run.

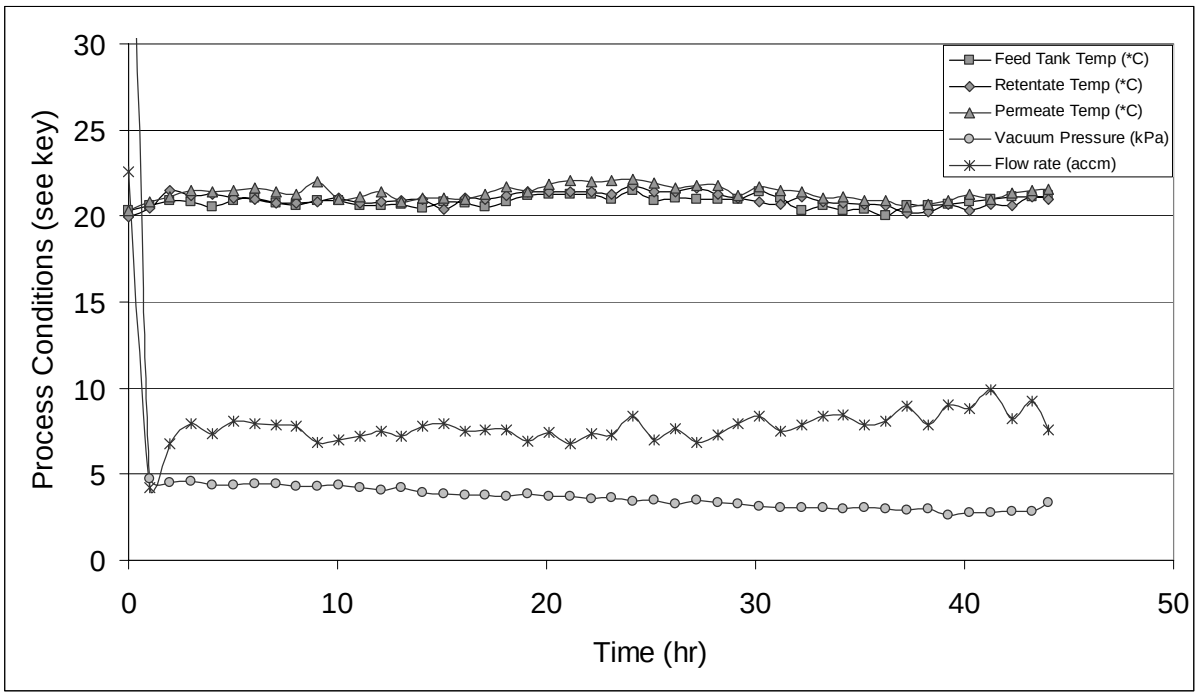

Figure 5:25 Process variables for pervaporation run: LDPE – 120404 (28.7 μm).

The average steady-state temperatures for experiments conducted at waterbath temperatures of 20°C were ($\widetilde{T}_f$ = 21.00°C (± 0.40°C), $\widetilde{T}_r$ = 21.02°C (± 0.54°C), and $\widetilde{T}_p$ = 21.65°C (± 0.78°C) for feed, retentate and permeate temperatures respectively. The bulk of the uncertainty is due to the variability of signal output from the thermocouples (± 0.49°C). Permeate temperature had the largest degree of variation due to its distance from the primary source of temperature control and the effects of room temperature fluctuations. Temperature variation within a single run was ±2°C.

Variation in steady-state permeate pressure ($\widetilde{P}_p$: 2.64 – 8.77 kPa) from run to run had no significant influence on selectivity. Permeate pressure averaged between $\overline{P}_p$ = 1.94 and $\overline{P}_p$ = 2.34 kPa (± 0.20 kPa) for offline runs and between $\overline{P}_p$ = 3.41 and $\overline{P}_p$ = 7.31 kPa (± 0.65 kPa) for online sampling runs. Steady-state permeate pressure depended slightly on membrane thickness. The thicker (24.7 – 31.5 μm) membranes averaged lower steady-state permeate pressures than the thinnest (11.3 – 14.8 μm) membranes (Figure 5:26). Thicker

membranes may have been less susceptible to pinhole imperfections and/or may have formed a better seal with the 'o'rings in the membrane unit.

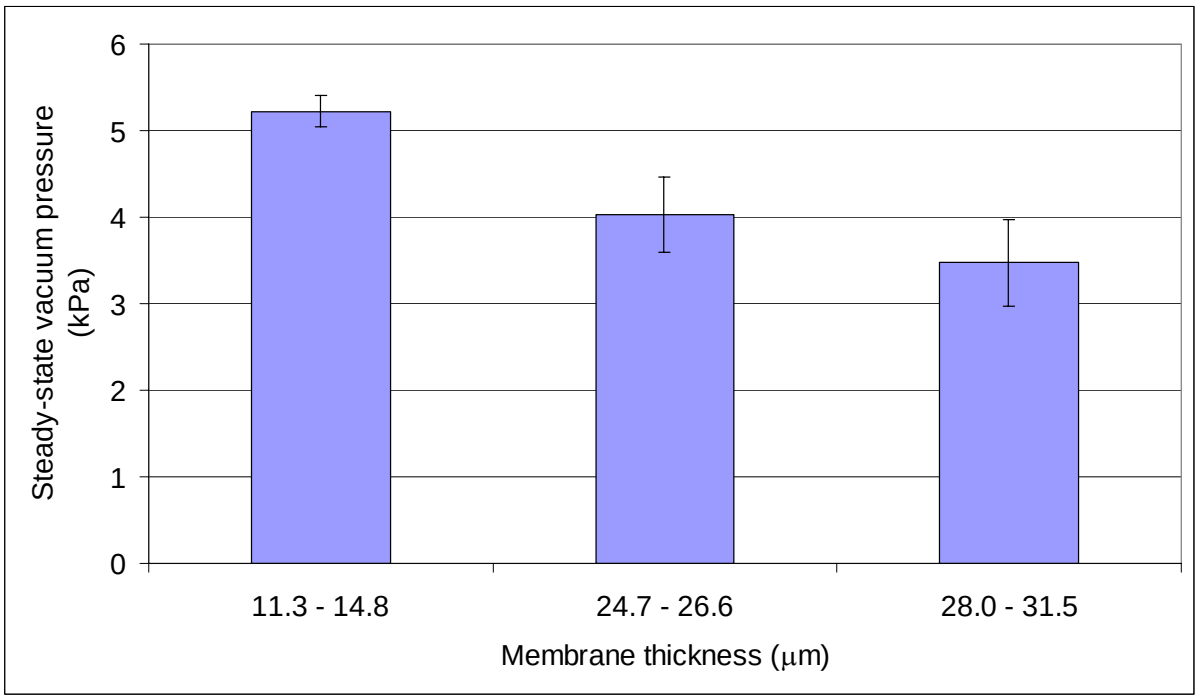

Figure 5:26 Average steady-state permeate pressure observed for various membrane thickness.

Criteria for rejecting data

Data from several runs was rejected from analysis where observed permeate flow rates were several times higher than the norm and they failed to reach steady-state conditions between 30-44 hours. In these cases it was likely that leaks occurred across membranes (e.g., pinholes) or in process lines.

5.1.7.2 Influence on membrane swelling

Dimensions and weights of LDPE membranes before and after soaking in feed solution, are given in Table 5:01. For each membrane, dry diameters were averaged from measurements across four quadrants of the membrane, dry thickness averaged from six random measurement points and dry weights averaged from six measurements. Wet weights were measured against time as solvent evaporated quickly. The zero intercept from three consecutive measurements was taken as the wet weight immediately after soaking.

Table 5:01 LDPE membrane parameters for multiple replicate experimental runs.

Run Designation	Dry Thickness (μm)	Dry Diameter (mm)	Dry Weight (g)	Wet Weight (g) [§]
LDPE – 180404	31.5	127.69	0.3822	0.3926
LDPE – 050404	29.5	126.75	0.3522	0.3583
LDPE – 120404	28.7	127.40	0.3456	0.3516
LDPE – 200404	28.0	127.05	0.3312	0.3374
LDPE – 220404	26.6	126.91	0.3013	0.3048
LDPE – 070404	26.2	127.10	0.3165	0.3317
LDPE – 140404	25.5	127.14	0.3146	0.3223
LDPE – 260404	25.3	126.78	0.2878	0.2942
LDPE – 240404	24.9	127.59	0.2880	0.2925
LDPE – 290304	24.7	127.07	0.2979	0.3034
LDPE – 080604	14.8	126.33	0.1559	0.1628
LDPE – 020504	13.5	126.84	0.1584	0.1610
LDPE – 150604	13.5	127.02	0.1509	0.1568
LDPE – 290404	13.2	126.87	0.1572	0.1599
LDPE – 020604	11.3	126.25	0.1409	0.1562
Average:		126.99 ± 0.40		

[§] Zero intercept

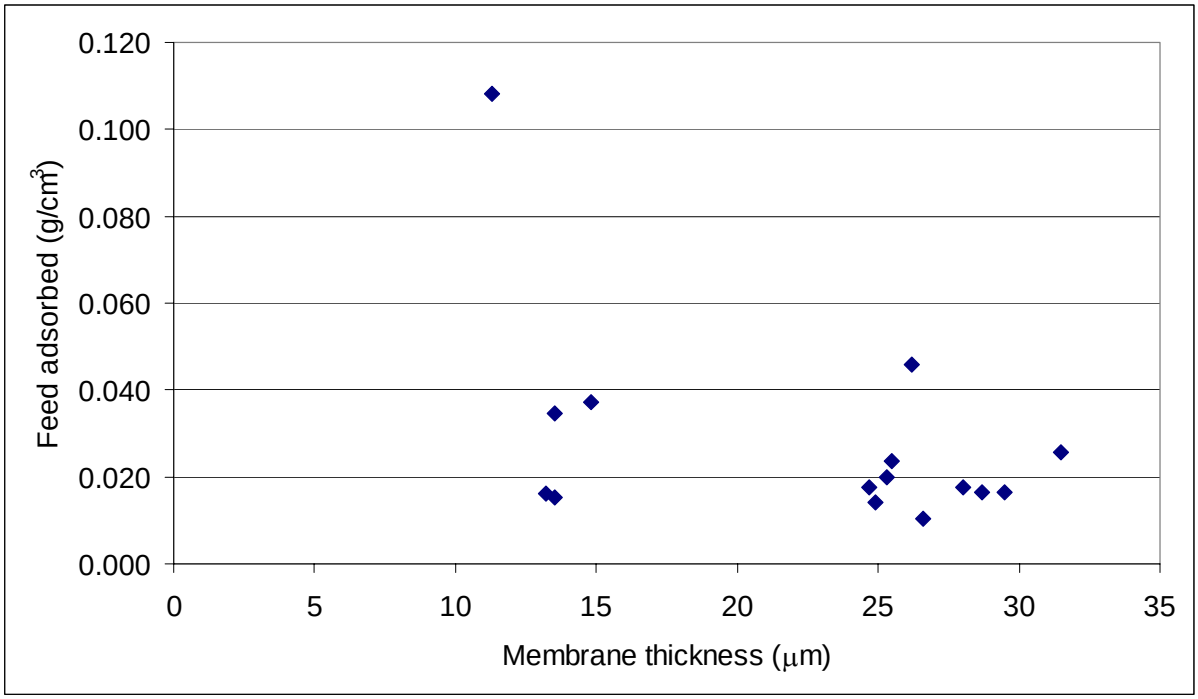

Figure 5:27 Adsorbtion of feed solution per unit volume of LDPE polymer.

The uniformity of the amount of feed absorbed per cm^3 of polymer (Figure 5:27) indicates that despite differences in thickness, the LDPE membranes are relatively homogeneous. The process of forming different thickness LDPE membranes appears to have had little affect on the degree of crystallinity in the polyethylene structure and subsequently its absorbtive capacity.

5.1.7.3 Influence on selectivity

Analysis of permeate vapour composition was carried out using online sampling of the process line via gas chromatography. Membrane selectivity was calculated from this data and known feed compositions. Figures 5:27 and 5:28 show representative graphs. Note that linalyl acetate (■)preferentially permeates through this LDPE membrane ($\alpha < 1.0$) with respect to the permeation of linalool.

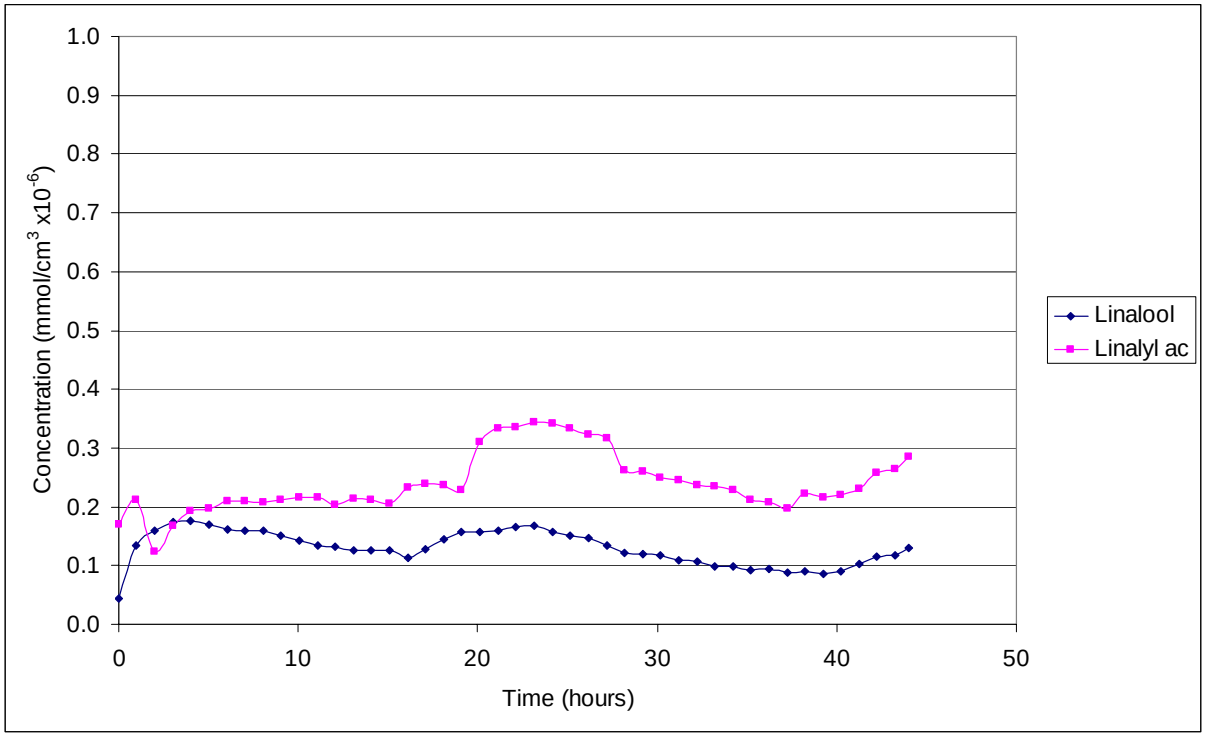

Figure 5:28 Composition of permeate vapour throughout pervaporation run: LDPE – 120404 (28.7 μm).

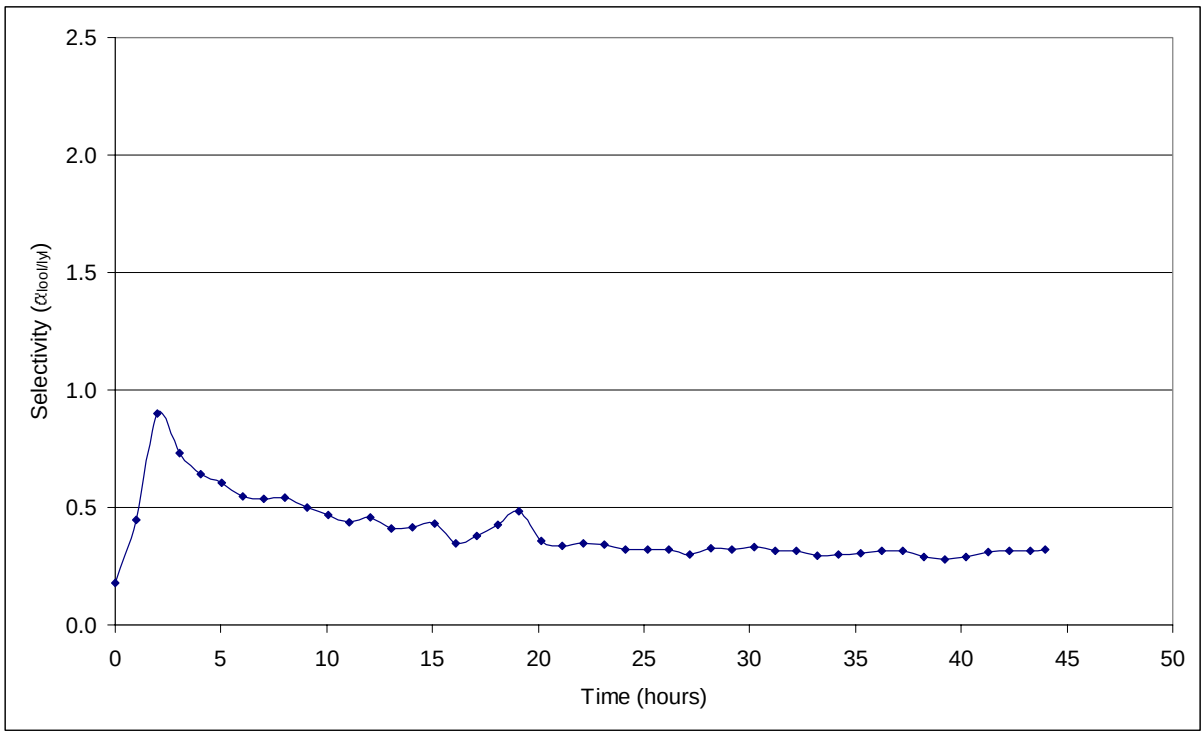

Figure 5:29 Selectivity ($\alpha_{lool/lyl}$) of permeate vapour throughout pervaporation run: LDPE – 120404 (28.7 μm).

The majority of pervaporation runs reached steady-state selectivity between 20 – 30 hours, thus steady-state data is collated from >30 hours.

Figure 5:30 shows the steady-state selectivity data for membranes of various thicknesses. Membranes of thickness above 24.7 μm did not appear to show any relationship between selectivity and membrane thickness. However, selectivity was poor for the thinnest membranes (11.3 – 14.8 μm), as α approaches unity. This contradicts the literature, which reports that selectivity should remain approximately constant despite varying membrane thickness (Binning *et al.*, 1961; Sridhar *et al.*, 2000). Binning *et.al.* (1961) qualified this statement by saying that "selectivity is independent of film thickness in the range of thickness considered practical for commercial use", which with state-of-the-art polymer manufacturing practices in 1961 was membranes of 300 μm thickness, vastly different from the 10 μm homogeneous membranes commercially available from Goodfellow Ltd. (Cambridge, UK) in 2001. Sridhar *et.al.* (2000), studied the effects of membrane thickness on selectivity, and utilised membranes ranging from 25 – 120 μm thick, thus the thinnest membranes in the current study are outside the scope of current literature.

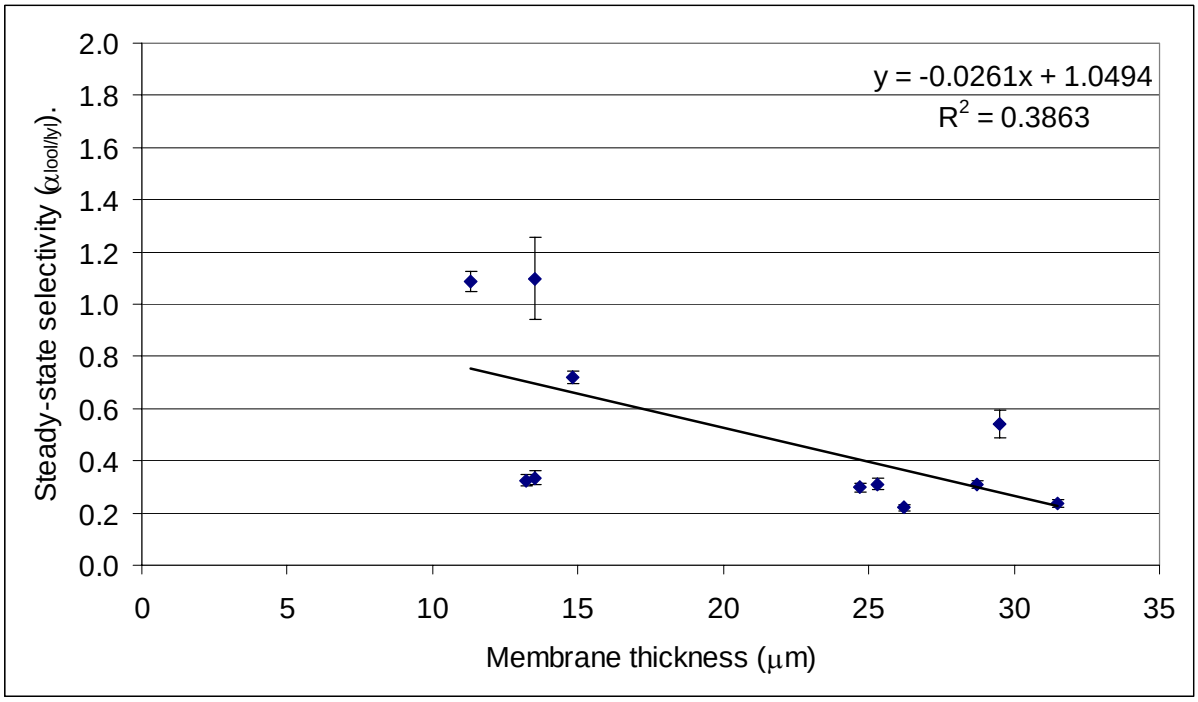

Figure 5:30 Correlation between membrane thickness and selectivity, calculated via online sampling of vapour permeate.

Thus the loss of selective permeability of the thinner membranes may indicate the limit to the membrane thinness which can be used in pervaporation and still maintain the ability to selectively permeate desired feed components. It is a matter of conjecture whether poor selectivity was due to an inability to reliably obtain pinhole-free homogeneous membranes of this thickness, or simply that there was not a thick enough "dry layer" on the downstream side of the membrane for interaction between membrane and permeants to occur.

5.1.7.4 Influence on flow rate

The volume of condensate collected in cold traps is shown in Figure 5:31, and represents an average of the flow of permeants throughout the entire process run. The logarithmic y-axis scale emphasises the extreme differences in overall permeate flow through membranes, with the thinnest membranes (11.3 – 14.8 μm) producing a volume of condensate an order of magnitude higher than the flow rates for membranes > 25 μm.

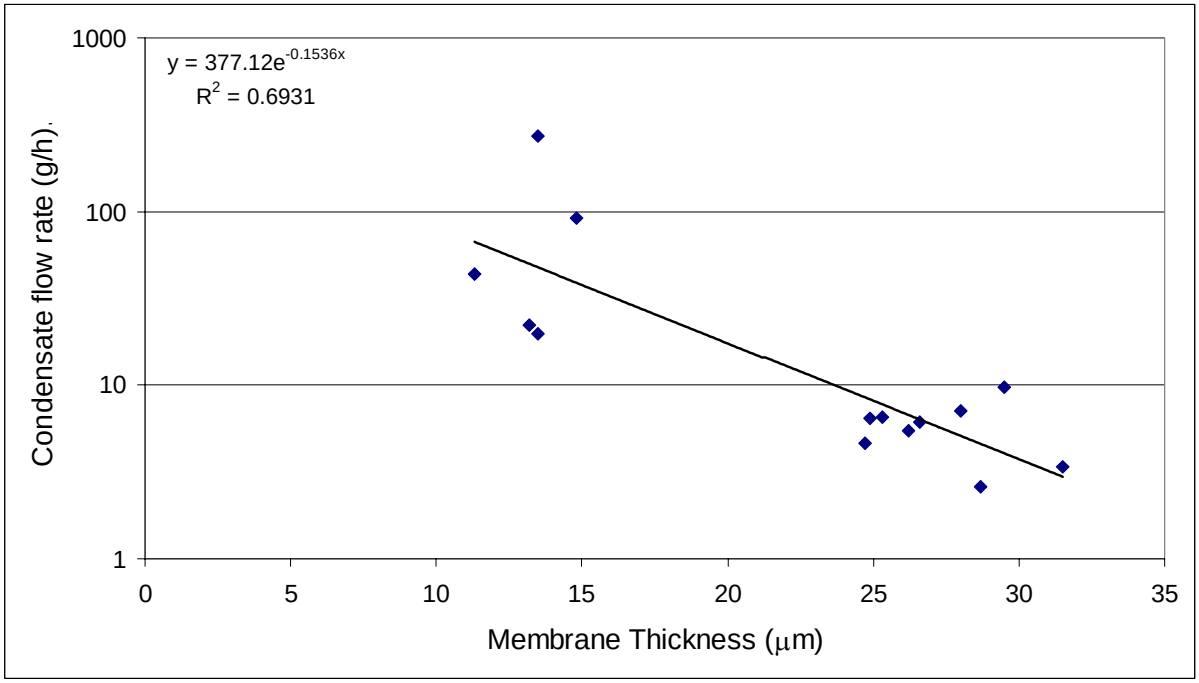

Figure 5:31 Correlation between membrane thickness and flow rate, calculated via volume of permeate condensate collected in cold traps.

By comparison, the steady-state flow rates (30-44 hours) acquired using an online electronic flow meter show that there is no significant difference in flow rates once the membrane has reached steady state conditions (Figure 5:32).

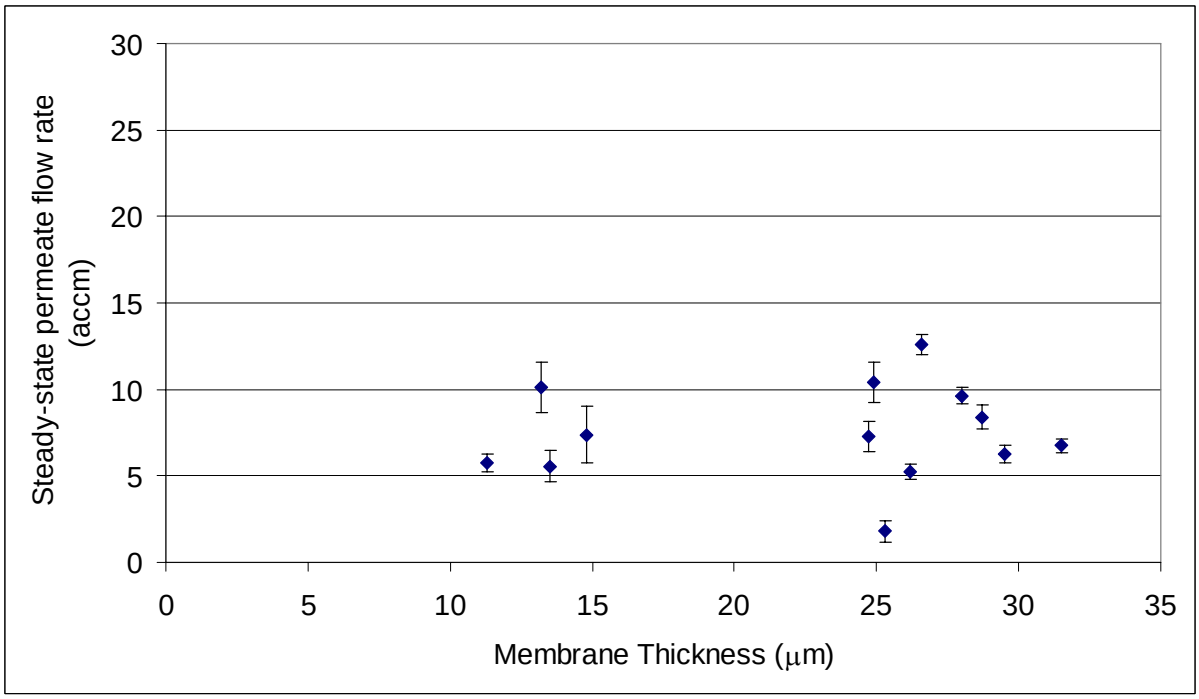

Figure 5:32 Effect of membrane thickness on steady-state flow rate through LDPE membranes of various thicknesses (accm calculation in Appendix 1).

This highlights the importance of allowing the PV process to reach steady-state conditions before collection of permeate product occurs. Standard deviations (error bars on Figure 5:32) were higher for thinner membranes than that of membranes > 25 μm thick, indicating a higher degree of fluctuation within process conditions, and a greater degree of variation in results from these membranes.

The lack of correlation between steady-state permeate flow rates and membrane thickness suggests that pinhole imperfections are unlikely to be the cause of the deterioration of selectivity with membrane thickness. Thus, membranes < 14.8 mm are not thick enough to produce enough interaction between membrane and permeants.

Steady-state permeate pressures obtained for membranes > 25 μm were significantly lower than the thinnest membranes (< 15 μm). However this variation is minimal in the context of transmembrane pressure where the driving force varied by 1-2% (ΔP_{mem}: 96 – 97 kPa).

5.1.8 Summary of process variable effects

Permeate Temperature took 3-4 hours to reach steady-state depending on temperature setting and room temperature. There was no statistically significant effect of temperature on selectivity at permeate temperatures ranging from 22-34°C, and fluctuations of up to 4°C within runs had no significant influence on selectivity and permeate flow rate. As temperature increased from 22-34°C, permeate flow rates through the membrane increased significantly.

Permeate pressure had no significant influence on selectivity when maintained at < 10 kPa. However, as permeate pressure increased, permeate flow rate decreased slightly within most runs, as the driving force of the trans-membrane pressure was reduced.

Membrane impinging jet height had no detectable influence on selectivity, however the permeate flow rate varied significantly with the height of the conical impinging jet from the membrane. Adapter heights of 1.36 and 2.36 mm produced higher steady-state permeate flow rates than 0.36 and 3.36 mm runs, but an impinging jet height of 1.36 mm had the highest reproducibility. Adapter heights of ≥ 1.36 mm reached steady-state permeate flow rates between 5-10 hours, whereas an impinging jet height of 0.36 mm took 15-20 hours to reach steady-state.

Despite Miranda & Campos (1999) stating that a feed flow with a Reynolds number of 1600 is optimal for pervaporation using a membrane unit with a concial flow distributor, feed flow rate had no statistically significant effect on permeate flow rates and selectivity of HDPE membranes tested.

Concentrations ranging between 1.78 – 6.01 % v/v linalool and linalyl acetate in ethanol had no statistically significant effect on selectivity or permeate flow rates. This was predominantly due to the scatter of data in these experiments.

Pre-soaking of membranes reduced the time to reach steady-state pervaporation conditions. Membranes which started pervaporation dry took up to 5 hours longer to reach steady-state conditions than those which had been previously soaked in the feed solution.

Literature states that selectivity should remain approximately constant despite varying membrane thickness, however the thinnest membranes (11.3 – 14.8 μm) studied had very poor selectivity in comparison to membranes >24.7 μm. LDPE membrane ranging in thickness from 24.7 – 31.5 μm showed relatively constant selectivity. Steady state permeate flow rates were independent of membrane thickness indicating that the likely cause of deterioration in selectivity with membrane thickness was insufficient 'dry-layer' for membrane-permeant interaction to take place.

5.2 Effect of polymer type on pervaporation

Membrane materials chosen using Hansen solubility parameters to be selectively permeable for one component over another, as well as the necessary mechanical and chemical stability included; Polyamide (PA: 26.9 μm), Polycarbonate (PC: 20.5 μm), Polyether imide (PEI: 29.2 μm), Polyether sulphone (PES: 27.6 μm), Polyimide (PI: 30.0 μm), Polypropylene (PP: 15.9 μm), and Polytetrafluoroethylene (PTFE: 26.7 μm).

5.2.1 Pervaporation performance of various polymers

Experiments were run at $\widetilde{T}_p$ = 30.97°C ± 0.46°C, $\widetilde{P}_p$ < 10 kPa, membrane unit impinging jet height = 1.36 mm, feed concentrations ≈ 5% v/v linalool and linalyl acetate in ethanol, and a feed flow rate of ≈ 804 mL/min.

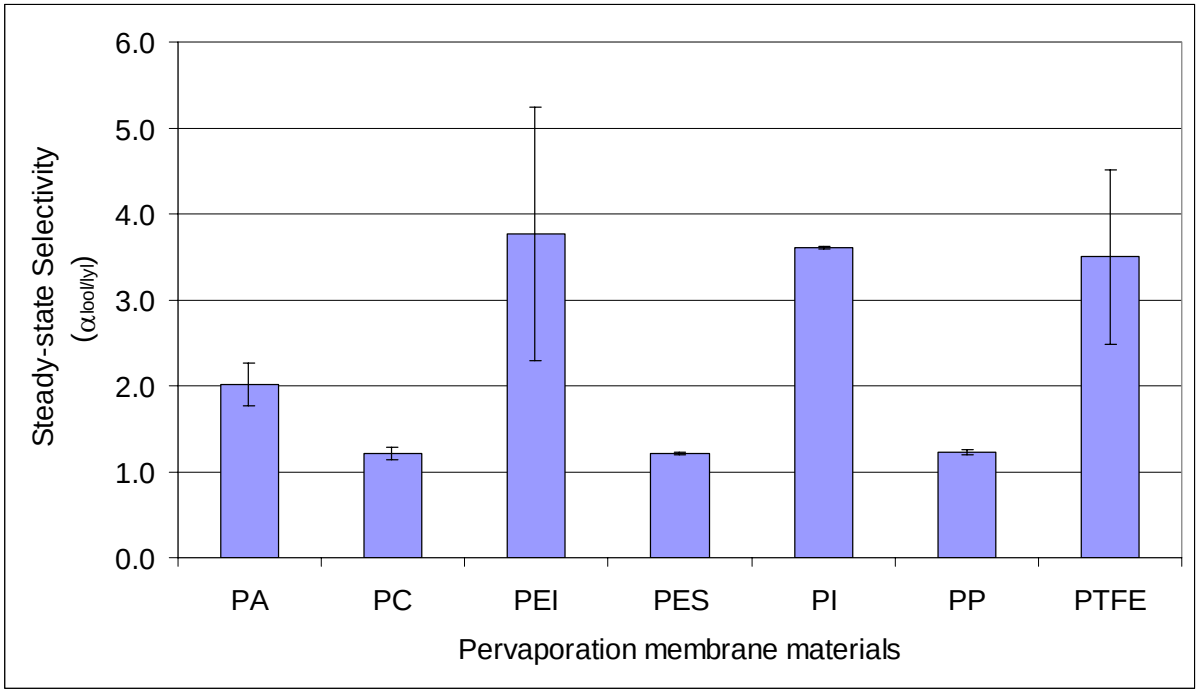

Figure 5:33 Selectivity of various polymer membrane materials.

All of the membranes displayed in Figure 5:33 when analysed via online sampling of permeate vapour, preferentially permeated linalool ($\alpha > 1$) with respect to linalyl acetate. Membranes that produced the highest selectivities were PEI ($\alpha = 3.767$), PI ($\alpha = 3.608$) and PTFE ($\alpha = 3.502$). PA was moderately good ($\alpha = 2.015$), but PC ($\alpha = 1.212$), PES ($\alpha = 1.213$) and PP ($\alpha = 1.226$) were barely above unity. Feng and Huang (1997) stated that polymers with high selectivity are often preferred for further study because the disadvantage associated with low permeability can be partly compensated by introducing asymmetricity to the membrane structure, thereby reducing the effective thickness of the membrane while maintaining mechanical strength. Thus PA, PI, PEI and PTFE show optimal selectivity for further analysis.

Of the membranes which produced moderate to high selectivity, PA (30 hours), PEI (20 hours) and PI (30 hours) took considerably longer to reach steady-state than PTFE (5 hours), despite pre-soaking all membranes. PC, PES and PP all reached steady-state withing 3-5 hours. This may have been due to a greater degree of interaction between polymer and permeants. The thickness of these membranes had a very minor influence on the time taken to reach steady-state, as PA, PEI and PI were 26.9, 29.2 and 30.0 μm thick respectively. By comparison, PTFE, PC, PES, and PP were 26.7, 20.5, 27.6, and 15.9 μm respectively.

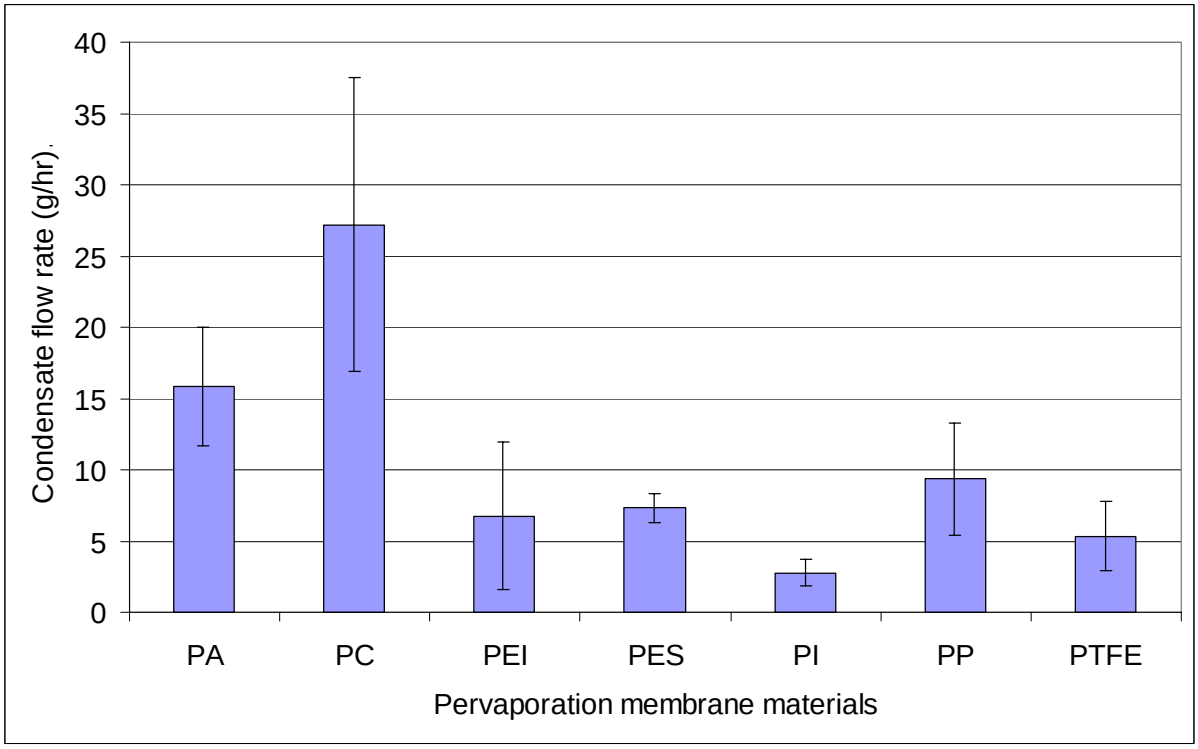

Figure 5:34 Permeate flow rate of various polymer membrane materials.

Figure 5:34 shows that PA and PC produced the highest permeate flow rates at 15.86 and 27.19 mg/h respectively. However, PC proved to be very brittle with membrane failure occurring during processing (after 18 and 43 hours) for two of the three online sampling runs where the membrane had been pre-soaked in feed solution. In addition to the membranes shown above, Poly methyl methacrylate (PMMA) was also examined, however it disintegrated in the feed solution.

When permeate flow rate is observed in conjunction with selectivity, Figure 5:35 shows that PA, PC, PEI and PTFE are the membranes with the highest efficiency of the homogeneous membranes studied.

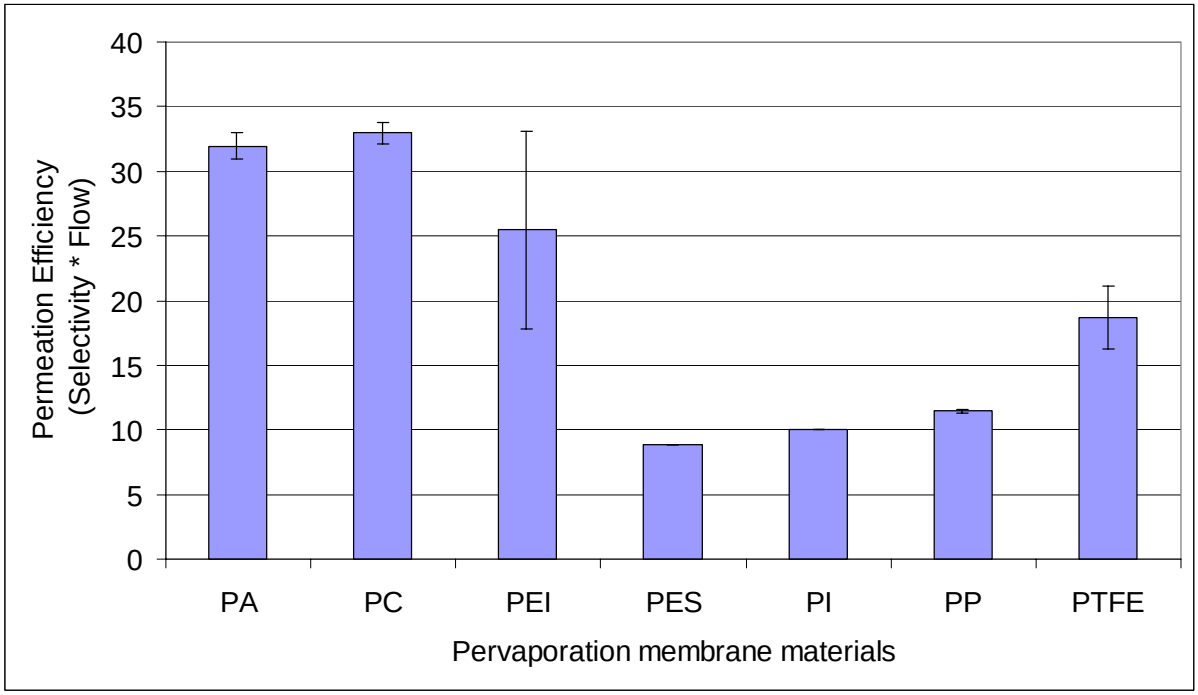

Figure 5:35 Overall efficiency of various polymer membrane materials.

However, as selectivity is more difficult to improve than flux, polymers with the greatest potential for further research are those with highest selectivity PA, PEI, PI and PTFE show the greatest promise.

5.2.2 Comparison with HSP predictions

The smaller the $\Delta\delta_{(S-P)}$, the more attracted a polymer is to each permeant (Eqn. 2:16). Thus based on the averaged Hansen solubility parameters calculated in Chapter 4, it was expected that PC, PP and PTFE would preferentially permeate linalyl acetate as the $\Delta\delta_{(S-P)}$ for this component is smaller than that of linalool. Conversely, PA, PEI, PES, and PI were expected to preferentially permeate linalool (Figure 5:36).

However, Figure 5:33 previously showed that all of the polymers tested selectively permeated linalool in preference to linalyl acetate. This may have been due to the difference in size of these molecules. The molar volume (molecular weight / density) of linalool ($C_{10}H_{18}O$) was 177.1 cm^3/mol and linalyl acetate ($C_{12}H_{20}O_2$) was 217.9 cm^3/mol. Thus with its larger size and steric hindrance, permeation of linalyl acetate may have been dominated by diffusive selectivity rather than sorption selectivity.

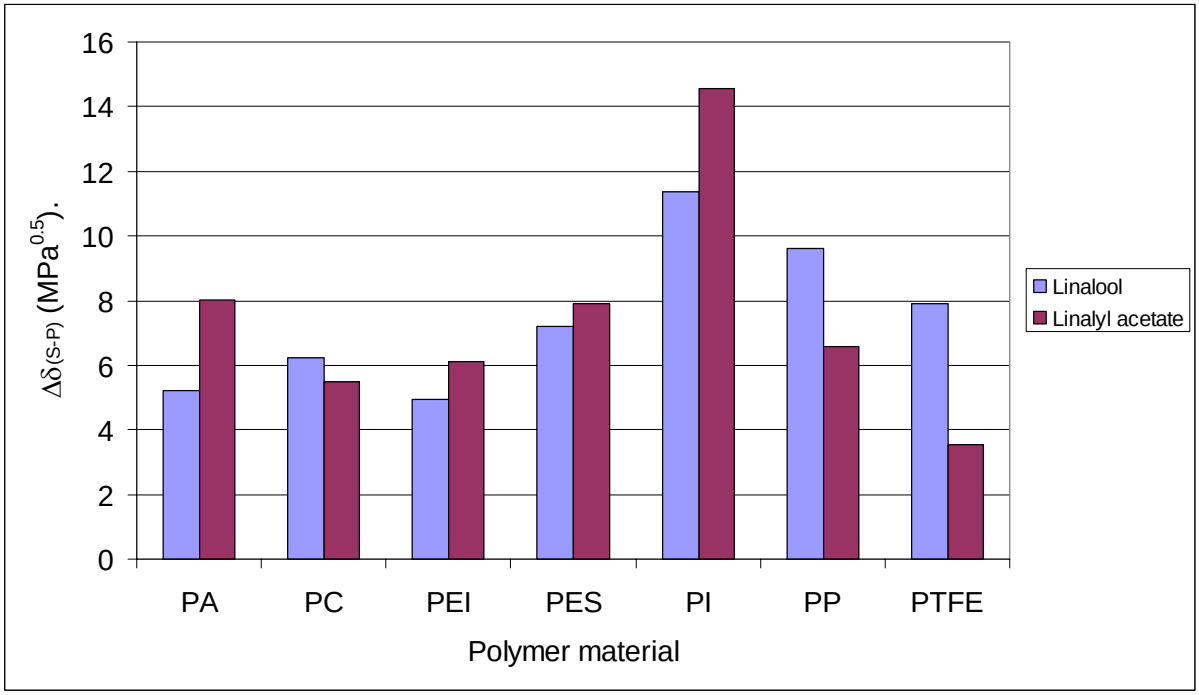

Figure 5:36 Relative energy differences between permeants and various polymers.

Figure 5:37 shows there is very little correlation between the selectivity of each membrane material and their solubility solely in linalool. One would expect the smaller the distance linalool lies from the polymer ($\Delta\delta_{(lool\text{-}polymer)}$) the better the selectivity. However, this relationship is not immediately obvious.

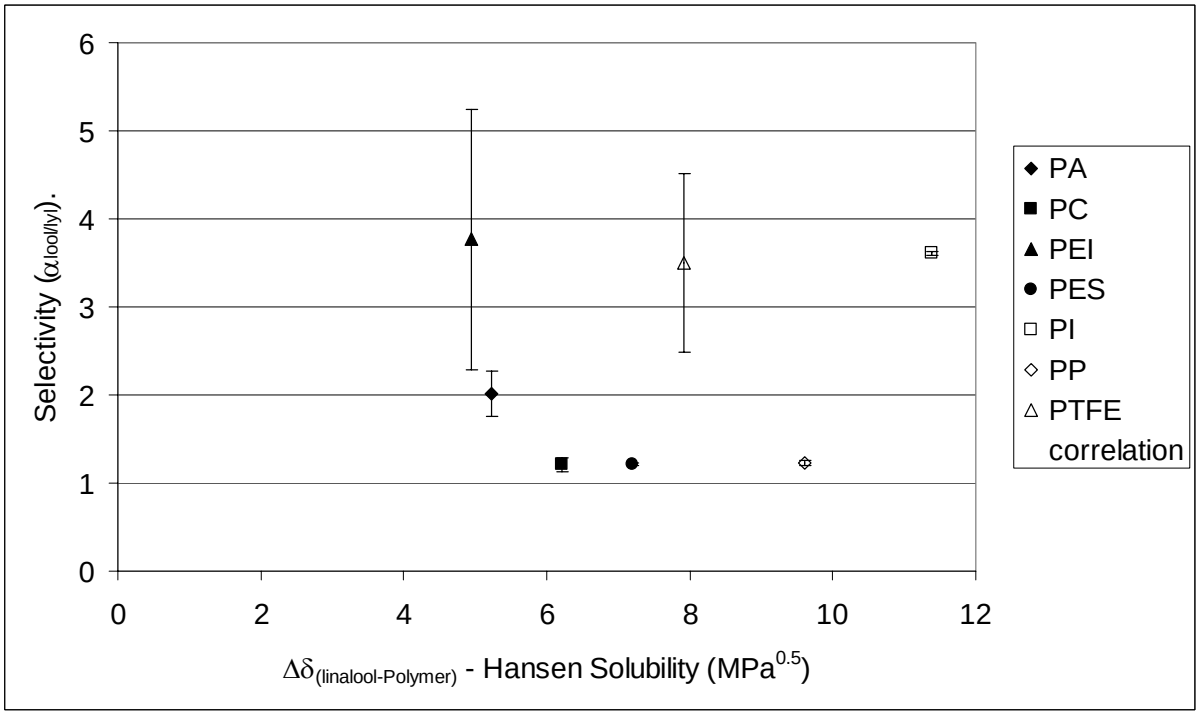

Figure 5:37 Relationship between selectivity of various polymer membrane materials and their attraction to linalool ($\Delta\delta_{(lool\text{-}p)}$).

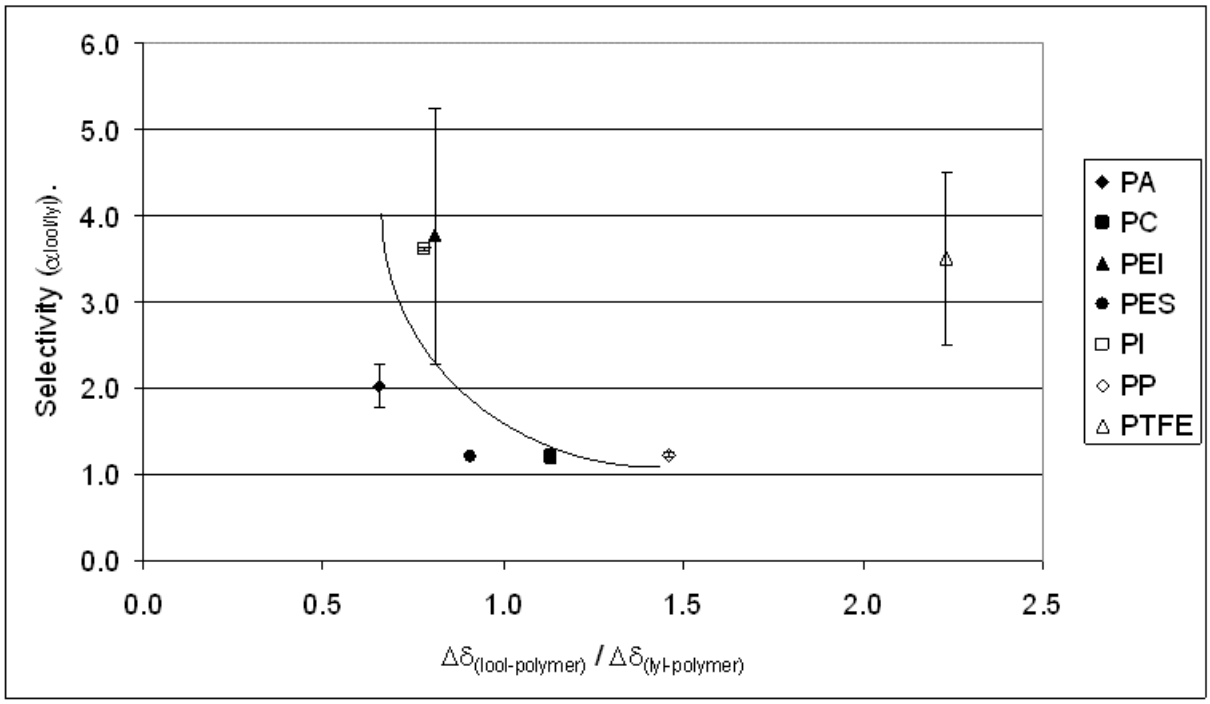

Figure 5:38 Relationship between selectivity of various polymer membrane materials and their attraction to linalool ($\Delta\delta_{(lool\text{-}p)}$) relative to linalyl acetate ($\Delta\delta_{(lyl\text{-}p)}$).

Figure 5:38 shows the correlation between the selectivity of each membrane material (except PTFE) and their solubility in linalool with respect to linalyl acetate ($\Delta\delta_{(lool\text{-}polymer)}$ / $\Delta\delta_{(lyl\text{-}polymer)}$). Here, the smaller the distance linalool lies from the polymer with respect to linalyl acetate, the better the selectivity. As could be expected, membrane materials where linalool and linalyl acetate are equidistant from the polymer in HSP space, show little preferential selectivity ($\alpha \approx 1.0$).

PTFE appeared to behave anomalously in Figure 5:38, as according to its HSP, it should have preferentially permeated linalyl acetate, however this was not observed in PV experiments. This may have been due to the influence of diffusivity, with linalyl acetate being a much larger molecule and therefore less volatile and having a lower diffusion coefficient than linalool. Alternatively there may have been bias in the calculation of HSP, as literature values and group contribution methods make no accounting for additives and other residues that may be present in the polymer, especially in light of the vastly different values obtained for the H-bonding component of PTFE from literature, group contribution and swelling experiments (Table 4:23).

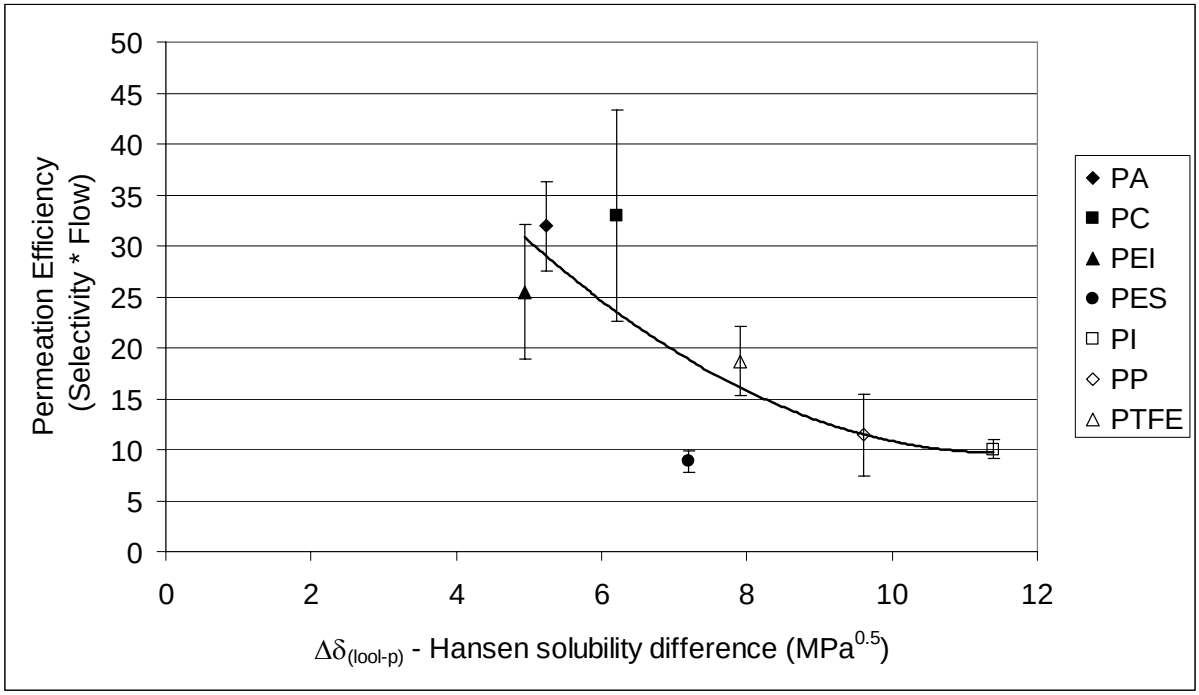

Figure 5:39 Relationship between Overall efficiency of various polymer membrane materials and their attraction to linalool ($\Delta\delta_{(lool\text{-}p)}$). Error bars are additive standard errors α+Q.

The relationship between permeation efficiency and $\Delta\delta_{(lool\text{-}polymer)}$ is shown in Figure 5:39. In general, the smaller the Hansen solubility difference ($\Delta\delta_{(S\text{-}P)}$) between the solubility parameters of linalool and polymer, the more attracted they are to each other and the greater the efficiency in pervaporation separations. PA, PC and PEI had smaller $\Delta\delta_{(S\text{-}P)}$ (5.23, 6.21, 4.94 respectively), in comparison to PES, PI, PP and PTFE ($\Delta\delta_{(S\text{-}P)}$ = 7.20, 11.39, 9.60, 7.92 respectively), and the former group had highest permeate flow rates and selectivity towards linalool.

Figure 5:40 shows the correlation between the permeation efficiency of each membrane and their solubility in linalool with respect to linalyl acetate ($\Delta\delta_{(lool\text{-}polymer)}$ / $\Delta\delta_{(lyl\text{-}polymer)}$). Those with a solubility difference greater than 1.0 should preferentially permeate linalyl acetate, and those with solubility difference < 1.0 preferentially permeate linalool. As mentioned previously, PTFE behaved anomalously, and PC was very brittle. This brittleness of PC could potentially have lead to leakage (prior to membrane failure), and boosted the permeate flow component of the efficiency calculation. This theory of pre-membrane failure leakage is reinforced by the large error bars in Figure 5:34 for PC (std error ± 10.3 g/h).

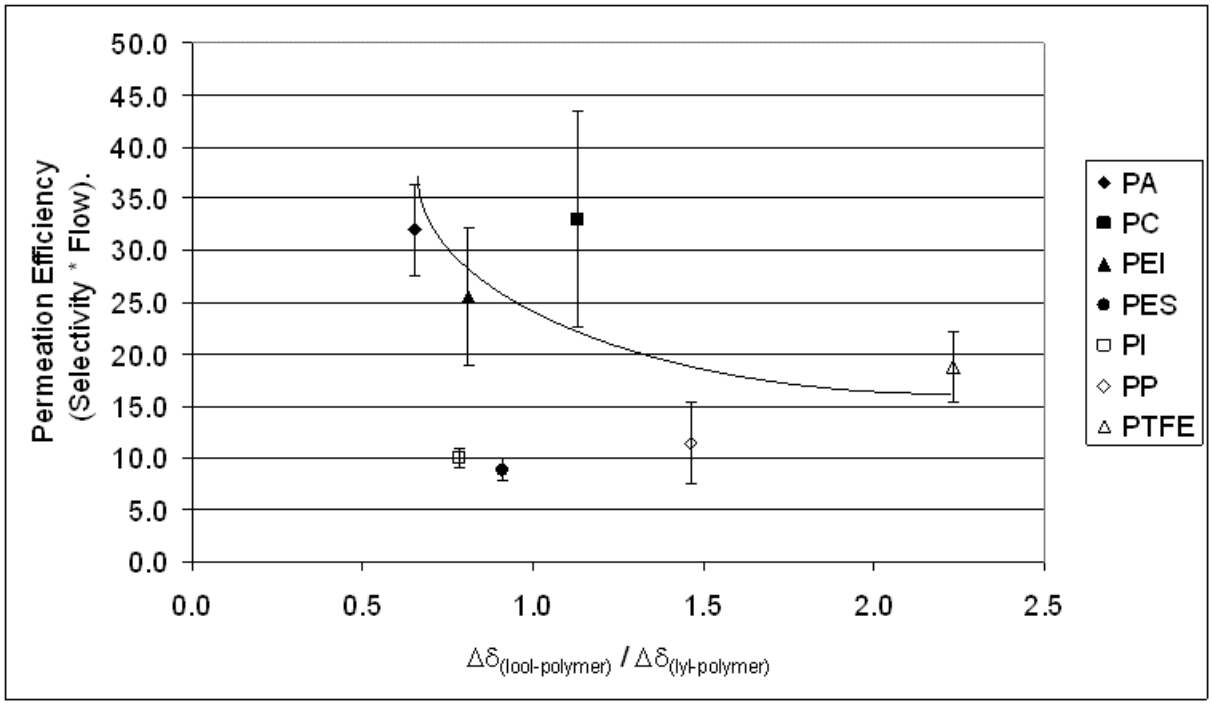

Figure 5:40 Relationship between Overall efficiency of various polymer membrane materials and their attraction to linalool ($\Delta\delta_{(lool-p)}$) relative to linalyl acetate ($\Delta\delta_{(lyl-p)}$.

5.2.3 Summary of PV with various membrane materials

On the basis of natural efficiency of the homogeneous polymer, PA, PC, PEI and PTFE would be the best options for further study with the processing of the lavender essential oil rather than the model solution used in this study. The brittle nature of PC under model solution pervaporation conditions indicates it is unlikely to withstand the chemical stresses placed on it when pervaporating pure lavender oil, leaving PA, PEI and PTFE as the homogeneous membranes with the best potential for enrichment of linalool from lavender oil. PC may show improved stability if combined with another polymer material which would allow the PC to act as the selective layer while providing the necessary mechanical support to minimise the likelihood of membrane rupture.

According to Koops and Smolders (Koops and Smolders, 1991), it is easier to increase flux at a later date than to increase selectivity. On this basis; PEI, PI and PTFE should be chosen for further investigation to improve stability and flux rates by modification of the polymer morphology into asymmetric or composite membranes, or structurally using crosslinking, blending, grafting or copolymerisation.

Interestingly, the membranes with the best selectivity also tended to take the longest to reach steady-state pervaporation conditions. This may have been due to a greater degree of interaction between polymer and permeants.

PA, PEI and PTFE had the highest natural efficiency and for permeating linalool of the homogeneous polymers, plus the required mechanical and chemical stability for pervaporation processes. These polymers should be chosen for further investigation into improving stability and flux rates so they might be suitable for processing of pure essential oil.

Pervaporation selectivity did not always follow the trends predicted by HSP. Polymers such as PA, PEI, PES, and PI did preferentially permeate linalool as expected, but PC, PP and PTFE did not permeate linalyl acetate preferentially. This may have been due to the difference in size and diffusivity of these molecules, which meant that the larger molecule (linalyl acetate) did not follow the sorption selectivity predictions.

The smaller the Hansen solubility difference ($\Delta\delta_{(S-P)}$) between the solubility parameters of linalool and polymer, the more attracted they were to each other and the greater the efficiency in pervaporation separations. As expected, membrane materials where linalool and linalyl acetate were equidistant from the polymer in HSP space, showed little preferential selectivity ($\alpha \approx 1.0$).

5.3 Membrane selection procedure

Based on the research carried out in this thesis, the following basic procedure has been determined to be best practice for selecting membrane materials using HSP (Figure 5:41).

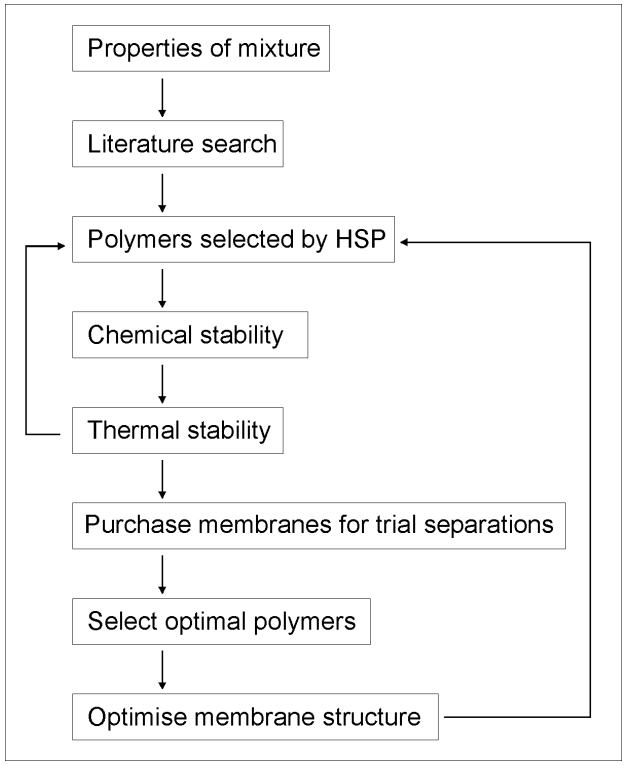

Figure 5:41 Systematic approach to selection of membrane materials using HSP.

1. *Properties of the mixture*

   This involves identification of the feed composition, desired permeant, major and minor components, feed variability and contaminants that may cause problems. Based on the feed composition and desired permeant, a first estimate can be made as to hydrophilic/hydrophobic/organophilic membrane requirements.

2. *Literature search*

   Determine through literature search if the feed components have been studied before, and identify what membrane materials were successfully used to separate feeds with comparable functional groups to the current feed components.

3. *Polymers selected by HSP*

   Select membrane materials for preferential sorption of the desired permeant over the other feed components. Potential membrane materials are chosen using HSP where the minor/desired component is inside the solubility sphere, and other feed components outside the solubility sphere of the polymer.

4. *Chemical & Thermal stability*

   Determine if potential polymer materials have the chemical resistance and thermal stability required to withstand PV processing conditions. If polymers are likely to disintegrate or degrade, return to step 3 and choose alternate polymer materials.

5. *Purchase membranes for trial separations*

   Based on selection criteria in steps 3 & 4, obtain homogeneous thin film polymer materials of approximately 20-25 μm thickness from commercial supplier, or manufacture them yourself. Carry out test PV runs with these membranes using the feed mixture.

6. *Select optimal polymers*

   From these PV runs choose those membranes that perform best in both selectivity and flux rates.

7. *Optimise membrane structure*

   For those membranes with the best selectivity, the polymer material can be optimised for flux by altering the membrane morphology (asymmetric or composite membranes). Composite membrane materials can be chosen by returning to step 3 and using HSP to find compatible polymeric materials. Other membrane modification procedures can be used to optimise membrane performance including; altering the crystallinity, density, blending, grafting, copolymerization, and degree of cross-linking.

The procedure outlined above is primarily designed for selection of membrane materials for organic/organic liquid mixture separations, where the components are of comparable molecular size. Liquid mixtures where there is significant disparity in the size of the constituents (as seen in most aqueous/organic feeds), are systems which are likely to be dominated by diffusion rather selectivity; hence the limited ability of HSP to predict preferential permeation.

Chapter

6

Conclusions & Recommendations

This section details conclusions made about membrane selection, HSP calculation, PV process variable effects, and the optimum membrane materials for selective permeation of model solution components. Recommendations are made about practical applications and the implications for future research.

6.1.1 Summary of conclusions

HSP prediction of PV selectivity

The Hansen solubility parameter approach successfully predicted the separation characteristics of the majority of benzene/organic, alcohol/alkene, and alkane/organic solutions. However, it was unable to consistently predict the separation characteristics of halogenated/organic and xylene isomer mixtures.

Membrane selection

The HSP membrane selection method indicated that PA 6,6, POMH, PSU, PBT, PTFE, and PP had the greatest potential for selectively permeating lavender essential oil components, with PS, PC, PEI, PVC also showing promise. Of these, PA 6,6, PC, PEI and PTFE had the highest natural efficiency in homogeneous membrane form, indicating these polymers have the greatest potential for modification into asymmetric or composite membranes to achieve improved permeation characteristics. PC in particular would benefit most from modifications to its morphology which would improve its chemical stability and mechanical strength under processing condtitions.

Pervaporation selectivity did not always follow the trends predicted by HSP. Polymers such as PA, PEI, PES, and PI did preferentially permeate linalool as expected, but PC, PP and PTFE did not permeate linalyl acetate preferentially. This may have been due to the difference in size of these molecules, which meant that permeation of the larger molecule (linalyl acetate) was dominated by diffusion selectivity. Alternatively, the inaccuracies inherent in the use of group contribution method of HSP determination may have influenced the reliability of the predicted selective permeation.

HSP calculation

The polymer swelling method was better than the solubility method for determining HSP as it was simple, time efficient and used a far lower number of potentially toxic solvents. If electrical data are available for polymers, the refractive index method is excellent for determining δ_d, and the dielectric constant gives good relative δ_p values within a set of polymers. Possibly the least accurate method of determining HSP was the group contribution method, as it made a large number of assumptions based on generic polymer species, and took no account of individual variations due to manufacturing process and additives.

Process Variable Effects

As predicted by literature, permeate flow rates increased with temperature, and temperature did not significantly effect selectivity for permeate temperatures ranging from 22-34°C. Permeate pressure maintained at < 10 kPa had no significant influence on selectivity. However, as permeate pressure increased, permeate flow rate decreased slightly within most runs, as the driving force of the trans-membrane pressure was reduced.

Membrane impinging jet height had no detectable influence on selectivity. Permeate flow rate, reproducibility and time to reach steady-state were optimal at an impinging jet height of 1.36 mm above the membrane. Feed flow rate through the concial flow distributor had no statistically significant effect on permeate flow rates or selectivity.

Due to the scatter in data, selectivity and permeate flow rates showed no statistically significant differences in means at various feed concentrations (1.78 – 6.01 % v/v linalool and linalyl acetate in ethanol).

Pre-soaking of membranes reduced the time to reach steady-state pervaporation conditions. Membranes with the highest selectivity also tended to take the longest to reach steady-state pervaporation conditions. This may have been due to a greater degree of interaction between polymer and permeants.

Contrary to literature membrane thickness did effect selectivity. Membranes of thickness 11.3 – 14.8 μm had poor selectivity in comparison to membranes >24.7 μm thickness. Steady state permeate flow rates were independent of membrane thickness indicating that the likely cause

of deterioration in selectivity with membrane thickness was insufficient 'dry-layer' for membrane-permeant interaction to take place.

Polymers selected using HSP successfully preferentially permeated linalool over linalyl acetate in a model organic liquid mixture. Modest selectivities in favour of linalool averaging 3.8, 3.6, and 3.5 were achieved for PEI, PI and PTFE respectively, and low selectivities were achieved by PA ($\alpha_{lool/lyl}$ = 2.02) and PC ($\alpha_{lool/lyl}$ = 1.21). Good permeate flow rates were achieved for PA and PC at 15.86 and 27.19 mg/h respectively, and modest flow rates were achieved by PEI (6.77 mg/h), PI (2.78 mg/h) and PTFE (5.34 mg/h). PES and PP had modest selectivities and flow rates (PES: $\alpha_{lool/lyl}$ = 2.02, 7.30 mg/h; PP: $\alpha_{lool/lyl}$ = 1.23, 9.34 mg/h).

6.1.2 Attainment of objectives

The use of Hansen solubility parameters (HSP) as a method for membrane selection successfully fulfils the criteria of being quick, easy, reproducible and valid for separating a variety of organic liquid mixtures. However, HSP are less reliable at predicting selective permeation when feed components vary significantly in molecular size, as diffusivity dominates permeation rather than selectivity. Because it is easier to increase flux by altering membrane morphology than to increase selectivity (Koops and Smolders, 1991), selection of preliminary polymer membrane materials on the basis of polymer-feed component affinity using HSP is still valid.

Hansen solubility parameters (HSP) have proved to be a good first estimate for selecting membrane materials for specific organic-organic separations.

6.1.3 Future research

Future work on PV of essential oils should include a series of PV experiments testing the polymers identified as having the best potential selective permeation on pure essential oil feeds. Also, improvement of polymer membrane permeation characteristics through modification into asymmetric or composite form will be essential to obtaining commercial application.

Inverse gas chromatography

Another idea stimulated by this research project includes extending the use of inverse gas chromatography to calculation of HSP. Although rectangular thin-channel column inverse gas chromatography (RTCC-IGC) (Huang *et al.*, 2001) was found to be impractical for selecting novel membrane materials for permeating large organic molecules (b.p. > 100°C), it does show promise as a technique for obtaining HSP. The RTCC-IGC unit could be used to quickly obtain HSP of a wide variety of polymers by running a range of solvent probes over the thin film membrane 'column', and correlating their retention times with probe HSP in much the same way as the swelling experiments in section 3.4 were carried out. Not only are smaller quantities of potentially toxic solvent probes required (c.f. HSP solubility or swelling experiments), but the set-it-and-forget-it nature of a modern GC-FID with autosampler, means it is less labour intensive. Absence of the need to weigh polymer samples pre- and post-sampling will also reduce labour intensiveness of swelling experiments, in addition to improving accuracy and precision of HSP obtained.

The only draw-back foreseen is the difficulty of getting enough high h-bonding solvents, as water cannot be detected on a GC-FID. However, because such small quantities of unusual solvents are required; dimethyl sulfide, 2-propanethiol, 3-Methylcyclohexanone or 3-Penten-2-one etc., could be substituted. Alternatively a different detector could be fitted to the GC.

6.1.4 Practical applications

Practical applications for PV of essential oils include the production of specifically tailored flavour and fragrance mixtures. Alteration of the composition of thermo-labile essential oil using this technique could yield high value natural products easily tailored to the end users specifications. Essential oils which currently do not reach industry standards or suffer significant compositional variation from season to season can be modified to fit the desired composition.

Enrichment of valuable pharmaceutical products or reduction in the concentration of potentially harmful essential oil components could produce a more valuable product that is safer to use. PV membrane processing of essential oils could produce a desirable product

well in advance of programs to selectively breed plants yielding a desirable composition, giving the advantage of shorter lead time to market place.

References

Abboud, J. L., M. J. Kamlet and R. W. Taft (1977). "Regarding a generalized scale of solvent polarities." Journal of the American Chemical Society 99(25): 8325-8327.

Aburjai, T. and F. M. Natsheh (2003). "Plants used in cosmetics." Phytotherapy Research 17(9): 987-1000.

Acharya, H. R., S. A. Stern, Z. Z. Liu and I. Cabasso (1988). "Separation of liquid benzene/cyclohexane mixtures by perstraction and pervaporation." Journal of Membrane Science 37(3): 205-232.

Ahmad, H. (1982). "Parameter of acrylamide series polymers through its components and group contribution technique." Journal of Macromolecular Science A17: 585-600.

Akgün, M., N. A. Akgün and S. Dinçer (2000). "Extraction and modeling of lavender flower essential oil using supercritical carbon dioxide." Industrial & Engineering Chemistry Research 39(2): 473-477.

Al-Amier, H., B. M. M. Mansour, N. Toaima, R. A. Korus and K. Shetty (1999). "Tissue culture based screening for selection of high biomass and phenolic producing clonal lines of lavender using pseudomonas and azetidine-2-carboxylate." Journal of Agricultural & Food Chemistry 47(7): 2937-2943.

Anastasiadis, S. H., I. Gancarz and J. T. Koberstein (1988). "Interfacial tension of immiscible polymer blends: Temperature and molecular weight dependence." Macromolecules 21(10): 2980-2987.

Aptel, P., J. Cuny, J. Jozefowicz, G. Morel and J. Neel (1972). "Liquid transport through membranes prepared by grafting of polar monomers onto poly(tetrafluoroethylene) films. I. Some fractionations of liquid mixtures by pervaporation." Journal of Applied Polymer Science 16: 1061-1076.

Aptel, P., J. Cuny, J. Jozefonvicz, G. Morel and J. Neel (1974). "Liquid transport through membranes prepared by grafting of polar monomers onto poly(tetrafluoroethylene) films. Ii. Some factors determining pervaporation rate and selectivity." Journal of Applied Polymer Science 18: 351-364.

Aptel, P., N. Challard, J. Cuny and J. Neel (1976). "Application of the pervaporation process to separate azeotropic mixtures." Journal of Membrane Science 1: 271-287.

Auerbach, M. H. (1995). "A novel membrane process for folding essential oils." Flavour Technology ACS Symposium Series 610: 127-138.

Baddour, R. F., A. S. Michaels, H. J. Bixler, R. P. De Filippi and J. A. Barrie (1964). "Transport of liquids in structurally modified polyethylene." Journal of Applied Polymer Science 8: 897-933.

Baudot, A. and M. Marin (1996). "Dairy aroma compounds recovery by pervaporation." Journal of Membrane Science 120: 207-220.

Baudot, A. and M. Marin (1997). "Pervaporation of aroma compounds: Comparison of membrane performances with vapour-liquid equilibria and engineering aspects of process improvement." Transactions of the Institution of Chemical Engineers, (Food and Bioproducts Processing) 75(Part C): 117-142.

Beauchêne, D., J. Grua-Priol, T. Lamer, M. Demaimay and F. Quémeneur (2000). "Concentration by pervaporation of aroma compounds from fucus serratus." Journal of Chemical Technology & Biotechnology 75(6): 451-458.

Beerbower, A., P. L. Wu and A. Martin (1984). "Expanded solubility parameter approach. I: Naphthalene and benzoic acid in individual solvents." Journal of Pharmaceutical Sciences 73(2): 179-188.

Bengtsson, E., G. Tragardh and B. Hallstrom (1989). Enrichment of aroma compounds by pervaporation. Engineering and food, vol. 3, advanced processes. W. E. L. Spiess and H. Schubert. London, UK, Elsevier**:** 270-279.

Bhattacharya, S. and S.-T. Hwang (1997). "Concentration polarization, separation factor, and peclet number in membrane processes." Journal of Membrane Science 132(1): 73-90.

Bienvenu, F. (1995). Lavender growing for oil production. Agriculture Notes, Ovens Research Station, Myrtleford, Australia. Notes Series No AG0450.

Billmeyer, F. W. (1984). Cited in Miller-Cho, B. A. and Koenig, J. L. (2003) "Dissolution of Symmetric Diblock Copolymers with Neutral Solvents, a Selective Solvent, a Nonsolvent, and Mixtures of a Solvent and Nonsolvent Monitored by FT-IR Imaging." Macromolecules. Vol 36(13): 4851-4861

Binning, R. C. and F. E. James (1958). "Permeation. A new commercial separation tool." Petroleum Engineer 30: C14, Cited in Feng, X. and R. Y. M. Huang (1997). Liquid Separation by Membrane Pervaporation: A Review. Industrial & Engineering Chemistry Research 1936: 1048-1966.

Binning, R. C., R. J. Lee, J. F. Jennings and E. C. Martin (1961). "Separation of liquid mixtures by permeation." Industrial and Engineering Chemistry 53(1): 45-50.

Binning, R. C., J. F. Jennings and E. C. Martin (1962). Removal of water from organic chemicals. U.S. Patent 3,035,060. USA. Cited in Feng, X. and R. Y. M. Huang (1997). Liquid Separation by Membrane Pervaporation: A Review. Industrial & Engineering Chemistry Research 36: 1048-66.

Blume, I., J. G. Wijmans and R. W. Baker (1990). "The separation of dissolved organics from water by pervaporation." Journal of Membrane Science 49: 253-286.

Böddeker, K. W. and G. Bengtson (1990). "Pervaporation of low volatility aromatics from water." Journal of Membrane Science 53: 143-158.

Böddeker, K. W., G. Bengtson and H. Pingel (1990). "Pervaporation of isomeric butanols." Journal of Membrane Science 54(1-2): 1-12.

Bowen, T. C. (2003). Fundamentals and applications of pervaporation through zeolite membranes. Chemical Engineering. CO, USA, University of Colorado.

Brun, J. P., C. Larchet, R. Melet and G. Bulvestre (1985). "Modelling of the pervaporation of binary mixtures through moderately swelling, non-reacting membranes." Journal of Membrane Science 23: 257-283.

Bryant, D. L., R. D. Noble and C. A. Kovac (1997). "Facilitated transport of benzene and cyclohexane with poly(vinyl alcohol)–agno3 membranes." Journal of Membrane Science 127: 161-170.

Buckley-Smith, M. K. and C. J. Fee (2001). A technique for the selection of pervaporation membrane materials for aqueous organic separations. 8th Annual New Zealand Engineering and Technology Postgraduate Conference, University of Waikato, Hamilton, New Zealand, Campus Copy, The University of Waikato, Hamilton, New Zealand.

Buckley-Smith, M. K. and C. J. Fee (2002a). The use of hansen solubility parameters as a membrane selection procedure. The 9th Annual Engineering and Technology Postgraduate Conference, 24 St. Paul Street, Auckland City, New Zealand, AUT (Auckland University of Technology), Auckland, New Zealand.

Buckley-Smith, M. K. and C. J. Fee (2002b). The use of hansen solubility parameters for the selection of materials for organic/organic separations by pervaporation. 9th APCChE Congress and CHEMECA 2002, Christchurch, NZ, Department of Chemical and Process Engineering, University of Canterbury, Christchurch, New Zealand.

Burke, J. (1984). "Solubility parameters: Theory and application." AIC Book and Paper Group Annual 3: 13-58.

Cabasso, I., J. Jagur-Grodzinski and D. Vofsi (1974a). "Polymeric alloys of polyphosponates and acetyl cellulose. I. Sorption and diffusion of benzene and cyclohexane." Journal of Applied Polymer Science 18: 2117-2136.

Cabasso, I., J. Jagur-Grodzinski and D. Vofsi (1974b). "A study of permeation of organic solvents through polymeric membranes based on polymeric alloys of polyphosphonates and acetyl cellulose. Ii. Separation of benzene, cyclohexene, and cyclohexane." Journal of Applied Polymer Science 18(7): 2137-2147.

Cabasso, I. (1983). "Organic liquid mixtures by perselective polymer membranes. 1. Selection and characteristics of dense isotropic membranes employed in the pervaporation process." Industrial and Engineering Chemistry Product Research and Development 22: 313-319.

Cao, B. and M. A. Henson (2002). "Modeling of spiral wound pervaporation modules with application to the separation of styrene/ethylbenzene mixtures." Journal of Membrane Science 197(1-2): 117-146.

Carter, J. W. and B. Jagannadhaswamy (1964). "Separation of organic liquids by selective permeation through polymeric films." British Chemical Engineering 9(8): 523-526.

Charbit, G., F. Charbit and C. Molina (1997). "Study of mass transfer limitations in the deterpenation of waste waters by pervaporation." Journal of Chemical Engineering of Japan 30(3): 382-387.

ChemFinder. (2002). "Database searching using chemical name, cas number, molecular formula, or molecular weight." from http://www.chemfinder.com or http://chemfinder.cambridgesoft.com/.

Chen, H. L., L. G. Wu, J. Tan and C. L. Zhu (2000). "Pva membrane filled beta-cyclodextrin for separation of isomeric xylenes by pervaporation." Chemical Engineering Journal 78(2-3): 159-164.

Chen, M. S. K., G. R. Markiewicz and K. G. Venugopal (1989). "Development of membrane pervaporation trim™ process for methanol from ch3oh/mtbe/c4 mixtures." AIChE Symposium Series 85(272): 82-88.

CIPO. (2005). "Canadian intellectual property office, http://patents1.Ic.Gc.Ca/intro-e.Html." Retrieved July 2005.

Clark, G. S. (1988). "Linalool: An aroma chemical." Perfumer & Flavorist 13(Aug/Sept): 49-54.

Croll, L. M. and H. D. H. Stöver (2003). "Formation of tectocapsules by assembly and cross-linking of poly(divinylbenzene-alt-maleic anhydride) spheres at the oil-water interface." Langmuir 19(14): 5918-5922.

Cunha, V. S., R. Nobrega and A. C. Habert (1999). "Fractionation of benzene/n-hexane mixtures by pervaporation using polyurethane membranes." Brazilian Journal of Chemical Engineering 16(3): 297-308.

Cunha, V. S., M. L. L. Paredes, C. P. Borges, A. C. Habert and R. Nobrega (2002). "Removal of aromatics from multicomponent organic mixtures by pervaporation using polyurethane membranes: Experimental and modeling." Journal of Membrane Science 206(1-2): 277-290.

Dagaonkar, M. V., S. B. Sawant, J. B. Joshi and V. G. Pangarkar (1998). "Sorption and permeation of aqueous alkyl-piperazines through hydrophilic and organophilic membranes: A transport analysis." Separation Science & Technology 33(3): 311.

Darkow, R., M. Yoshikawa, T. Kitao, G. Tomaschewski and J. Schellenberg (1994). "Photomodification of a poly(acrylonitrileco-butadiene-co-styrene) containing diaryltetrazolyl groups." Journal of Polymer Science Part A: Polymer Chemistry 32(9): 1657-1664.

Deng, S., S. Sourirajan, K. Chan, B. Farnand, T. Okada and T. Matsuura (1991). "Dehydration of oil-water emulsion by pervaporation using porous hydrophilic membranes." Journal of Colloid and Interface Science 141(1): 218-225.

Drioli, E. and M. Romano (2001). "Progress and new perspectives on integrated membrane operations for sustainable industrial growth." Industrial & Engineering Chemistry Research 40(5): 1277-1300.

Dutta, B. K. and S. K. Sikdar (1991). "Separation of azeotropic organic liquid mixtures by pervaporation." AIChE Journal 37(4): 581-588.

Ellinghorst, G., A. Niemoller, H. Scholz, M. Scholz and H. Steinhauser (1987). Second International Conference on Pervaporation Processes in the Chemical Industry, San Antonio, USA, Bakish Material Corporation, New Jersey, USA.

Enneking, L., A. Heintz and R. N. Lichtenthaler (1996). "Sorption equilibria of the ternary mixture benzene/cyclohexene/cyclohexane in polyurethane- and peba-membrane polymers." Journal of Membrane Science 115(2): 161-170.

EPO. (2005). "European patent office, http://ep.Espacenet.Com/search97cgi/s97_cgi.Exe?Action=formgen&template=ep/en/advanced.Hts." Retrieved July 2005.

Farber, L. (1935). "Applications of pervaporation." Science 82(2120): 158.

Felder, R. M. and R. W. Rousseau (1986). Elementary principles of chemical processes. New York, USA, John Wiley & Sons.

Feng, X. and R. Y. M. Huang (1997). "Liquid separation by membrane pervaporation: A review." Industrial & Engineering Chemistry Research 36: 1048-1066.

Ferreira, L. B. (1998). The feasibility of pervaporation in the purification of ethanol. Process and Environmental Technology. Palmerston North, New Zealand, Massey University.

Ferreira, L., M. Kaminski, A. J. Mawson, D. J. Cleland and S. D. White (2001). "Development of a new tool for the selection of pervaporation membranes for the separation of fusel oils from ethanol/water mixtures." Journal of Membrane Science 182: 215-226.

Ferreira, L., M. Kaminski, D. J. Cleland and A. J. Mawson (2002). Pervaporation with organophilic membranes: Selectivity towards alcohols and integration with a distillation unit. 9th APCChE Congress and CHEMECA 2002, Christchurch, New Zealand, Department of Chemical and Process Engineering, University of Canterbury, N.Z.

Flanders, C. L., V. A. Tuan, R. D. Noble and J. L. Falconer (2000). "Separation of c6 isomers by vapor permeation and pervaporation through zsm-5 membranes." Journal of Membrane Science 176(1): 43-53.

Frank, T. C., J. R. Downey and S. K. Gupta (1999). Quickly screen solvents for organic solids. Chemical Engineering Progress. 95**:** 41-61.

Froehling, P. E., D. M. Koenhen, A. Bantjes and C. A. Smolders (1976). "Swelling of linear polymers in mixed swelling agents; predictability by means of solubility parameters." Polymer 17: 835-836.

Funke, H. H., A. M. Argo, J. L. Falconer and R. D. Noble (1997). "Separation of cyclic, branched and linear hydrocarbon mixtures through silicate membranes." Industrial Engineering Chemistry Research 36(1): 137 -143.

Geng, Q. and C. H. Park (1994). "Pervaporative butanol fermentation by clostridium acedobutylicum." Biotechnology and Bioengineering 43: 978-986.

George, S. C., K. Prasad, J. P. Misra and S. Thomas (1999). "Separation of alkane-acetone mixtures using styrene-butadiene rubber/natural rubber blend membranes." Journal of Applied Polymer Science 74(13): 3059-3068.

Ghosh, I., S. K. Sanyal and R. N. Mukherjea (1987). "Separation of organic liquid mixtures by pervaporation - effect of some physico-chemical parameters." J. Inst. Eng. (India), Part CH 68(1): 30-34.

Goodfellow. (2002). "Goodfellow. Serving the research needs of science and industry worldwide: Technical data." from http://www.goodfellow.com/.

Goodfellow. (2004). "Technical data - polymer properties."

Gump, C. J., R. D. Noble and J. L. Falconer (1999). "Separation of hexane isomers through nonzeolite pores in zsm-5 zeolite membranes." Industrial & Engineering Chemistry Research 38(7): 2775-2781.

Gump, C. J., X. Lin, R. D. Noble and J. L. Falconer (2000). "Experimental configuration and adsorption effects on the permeation of c4 isomers through zsm-5 zeolite membranes." Journal of Membrane Science 173(1): 35-52.

Hancock, B. C., P. York and R. C. Rowe (1997). "The use of solubility parameters in pharmaceutical dosage form design." International Journal of Pharmaceutics 148(1): 1-21.

Hansen, C. M. (1967). "I. Solvents, plasticizers, polymers, and resins - the three dimensional solubility parameter - key to paint component affinities." Journal of Paint Technology 39(505): 104-117.

Hansen, C. M. (1969). "The universality of the solubility parameter." Industrial & Engineering Chemistry Product Research and Development 8(1): 2-11.

Hansen, C. M. (2000). Hansen solubility parameters. A user's handbook. Boca Raton, Florida, USA, CRC Press LLC.

Hansen, C. M. (2004a). "50 years with solubility parameters - past and future." Progress in Organic Coatings 51(1): 77-84.

Hansen, C. M. (2004b). "Polymer additives and solubility parameters." Progress in Organic Coatings 51(2): 109-112.

Hansen, C. M. and A. L. Smith (2004). "Using hansen solubility parameters to correlate solubility of c60 fullerene in organic solvents and in polymers." Carbon 42(8-9): 1591-1597.

Hao, J., K. Tanaka, H. Kita and K. Okamoto (1997). "The pervaporation properties of sulfonyl-containing polyimide membranes to aromatic/aliphatic hydrocarbon mixtures." Journal of Membrane Science 132(1): 97-108.

He, D. (2000). A pilot pervaporation system: Design and evaluation. Materials & Process Engineering. Hamilton, New Zealand, University of Waikato.

Heintz, A. and W. Stephan (1994). "A generalized solution-diffusion model of the pervaporation process through composite membranes part i. Prediction of mixture solubilities in the dense active layer using the uniquac model." Journal of Membrane Science 89(1-2): 143-151.

Heisler, E. G., A. S. Hunter, J. Siciliano and R. H. Treadway (1956). "Solute and temperature effects in the pervaporation of aqueous alcoholic solutions." Science 124(3211): 77-79.

Hickey, P. J., F. P. Juricic and C. S. Slater (1992). "The effect of process parameters on the pervaporation of alcohols through organophilic membranes." Separation Science and Technology 27(7): 843-861.

Hildebrand, J. H. and R. L. Scott (1964). The solubility of nonelectrolytes. New York, USA, Dover Publications, Inc.

Hömmerich, U. and R. Rautenbach (1998). "Design and optimization of combined pervaporation/distillation processes for the production of mtbe." Journal of Membrane Science 146(1): 53-64.

Horst, R. and B. A. Wolf. (2005). "Thermodynamics of polymer solutions." from http://wolf.chemie.uni-mainz.de/Internet/Students/thermodynamics_of_polymer_solutions.pdf.

Hoy, K. L. (1985). Tables of solubility parameters, Solvent and Coatings Materials Research and Development Department, Union Carbide Corporation. Cited in Van Krevelen, D.W. (1990). Properties of Polymers. Their correlation with chemical structure; their numerical estimation and prediction from additive group contributions. Chapter 7 - Cohesive properties and solubility. Third, completely revised edition, Amsterdam, Netherlands: Elsevier. 189-225.

Huang, R. Y. M. and V. J. C. Lin (1968). "Separation of liquid mixtures by using polymer membranes. I. Permeation of binary organic liquid mixtures through polyethylene." Journal of Applied Polymer Science 12: 2615-2631. Cited in: Villaluenga, J. P. G. and A. Tabe-Mohammadi (2000). A review on the separation of benzene/cyclohexane mixtures by pervaporation processes. Journal of Membrane Science, 2169: 2159-2174.

Huang, R. Y. M. and J. W. Rhim (1991). Chapter 2 - separation characteristics of pervaporation membrane separation processes. Pervaporation membrane separation

processes. R. Y. M. Huang. Amsterdam, Netherlands, Elsevier Science Publishers**:** 111-181.

Huang, R. Y. M., P. Shao, G. Nawawi, X. Feng and C. M. Burns (2001). "Measurements of partition, diffusion coefficients of solvents in polymer membranes using rectangular thin-channel column inverse gas chromatography (rtccigc)." Journal of Membrane Science 188(2): 205-218.

Hubert, C., D. Fichou, P. Valat, F. Garnier and B. Villeret (1995). "A solvatochromic dye-doped polymer for detection of polar additives in hydrocarbon blends." Polymer 36(13): 2663-2666.

Hwang, S.-T. and K. Kammermeyer (1984). Chapter vii - pervaporation. *In* membrane separations. New York, Wiley.

Inui, K., T. Miyata and T. Uragami (1997a). "Permeation and separation of benzene/cyclohexane mixtures through liquid-crystalline polymer membranes." Journal of Polymer Science Part B: Polymer Physics 35(4): 699-707.

Inui, K., H. Okumura, T. Miyata and T.-I. Uragami (1997b). "Permeation and separation of benzene/cyclohexane mixtures through cross-linked poly(alkyl methacrylate) membranes." Journal of Membrane Science 132(2): 193-202.

Inui, K., H. Okumura, T. Miyata and T. Uragami (1997c). "Characteristics of permeation and separation of dimethyl acrylamide–methyl methacrylate random and graft copolymer membranes for a benzene/cyclohexane mixture." Polymer Bulletin 39: 733-740.

Inui, K., T. Miyata and T. Uragami (1998a). "Permeation and separation of binary organic mixtures through a liquid-crystalline polymer membrane." Macromolecular Chemistry and Physics 199(4): 589-595.

Inui, K., K. Tsukamoto, T. Miyata and T. Uragami (1998b). "Permeation and separation of a benzene/cyclohexane mixture through benzoylchitosan membranes." Journal of Membrane Science 138(1): 67-75.

Inui, K., K. Noguchi, T. Miyata and T. Uragami (1999). "Pervaporation characteristics of methyl methacrylate-methacrylic acid copolymer membranes ionically crosslinked with metal ions for a benzene/cyclohexane mixture." Journal of Applied Polymer Science 71(2): 233-241.

Ishida, M. and N. Nakagawa (1985). "Exergy analysis of a pervaporation system and its combination with a distillation column based on an energy utilization diagram." Journal of Membrane Science 24: 271-283.

Ishihara, K. and K. Matsui (1987). "Pervaporation of ethanol-water mixture through composite membranes composed of styrene-fluoroalkyl acrylate graft copolymers and cross-linked polydimethylsiloxane membrane." Journal of Applied Polymer Science 34: 437-440.

Jiang, J.-S., D. B. Greenberg and J. R. Fried (1997). "Pervaporation of methanol from a triglyme solution using a nafion membrane: 2. Concentration polarization." Journal of Membrane Science 132(2): 263-271.

Johnson, T. and S. Thomas (1999). "Pervaporation of acetone-chlorinated hydrocarbon mixtures through polymer blend membranes of natural rubber and epoxidized natural rubber." Journal of Applied Polymer Science 71(14): 2365-2379.

Jonquières, A., D. Roizard, J. Cuny and P. Lochon (1996). "Solubility and polarity parameters for assessing pervaporation and sorption properties. A critical comparison for ternary

systems alcohol/ether/polyurethaneimide." Journal of Membrane Science 121(1): 117-133.

Jonquières, A., R. Clément, P. Lochon, J. Néel, M. Dresch and B. Chrétien (2002). "Industrial state-of-the-art of pervaporation and vapour permeation in the western countries." Journal of Membrane Science 206(1-2): 87-117.

Jou, J.-D., W. Yoshida and Y. Cohen (1999). "A novel ceramic-supported polymer membrane for pervaporation of dilute volatile organic compounds." Journal of Membrane Science 162(1-2): 269-284.

Kanani, D. M., B. P. Nikhade, P. Balakrishnan, G. Singh and V. G. Pangarkar (2003). "Recovery of valuable tea aroma components by pervaporation." Industrial & Engineering Chemistry Research 42(26): 6924-6932.

Kao, S. T., F. J. Wang and S. J. Lue (2002). "Sorption, diffusion, and pervaporation of benzene/cyclohexane mixtures on silver-nafion membranes." Desalination 149(1-3): 35-40.

Karlsson, H. O. E. and G. Trägårdh (1993a). "Aroma compound recovery with pervaporation - feed flow effects." Journal of Membrane Science 81: 163-171.

Karlsson, H. O. E. and G. Trägårdh (1993b). "Pervaporation of dilute organic-waters mixtures. A literature review on modelling studies and applications to aroma compound recovery." Journal of Membrane Science 76: 121-146.

Karlsson, H. O. E. and G. Trägårdh (1994). Pervaporation of aroma compounds: Models and experiments. Food Engineering, Lund University, Sweden.

Karlsson, H. O. E. and G. Trägårdh (1996). "Applications of pervaporation in food processing." Trends in Food Science & Technology 7(March): 78-83.

Kim, S.-G., G.-T. Lim, J. Jegal and K.-H. Lee (2000). "Pervaporation separation of mtbe (methyl tert-butyl ether) and methanol mixtures through polyion complex composite membranes consisting of sodium alginate/chitosan." Journal of Membrane Science 174(1): 1-15.

Knight, K. F., A. Duggal, R. A. Shelden and E. V. Thomson (1986). "Dependence of diffusive permeation rates on upstream and downstream pressures. V. Experimental results for the hexane-heptane (ideal) and toluene-ethanol (nonideal)." Journal of Membrane Science 26: 31-50.

Kober, P. A. (1917). "Pervaporation, perstillation and percrystallization." Journal of the American Chemical Society 39(5): 944-948.

Koenhen, D. M. and C. A. Smolders (1975). "The determination of solubility parameters of solvents and polymers by means of correlations with other physical quantities." Journal of Applied Polymer Science 19: 1163-1179.

Koenitzer, B. A. (1990). Polyurethane-imide membranes and their use for separation of aromatics from non-aromatics, us patent 4,929,358. USA, Exxon Research and Engg. Co.,**:** Cited in Smitha, B., D. Suhanya, *et al.* (2004). Separation of organic-organic mixtures by pervaporation - a review. Journal of Membrane Science 2241(2001): 2001-2021.

Koops, G. H. and C. A. Smolders (1991). Chapter 5 - estimation and evaluation of polymeric materials for pervaporation membranes. Pervaporation membrane separation processes. R. Y. M. Huang. Amsterdam, The Netherlands, Elsevier Science Publishers**:** 253-278.

Kosower, E. M. (1958). "The effect of solvent spectra. I. A new empirical measure of solvent polarity: Z-values." Journal of the American Chemical Society 80(13): 3253-3270.

Kucharski, M. and J. Stelmaszek (1967). "Separation of liquid mixture by permeation." International Journal of Chemical Engineering 7: 618-622.

Lee, Y. M., D. Bourgeois and G. Belfort (1987). Selection of polymer membrane materials for pervaporation. Proceedings of the 2nd International Conference on Pervaporation Processes in the Chemical Industry, San Antonio, Texas.

Lee, Y. M., D. Bourgeois and G. Belfort (1989). "Sorption, diffusion and pervaporation of organics in polymer membranes." Journal of Membrane Science 44: 161-181.

Lipnizki, F., S. Hausmanns, P. K. Ten, R. W. Field and G. Laufenberg (1999). "Organophilic pervaporation: Prospects and performance." Chemical Engineering Journal 73: 113-129.

Lloyd, D. R. and T. B. Meluch (1985). "Selection and evaluation of membrane materials for liquid separations." American Chemical Society symposium series. Materials Science of Synthetic Membranes. 269: 49-79.

Lomascolo, A., C. Stentelaire, M. Asther and L. Lesage-Meessen (1999). "Basidiomycetes as new biotechnological tools to generate natural aromatic flavours for the food industry." Trends in Biotechnology 17(7): 282-289.

Lotus Oils. (2005). "Retail product & price list." Retrieved 24 August, 2005, 2005, from http://www.lotusoils.co.nz/Retail%20Price%20List.htm.

Lue, S. J., F. J. Wang and S.-Y. Hsiaw (2004). "Pervaporation of benzene/cyclohexane mixtures using ion-exchange membrane containing copper ions." Journal of Membrane Science 240(1-2): 149-158.

Luo, G. S., M. Niang and P. Schaetzel (1997). "Pervaporation separation of etbe/etoh mixtures with blended membranes." Journal of Membrane Science 125(2): 237-244.

Macrogalleria. (1996). from http://www.pslc.ws/macrog/index.htm.

Mandal, S. and V. G. Pangarkar (2002a). "Pervaporative dehydration of 1-methoxy propanol with acrylonitrile based co-polymer membranes prepared through emulsion polymerization: A solubility parameter approach and study of structural impact." Journal of Membrane Science 209(1): 53-66.

Mandal, S. and V. G. Pangarkar (2002b). "Separation of methanol–benzene and methanol–toluene mixtures by pervaporation: Effects of thermodynamics and structural phenomenon." Journal of Membrane Science 201(1-2): 175-190.

Mandal, S. and V. G. Pangarkar (2003). "Effect of membrane morphology in pervaporative separation of isopropyl alcohol-aromatic mixtures - a thermodynamic approach to membrane selection." Journal of Applied Polymer Science 90(14): 3912-3921.

Mangaraj, D., S. Patra and S. Rashid (1963a). "Cohesive energy densities of high polymers part 2. Cohesive energy densities of poly-acrylates and polymethacrylates from swelling measurements." Makromolekulare Chemie 65: 39-46.

Mangaraj, D., S. Patra and S. B. Rath (1963b). "Cohesive energy densities of high polymers part 4. C.E.D. Of polyacrylates." Makromolekulare Chemie 67: 84-89.

Martin, E. C. and J. T. Kelly (1961). Us patent #2,981,730 and #3,150,456.

Massey, B. S. (1979). Mechanics of fluids, 4th edition. New York, USA, Van Nostrand Reinhold Company.

Mastelic, J., M. Milos, D. Kustrak and A. Radonic (2000). "Essential oil and glycosidically bound volatile compounds from the needles of common juniper (*juniperus communis* l.)." Croatica Chemica Acta. 73(2): 585-593.

Mathias, L. J. (2004). "The Macrogalleria." Department of Polymer Science, The University of Southern Mississippi, USA. http://www.psrc.usm.edu/macrog/index.htm

Mathys, R. G., W. Heinzelmann and B. Witholt (1997). "Separation of higher molecular weight organic compounds by pervaporation." Chemical Engineering Journal 67: 191-197.

Matsui, S. and D. R. Paul (2002). "Pervaporation separation of aromatic/aliphatic hydrocarbons by crosslinked poly(methyl acrylate-co- acrylic acid) membranes." Journal of Membrane Science 195(2): 229-245.

Matsui, S. and D. R. Paul (2003). "Pervaporation separation of aromatic/aliphatic hydrocarbons by a series of ionically crosslinked poly(n-alkyl acrylate) membranes." Journal of Membrane Science 213(1-2): 67-83.

MatWeb. (2002). "Plastics abbreviations and acronyms." from http://www.matweb.com/abbreviations.htm.

McCandless, F. P., D. P. Alzheimer and R. B. Hartman (1974). "Solvent membrane separation of benzene and cyclohexane." Industrial & Engineering Chemistry Process Design and Development 13(3): 310-312.

Michaels, A. S., R. F. Baddour, H. J. Bixler and C. Y. Choo (1962). "Conditioned polyethylene as a permselective membrane. Separation of isomeric xylenes." Industrial & Engineering Chemistry., Process Design and Development 1(1): 14-25.

Miranda, J. M. and J. B. L. M. Campos (1999). "Impinging jets confined by a conical wall: Laminar flow predictions." AIChE Journal 45(11): 2273-2285.

Miranda, J. M. and J. B. L. M. Campos (2001a). "Concentration polarization in a membrane placed under an impinging jet confined by a conical wall – a numerical approach." Journal of Membrane Science 182(1-2): 257-270.

Miranda, J. M. and J. B. L. M. Campos (2001b). "Impinging jets confined by a conical wall: High schmidt mass transfer predictions in laminar flow." International Journal of Heat and Mass Transfer 44(7): 1269–1284.

Molina, C., A. Steinchen, G. Charbit and F. Charbit (1997). "Model for pervaporation: Application to ethanolic solutions of aroma." Journal of Membrane Science 132: 119-129.

Mulder, M. H. V., F. Kruitz and C. A. Smolders (1982). "Separation of isomeric xylenes by pervaporation through cellulose ester membranes." Journal of Membrane Science 11: 349-363.

Mulder, M. H. V., T. Franken and C. A. Smolders (1985). "Preferential sorption versus preferential permeability in pervaporation." Journal of Membrane Science 22: 155-173.

Mulder, M. H. V. and C. A. Smolders (1986). "Pervaporation, solubility aspects of the solution diffusion model." Separation and Purification Methods 15(1): 1-19.

Mulder, M. (1991). Basic principles of membrane technology. Dordrecht, Netherlands, Kluwer Academic Publishers.

Mulder, M. H. V., J. O. Hendrickman, H. Hegeman and C. A. Smolders (1983). "Ethanol-water separation by pervaporation." Journal of Membrane Science 16: 269-284, Cited in Smitha, B., D. Suhanya, et al. (2004). Separation of organic-organic mixtures by pervaporation - a review. Journal of Membrane Science 2241(2001): 2001-2021.

Nair, S., Z. Lai, V. Nikolakis, X. George, B. Griselda and M. Tsapatsis (2001). "Separation of close-boiling hydrocarbon mixtures by mfi and fau membranes made by secondary growth." Microporous and Mesoporous Materials 48(1-3): 219-228.

Néel, J. (1991). Chapter 1 - introduction to pervaporation. Pervaporation membrane separation processes. R. Y. M. Huang. Amsterdam, Netherlands, Elsevier Science Publishers**:** 1-109.

Nijhuis, H. H., M. H. V. Mulder and C. A. Smolders (1993). "Selection of elastomeric membranes for the removal of volatile organics from water." Journal of Applied Polymer Science 47(12): 2227-2243.

Nikolakis, V., G. Xomeritakis, A. Abibi, M. Dickson, M. Tsapatsis and D. G. Vlachos (2001). "Growth of a faujasite-type zeolite membrane and its application in the separation of saturated/unsaturated hydrocarbon mixtures." Journal of Membrane Science 184(2): 209-219.

Orme, C. J., M. K. Harrup, J. D. McCoy, D. H. Weinkauf and F. F. Stewart (2002). "Pervaporation of water–dye, alcohol–dye, and water–alcohol mixtures using a polyphosphazene membrane." Journal of Membrane Science 197(1-2): 89-101.

Pal, S. M. and V. G. Pangarkar (2005). "Acrylonitrile-based copolymer membranes for the separation of methanol from a methanol-toluene mixture through pervaporation." Journal of Applied Polymer Science 96(1): 243-252.

Paris, J., C. Molina-Jouve, D. Nuel, P. Moulin and F. Charbit (2004). "Enantioenrichment by pervaporation." Journal of Membrane Science 237(1-2): 9-14.

Park, H. C., R. M. Meertens, M. H. V. Mulder and C. A. Smolders (1994). "Pervaporation of alcohol-toluene mixtures through polymer blend membranes of poly(acrylic acid) and poly(vinyl alcohol)." Journal of Membrane Science 90(3): 265-274.

Park, H. C., R. M. Meertens and M. H. V. Mulder (1998). "Sorption of alcohol-toluene mixtures in poly(acrylic acid)-poly(vinyl alcohol) blend membranes and its role on pervaporation." Industrial & Engineering Chemistry Research 37(11): 4408-4417.

Peng, M. (2004). Modeling mass transfer in volatile organic compounds separation by pervaporation (pv) and application of pv in blueberry aroma recovery. New Brunswick, NJ, USA, Rutgers - The State University of New Jersey.

Peters, M. S. and K. D. Timmerhaus (1991). Plant design and economics for chemical engineers. New York, USA, McGraw-Hill, Inc.

Plastics USA. (2005). "Polymerweb. Technical information on plastic materials: Polymer tradenames."

Porter, N. G. (2001). Essential oils and their production. www.crop.cri.nz, New Zealand Institute for Crop & Food Research Ltd. Broad sheet # 39.

Price, G. J. and I. M. Shillcock (2002). "Inverse gas chromatographic measurement of solubility parameters in liquid crystalline systems." Journal of Chromatography A, 964(1-2): 199-204.

Psaume, R., P. Aptel, Y. Aurelle, J. C. Mora and J. L. Bersillon (1988). "Pervaporation: Importance of concentration polarization in the extraction of trace organics from water." Journal of Membrane Science 36: 373-384.

Qariouh, H., R. Schué, F. Schué and C. Bailly (1999). "Sorption, diffusion and pervaporation of water/ethanol mixtures in polyetherimide membranes." Polymer International 48(3): 171-180.

Rapin, J. L. (1988). The betheniville pervaporation unit: The first large-scale productive plant forthe dehydration of ethanol. Proceedings of the 3rd International Conference on Pervaporation Processes, Bakish Materials Corporation, Englewood, USA.

Rautenbach, R. and R. Albrecht (1980). "Separation of organic binary mixtures by pervaporation." Journal of Membrane Science 7: 203-223.

Ravindra, R., S. Sridhar, A. A. Khan and A. K. Rao (2000). "Pervaporation of water, hydrazine and monomethylhydrazine using ethylcellulose membranes." Polymer 41(8): 2795-2806.

Ray, S. K., S. B. Sawant, J. B. Joshi and V. G. Pangarkar (1997). "Development of new synthetic membranes for separation of benzene-cyclohexane mixtures by pervaporation: A solubility parameter approach." Industrial & Engineering Chemistry Research 36(12): 5265-5276.

Ray, S. K., S. B. Sawant, J. B. Joshi and V. G. Pangarkar (1999a). "Methanol selective membranes for separation of methanol-ethylene glycol mixtures by pervaporation." Journal of Membrane Science 154: 1-13.

Ray, S. K., S. B. Sawant and V. G. Pangarkar (1999b). "Development of methanol selective membranes for separation of methanol-methyl tertiary butyl ether mixtures by pervaporation." Journal of Applied Polymer Science 74(11): 2645-2659.

Reichardt, C. (1988). Solvents and solvent effects in organic chemistry. Weinheim, Federal Republic of Germany, VHC Verlagsgesellschaft mbH.

Ren, J., C. Staudt-Bickel and R. N. Lichtenthaler (2001). "Separation of aromatics/aliphatics with crosslinked 6fda-based copolyimides." Separation and Purification Technology 22-23(1): 31-43.

Rey-Mermet, C., P. Ruelle, H. Nam-Tram, M. Buchmann and U. W. Kesselring (1991). "Significance of partial and total cohesion parameters of pharmaceutical solids determined from dissolution calorimetric measurements." Pharmaceutical Research 8(5): 636-642.

Roberts, S. L., C. A. Koval and R. D. Noble (2000). "Strategy for selection of composite membrane materials." Industrial & Engineering Chemistry Research 39(6): 1673-1682.

Robello, D. (2004). Lecture Notes Chem424 - Synthetic Polymer Chemistry, Class 3 - Step Polymerization III, Department of Chemistry, University of Rochester, NY, USA. http://www.chem.rochester.edu/~chem424/class3.htm

Roizard, D., Jonquières, C. Léger, I. Noezar, L. Perrin, Q. T. Nguyen, R. Clément, H. Lenda, P. Lochon and J. Néel (1999). "Alcohol/ether separation by pervaporation. High performance membrane design." Separation Science and Technology 34(3): 369 - 390.

Roizard, D., A. Nilly and P. Lochon (2001). "Preparation and study of crosslinked polyurethane films to fractionate toluene-n-heptane mixtures by pervaporation." Separation & Purification Technology 22(3): 45-52.

Rose-Pehrsson, S. L. and J. H. Krech (1995). Solvatochromic dyes incorporated into polymer matrices for the optical detection of volatile organic compounds. Abstract # 1003. 188th meeting of the electrochemical society, Chicago, Illinois, USA.

Rudolf (1995) Cited in Hancock, B. C., P. York and R. C. Rowe (1997). "The use of solubility parameters in pharmaceutical dosage form design." International Journal of Pharmaceutics 148(1): 1-21.

Runham, S. R. (1996). An updated review of the potential uses of plants grown for extracts including essential oils and factors affecting their yield and composition. Mepal, UK, ADAS Arthur Rickwood**:** 75.

Sampranpiboon, P., R. Jiraratananon, D. Uttapap, X. Feng and R. Y. M. Huang (2000). "Separation of aroma compounds from aqueous solutions by pervaporation using polyoctylmethyl siloxane (poms) and polydimethyl siloxane (pdms) membranes." Journal of Membrane Science 174(1): 55-65.

Schäfer, T., G. Bengtson, H. Pingel, K. W. Böddeker and J. P. S. G. Crespo (1999). "Recovery of aroma compounds from a wine-must fermentation by organophilic pervaporation." Biotechnology and Bioengineering 62(4): 412-421.

Schleiffelder, M. and S. B. Claudia (2001). "Crosslinkable copolyimides for the membrane-based separation of p-/o-xylene mixtures." Reactive and Functional Polymers 49(3): 205-213.

Schrodt, V. N., R. F. Sweeny and A. Rose (1961). Membrane permeation of liquids. Symposium on Less Common Separation Methods in Petroleum Industry, St. Louis, USA, Division of Petroleum Chemistry, American Chemical Society.

Seymour, R. B. and C. E. Carraher (1988). Polymer chemistry: An introduction. New York, USA, Marcel Dekker, Inc.

Sferrazza, R. A. and C. H. Gooding (1988). Prediction of sorption selectivity in pervaporation membranes. Proc. Int. Conf. Pervaporation Processes Chem. Ind., 3rd., Bakish Mater. Corp., Englewood, N.J., USA.

Shah, V. and C. Bartels (1991). Engineering considerations in pervaporation applications. Proceedings of the Fifth International Conference on Pervaporation Processes in the Chemical Industry, Heidelberg, Germany, Bakish Materials Corporation.

Shao, P. (2003). Pervaporation dehydration membranes based on chemically modified poly(ether ether ketone). Waterloo, Canada, University of Waterloo.

Sierra Instruments Inc. (1994). Sierra 820 series top-trak mass flow meters instruction manual, Part Number IM-82, Revision C 06-99, Monterey, CA, USA. http://www.sierrainstruments.com.

Singleton, W. S., T. L. Ward and F. G. Dollear (1950). "Physical properties of fatty acids. I. Some dilatometric and thermal properties of stearic acid in two polymorphic forms." The Journal of the American Oil Chemists' Society. 27: 143-146.

Small, P. A. (1953). "Some factors affecting the solubility of polymers." Journal of Applied Chemistry 3: 71-80.

Smitha, B., D. Suhanya, S. Sridhar and M. Ramakrishna (2004). "Separation of organic-organic mixtures by pervaporation - a review." Journal of Membrane Science 241(1): 1-21.

Souchon, I., F. X. Pierre, V. Athes-Dutour and M. Marin (2002). "Pervaporation as a deodorization process applied to food industry effluents: Recovery and valorisation of aroma compounds from cauliflower blanching water." Desalination 148(1-3): 79-85.

Spitzen, J. W. F., E. Elsinghorst, M. H. V. Mulder and C. A. Smolders (1987). Solution-diffusion aspects in the separation of ethanol/wter mixtures with pva membranes. Proceedings of the Second International Conference on Pervaporation Processes in the Chemical Industry, San Antonio, Texas, USA, Bakish Materials Corporation, Englewood, New Jersey.

Sridhar, S., R. Ravindra and A. A. Khan (2000). "Recovery of monomethylhydrazine liquid propellant by pervaporation technique." Industrial & Engineering Chemistry Research 39(7): 2485-2490.

Srikanth, G. (2000). "Membrane separation processes - technology and business opportunities." Retrieved March 2005, 2005, from http://www.tifac.org.in/news/memb.htm.

Stavroudis, C. and S. Blank (1989). "Solvents & sensibility." Western Association for Art Conservation (WAAC) Newsletter 11(2): 2-10.

Sulzer ChemTech. (2005). "Pervaporation systems." Retrieved March 2005, 2005, from http://www.sulzerchemtech.com/eprise/SulzerChemtech/Sites/products_services/pervap.html.

Sun, F. and E. Ruckenstein (1995). "Sorption and pervaporation of benzene-cyclohexane mixtures through composite membranes prepared via concentrated emulsion polymerization." Journal of Membrane Science 99(3): 273-284.

Suzuki, F. and K. Onozato (1982). "Pervaporation of benzene-cyclohexane mixture by poly(-methyl l-glutamate) membrane and synergetic effect of their mixture on diffusion rate." Journal of Applied Polymer Science 27(11): 4229-4238.

Sweeny, R. F. and A. Rose (1965). "Factors determining rates and separation in barrier membrane permeation." Industrial & Engineering Chemistry Product Research and Development 4(4): 248-251.

Tanihara, N., K. Tanaka, H. Kita and K.-I. Okamoto (1994). "Pervaporation of organic liquid mixtures through membranes of polyimides containing methyl-substituted phenylenediamine moieties." Journal of Membrane Science 95(2): 161-169.

Tanihara, N., N. Umeo, T. Kawabata, K. Tanaka, H. Kita and K. Okamoto (1995). "Pervaporation of organic liquid mixtures through poly(ether imide) segmented copolymer membranes." Journal of Membrane Science 104: 181-192.

Terada, J., T. Hohjoh, S. Yoshimasu, M. Ikemi and I. Shinohara (1982). "Separation of benzene-cyclohexane azeotropic mixture through polymeric membranes with microphase separated structures." Polymer Journal 14(5): 347-353.

Ulbricht, M. and H. Schwarz (1997). "Novel high performance photo-graft composite membranes for separation of organic liquids by pervaporation." Journal of Membrane Science 136: 25-33.

Unnikrishnan, G., P. H. Gedam, V. S. K. Prasad and S. Thomas (1997). "Separation of n-hexane/acetone mixtures by pervaporation using natural rubber membranes." Journal of Applied Polymer Science 64(13): 2597-2603.

Uragami, T., K. Tsukamoto, K. Inui and T. Miyata (1998). "Pervaporation characteristics of a benzoylchitosan membrane for benzene-cyclohexane mixtures." Macromolecular Chemistry and Physics 199(1): 49-54.

USPTO. (2005). "United states patent and trademark office." Retrieved July 2005, from http://www.uspto.gov/patft/.

Van Krevelen, D. W. and P. J. Hoftyzer (1976). Properties of polymers: Their estimation and correlation with chemical structure. Amsterdam, Netherlands, Elsevier. Cited in Van Krevelen, D.W. (1990). Properties of Polymers. Their correlation with chemical structure; their numerical estimation and prediction from additive group contributions. Chapter 7 - Cohesive properties and solubility. Third, completely revised edition, Amsterdam, Netherlands: Elsevier. 189-225.

Van Krevelen, D. W. (1990). Properties of polymers. Their correlation with chemical structure; their numerical estimation and prediction from additive group contributions. Chapter 7 - cohesive properties and solubility. Amsterdam, Netherlands, Elsevier.

Vaz Freire, L. M. T., A. M. C. Freitas and A. M. Relva (2001). "Optimization of solid phase microextraction analysis of aroma compounds in a portuguese muscatel wine must." Journal of Microcolumn Separations 13(6): 236-242.

Villaluenga, J. P. G. and A. Tabe-Mohammadi (2000). "A review on the separation of benzene/cyclohexane mixtures by pervaporation processes." Journal of Membrane Science 169: 159-174.

Villaluenga, J. P. G., M. Khayet, P. Godino, B. Seoane and J. I. Mengual (2003). "Pervaporation of toluene/alcohol mixtures through a coextruded linear low-density polyethylene membrane." Industrial & Engineering Chemistry Research 42(2): 386-391.

Voilley, A., B. Schmidt, D. Simatos and S. Baudron (1988). Extraction of aroma compounds by the pervaporation technique. Proceedings of Third International Conference on Pervaporaiton Processes in the Chemical Industry, Bakish Materials Corporation, Englewood, NJ.

Wang, H., X. Lin, K. Tanaka, H. Kita and K. Okamoto (1998). "Preparation of plasma-grafted polymer membranes and their morphology and pervaporation properties toward benzene/cyclohexane mixtures." Journal of Polymer Science Part A: Polymer Chemistry 36: 2247-2259.

Wang, H., K. Tanaka, H. Kita and K. Okamoto (1999). "Pervaporation of aromatic/non-aromatic hydrocarbon mixtures through plasma-grafted membranes." Journal of Membrane Science 154: 221-228.

Wang, H. Y., T. Ugomori, K. Tanaka, H. Kita, K. Okamoto and Y. Suma (2000). "Sorption and pervaporation properties of sulfonyl-containing polyimide membrane to aromatic/non-aromatic hydrocarbon mixtures." Journal of Polymer Science Part B: Polymer Physics 38(22): 2954-2964.

Wang, Y.-C., C.-L. Li, J. Huang, C. Lin, K.-R. Lee, D.-J. Liaw and J.-Y. Lai (2001). "Pervaporation of benzene/cyclohexane mixtures through aromatic polyamide membranes." Journal of Membrane Science 185(2): 193-200.

Wang, Y., S. Hirakawa, H. Wang, K. Tanaka, H. Kita and K.-I. Okamoto (2002). "Pervaporation properties to aromatic/non-aromatic hydrocarbon mixtures of cross-linked membranes of copoly(methacrylates) with pendant phosphate and carbamoylphosphonate groups." Journal of Membrane Science 199(1-2): 13-27.

Weast, R. C., Ed. (1988). Crc handbook of chemistry and physics. Boca Raton, Florida, USA, CRC Press, Inc.

Wegner, K., J. Dong and Y. S. Lin (1999). "Polycrystalline mfi zeolite membranes: Xylene pervaporation and its implication on membrane microstructure." Journal of Membrane Science 158: 17-27.

Wenzlaff, A., K. W. Böddeker and K. Hattenbach (1985). "Pervaporation of water-ethanol through ion exchange membranes." Journal of Membrane Science 22(2-3): 333-344.

Wessling, M., U. Werner and S. T. Hwang (1991). "Pervaporation of aromatic c8-isomers." Journal of Membrane Science 57(2-3): 257-270.

Wijmans, J. G. and R. W. Baker (1995). "The solution-diffusion model: A review." Journal of Membrane Science 107: 1-21.

Wijmans, J. G., A. L. Athayde, R. Daniels, J. H. Ly, H. D. Kamaruddin and I. Pinnau (1996). "The role of boundary layers in the removal of volatile organic compounds from water by pervaporation." Journal of Membrane Science 109(1): 135-146.

Yamaguchi, T., S. Nakao and S. Kimura (1992). "Solubility and pervaporation properties of the filling polymerised membrane prepared by plasma-graft polymerisation for pervaporation of organic-liquid mixtures." Ind. Eng. Chem. Res. 31: 1914-1919.

Yamaguchi, T., S. Nakao and S. Kimura (1993). "Design of pervaporation membrane of organic-liquid separation based on solubility control by plasma-graft filling polymerization technique." Ind. Eng. Chem. Res. 32(5): 848-853.

Yamasaki, A., T. Shinbo and K. Mizoguchi (1997). "Pervaporation of benzene/cyclohexane and benzene/n-hexane mixtures through pva membrane." Journal of Applied Polymer Science 64(6): 1061-1065.

Yanagishita, H., D. Kitamoto, T. Ikegami, H. Negishi, A. Endo, K. Haraya, T. Nakane, N. Hanai, J. Arai, H. Matsuda, Y. Idemoto and N. Koura (2002). "Preparation of photo-induced graft filling polymerized membranes for pervaporation using polyimide with benzophenone structure." Journal of Membrane Science 203(1-2): 191-199.

Yeom, C. K., J. M. Dickson and M. A. Brook (1996). "A characterization of pdms pervaporation membranes for the removal of trace organic from water." Korean Journal of Chemical Engineering 13(5): 482-488.

Yoshida, W. and Y. Cohen (2003). "Ceramic-supported polymer membranes for pervaporation of binary organic/organic mixtures." Journal of Membrane Science 213(1-2): 145-157.

Yoshikawa, M., N. Ogata and T. Shimidzu (1986). "Polymer membrane as a reaction field iii. Effect of membrane polarity on selective separation of a water-ethanol binary mixture through synthetic polymer membranes." Journal of Membrane Science 26: 107.

Young, C. A. J. (1973). "The chemical and petrochemical industries." Philosophical Transactions of the Royal Society of London. Series A, Mathematical and Physical Sciences 275(1250): 329-355.

Zellers, E. T. (1993). "Three-dimensional solubility parameters and chemical protective clothing permeation. I modelling the solubility of organic solvents in viton ® gloves." Journal of Applied Polymer Science 50: 513.

Zellers, E. T., D. H. Anna, R. Sulewski and X. Wei (1996a). "Critical analysis of the graphical determination of hansen's solubility parameters for lightly crosslinked polymers." Journal of Applied Polymer Science 62(12): 2069-2080.

Zellers, E. T., D. H. Anna, R. Sulewski and X. Wei (1996b). "Improved methods for the determination of hansen's solubility parameters and the estimation of solvent uptake for lightly crosslinked polymers." Journal of Applied Polymer Science 62(12): 2081-2096.

Zhang, S. and E. Drioli (1995). "Pervaporation membranes." Separation Science and Technology 30(1): 1-31.

Appendix 1

Data analysis

Calculation of Concentration

Liquid samples of linalool, injected manually into the GC-FID were correlated directly to the peak area of the internal standard (Octanol) in order to calculate concentration.

Table A1:2. Peak Area of manually injected liquid solution components.

Conc. (%v/v)	Octanol	Linalool	Linalyl acetate
0.1	2362.4	52.2	14.4
1.0	835.6	253.4	204.3
4.0	2631.4	2503.1	2382.6
5.0	2915.6	3200.7	3199.9
6.0	2589.99	3445.4	3539.2
10.0	2947.9	6175.4	6709.8

Table A1:3. Physical properties of permeate components (ChemFinder, 2002).

Material	Density (g/cm^3)	Molecular weight (g/mol)
Ethanol (EtOH)	0.789	46.0688
Linalool (lool)	0.868	154.2516
Linalyl acetate (lyl)	0.901	196.2888

Concentration of standard solutions were calculated using the following equation, using volumes pipetted (Gilson: 10 μL, 250 μL, 1000 μL), density and molecular weight (Table A1:3):

$$Conc.(mol.L^{-1}) = \frac{\left(Conc.(v/v) * Density(g.mL^{-1}) * 1000(mL.L^{-1})\right)}{\left(Mol.wt.(g.mol^{-1})\right)} \qquad \text{(A1:1)}$$

Table A1:4 Calculation of linear relationship between organic concentration and internal standard peak areas.

Conc. (%v/v)	Conc. Lool	Ratio	Conc. Lyl	Ratio

	(mol/L)	(Lool:Oct)	(mol/L)	(Lyl:Oct)
0.1	0.0056	0.022	0.0046	0.006
1.0	0.0563	0.303	0.0459	0.244
4.0	0.2251	0.951	0.1836	0.905
5.0	0.2814	1.098	0.2295	1.098
6.0	0.3376	1.330	0.2754	1.366
10.0	0.5627	2.095	0.4590	2.276

The peak area ratio was then calculated between the organic component and the internal standard (Table A1:4) and displayed in Figure A1:12.

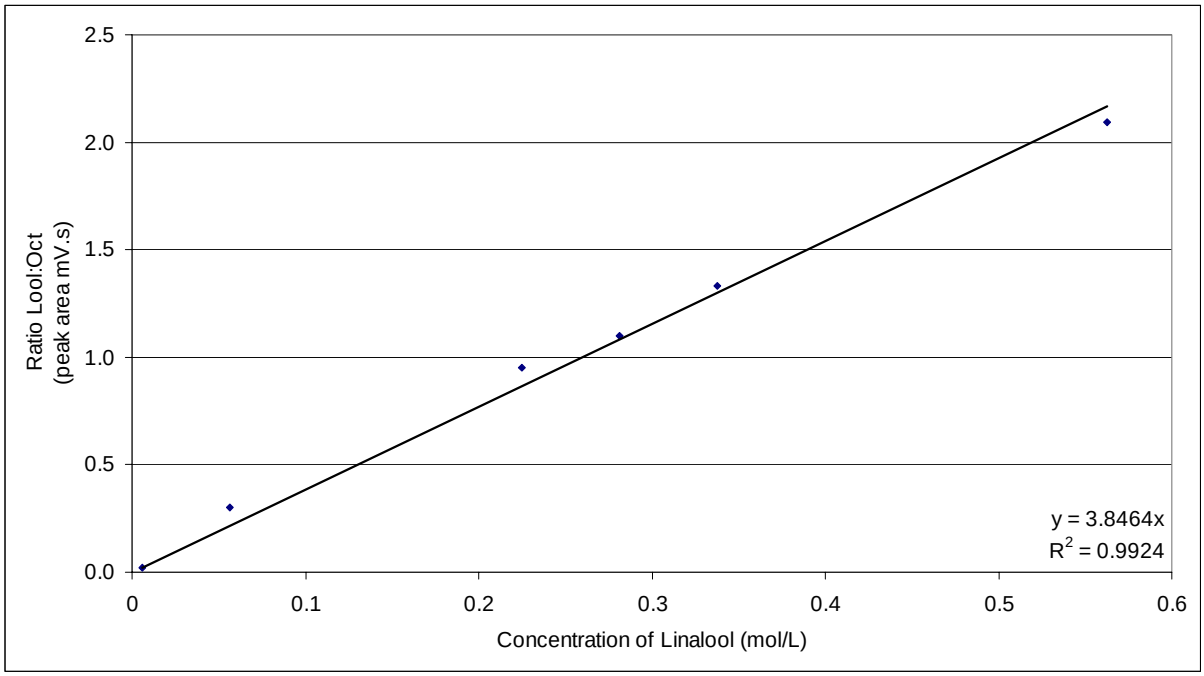

Figure A1:12 Correlation between Linalool and internal standard, Octanol (5% v/v).

Thus linalool concentrations were calculated in the same manner using the correlation indicated in Figure A1:12 above to give the equation:

$$Concentration_{lool}(mol/L) = \frac{Ratio_{lool:oct}}{3.8464} \qquad \text{(A1:2)}$$

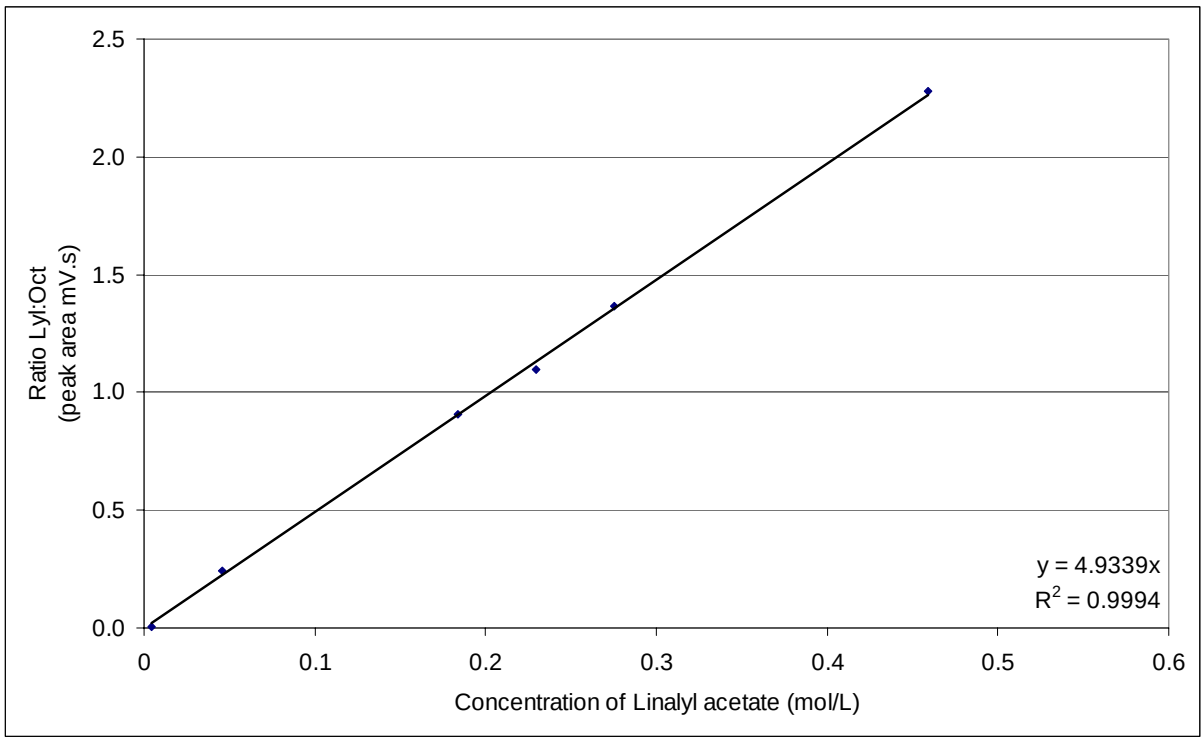

Figure A1:13 Correlation between Linalyl acetate and internal standard, Octanol (5% v/v).

The correlation sown in Figure A1:13 gives the function for calculating concentration of linalyl acetate from GC-FID peak area:

$$Concentration_{lyl}(mol/L) = \frac{Ratio_{lyl:oct}}{4.9339}$$

Table A1:5 Calculation of organic concentration from ratio with internal standard.

Starting Feed Concentration	Peak Area (mV.s)	Ratio (org:oct)	Conc. (mol/L)	Conc. (%v/v)
Octanol	2457.8			
Linalool	3793.0	1.54	0.4012	7.13%
Linalyl acetate	3522.9	1.43	0.2905	6.33%

Thus for any given sample, the Ratio of component to octanol can be used to calculate concentration (Table A1:5).

Gas sampling valve

For calculation of vapour sample (1.0 cm^3), direct correlation to the peak area of manually injected liquid samples were used.

Table A1:6 Data for calculation of standard curve for GC-FID to organic solutions.

Conc. %v/v in 50uL	Dilution 50 µL / 1000µL	Peak Area (mV.s) Octanol	Linalool	Linalyl acetate	Ratio Lool:Oct	Ratio Lyl:Oct
0.1	0.005	2362.4	52.2	14.4	0.02	0.01
1	0.05	835.6	253.4	204.3	0.30	0.24
4	0.2	2631.4	2503.1	2382.6	0.95	0.91
5	0.25	2915.6	3200.7	3199.9	1.10	1.10
6	0.3	2590.0	3445.4	3539.2	1.33	1.37
10	0.5	2947.9	6175.4	6709.8	2.09	2.28
	Average:	2380.48				

Table A1:6 above shows the degree of variation found in manual injections. The peak area for octanol at the 1%v/v aliquot is significantly less than the average shown at the bottom of the table, indicating human error introduced when manually injecting a volume of sample onto the GC-FID. However this effect is moderated by the use of ratio's to the internal standard, as all of the organic components have smaller peak area's and are relative to that of octanol. The ratio of organic:octanol was multiplied by the average peak area for Octanol to give the standardised peak area for both linalool and linalyl acetate. See Table A1:7 below.

Table A1:7 Standardised peak areas.

Conc. (mol/L)	Mol injected (0.1µL)	Std. Linalool	Std. Linalyl acetate
0.000281	2.81359×10^{-8}	52.60	14.51
0.002814	2.81359×10^{-7}	721.89	582.02
0.011254	1.12543×10^{-6}	2264.42	2155.41
0.014068	1.40679×10^{-6}	2613.26	2612.60
0.016882	1.68815×10^{-6}	3166.70	3252.91
0.028136	2.81359×10^{-6}	4986.75	5418.28

This data is displayed graphically below, along with the trendline correlations for calculating the concentration of linalool (Figure A1:14) and linalyl acetate (Figure A1:15) from their peak area's.

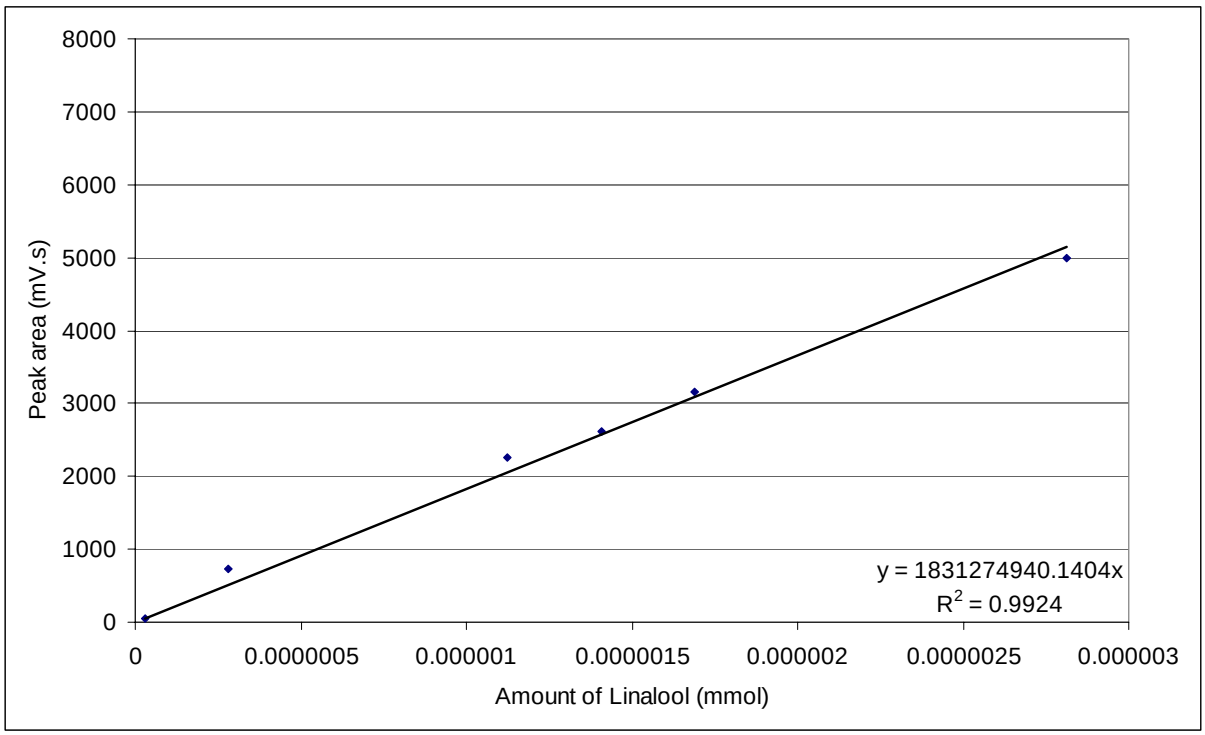

Figure A1:14 Standard Curve Correlation; GC-FID response to Concentration of known Linalool solutions

Because the detector conditions (range and attenuation) are the same for both liquid and vapour sampling, they have equivalent correlations to detector response (peak area). Thus any injection of sample via the gas sampling valve (GSV) will be determined by the relationship:

$$x_{(lool)}\ (mmol/cm^3) = Peak\ area_{(lool)} / 1{,}831{,}274{,}940 \qquad (A1:3)$$

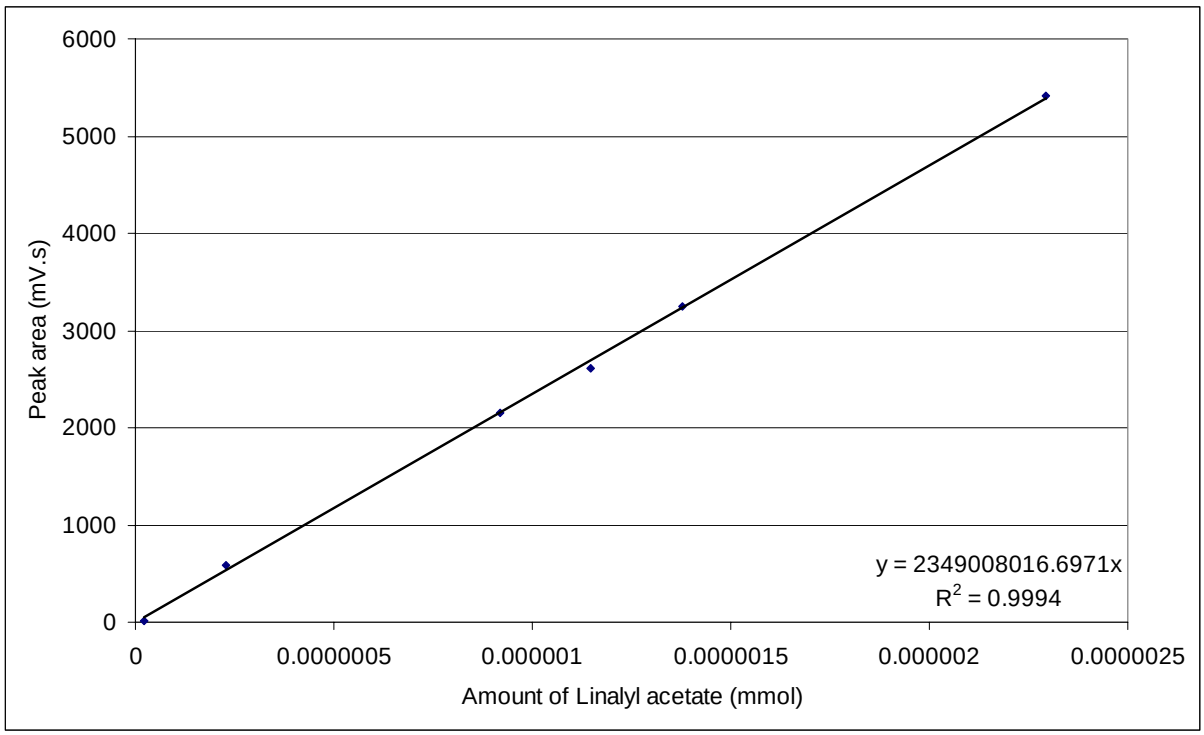

Figure A1:15 Standard Curve Correlation; GC-FID response to Concentration of known Linalyl acetate solutions

$$x_{(lyl)}\ (mmol/cm^3) = Peak\ area_{(lyl)} / 2{,}349{,}008{,}017 \qquad (A1:4)$$

The problem with this method of calculation, i.e., lack of internal standard, is that the detector response may drift higher or lower depending on temperature of gas supply lines (summer to winter room temperatures), gradual drift of FID gas flow rates, soot build-up on FID components etc. This can be minimised as much as possible with good preventive maintenance of GC-FID, but the best option for minimising the degree of drift is to use manual injections prior to GSV injections as an external standard (peak area of octanol (5% v/v) from liquid samples).

Mass Balance Analysis

A complete mass balance of the PV process is difficult due to constraints in both the experimental and process design, and the sensitivity of analytical equipment.

The balance between the amount of solution lost from the feed stream, permeating through the membrane and collected in the cold trap is difficult to measure accurately because of (a)

the large relative volume of the feed tank (≈2000mL), and (b) the small volume of permeate collected in the cold trap (≈1-5mL). The loss of a few millilitres from the bulk feed during the course of an experiment is undetectable in the concentration of the feed as measured by GC-FID. The sampling error due to manual GC-FID analysis technique is larger than the difference in the concentration before and after processing of the feed.

Limitations in the pilot scale process design ruled out the possibility of monitoring the feed mass gravimetrically. A stainless steel feed tank, firmly attached to a waterbath to control feed temperature precluded the ability to weigh the feed tank with any accuracy.

The only other alternative for monitoring the mass balance within the process was to link the flow transmitter output to the mass fraction of permeate detected via online sampling on the GC-FID, and compare mass flows with that collected in cold traps. Thereby verifying the completeness of condensation and validate the potential for loss of permeate through leaks in the process lines, valves and connections.

Validation of mass balance

An experiment was run that validated the mass balance between permeate collected and manually sampled from cold traps, and that sampled via the GC-GSV in vapour form. A 40 hour PV run consisting of four 10 hourly manual samples, and hourly GSV sampling gave the following results.

Standard Process Conditions

Fixed process conditions:

V = 1 cm^3 (Sampling loop)
T = 140°C (External oven for GC-FID sampling loop)

HDPE Membrane particulars:

Dry diameter = 126.70 mm
Dry thickness = 0.0104 mm (≈10μm)
Dry weight = 0.12205 g
Wet weight = 0.12738 g (pre-soaked in feed solution)

Process run with online sampling

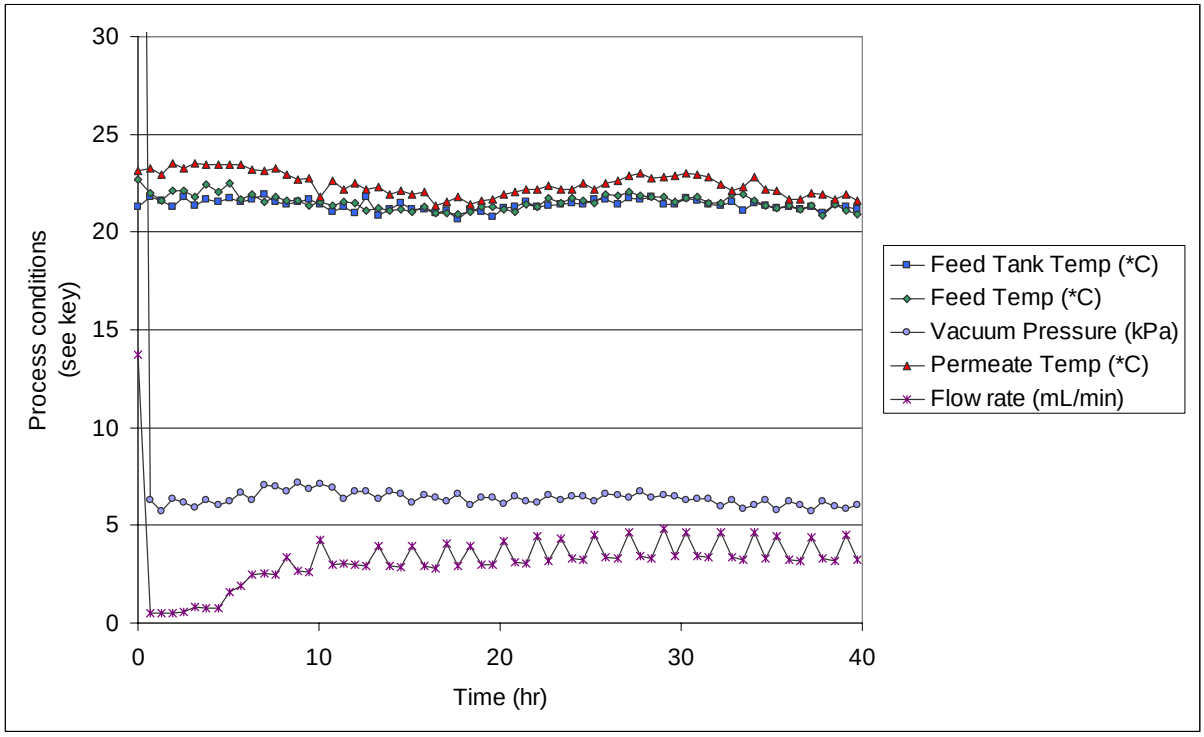

Figure A1:16 Process variables for pervaporation of 5% v/v solutions of Linalool and Linalyl acetate in Ethanol using an HDPE membrane (11/03/04) under standard operating conditions.

Average process conditions at approximate steady state (10hrs to 40hrs):

P = 6.341 kPa

Q = 3.59 $sccm_{(EtOH)}$

T_f = 21.32°C (Feed tank)

T_r = 21.41°C (Retentate)

T_p = 22.20°C (Permeate)

Analysis of Cold Trap samples

The volumetric amounts of permeate collected in the cold traps over the 10 hour intervals of this experiment (Figure A1:17), closely mirrors flow rates (Figure A1:16). The first 10 hours in the pervaporation experiment showed the lowest permeate flux rate, gradually increasing until it reached approximate steady state between 20 and 40 hours.

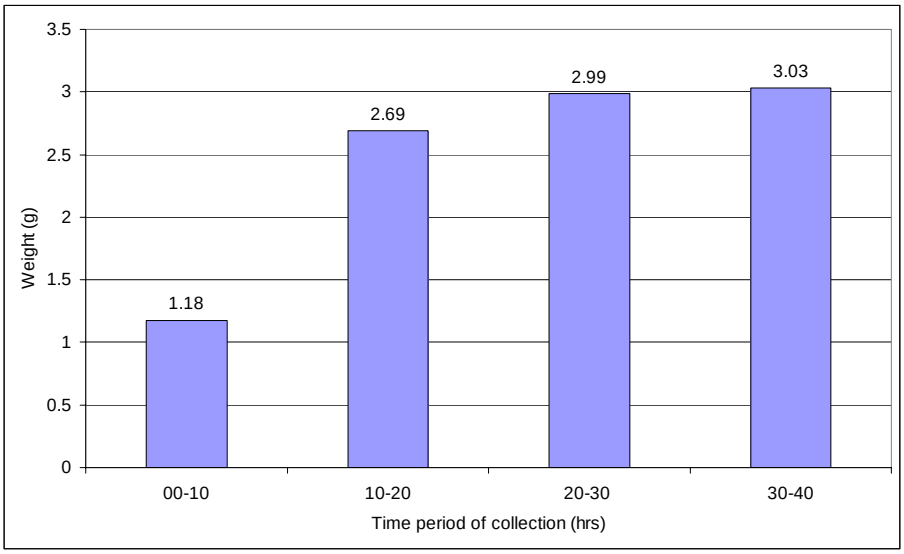

Figure A1:17 Permeate collected in cold traps from pervaporation process.

Concentrations of these cold trap samples are (Figure A1:18) below where linalyl acetate dominates the mixture that permeated through the HDPE membrane.

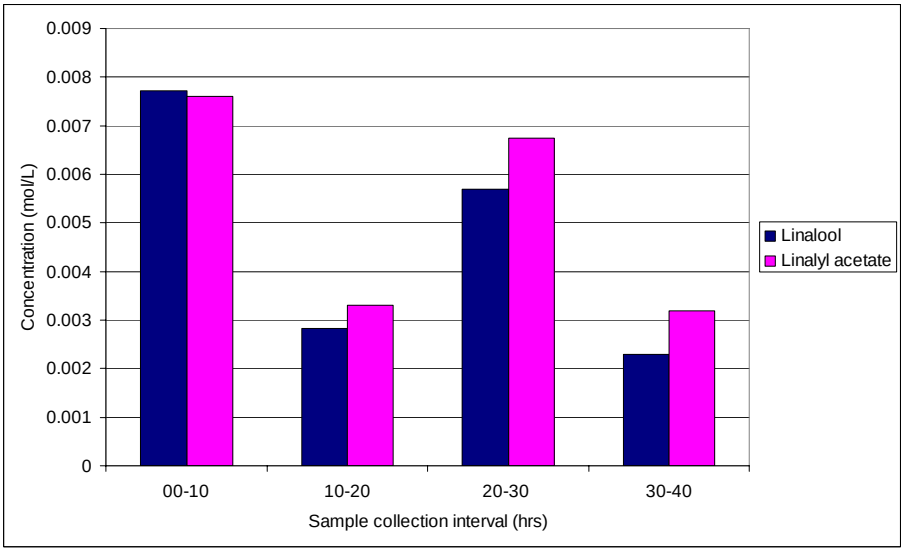

Figure A1:18 GC-FID analysis of permeate concentration from condensed samples collected at intervals in cold traps (manual injections, with internal standards).

Below are example calculations of the mass flow rates of permeate samples collected in cold traps, and a summary in Table A1:8.

Linalool mass flow rate:

$$x = \frac{\left(Conc.(mol.L^{-1}) * Mol.wt.(g.mol^{-1})\right)}{\left(Density(g.mL^{-1}) * 1000(mL.L^{-1})\right)}$$

$$x_{(lool)} = \frac{\left(0.007722(mol.L^{-1}) * 154.2516(g.mol^{-1})\right)}{\left(0.868(g.mL^{-1}) * 1000(mL.L^{-1})\right)}$$

$x_{(lool)}$ = 0.001372 v/v

$Q_{(lool)}$ = (0.001372 v/v) * (1.18g/10hrs)

$Q_{(lool)}$ = 0.0001619 g/hr

$Q_{(lool)}$ = 0.1619 mg/hr

Table A1:8 Concentrations of Coldtrap liquid samples.

Time (hrs)	Mass of Coldtrap (g)	Linalool (mol/L)	Mass fraction linalool	Flow rate linalool (mg/hr)	Linalyl acetate (mol/L)	Mass fraction lyl.ac.	Flow rate lyl.ac. (mg/hr)
00-10	1.18	0.007722	0.001372	0.162	0.007598	0.001655	0.195
10-20	2.69	0.002831	0.000503	0.135	0.003306	0.000720	0.194
20-30	2.99	0.005689	0.001011	0.302	0.006745	0.001469	0.439
30-40	3.03	0.002291	0.000407	0.123	0.003192	0.000695	0.211

Analysis of Vapour samples

Table A1:9 contains the average process conditions observed in the PV experiment over each 10 hour sampling interval.

Table A1:9 Average process conditions over 10hr sampling intervals.

Sampling interval (hrs):	Feed Tank Temp. (ºC)	Retentate Temp. (ºC)	Permeate Temp. (ºC)	Vacuum Pressure (kPa)	Flow rate $sccm_{(EtOH)}$ (mL/min)
00-10	21.6	21.9	23.2	6.46	1.6
10-20	21.1	21.2	21.9	6.52	3.3
20-30	21.5	21.6	22.5	6.42	3.7
30-40	21.3	21.4	22.2	6.08	3.8

Permeate concentrations observed in the condensed samples (see Fig A1:18 in cold trap analysis section) closely mirrored the trend observed in GC-FID detector response when vapour was sampled online (Figure A1:19).

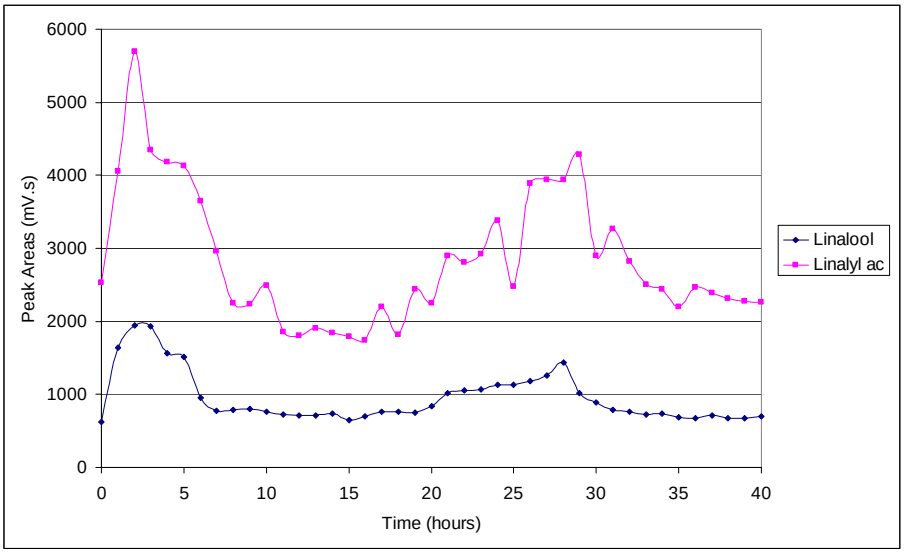

Figure A1:19 GC-FID analysis of permeate vapour from online sampling.

GC-FID peak area was converted to concentration using conversion factor discussed previously in the GC analysis section (Equations A1:3 & A1:4).

Mass Balance based on ideal gas laws

Ideal gas law (Felder and Rousseau, 1986):

$$PV = nRT \qquad \text{(A1:5)}$$

Where:

P = absolute pressure of gas

V = volume or volumetric flow rate of the gas

n = number of moles or molar flow rate of the gas

R = the gas constant, (volume)(pressure)/(mole)(temperature)

T = absolute temperature of the gas

Constants (Peters and Timmerhaus, 1991):

1 mol of an ideal gas at 0°C and 1 atm occupies 22.415 litres.

$$R = 82.06 \ (cm^3)(atm)/(mol)(K) \qquad \text{(A1:6)}$$

Calculation (at steady state 10-40 hours):

P = 6.341 kPa = 0.06258 atm

$V = 1.0\ cm^3$

n_{total} = unknown

$R = 82.06\ (cm^3)(atm)/(mol)(K)$

$T = 413.1\ K\ (140°C)$

$n_{total} = (0.06258\ atm)(\ 1.0\ cm^3)/(82.06\ (cm^3)(atm)/(mol)(K))(413.1\ K)$

$n_{total} = 0.000,001,846\ mol$

$n_{total} = 1.846\ x10^{-6}\ mol$

$n_{total} = n_{lool} + n_{lyl} + n_{EtOH}$

Summary of these calculations can be (Table A1:10) for the four time intervals studied in this PV run.

Table A1:10 Averaged vapour permeate concentrations of Linalool and linalyl acetate over 10 hour sampling intervals.

Time (hours)	Pressure (atm)	Linalool (mol x10^{-9} /cm^3)	Linalyl acetate (mol x10^{-9} /cm^3)	n_{total} (mol x10^{-9} /cm^3)
00-10	0.063740142	0.68427464	1.534256151	1880.296407
10-20	0.064379211	0.397657383	0.846046495	1899.148576
20-30	0.063355882	0.608614237	1.395972247	1868.960991
30-40	0.059993304	0.398640305	1.088382833	1769.766911

Following are example calculations of the molar flow rates of permeate samples collected via gas sampling valve, and summarised in Table A1:11.

<u>Linalool molar flow rate:</u>

$$x_{(lool)} = \frac{n_{lool}}{n_{total}}$$

$$x_{(lool)} = \frac{0.68427464\ x10^{-9}\ mol}{1880.296407\ x10^{-9}\ mol}$$

$x_{(lool)} = 0.000,363,918$

$x_{total} = x_{lool} + x_{lyl} + x_{EtOH} = 1$

$x_{EtOH} = 1 - (x_{lool} + x_{lyl})$

Table A1:11 Mole fraction of solution components over time intervals.

Time (hrs)	Mole fraction linalool	Mole fraction linalyl acetate	Mole fraction ethanol
00-10	0.000363918	0.000815965	0.99882012
10-20	0.000209387	0.000445487	0.99934513
20-30	0.000325643	0.000746924	0.99892743
30-40	0.00022525	0.000614987	0.99915976

Flow rate of vapour permeate

The Top-Trak™ mass flow meter was calibrated in factory to the flow of Nitrogen at standard conditions 21°C and 760 mmHg (Sierra Instruments Inc., 1994). Flow meter output was converted to $Ethanol_{(g)}$ via the K-factor, which is derived from the first law of thermodynamics applied to the sensor tube.

$$H = \frac{\dot{m} C_p \Delta T}{N}$$

K-factor for ethanol:

$$\frac{Q_{EtOH}}{Q_{N_2}} = \frac{K_{EtOH}}{K_{N_2}}$$

$$Q_{EtOH} = \frac{0.39}{1.00} * Q_{N_2}$$

Translation from factory calibrated flow rate at standard conditions sccm (standard cm^3/min at 21°C, 1atm) to accm (actual cm^3/min) requires the following conversions:

$$Q_{accm} = \frac{P_{std}}{P_{act}} * \frac{T_{act}}{T_{std}} * Q_{sccm}$$

$$Q_{accm} = \frac{101.325kPa}{6.46kPa} * \frac{273.15^\circ K + 23.2^\circ C}{273.15^\circ K + 21.0^\circ C} * 1.6sccm$$

$$Q_{accm} = 25.38accm$$

Q_{Mr} = Flow rate $accm_{(EtOH)}$ (cm^3/min) * n_{total} (mol/cm^3)

Q_{Mr} = 25.38 $accm_{(EtOH)}$ * 1.880296407 x10^{-6} (mol/cm^3)

Q_{Mr} = 4.77274 x10^{-5} (mol/min) * 60 (min/hr)

Q_{Mr} = 0.002863647 (mol/hr)

$Mr_{(total)} = x_{lool}*Mr_{lool} + x_{lyl}*Mr_{lyl} + x_{EtOH}*Mr_{EtOH}$

$Mr_{(total)}$ = (0.000363918*154.2516) + (0.000815965*196.2888) + (0.99882012*46.0688)

$Mr_{(total)}$ = 46.23074399 g/mol

Mass flow rate

$Q_{mass} = Q_{Mr}$ (mol/hr) * $Mr_{(total)}$ (g/mol)

Q_{mass} = 0.002863647 (mol/hr) * 46.23074399 (g/mol)

Q_{mass} = 0.132388515 (g/hr)

Q_{mass} = 1.32388515 (g/10hrs)

This conversion is summarised in Table A1:12.

Table A1:12 Flow rates of Linalool and Linalyl acetate over time intervals.

Time (hrs)	Flow rate $accm_{(EtOH)}$ (cm^3/min)	n_{total} (mol x10^{-6} /cm^3)	Flow rate (mol/hr)	Total molecular weight (g/mol)	Mass flow rate (g/10hrs)
00-10	25.38	1.880296407	0.00286365	46.2307	1.32
10-20	51.10	1.899148576	0.00582255	46.1584	2.69
20-30	59.17	1.868960991	0.00663476	46.2162	3.07
30-40	62.83	1.769766911	0.00667190	46.1856	3.08

Comparison of vapour permeate and condensate analysis.

Figure A1:21 shows a very good correlation between vapour samples collected in cold traps and the predicted mass flow over this time period. Time interval 00-10hrs showed the largest difference (Δ= 11.77%) between the flow meter reading and that of the cold trap, 10-20hrs varied by Δ= 0.21%, 20-30hrs Δ= 2.63%, and 30-40hrs showed Δ= 1.68% difference.

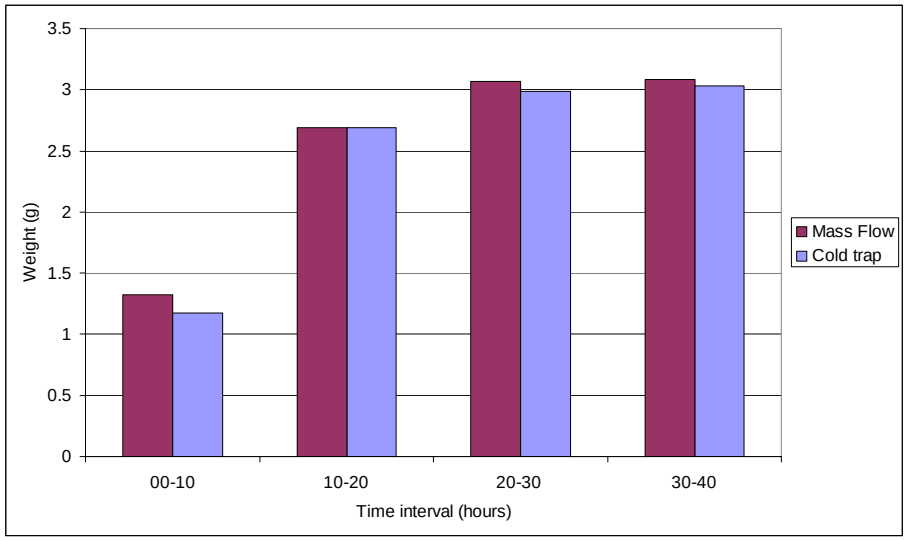

Figure A1:21. Comparison of expected mass flow of vapour permeate over 10 hour period, and that collected in coldtraps.

The mass flow meter manufacturer stated that the K-factors for conversion from N_2 to other gases is only a rough approximation, and inaccuracy of measurement can range from ± 5-10% (Sierra Instruments Inc., 1994). This is further complicated by the fact that although the vapour permeate is predominantly ethanol, it does contain linalool and linalyl acetate which have different heat capacities and will affect the operation of the mass flow meter (temperature difference between resistance temperature detector (RTD) coils); plus the composition of the permeate vapour will vary throughout the course of a pervaporation run.

Further error may be introduced by the ability of the cold trap immersed in liquid nitrogen to retain all volatile organic molecules passing through the system. However, the difference between the permeate vapour calculated via the mass flow meter and that measured from the cold trap is very small, leading to the conclusion that the cold trap does indeed collect the vast majority of volatile molecules, and that the assumptions made about the heat capacity of the vapour permeate (predominantly ethanol) are valid.

Appendix 2

Effect of Feed Flow rate on Pervaporation

The effect of feed flow rate on pervaporation was studied using HDPE membranes (10 μm thick). These experiments were run at $\widetilde{T}_p$ = 22.6°C ± 0.77°C, $\widetilde{P}_p$ < 10 kPa, membrane unit impinging jet height = 1.36 mm, feed concentrations ~ 5% v/v linalool and linalyl acetate in ethanol, and a feed flow rate ranging from approximately 541– 1328 mL/min ($\pm_{max}$ 28 mL/min). The linear range for the pervaporation feed flow rate was calibrated manually *in-situ* using water, a stopwatch and measuring cylinder, and was found to be between 378 – 1656 mL/min (Figure A2:01). Feed pump speeds below 10% were irreproducible, and speeds above 40% were non-linear.

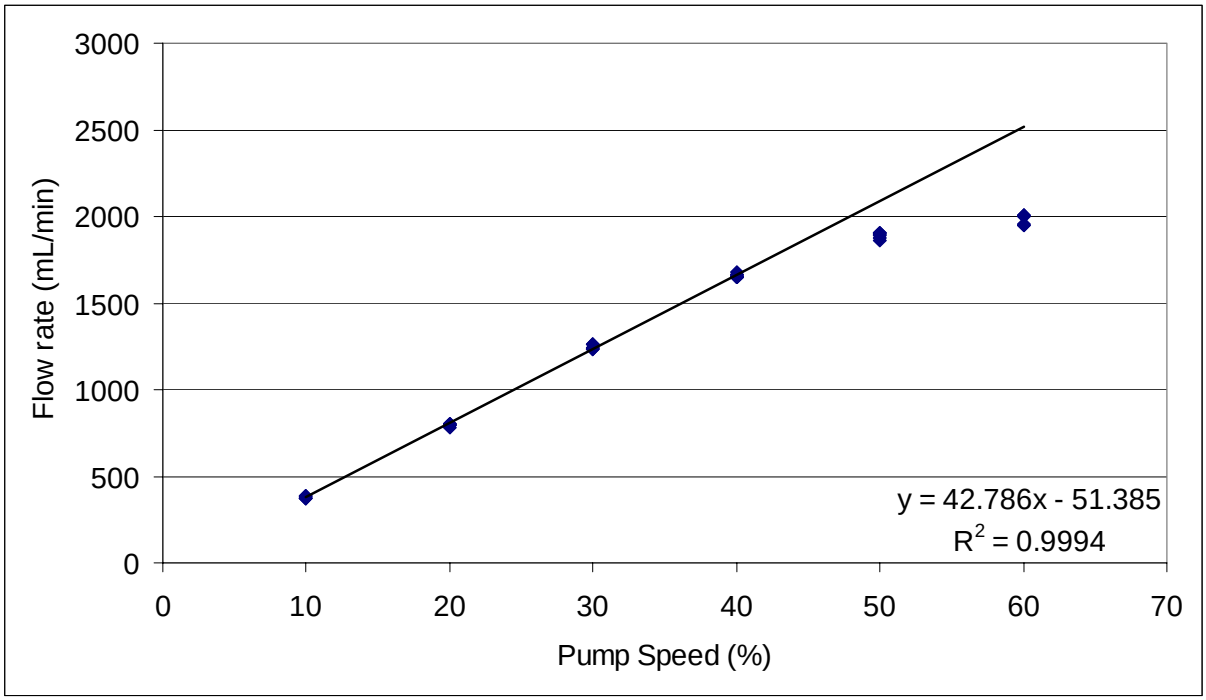

Figure A2:01 Capacity of feed pump and calibration of linear region of flow.

Turbulence within a membrane unit is desirable to minimise the effects of fouling and concentration polarization in the boundary layer. Changes in the diameter of the pipe, as seen in the flow distributor for the membrane unit (Figure A2:02); can cause changes in the critical

Reynolds number (*Re* = 2000). If a pipe converges, the critical Reynolds number required to achieve turbulence is higher, whereas divergence such as seen in the membrane unit flow distributor produces a lower value for Newtonian fluids (Massey, 1979). The divergence occurring at the flow distributor increases the likelihood that feed flowing through the membrane unit will in fact be turbulent.

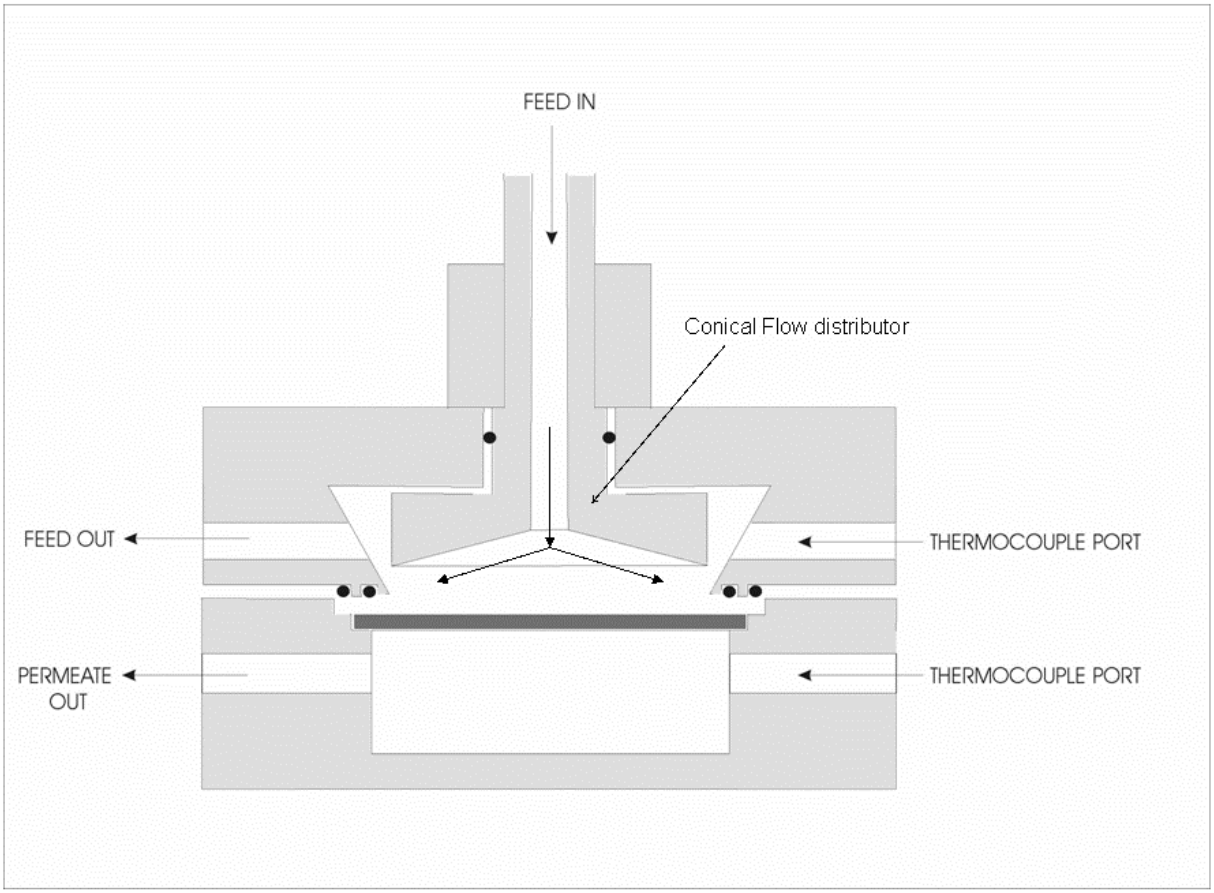

Figure A2:02 Schematic diagram of membrane cell (He, 2000), reproduced from Figure 5:17.

The transition from laminar to turbulent flow regime within a conical membrane cell flow distributor was studied by Miranda & Campos (1999). They found that in a conical flow distributor, the critical value of jet Reynolds number was approximately *Re* = 1600.

Reynolds numbers were calculated to measure the turbulence at the Jet nozzle in the membrane unit (Miranda and Campos, 2001a).

$$\mathrm{Re} = \frac{\rho_o * V_j * D_j}{\mu_o} \qquad \text{(Eqn A2:1)}$$

where V_j is the average jet velocity at the nozzle exit, D_j the diameter of the jet, ρ_o and μ_o, the density and the viscosity of the feed solution. The density and viscosity were approximated

to that of ethanol $\rho_{o\ EtOH}$ = 789 kg/m^3 and $\mu_{o\ EtOH}$ = 0.00119 kg/(m·s) at 20°C, and the jet diameter D_j = 0.00873 m. Linear flow rates were calculated from volumetric flow rate (m^3/sec) divided by the jet area = 5.98575 x10^{-05} m^2. (see dimensions in Chapter 3, Figure 3:5).

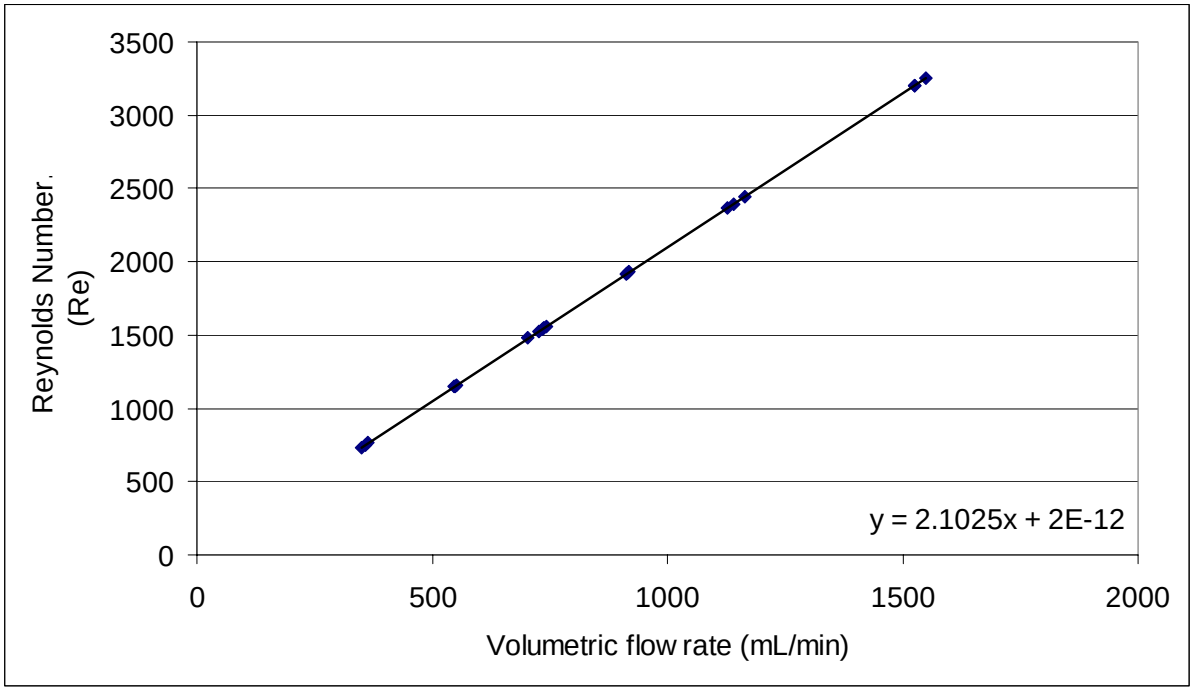

Figure A2:03 Corelation between volumetric flow rate and Reynolds number for impinging jet membrane unit.

At pump flow rate 804 ± 9 mL/min, flow at the jet nozzle gives an average Reynolds Number of 1691 (using Eqns. in Figures A2:01 and A2:03), close to the *Re* = 1600 recommended by Miranda & Campos (2001a).